Amyloid peptides and the vascular system : the link between cerebrovascular angiopathy and Alzheimer's disease

Alsheikh Abubaker, Aisha

Award date:
2019

Awarding institution:
University of Bath

DOCTORAL THESIS

AMYLOID PEPTIDES AND THE VASCULAR SYSTEM: THE LINK BETWEEN CEREBROVASCULAR ANGIOPATHY AND ALZHEIMER'S DISEASE

Aisha Saleh Hussein Alsheikh Abubaker BSc (Hons), MRes

A thesis submitted for the degree of Doctor of Philosophy

University of Bath

Department of Pharmacy and Pharmacology

March 2019

This research was performed under the supervision of

Dr. Giordano Pula and Dr. Ian Eggleston

COPYRIGHT

Signed: …….. Date: ……..……..

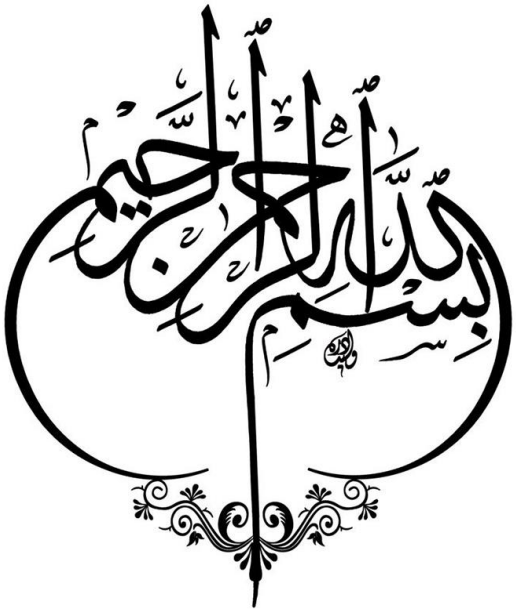

أكرس رسالة الدكتوراه هذه إلى جدتي الراحلة (رحمها الله)

والدتي التي لم تتوقف أبداً عن العطاء والمحبة ودعم بلا حدود

In the name of God, the Most Gracious, the Most Merciful

I dedicate this thesis to my late grandmother (God rest her soul)

and to my mother who never stopped loving, giving, and

supporting me.

TABLE OF CONTENTS

TABLE OF CONTENTS III
ABSTRACTT…….…. VI
ACKNOWLEDGMENT VIII
PUBLICATIONS…… IX
LIST OF TABLES…. X
LIST OF FIGURES XI
ABREVIATIONS…… XIV

CHAPTER 1…….. 1
1. INTRODUCTION 2
1.1. DEMENTIA AND ALZHEIMER'S DISEASE 2
1.2. ETIOPATHOGENESIS AND ALZHEIMER'S DISEASE 3
1.2.1. Neuropathology 3
1.2.2. Amyloid Precursor Protein 4
1.2.3. Aβ peptide Production and Clearance 6
1.2.4. Amyloid and Vascular Hypotheses of AD Onset and Development 9
1.3. CEREBRAL AMYLOID ANGIOPATHY AND ALZHEIMER'S DISEASE 12
1.3.1. Clinical Manifestation of CAA 12
1.3.2. Sources and Mechanisms of Aβ Deposition in CAA 13
1.4. PLATELETS AND ALZHEIMER'S DISEASE 15
1.4.1. Platelet Overview 15
1.4.2. Platelet Morphology 15
1.4.3. Platelet Role in Haemostasis and Thrombosis 17
Primary Haemostasis 18
Platelets and Blood Flow 18
Mechanisms of Platelet Adhesion, Activation, and Signalling 20
Collagen 20
Von Willebrand Factor (VWF) and GPIB-V-IX 21
Integrin $\alpha_2\beta_1$ (GPIa/IIa) 23
Glycoprotein VI (GPVI) 24
Cytoskeleton Rearrangement 25
Secretion of Granule Contents 26
ADP and its Receptors 29
Thromboxane A_2 (TxA_2) and its Receptor 30
Integrin $\alpha_{IIb}\beta_3$ (GPIIb-IIIa) 30
Thrombin and its Receptors 33
Secondary Haemostasis 35
1.4.4. Platelet Abnormalities in AD 40
1.4.5. Amyloid β Peptides and Platelet Activation 41
1.5. RESEARCH HYPOTHESIS 45
1.6. AIMS OF THE STUDY 45

CHAPTER 2…….…. 42
2. MATERIALS & METHODS 43
2.1. EXPERIMENTAL SECTION A: PEPTIDE SYNTHESIS 43
2.1.1. Aβ25-35 Solid Phase Peptide Synthesis (SPPS) 43
2.2. EXPERIMENTAL SECTION B: PLATELET STUDIES 48
2.2.1. MATERIALS 48
2.2.2. METHODOLOGY 51
2.2.2.1. Platelet Isolation 51
2.2.2.2. Adhesion Assay 51
2.2.2.3. Platelet Aggregation Assay by Suspension Turbidimetry 52
2.2.2.4. Thrombus Formation Assay under Physiological Flow 52
2.2.2.5. Platelet α-Degranulation and αIIbβ3 Activation by Flow cytometry 53
2.2.2.6. Detection of Platelet binding to FITC-labelled Aβ Peptides 53
2.2.2.7. Detection of ROS by Microplate Reader 54
2.2.2.8. Detection of Intracellular ROS in Platelets by Flow Cytometry 54
2.2.2.9. Detection of Superoxide Anion in Platelets by Flow Cytometry 55
2.2.2.10. Detection of Superoxide Anion by Electron Paramagnetic Resonance (EPR) 55
2.2.2.11. Amyloid Peptide β Fibrillation in Real Time Using Thioflavin T Assay 56

CHAPTER 3……. 57
3. RESULTS 58
3.1. BACKGROUND 58
3.2. AIMS & OBJECTIVES 62
3.3. RESULTS 63
3.3.1. Aβ25-35 solid phase peptide synthesis (SPPS) 63
3.3.2. Aβ peptides support platelet adhesion under static conditions 64
3.3.3. Effects of Aβ peptides as agonists or co-agonists on platelet aggregation 71
3.3.4. Aβ1-42 increases thrombus formation in whole blood under physiological venous flow conditions…… 74
3.3.5. Aβ1-42 induces platelet activation and expression of integrin $\alpha_{IIb}\beta_3$ 76
3.4. SUMMARY OF RESULTS 78
3.5. DISCUSSION 79

CHAPTER 4…… 84
4. RESULTS 85
4.1. BACKGROUND 85
4.2. AIMS & OBJECTIVES 90
4.3. RESULTS 91
4.3.1. ROS detection in platelet using DCFDA 91
4.3.2. Superoxide detection in platelets using Dihydroethidium 95
4.3.3. Superoxide detection in platelet using electron paramagnetic resonance (EPR) 101
4.4. SUMMARY OF RESULTS 108
4.5. DISCUSSION 109

CHAPTER 5…… 114
5. RESULTS 115
5.1. BACKGROUND 115
5.2. AIMS & OBJECTIVES 117
5.2. RESULTS 118
5.2.1. Effects of ROS inhibition on Aβ1-42-induced platelet adhesion and spreading under static conditions…… 118
5.2.2. NOX inhibition attenuated thrombus formation potentiated by Aβ1-42 under physiological venous flow conditions…… 125
5.2.3. Aβ1-42 stimulated platelets induce $\alpha_{IIb}\beta_3$ activation in a NOX-dependent manner 126
5.2.4. Aβ1-42-induced platelet aggregation is NOX-dependent 128
5.2.5. Identification of potential platelet receptors involved in binding to Aβ1-42 using inhibitors……...…….. 132
5.3. SUMMARY OF RESULTS 144
5.4. DISCUSSION 145

CHAPTER 6…… 149
6. GENERAL CONCLUSIONS 150
FUTURE WORK 154

REFERENCES……. 155

APPENDIX…… 177
HPLC and MS for Aβ peptide from Life-Protein 177
Publications…….…. 181

ABSTRACT

Alzheimer's disease (AD) is a multifactorial neurodegenerative disorder that results in progressive impairment of brain cognitive functions and memory. Amyloid beta (Aβ) peptides are protein fragments present as insoluble and misfolded polymeric depositions in the brain parenchyma and cerebral blood vessel walls of AD patients. Pathological accumulation of Aβ peptides within the cerebrovasculature, especially cerebral cortex and leptomeninges vessels, is referred to as cerebral amyloid angiopathy (CAA) and it can compromise the blood brain barrier (BBB) integrity. In addition, capillary dysfunction, such as pericyte degradation and pericapillary fibrosis, is also observed in AD. These conditions affect blood rheology and hemodynamics leading to impaired cerebral blood flow to tissues.

Circulating blood platelets are responsible for haemostasis and thrombosis, and have also been shown to mediate immunity, tissue repair, and inflammation. Several studies have revealed that platelets in AD patients exhibited abnormalities, including an aberrant pre-activation state. When combined together with compromised blood vessels integrity, a highly pro-thrombotic environment within the cerebrovascular system is established, which leaves AD patients extremely vulnerable to the formation of microthromboses and thromboembolic events. This further exacerbates brain tissue degeneration. The exact intracellular mechanisms underlying platelet activation triggered by Aβ peptides are not well established. Emerging evidence suggests a strong correlation between Aβ peptide effects on platelets and reactive oxygen species (ROS) generation, but a complete picture of the link between Aβ peptides and platelet redox homeostasis is still missing. Therefore, the present PhD project aimed to investigate the mechanisms underlying Aβ peptide-dependent activation of platelets and the potential role of ROS in this pathophysiological event.

In phase I, the effects of Aβ peptides on platelet functional responses were explored, such as adhesion, aggregation, and thrombus formation under static and physiological flow conditions. Phase II, explores different methodologies to assess oxidative changes in platelets upon treatment with Aβ peptides. Finally in Phase III, the redox- and NADPH oxidase-dependence of platelet functional alterations induced by Aβ peptides was investigated. Taken together, this work suggests that Aβ1-42 binds to platelets through collagen receptor GPVI, which induces intracellular redox stress and potentiates platelet activation. Aβ1-42 most likely also binds to scavenger receptor CD36 (GPIV). Aβ1-42

induced significant platelet adhesion and thrombus formation in whole blood under venous flow condition, while other Aβ peptides did not. This suggests a role for this peptide in the cerebrovascular abnormalities associated with AD. Finally, we highlighted the importance of NOXs in the activation of platelets in response to Aβ1-42 peptides and have shown that both NOX1 and NOX2 are important for the induction of superoxide anion formation in platelets activated by Aβ1-42. This work sheds new light on the pro-thrombotic activity of amyloid peptides and provides new insights into the molecular mechanisms underlying cerebral microthrombosis and impaired blood flow in the cerebrovasculature associated with AD progression.

ACKNOWLEDGMENT

First and foremost, I would like to express my profoundly indebted and sincere gratitude to both my main supervisor, Dr. Giordano Pula for giving me this great research opportunity and for being an inspirational mentor, and my co-supervisor Dr. Ian Eggleston. Both relentlessly gave me continuous guidance, support, and patience throughout the years and taught me invaluable knowledge and skills. I would also like to sincerely thank Dr. Ruggero Dondi for his countless efforts to assist and guide me throughout the peptide synthesis experiments in the laboratory. Furthermore, I would like to acknowledge with much gratitude and appreciation Dr. Dina Vara and Dr. Tiago Fortunato for their encouragement and assistance during various phases of my project. Moreover, I would like to express a special thanks to Ms. Jo Carter, for supervising and guiding me in learning venipuncture techniques, Dr. Adrian Rogers for training me on Flow Cytometry and Microplate Reader, and Dr. Anneke Lubben for Mass Spectrometry training, Ms. Bridget Knight who has been an incredible support for providing blood donors at the RD&E NHS foundation Trust, and Dr. Pia Leete for training me in Fluorescence Microscopy. I am also grateful for the support and guidance from Dr. Ilaria Canobbio in the University of Pavia Italy; and from the University of Bath, Dr. Khaled Almansour, Dr. Amanda Mackenzie, Dr. Lorenzo Caggiano, Dr. Sergey Smirnov, Dr. Kunal Tewari, Mr. Pascal Loizeau, Dr. Majdah Alotaibi, Dr. Mike Kenny, and Dr. Bayan Alkhawaja; and from the University of Exeter, Dr. Afi Leslie, and Dr. Eseoghene Ifie who helped me countlessly. I would like to acknowledge with much gratitude all the blood donors, especially Mr. Husain Naqi, without whom my experiments wouldn't have been possible, and also the people who patiently and tirelessly allowed me to practice my phlebotomy techniques on them at the start. I am also grateful to the Department of Pharmacy and Pharmacology at the University of Bath for providing excellent research facilities and work environment. In addition, I am also grateful to the University of Exeter for providing excellent research facilities, which allowed me to continue my final year experiments. Last, but not least, I would like to dedicate to greatest extent my deepest love, gratitude and ultimate appreciation to my mother for all the sacrifices and support she gave me every step of the way in order for me to attain my higher education and pursuing my dreams.

"There are not enough words in the world to describe how much I love you mum, you have been my rock, my inspiration, my superhero, and an irreplaceable blessing from God. This work is my gift to you."

PUBLICATIONS

Publications from Thesis

Alsheikh-Abubaker, A., Vara, D., Visconte, C., Eggleston, I., Torti, M., Canobbio, I. and Pula, G., 2019. Amyloid Peptide β1-42 induces integrin αIIbβ3 activation, platelet adhesion, and thrombus formation in a NADPH oxidase-dependent manner. Oxidative Medicine and Cellular Longevity, 2019, pp. 1-12. (Chapters 3 and 5)

Alsheikh-Abubaker, A., Vara, D., Eggleston, I., Canobbio, I. and Pula, G., 2017. A novel flow cytometry assay using dihydroethidium as redox-sensitive probe reveals NADPH oxidase-dependent generation of superoxide anion in human platelets exposed to amyloid peptide beta. Platelets, pp. 1-9. (Chapter 2)

Other Publications

Visconte, C., Canino, J., Guidetti, G.F., Zara, M., Seppi, C., Alsheikh-Abubaker, A., Pula, G., Torti, M. and Canobbio, I., 2018. Amyloid precursor protein is required for in vitro platelet adhesion to amyloid peptides and potentiation of thrombus formation. Cellular Signalling, 52, pp. 95-102.

Canobbio, I., Alsheikh-Abubaker, A., Visconte, C., Torti, M. and Pula, G., 2015. Role of amyloid peptides in vascular dysfunction and platelet dysregulation in Alzheimer's disease. Frontiers in Cellular Neuroscience, 9.

Posner, M.G., Upadhyay, A., Alsheikh-Abubaker, A., Fortunato, T.M., Vara, D., Canobbio, I., Bagby, S. and Pula, G., 2016. Extracellular fibrinogen-binding protein (Efb) from Staphylococcus aureus inhibits the formation of platelet-leukocyte complexes. J Biol Chem, 291(6), pp. 2764-2776.

Conferences and Posters

Jan 2015: GW4 Ageing and Dementia Meeting, Bristol, Poster presentation

Sep 2015: UK Platelet Meeting, Leicester, Poster presentation. 'Live Platelet Assay for the Detection of ROS Generation'.

Jan 2016: Dementia HIT Clinical Research Showcase (Conference), Bristol.

Sep 2017: 1st Italian-UK Platelet Meeting, Bath, Poster presentation. ‘Detection of Reactive Oxygen Species by Amyloid Peptides β in Human Platelets using Dihydroethidium’

LIST OF TABLES

Table 1 | Summary of dementia types clinical manifestation. 2

Table 2 | Main bioactive molecules and receptor proteins for platelet granules 28

Table 3 | Coagulation proteins nomenclature, pathways involved, and function. 38

Table 4 | Fmoc-protected amino acids for synthesis of Aβ25-35 44

Table 5 | Sequences and molecular formulae of Life Tein Aβ peptides 47

Table 6 | Platelet Stimuli 48

Table 7 | Platelet Inhibitors 48

Table 8 | Amyloid Peptides β 49

Table 9 | Antibodies, Molecular & Fluorescent Probes 49

Table 10 | Other Reagents 49

Table 11 | Instruments & Software 50

LIST OF FIGURES

CHAPTER 1

Figure 1.1: Cross-sectional comparison between normal brain and atrophied brain in advanced AD. 4
Figure 1.2: Summary of APP proteolytic processing in the amyloidogenic and non-amyloidogenic pathways, and putative physiological and pathological roles of APP and its generated fragments. 6
Figure 1.3: Normal physiological maintenance of the homeostatic balance between Aβ production and clearance in the brain and the periphery. 8
Figure 1.4: Types and development of CAA 13
Figure 1.5: Summary of discoid platelet structural features seen from an equatorial plane view. 16
Figure 1.6: Summary of parabolic velocity profile and blood flow properties under physiological and pathological conditions. 19
Figure 1.7: Simplified diagram for the process of platelet initial tethering, rolling and firm adhesion and to collagen through VWF and the three main adhesion receptors as shown……..22
Figure 1.8: Main platelet receptors and their signalling mechanisms involved in initial adhesion and activation to collagen. 25
Figure 1.9: Fibrinogen molecular structure…….31
Figure 1.10: Platelet signalling downstream for different GPCRs upon stimulation with its soluble agonists ADP, thrombin, and thromboxane A2. 34
Figure 1.11: Summary of coagulation cascade model 36
Figure 1.12: Summary of the different stages for maintaining haemostasis, and mechanisms of anticoagulation system involving endothelial cells. 39

CHAPTER 2

Figure 2.1: Illustration of the basic principles in SPPS. 43

CHAPTER 3

Figure 3.1: Aβ25-35 peptide synthesis. 63
Figure 3.2: Platelet adhesion and spreading area over collagen or fibrinogen-coated surfaces under static conditions. 65
Figure 3.3: Aβ peptides support platelet adhesion under static conditions. 67
Figure 3.4: Platelet adhesion and spreading onto dual coated surfaces with collagen and Aβ peptides under static conditions. 69
Figure 3.5: Aβ peptides potentially enhance platelet adhesion in the presence of fibrinogen. 70
Figure 3.6: Platelet aggregation in response to thrombin or collagen. 71
Figure 3.7: Examining platelet aggregation in response to amyloid peptides as agonists. 72
Figure 3.8: Potentiation of platelet aggregation in response to amyloid peptides with collagen. 73
Figure 3.9: Potentiation of platelet aggregation in response to amyloid peptides with thrombin. 74
Figure 3.10: Platelet adhesion to amyloid peptides under physiological shear stress. 75

Figure 3.11: Activation of integrin $\alpha_{IIb}\beta_3$ by Aβ1-42. 76
Figure 3.12: Binding of FITC-labelled Amyloid peptides to platelets. 77

CHAPTER 4

Figure 4.1: Summary of platelet sources of ROS, free radical formation, and antioxidant enzymes. 86
Figure 4.2: Schematic representation of structure of NADPH oxidase enzymes (1 and 2) and assembly of subunits. 87
Figure 4.3: Preliminary study on ROS generation in live platelet suspension using microplate reader. 92
Figure 4.4: Determination of optimum concentrations for 6 different stimuli to detect ROS generation in live platelet suspensions by flow cytometry. 93
Figure 4.5: Optimum time and concentration for use of NAC as ROS scavenger on stimulated platelet suspensions. 94
Figure 4.6: Effects of different Aβ peptides on ROS generation in live platelet suspensions detected by flow cytometry. 94
Figure 4.7: Use of DHE to detect superoxide anion formation in platelets. 96
Figure 4.8: Determination of the concentration dependence of superoxide anion generation for 6 different stimuli. 97
Figure 4.9: Investigation of the effects of the ROS scavenger NAC at different concentrations on platelet superoxide anions formation by different physiological stimuli. 98

CHAPTER 5

Figure 5.1: Effects of ROS inhibition with NAC on platelet adhesion and spreading over Aβ1-42-coated surfaces. 119
Figure 5.2: Effects of ROS inhibition with NAC on platelet adhesion and spreading over dual coated surfaces with collagen and Aβ1-42. 120
Figure 5.3: Effects of ROS inhibition with NAC on platelet adhesion and spreading area over dual coated surfaces with fibrinogen and Aβ1-42. 121
Figure 5.4: Aβ1-42 induces NOX-dependent platelet adhesion and spreading under static conditions. 122
Figure 5.5: NOX-dependent inhibition of platelet adhesion and spreading over dual coated surfaces with collagen and Aβ1-42. 123
Figure 5.6: NOX-dependent inhibition of platelet adhesion and spreading over dual coated surfaces with fibrinogen and Aβ1-42. 124
Figure 5.7: Effects of NOX inhibition on platelet adhesion to Aβ1-42 under physiological shear stress. 125
Figure 5.8: Activation of integrin αIIbβ3 by Aβ1-42 is NOX-dependent. 126
Figure 5.9: Effects of NOX inhibition on platelet aggregation stimulated by physiological agonists. 128
Figure 5.10: Aβ1-42 induced platelet aggregation is NOX-dependent. 129
Figure 5.11: NOX1 and NOX2 inhibition attenuated by Aβ1-42-induced platelet aggregation. 130
Figure 5.12: Aβ1-42 induced signalling in platelets. 131
Figure 5.13: Effects of PAR1 inhibition on platelet adhesion and spreading over Aβ1-42 under static conditions. 132
Figure 5.14: Effects of PAR1 inhibition on platelet adhesion and spreading over dual coated surfaces with Aβ1-42 and collagen. 134

Figure 5.15: Effects of PAR1 inhibition on platelet adhesion and spreading over dual coated surfaces with Aβ1-42 and fibrinogen. 135
Figure 5.16: Effects of CD36 inhibition on platelet adhesion and spreading over Aβ1-42 under static conditions. 137
Figure 5.17: Effects of CD36 inhibition on platelet adhesion and spreading over dual coated surfaces with Aβ1-42 and collagen. 138
Figure 5.18: Effects of CD36 inhibition on platelet adhesion and spreading over dual coated surfaces with Aβ1-42 and fibrinogen. 139
Figure 5.19: Effects of GPVI inhibition by losartan on Aβ1-42 induces platelet adhesion and spreading under static conditions. 141
Figure 5.20: Effects of GPVI inhibition by losartan on platelet adhesion and spreading over dual coated surfaces with Aβ1-42 and collagen. 142
Figure 5.21: Effects of GPVI inhibition by losartan on platelet adhesion and spreading over dual coated surfaces with Aβ1-42 and fibrinogen. 143

CHAPTER 6

Figure 6.1: Proposed model for the etiopathogenesis of AD and the role of platelets. 152

ABREVIATIONS

A	
AA	Amino acid
ACE	Angiotensin converting enzyme
AD	Alzheimer's disease
ADP	Adenosine diphosphate
ApoEε2/3/4	Apolipoprotein E allele 2, 3 or 4
ANOVA	Analysis of Variance
APP	Amyloid precursor protein
Akt	Protein kinase B (PKB) serine/threonine-specific protein kinase
B	
BBB	Blood brain barrier
Boc	tert. Butoxycarbonyl
C	
CAA	Cerebral Amyloid Angiopathy
CD36	Cluster of differentiation 36 (glycoprotein IV)
CM-H2DCFDA	5-(and-6)-chloromethyl-2′,7′-dichlorodihydrofluorescein diacetate
cPLA2	Cytosolic phospholipase A2
CMH	1-hydroxy-3-methoxycarbonyl-2,2,5,5-tetramethylpyrrolidine
D	
DCM	Dichloromethane
DIPEA/DIEA	N,N-Diisopropylethylamine
DMF	N,N-dimethyl formamide
DMSO	Dimethyl sulfoxide
DTT	Dithiothreitol
DAG	Diacylglycerol
DHE	Dihydroethidium
DBU	1,8-Diazabicyclo[5.4.0]undec-7-ene
E	
ECE	Endothelin converting enzyme
EDTA	Ethylenediaminetetraacetic acid
EDT	1,2-Ethanedithiol
EOAD	Early-onset Alzheimer's disease
ERK	Extracellular signal regulated kinases
ESI-MS	Electrospray Ionization Mass Spectrometry
Et2O	Diethyl ether
ECM	Extracellular matrix
EPR	Electron paramagnetic resonance
ET	Endothelin
ECE	Endothelin converting enzyme

F	
Fmoc	9-fluorenylmethoxycarbonyl
FITC	Fluorescein isothiocyanate
FTIR	Fourier transform infrared spectroscopy
FAK	Focal adhesion kinase
FcR- γ-chain	Fc receptor γ-chain
G	
GSH	Glutathione
GSSG	Glutathione disulphide
H	
HEPES	4-(2-Hydroxyethyl) piperazine-1-ethanesulfonic acid
HOBt	1-Hydroxybenzotriazole
HMPB	4-(4-Hydroxymethyl-3-methoxyphenoxy) butyric acid
I	
IP3	Inositol 1,4,5-triphosphate
J	
JNK	c-Jun N-terminal Kinases
L	
LOAD	Late-onset Alzheimer's disease
LRP1	Lipoprotein receptor-related protein 1
M	
MAPK	Mitogen-activated protein kinases
MeCN	Acetonitrile
MeOH	Methanol
$MgCl_2$	Magnesium chloride
MSNT	1-(Mesitylene-2-sulfonyl)-3-nitro-1,2,4-triazole
m/z	Mass-to-charge ratio
MLC	Myosin light chain
N	
NAC	N-Acetyl-L-cysteine
NaCl	Sodium chloride
NaHCO3	Sodium bicarbonate
NOX	NADPH oxidase
O	
OtBu	tert. Butoxy
oxLDL	Oxidised low density lipoprotein
P	
PGE1	Prostaglandin E1
PKC	Protein kinase C
PLCγ2	Phospholipase C gamma 2

PyBOP	Benzotriazol-1-yl-oxytripyrrolidinophosphonium hexafluorophosphate
PAR	Protease-activated receptor
Pyk2	Protein tyrosine kinase 2
PLCγ2	Phospholipase C γ2
PI3K	Phosphoinositide 3-kinase
PIP2	Phosphatidylinositol 4,5-bisphosphate
PIP3	Phosphatidylinositol 3,4,5-trisphosphate

R	
RP-HPLC	Reverse Phase High Performance Liquid Chromatography
RGD	Arginine-Glycine-Aspartate amino acid sequence
Rap	Ras-related Proteins (GTP-binding protein)
Rho	Ras homologous (member of Ras family of small GTPases)
ROS	Reactive oxygen species

S	
SPPS	Solid Phase Peptide Synthesis
Syk	Spleen tyrosine kinase
SH2	Src-homology 2 domains
SFKs	Src-family kinases

T	
tBu	tert. butyl
TFA	Trifluoroacetic acid
TIS	Triisopropylsilane
tPA	Tissue plasminogen activator
Trt	Trityl
TXA2	Thromboxane A2
TRITC	Tetramethylrhodamine isothiocyanate

V	
VWF	Von Willebrand Factor

CHAPTER 1

General Introduction

1. INTRODUCTION

1.1. DEMENTIA AND ALZHEIMER'S DISEASE

One of the hardest things to ever experience is to grieve the loss of a loved one who is still alive. Dementia is one the most common ageing-related pathologies and it is used as an umbrella term to define a state and a cluster of symptoms involving progressive impairment in brain cognitive functions and memory that can eventually lead to decreased quality of life, physical disability and institutionalization [1, 2]. It is estimated that there are approximately 50 million dementia sufferers globally and the figures are expected to escalate to 152 million by the year 2050 if no cure is available causing concern for a future worldwide health crisis [3]. In the UK alone, dementia now is considered the leading cause of death and places an overwhelming economic burden on social and health care systems costing £26 billion annually [4]. There many types and causes of dementia but the most common ones are categorised into: Alzheimer's dementia, vascular dementia, Lewy bodies dementia, and Frontotemporal dementia [5]. Table 1 below provides a summary of their clinical features. The most dominant causes that leads to dementia are Alzheimer's disease (AD; 60-80% of dementia cases) and vascular dementia (VaD, approximately 20% of cases) [3, 5].

Table 1 | Summary of dementia types clinical manifestation [5].

Dementia Type	Clinical Manifestation
Alzheimer's disease	• Insidious onset and slow progressive decline • Short-term memory impairment in early stage; deficit on 3-word or 5 word recall; executive function impairment in later stages
Vascular dementia (multi-infarct dementia)	• Sudden or gradual onset • Usually correlated with cerebrovascular disease (stroke, lacunar infarcts) and atherosclerotic comorbidities (diabetes, hypertension, coronary heart disease) • Mild memory impairment in early stage • Possible gait difficulties and falls (depending on the extent of the stroke)
Lewy body dementia	• Fluctuating cognition associated with parkinsonism • Poor executive function and visual hallucinations in early stage; deficits on tests designed to examine visual perception (pentagons, cube, trails, clock face)
Frontotemporal dementia	• More prominent personality changes (disinhibition) and behavioural disturbances (apathy, aggression, agitation with less memory impairment in early stage)

Alzheimer's disease (AD) is a multifactorial severe and progressive neurodegenerative brain disorder that represents one of the most prominent causes of dementia with an increasing prevalence worldwide [3]. It was first described by the German psychiatrist Alois Alzheimer

in 1906 as “a peculiar disease of the cerebral cortex” upon post-mortem histopathological examination of the brain of his patient, Auguste Deter, who had suffered the clinical symptomology of what was called pre-senile dementia [6]. Alzheimer discovered brain alterations and the presence of numerous forms of what he described as “plaques” and “tangles” in the cerebral cortex [7].This form of dementia later became referred to as “Alzheimer’s disease” since it was first presented and documented by Alzheimer. Re-examination of Auguste Deter’s medical records and brain specimens in 1997 using modern scientific methods confirmed Alzheimer’s original observations [8].

1.2. ETIOPATHOGENESIS AND ALZHEIMER’S DISEASE

1.2.1. Neuropathology

Since the initial observations by Alzheimer on brain alterations, significant advances have been made in understanding the neuropathological processes underlying this disease [9]. The prominent morphological hallmarks of the disease involve the presence of intraneuronal insoluble aggregates of the microtubule- associated protein, Tau, aberrantly found in a hyperphosphorylated state and forming neurofibrillary tangles (NFTs) [10, 11]. NFTs disrupt the communication and transportation system of neurons, and interfere with numerous intracellular functions, consequently leading to neuronecrosis [11-13].

The second prominent morphological hallmark is the presence of extraneuronal pathological accumulation of insoluble aggregates of misfolded polymeric protein fragments known as β-amyloid peptides (Aβ) in the form of oligomers, fibrils and plaques deposited in the brain parenchyma and mostly accompanied by inflammation due to neuronal and synaptic damage [14, 15]. There are two frequently observed forms of amyloid plaques and these are classified into diffused, and dense-core plaques [9]. Diffused plaques are composed of amorphous amyloid with irregular morphology and are commonly found in the normal ageing brain with no pathological association with cognitive impairment or synaptic loss [16]. Dense-core plaques however, are composed of dense fibrillar Aβ sheets at the core with random filaments projecting, and have a pathological association with neuronal degeneration and cognitive impairment [16, 17]. Soluble or monomeric form of Aβ peptides may also be present at elevated levels in the brain and cerebrospinal fluid [18]. In addition, accumulation of Aβ deposits have been observed within small to medium-sized cerebral blood vessel walls, especially areas of cortical and leptomeningeal arteries and capillaries [19, 20]. This contributes to cerebrovascular impairment and the development of cerebral amyloid angiopathy (CAA) [21]. These characteristic lesions are key diagnostic features and central to AD pathology [22]

(summarised in Figure 1.1). They are usually accompanied by chronic inflammation and oxidative stress leading to blood hypoperfusion and cerebrovascular lesions that damage the integrity of the blood brain barrier (BBB) [23-25]. The manifestation of these pathological conditions eventually leads to neurovascular dysfunction, neuronecrosis, cognitive decline, and ultimately death [26].

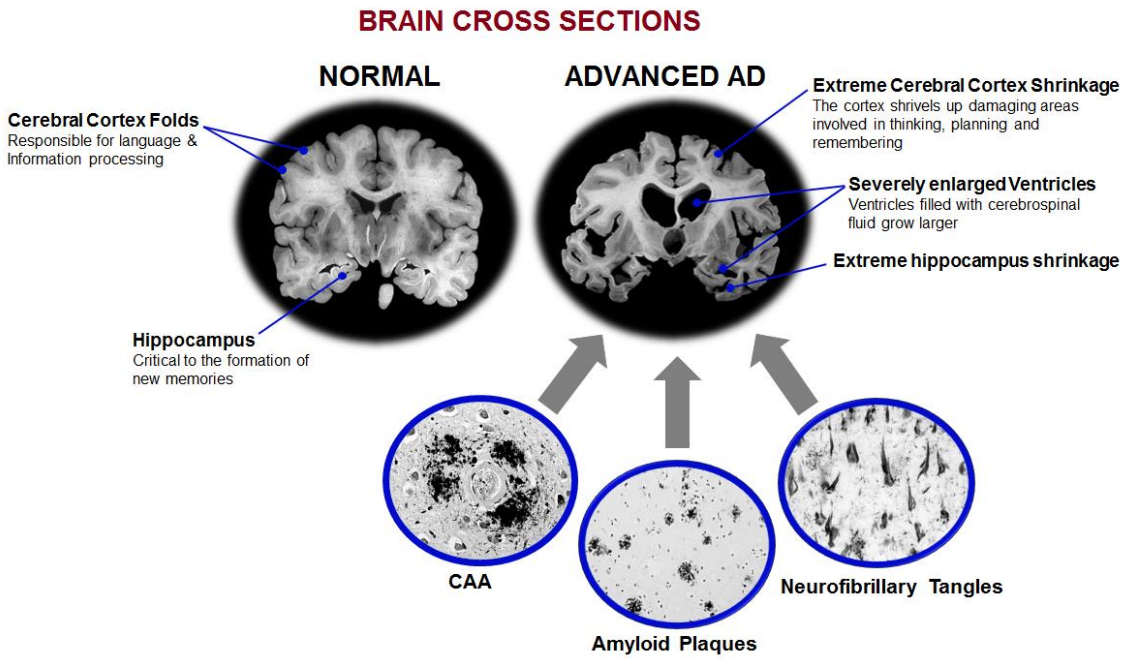

Figure 1.1: Cross-sectional comparison between normal brain and atrophied brain in advanced AD. (Original figure but the images are modified [7, 27-29]).

1.2.2. Amyloid Precursor Protein

The misfolded proteins, Aβ peptides, that are present in AD are derived from the metabolism of a transmembrane protein called amyloid precursor protein (APP) [30]. APP is considered to be a molecule with diverse functionality, expressed ubiquitously in cells throughout the body with 3 main isoforms identified in humans, namely, APP695, APP751 and APP770, generated by alternative splicing of its mRNA transcript [30, 31]. APP isoform ratios differ depending on the tissue types [31]. For example, APP695, is mainly expressed by neuronal cells and lacks the Kunitz-type serine inhibitory domain (KPI), while, KPI is present in the extracellular domain of isoforms APP751 and APP770 that are mainly expressed by platelets and peripheral cells [32, 33]. Processing of APP follows two alternative pathways, non-amyloidogenic and amyloidogenic.

In the non-amyloidogenic pathway, the sequential cleavage of APP by membrane-bound proteases, namely α- and γ-secretases, generates a large soluble extracellular APPα fragment (sAPPα), via ectodomain shedding, and a membrane-tethered intracellular C-terminal

fragment (C83) that is further cleaved by γ-secretase to generate P3 and APP intracellular domain (AICD) fragments [14, 34, 35] In the amyloidogenic pathway, β-, instead of α-secretase, together with γ-secretase, cleaves APP producing sAPPβ and C-terminal fragment (C99) that is also subjected to further γ-secretase proteolysis causing the liberation of Aβ peptides. Due to the fact that final γ-secretase proteolysis is not single-site specific, a variety of Aβ peptide species can be generated ranging from 37 up to 43 amino acids in length, with Aβ1-40 and Aβ1-42 being the most common species produced [14, 34, 35].

Under normal physiological conditions, the ratio of Aβ1-42 to Aβ1-40 in the brain is ~1:9, but in AD this ratio is altered and favours Aβ1-42 to Aβ1-40 [36].The hydrophobic and fibrillogenic nature of the longer Aβ peptides mean that they have a higher tendency to aggregate, especially Aβ1-42, which is the most commonly produced species in the brain [37, 38]. This can result in the transformation and misfolding from soluble monomeric species to more toxic oligomeric, protofibrils and then fibrils, which constitutes the majority of amyloid senile plaques observed in AD brains [38, 39]. Figure 1.2 summarises APP metabolism and the physiological and pathological roles of its by-products.

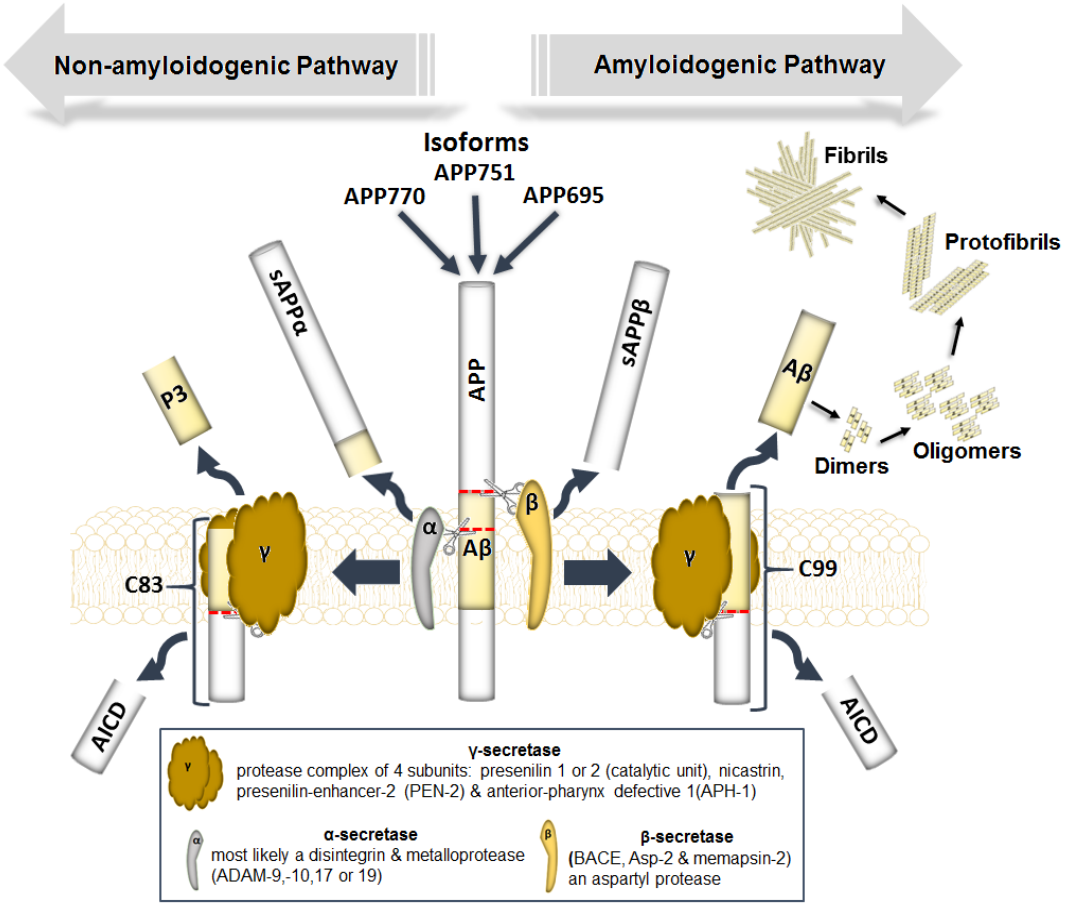

Figure 1.2: Summary of APP proteolytic processing in the amyloidogenic and non-amyloidogenic pathways, and putative physiological and pathological roles of APP and its generated fragments.
(Created from [30, 34, 40-44])

The aberrant build-up of aggregated Aβ fragments is a consequence of the imbalance between the rate of its production and clearance mechanisms [45].

1.2.3. Aβ peptide Production and Clearance

Physiological metabolism and homeostatic balance between Aβ production and clearance are maintained via several pathways throughout the body. In the central nervous system (CNS), Aβ is produced (predominantly Aβ1-42) by various brain cells, such as, astrocytes, oligodendrocytes, microglia, and neurons [46, 47]. Aβ is also produced (predominantly Aβ1-

40) by peripheral cells, such as, endothelial cells, platelets, fibroblasts, skeletal myocytes and osteoblasts [47, 48].

In the brain, several mechanisms are utilized for Aβ clearance and they involve receptor-mediated efflux (via lipoprotein receptor-related protein 1 or 2 (LRP1/2) and ATP dependent efflux transporter P-glycoprotein (P-gp)) of free Aβ and Aβ-bound to chaperone molecules (i.e. apolipoprotein E (ApoE) (APOE ε2 and ε3), ApoJ (Clusterin) and α-2-macroglobulin) into blood circulation across the blood brain barrier (BBB) [48, 49]. Aβ can also be cleared through transportation across the blood-cerebrospinal fluid barrier (BCSFB), by cerebrospinal fluid (CSF) absorption, and interstitial fluid (ISF) bulk flow drainage into the circulatory and lymphatic systems [50].

Extracellular soluble and oligomeric Aβ can be subject to degradation by proteolytic enzymes (e.g. neprilysin (a major amyloid-degrading enzyme that plays an important role neuropeptide signalling termination and brain function, but its activity decreases with age)[51-53], insulin-degrading enzyme (IDE; degrades both insulin and Aβ peptides and its activity is also decreased with age) [53, 54], endothelin converting enzyme 1 and 2 (ECE-1 and ECE-2; plays regulatory role of Aβ levels in the brain) [53, 55], angiotensin-converting enzyme (ACE; known to play a central role in renin-angiotensin system (RAS) for blood pressure, sodium, and body fluid maintenance) [56], plasmin, tissue plasminogen activator (tPA), and matrix metalloproteinases) [53, 57, 58]. Moreover, neuronal and glial cells can take up soluble Aβ via phagocytosis, endocytosis, and micropinocytosis and subject it to intracellular proteasomal and lysosomal degradation [59]. There are peripheral endogenous antibodies against Aβ and chaperone/bindable substances that are able to enter and exit the brain at low levels and have the ability to prevent Aβ aggregation and resolve Aβ fibrils [60].

Aβ present in the periphery is systemically cleared via peripheral cells, tissues or organs. This includes Aβ uptake and degradation via phagocytosis or endocytosis by immune cells (i.e. monocytes, macrophages, and neutrophils); Aβ clearance by blood-mediated proteins and cells (e.g. erythrocytes, albumin, and lipoproteins such as apolipoprotein E); or excretion from the body via the kidney or liver [48, 61-63]. A summary of Aβ production and clearance is presented in Figure 1.3.

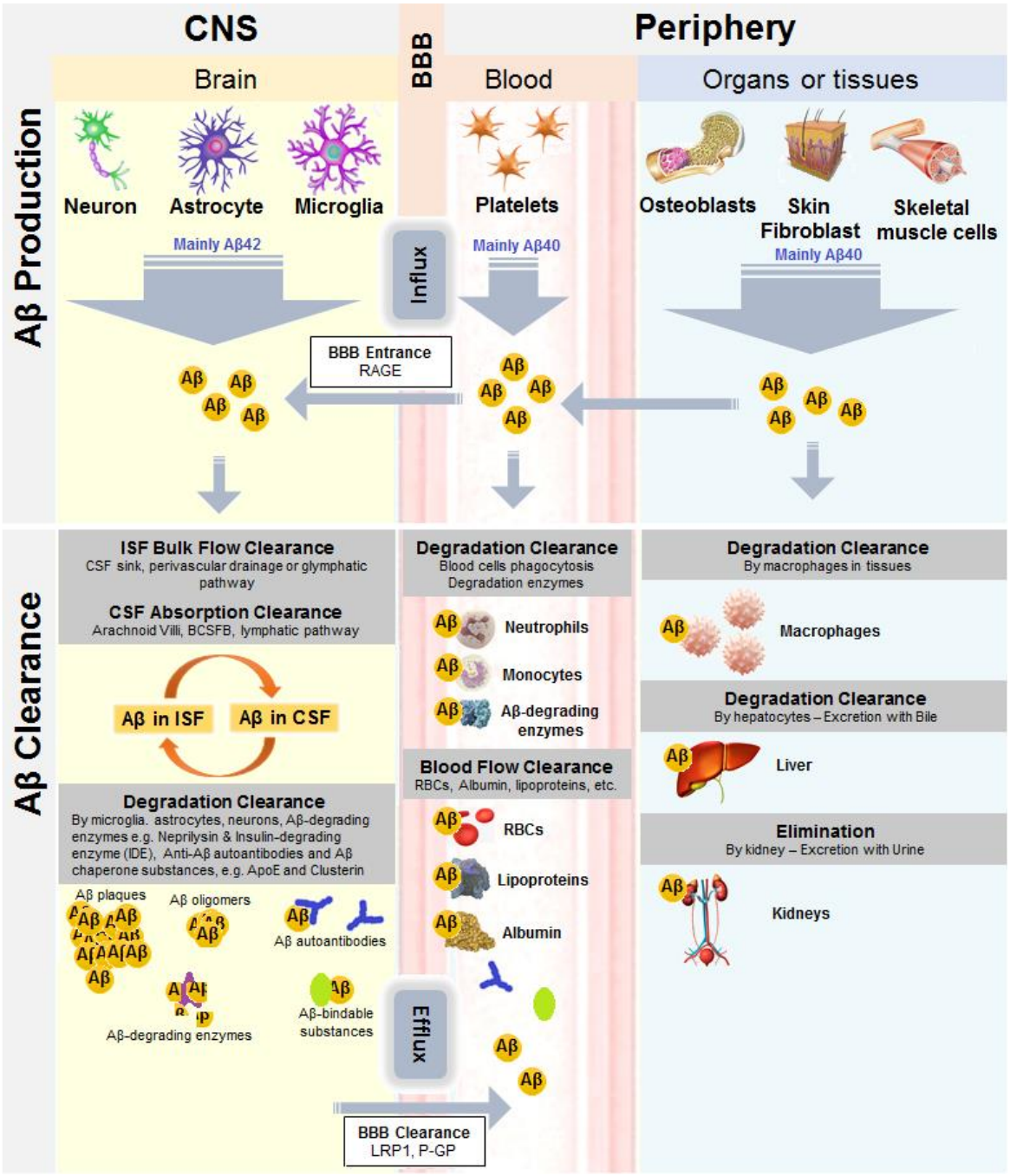

Figure 1.3: Normal physiological maintenance of the homeostatic balance between Aβ production and clearance in the brain and the periphery.
Aβ is produced by a variety of neuronal and glial cells in the brain and also by peripheral cells throughout the body such as skeletal muscle cells (myocytes), platelets, osteoblasts (bone cells) and skin fibroblast. Aβ is mainly transported across the blood brain barrier (BBB) by receptor-mediated influx (RAGE- receptor for advanced glycation end products) and efflux by lipoprotein receptor-related proteins (LRP) and ATP dependant efflux transporter P- glycoprotein (P-GP) on endothelial cells. In the central nervous system (CNS), Aβ is subjected to various clearance mechanisms which include intracellular phagocytic degradation by neurovascular unit cells or extracellular proteolytic enzymatic degradation. Aβ is also released following interstitial fluid (ISF) bulk flow or cerebrospinal fluid (CSF) drainage pathways. Aβ clearance can also occur by preventing its aggregation and resolving fibrils through the entrance of peripheral anti-Aβ autoantibodies and chaperone/bindable substances into the brain at low levels. Anti-Aβ autoantibodies bound to Aβ that is present in the periphery can also act as a peripheral sink to promote the Aβ efflux from the brain. In the periphery, some Aβ can be phagocytosed by blood cells, degraded by proteolytic enzymes, and some may bind to carriers that are transported to peripheral cells or organs for degradation and excretion from the body. Created and modified from [48, 62]. RBCs: red blood cells; ApoE: apolipoprotein E.

1.2.4. Amyloid and Vascular Hypotheses of AD Onset and Development

There are many theories that describe AD pathogenesis that are evidenced or still postulated. Several preliminary genetic studies found a number of familial mutations associated with the gene (APP) and also in the genes encoding γ-secretase catalytic subunits presenilin-1 or 2 (PSEN1/2). These mutations can lead to pathological overproduction of Aβ, which can ultimately result in its accumulation and oligomerisation and eventually lead to early onset of Alzheimer's disease (EOAD, age<65 years) [64, 65]. The formation and presence of cerebral amyloid plaques has been considered the primary pathological hub that leads to AD development as a consequence of their neurotoxic effects [64]. Therefore, the notion of "amyloid cascade hypothesis" was put forward as the main cause of AD, where aberrant Aβ deposition serves as the initial trigger to subsequent formation of NFTs, neurodegeneration, and dementia [41, 64].

However, this hypothesis accounts as a main cause for only 5% of gene-mutations related to EOAD, but does not account for the rest 95% of sporadic or late onset AD (LOAD, age>65 years) cases [66]. In the late onset form of AD, the underlying causality remains unknown due to its multifactorial nature. The increased risk of this form of AD has been associated with several genetic and non-genetic or environmental risk factors that most likely results in the failure of Aβ clearance mechanisms and not necessarily its overproduction [45, 67]. Genetic risk factors involved in LOAD include: certain TREM2 variants that expresses partial functional loss of TREM2 protein (a receptor aid in the uptake and clearance of Aβ by microglia cells) [68, 69]. In addition, individuals carrying ε4 allele of the apolipoprotein E gene (APOE) are at a greater risk of developing LOAD [70]. APOE gene exists as 3 polymorphic alleles (ε2. ε3, and ε4) and apolipoprotein E (ApoE) protein is a cholesterol transport protein that regulates lipid homeostasis by mediating its transport from one cell type to another [71]. ApoE is primarily synthesized by astrocytes and microglia in CNS, while in the peripheral tissues is mainly produced by the liver and macrophages [71, 72].

Aside from lipid transport, ApoE protein shown to play an important role in Aβ metabolism, where it facilitates Aβ uptake through cell surface receptors, e.g. LRP1 and LDLR (low density lipoprotein receptor), in an isoform-dependent fashion (E2>E3>E4) and influences the transport of Aβ within the CNS and also the formation of parenchymal amyloid plaques, especially with carriers of ApoE4, as it shown to be less effective in promoting enzyme-mediated degradation of Aβ and direct Aβ clearance due to its lower binding affinity compared to ApoE3 and ApoE2 [71, 73, 74]. In addition, ApoE-ε4 genotype expression is found to be much higher in AD patients than age-matched control and thus contributing towards

increasing the risk of AD by initiating and accelerating Aβ accumulation, aggregation and deposition in the brain. Other risk factors that may contribute towards the development of LOAD includes, ageing, hypercholesterolemia, obesity, type 2 diabetes, hypertension, and traumatic brain injury [75-80].

Epidemiological studies and post-mortem pathological examination have highlighted the substantial overlap between vascular risk factors and cerebrovascular dysfunction and AD [65]. These studies revealed significant shared pathophysiological correlations of AD with vascular diseases such as, hypertension, atherosclerosis, CAA, atrial fibrillation, macro/micro-infarcts, and strokes (ischemic and haemorrhagic) [81-84]. Numerous morphological and functional cerebrovasculature abnormalities were observed showing compromised BBB including altered endothelium processes, basement membrane thickening, and disruption due to collagen IV, laminin, proteoglycan deposition, intimal atrophy and decreased cerebrovascular density [30, 85].

Experimental and neuroimaging observational studies on humans and AD animal models have proposed that cerebrovascular dysfunction precedes the development of cognitive decline and AD pathology, [30, 86, 87] placing forward the idea of vascular dysfunction or "vascular hypothesis" as a potential cause of AD pathology [30, 88]. The vascular hypothesis proposes that advanced ageing, cardiovascular and cerebrovascular risk factors, such as arterial stiffness, atherosclerosis, hypertension, dyslipidaemia, diabetes type 2, smoking, obesity, and CAA, can lead to chronic cerebral hypoperfusion and diminished oxygen delivery and blood flow to the tissues and brain [30, 88]. This can result in the accumulation of Aβ and other blood-derived neurotoxic molecules, BBB breakdown, abnormal microvascular remodelling, and eventually the development of ischemic lesions and microhemorrhages causing neuronal injury, neurodegeneration, and cognitive deficits [30, 88, 89].

It has been reported that early vascular dysfunction of BBB affects neurovascular unit cells (i.e. endothelium, pericytes, vascular smooth muscle cells, neurons, and glial cells (astrocytes, microglia, and oligodendroglia) [90]. Pericytes regulate pivotal neurovascular functions necessary for neuronal homeostasis, such as, blood flow regulation in capillaries and toxic cellular by-products clearance, vascular stability and structure, and BBB formation and maintenance [91]. Recent studies highlighted the link between pericyte loss and/or malfunction (even in the absence of Aβ) and sufficient vascular-medicated and AD-like neurodegeneration [90-94]. Normally, pericytes facilitate Aβ clearance and degradation via their LRP-1 receptor. However, reduction of the number of pericytes and increased Aβ

accumulation in the brain can lead to increased uptake and cellular saturation of Aβ resulting in its degradation, thus contributing to further loss of perivascular cells [85, 95]. Pericyte loss and/or degeneration were observed in both the hippocampus and the cortex in human AD subjects and that is associated with key attributes of AD vascular pathology [93, 96].

Interestingly, many enzymatic proteins involved in Aβ-degradation and clearance also have vasomodulatory and cardiovascular roles that have been shown to be altered in AD subjects thus further compromising the vasculature. One of these proteins is neprilysin (NEP), cleaves numerous cardiovascular vasoactive peptides, and has vasodilatory or vasoconstrictive effects, but its expression found to be reduced in AD brains [55, 97-99]. ECE is also known to hydrolyse big endothelin (ET) molecules into smaller vasoactive molecules that act as potent vasoconstrictors, in addition to other biologically active peptides, such as bradykinin, which contributes significantly to the physiological maintenance of human vascular tone [100, 101]. The two ECE isoforms (ECE-1 and ECE-2) have similar biological activity but few studies have shown elevated expression of ECE-2 that was also influenced by Aβ [102], while no significant difference on ECE-1 expression was documented in AD subjects [103]. However, overexpression of ECE-1 was shown to have a protective effects against AD [104, 105]. Abnormalities in the expression of ECE and accumulation of Aβ can result in the reduction of blood flow in local microvasculature and the potential development of CAA, but how significant the contribution of ECE expression abnormalities towards AD progression, is yet to be clarified.

Other important Aβ-degrading enzymes are angiotensin converting enzymes (ACEs) that also play a key regulatory role in the renin-angiotensin system (RAS), which is an important hormonal system that maintains fluid homeostasis, and blood pressure regulation [106]. Renin present in plasma cleaves inactive angiotensinogen released by the liver into angiotensin I (Ang-I) which is then converted into a potent vasoconstrictor, angiotensin II (Ang-II), via the activity of ACEs. Ang-II acts on its receptors AT1R and AT2R throughout the body, thus exerting its hypertensive effects [106-108]. Under pathological conditions, RAS plays a critical role in the pathogenesis of hypertension, and can contribute towards associated cardiovascular diseases (CVDs) at variable severity, atherosclerotic lesions that compromise blood vessel integrity, and eventually the development of late onset AD and CAA (the sequence of these events is also referred to as the angiotensin hypothesis for AD) [107, 109-112]. Several components of RAS have been found to be altered in AD subjects including an increased perivascular ACE-1 activity with direct correlation to parenchymal Aβ load [113], and decreased activity of its homologue ACE-2 (the counter-regulatory enzyme that

degrades Ang-II to angiotensin and provides other additional vaso-protective effects) which is correlated inversely to ACE-1 activity and Aβ levels [114, 115]. Taking together the studies mentioned previously, a great number of pathogenic pathways relevant to cerebrovascular alteration and dysfunction are suggested as primary triggers and risk factors for neuronal dysfunction, which further supports and favours the vascular hypothesis as the initial trigger of late onset AD.

1.3. CEREBRAL AMYLOID ANGIOPATHY AND ALZHEIMER'S DISEASE

The presence of cerebral amyloid angiopathy (CAA) and atherosclerosis are considered the most prominent vascular lesions found in AD, with 80-100% of cases exhibiting CAA [116, 117]. Around 25% of AD patients have severe forms of CAA, while the majority have a moderate form, and it is also present in 30% of normal aging individuals >60 years of age [118]. In both sporadic and familial AD, the type of CAA associated with it occurs in sporadic form itself, while the hereditary form of CAA are generally rare and has an early onset with severe clinical manifestation [119]. The term CAA is given to describe the progressive deposition of Aβ peptides containing all Aβ forms but with higher ratio of Aβ1-40 to Aβ1-42 compared to the ones in senile plaques. Aβ peptides deposition occurs within neocortical and leptomeningeal small to medium sized arteries, especially areas of the vessel surrounding smooth cells, adventitia and the luminal side of tunica media [120-122]. Based on the presence or absence of Aβ in the capillaries, CAA was classified into 2 types: CAA-type 1 and CAA-type 2. In CAA-type 1, Aβ deposits in arteries and cortical capillaries and it is strongly associated with ApoE ε4 allele, but it is not associated with CAA-type 2 where Aβ deposits in bigger blood vessels and lacks the involvement of capillaries [123, 124].

1.3.1. Clinical Manifestation of CAA

Histological neurovascular alteration and deposition of amyloid peptides was initially described by Gustav Oppenheim in 1909 from autopsies of AD and demented brains [125]. Oppenheim found similarities between deposited substances found within degenerating blood vessel walls and substances found adjacent to necrotic brain parenchyma, and since his original finding, significant evidence has emerged to support his observations [125, 126]. There are 3 CAA severity levels that can be distinguished they include: mild CAA (Aβ mainly deposits in the outer basement membrane of the blood vessel wall), moderate CAA

(Aβ deposits in the outer basement membrane and between smooth muscle cells (SMCs), and severe CAA (extensive Aβ infiltration and focal fragmentations of the vessel wall and replacement of the other surrounding layers of the blood vessel) [123, 127, 128]. In severe CAA, loss of SMCs is apparent in tunica media with detachment and delamination of its outer layer causing a "double barrel" appearance, intimal alteration, fibrinoid necrosis and micro-aneurysm formation, perivascular leakage, microbleeds and inflammation (vasculitis) [128-132] (see Figure 1.4 for illustration). Ultimately this leads to vascular cerebrovascular degeneration, impaired blood flow and hypoperfusion, which further exacerbate the damage and contributes to the progression of cognitive decline [129, 133]. Clinical manifestations of CAA are associated with ischemic and intracerebral haemorrhages, cerebral infarcts, transient ischemic attacks, dementia, subarachnoid haemorrhage, and seizures [134, 135].

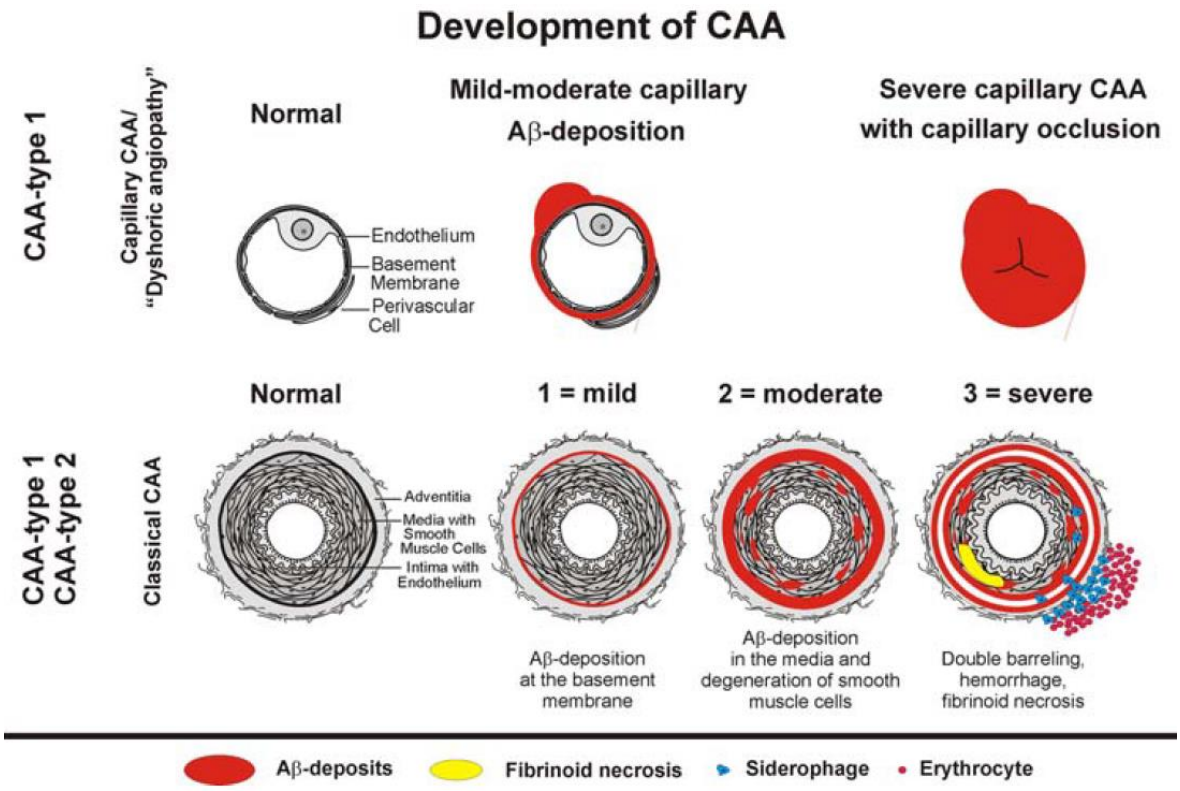

Figure 1.4: Types and development of CAA [123].

1.3.2. Sources and Mechanisms of Aβ Deposition in CAA

The sources and underlying mechanisms of the Aβ vascular deposits that lead to CAA are not well understood. There are three key hypotheses proposed with regards to the origins of Aβ observed in CAA: the vascular, systemic, and drainage hypotheses [136].

The vascular hypothesis suggests that Aβ found in CAA is derived from vascular wall constituents, i.e. endothelial cells, smooth muscle cells (SMCs), pericytes, adventitia, etc., as they have been shown to express APP and produce Aβ [137-139]. Several experimental studies have shown that overexpression of APP and overproduction of Aβ take place in cultured SMCs and human cerebral perivascular cells that were degenerating [120, 140, 141]. However, contrary observations on how larger arteries are less affected in severity to CAA than arterioles or capillaries despite the large number of vascular cells and layers, might indicate that Aβ produced by the vessel walls might not be the sole origin of Aβ in CAA [142].

The systemic hypothesis puts forward the notion that Aβ in CAA is primarily of haematogenous origin and it originates in the circulation from various APP-expressing cells throughout the body and enters the cerebral vessel walls and brain via a receptor for advanced glycation end-products (RAGE) [119, 136, 143]. A counterargument to this proposed hypothesis was raised when studies on transgenic mice inducing constitutive overproduction of human APP C-terminal fragment (C99) in multiple tissues showed significantly elevated plasma Aβ levels (approximately 17 times higher when compared to human Aβ plasma levels) [144]. However, no Aβ deposits occurring in cerebrovasculature were found in these mice up to age 29 months with the exception of some transgenic mice of one founder line, where Aβ deposits in the intestine were observed [144].

In the drainage hypothesis, it has been suggested that neuronal and glial cells are the source of vascular Aβ and this occurs due to failure of Aβ clearance from the brain along the perivascular lymphatic drainage pathway. Normally when Aβ is produced in the brain, it is cleared by its release from brain cells into the brain parenchyma extracellular space, and then into the capillary basement membrane from where it is drained and carried away by interstitial fluid (ISF) to arterial basement membranes. Aβ is then joined with other locally originated vascular wall Aβ and together they are carried away and out of the brain along the periarterial pathway via arterial pulsation [45, 142, 145, 146].

Soluble Aβ movement and clearance is reduced along the vessel wall usually with aging and also under vascular damage or onset of arteriosclerosis, which affects vascular tonality causing rigidity and decrease in arterial pulsation amplitude [147]. Consequently, soluble Aβ precipitation and the formation of insoluble amyloid β-sheet aggregates occurs, which impedes further Aβ elimination resulting in CAA [148]. This Aβ blockage also affects the clearance of brain solutes, metabolites and fluids causing disruption to brain homeostasis [45, 60, 149]. As a result, not only is Aβ metabolism affected in the brain, but it also invites a host

of other complications along with it including chronic inflammation, oxidative stress, blood hypoperfusion and pathological thrombus formation [150]. This further contributes to cerebrovascular damage, aberrant Aβ accumulation in the brain and blood vessels, and ultimately impairment in neuronal function [150]. Platelet activation has a fundamental role in thrombus formation and increasing evidence suggests their potential role in mediating the onset and development of CAA [151-153], since they also contain APP and have been shown to contribute >90% of Aβ in circulation [154-157].

1.4. PLATELETS AND ALZHEIMER'S DISEASE

1.4.1. Platelet Overview

Platelets are small enucleated discoid-shaped fragments released during megakaryocyte maturation processes and range in size from 2-4 μm in diameter [158, 159]. They are normally present at a physiological count of 2 to 3 x 10^8 / ml in human blood with a life span of about 10 days, whereupon they are transported to the spleen and removed from the circulation by neutrophils and macrophages [159]. Platelets are well known for their regulatory role in blood haemostasis and thrombosis, and their primary physiological aim is to prevent blood loss when blood vessels are injured by forming a platelet plug or clot at the site to seal the wound [160]. Platelets show versatility in their function in both health and disease due to their substantial content of receptors and secretory molecules, and they have been shown to act as a central hub mediating immunity, tissue repair, inflammation, cancer metastasis, angiogenesis, and thrombosis [161-167].

1.4.2. Platelet Morphology

Structurally, platelets consist of a standard biological phospholipid bilayer plasma membrane embedding an asymmetrical distribution of a wide range of constituents which include: neural membrane phospholipids, e.g. phosphatidylcholine and sphingomyelin (SPH); polar phospholipids e.g. phosphatidylinositol (PI), phosphatidylethanolamine (PE), and phosphatidylserine (PS); esterified cholesterol; integral transmembrane proteins; and a carbohydrate-enriched surface membrane coating, called glycocalyx, consisting of glycoproteins, proteoglycans, glycolipids, glycosaminoglycans, and oligosaccharides [168]. Upon platelet activation, the platelet surface membrane provides a pro-coagulation platform by rearranging its membrane composition and exposing its negatively charged phospholipids [168, 169]. In AD, there is an increased internal membrane fluidity[170], an altered ratio of cholesterol to phospholipid [170], and altered APP fragments[171].

The platelet surface plasma membrane also possesses a unique membrane system where the membrane invaginate inwards forming a cavity or canal, referred to as surface-connected open canalicular system (OCS). This provides an additional membrane reservoir that can be utilized for platelet shape change and spreading post-activation, and also as a bidirectional exchange area of substances between the platelet and plasma [172]. A remnant of the megakaryocyte rough endoplasmic reticulum called the dense tubular system (DTS), presenting intracellularly and aligned closely to OCS, provides the main storage sites for free calcium ions (Ca^{2+}), and enzymes involved in platelet activation, such as, phospholipase A2 (PLA2), thromboxane synthetase (TBXAS), and cyclooxygenase (COX) [168, 173].

The convex morphology of platelets is maintained by the circumferential microtubule system and the micro- and intermediate filament (actin filaments) network. Actin is a highly conserved protein present in a dynamic equilibrium inside the cell between the globular (G-actin) and polymeric filamentous form (F-actin), which can reversibly disassemble into G-actin subunits. The dynamics of both forms of actin are regulated by actin-binding proteins [168, 174] .

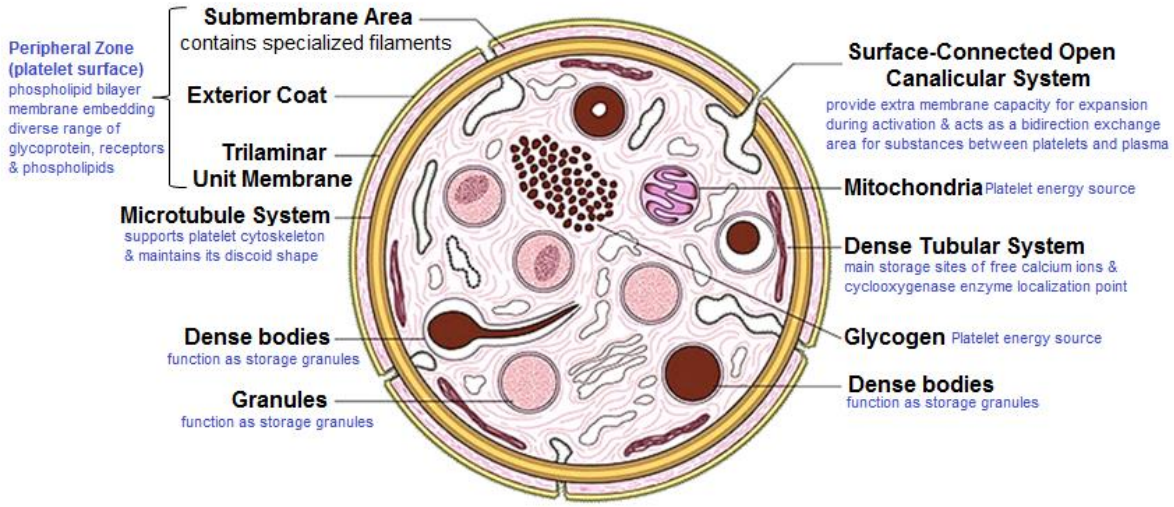

Figure 1.5: Summary of discoid platelet structural features seen from an equatorial plane view.
(modified from [173])

Platelet cytoskeleton reorganisation occurs upon platelet activation, where an increase in intracellular calcium (Ca^{2+}) induces the polymerisation of G-actin into F-actin in the intracellular submembrane area and the rapid formation of newly bundled actin filaments pushes the plasma membrane to form filopodia causing shape change [175]. Platelets contain different important cytosolic organelles aside from their cytoskeletal components, and they include specific secretory vesicles (α-granules, dense granules), lysosomes, peroxisomes,

glycosomes, free cytoplasmic glycogen, and a few randomly dispersed mitochondria[174]. A summary of platelet structure is shown in Figure 1.4.

Activated platelet secrete more than 300 active substances from their intracellular granules. Dense granules or dense bodies usually contain small pro-aggregation molecules, such as, Ca^{2+}, ADP, serotonin and ATP. On the other hand, platelet α-granules carry a cargo of diverse soluble proteins and membrane receptors categorized into adhesive proteins (e.g. P-selectin, fibrinogen, αIIbβ3, von Willebrand factor), mitogenic and angiogenic factors (e.g. platelet derived growth factor (PDGF), vascular endothelial growth factor (VEGF), transforming growth factor β (TGFβ)), cytokine-like proteins (e.g. β-thromboglobulin, PF4), coagulation factors (e.g. plasminogen, factor V, factor XI), chemokines and immune mediators (e.g. RANTES, CXCL1, complement C4, IgG), as well as an interestingly high content of APP and Aβ peptides [161, 176].

1.4.3. Platelet Role in Haemostasis and Thrombosis

Haemostasis is an intricate physiological process that occurs to prevent blood loss or haemorrhage from damaged blood vessels by sealing the injury with a localized clot while maintaining blood fluidity within the circulatory system [177]. This highly complex process provides a regulated interactive balance between blood vessels, platelets, plasma coagulation factors, and fibrinolytic proteins involved in blood clot formation or dissolution [177, 178] . Thrombosis on the other hand, is the pathological formation and development of blood clots within the blood vessels, both in arteries and veins, which can obstruct blood flow, impede blood vessel function, and lead to serious medical consequences [167, 177]. Under normal physiological conditions, the vascular system is under haemostatic balance, where procoagulant, anticoagulant, and fibrinolytic components are in equilibrium [179]. If the procoagulants are too active, this may lead to spontaneous thrombus generation causing, for example, deep vein thrombosis (DVT) and pulmonary emboli when present in veins, or myocardial infarction (heart attack) and strokes when present in the arteries [179, 180]. If the anti-coagulant or fibrinolytic proteins are too active, then bleeding problems will occur [177, 180]. Response to vascular injury occurs in two main phases called, primary haemostasis and secondary haemostasis [178].

Primary Haemostasis

Vasoconstriction is the earliest and most short-lived response to a vascular injury and can be initiated from various sources [181]. These include nerve endings around the injured site, where it is called neurogenic reflex vasoconstriction (NRF), myogenic constriction (MC) from injured smooth muscles [182], or endothelin release from injured endothelial cells that then acts on smooth muscles and contracts them [182, 183]. This event occurs instantaneously and is most relevant to minor injuries of small vessels to reduce blood loss and increase local shear forces [181]. Vascular injury also causes direct exposure of blood components to the sub-endothelial extracellular matrix (ECM) of blood vessels, which contains several adhesive proteins, such as collagen fibres, laminins, von Willebrand factor (VWF), fibronectin, and tissue factor (TF) [184]. These proteins serve as ligands that play a key role in the activation of specific platelet membrane receptors and their immediate adhesion to the injury site [185].

Platelets and Blood Flow

The localisation and adhesion of circulating platelets towards vascular injury sites is generally determined by local hemorheological and hemodynamic factors, such as blood density, velocity, shear rate, and vessel wall shear stress [186, 187]. Within the cardiovascular system, the normal fluidic motion of the blood in the vessels is in a laminar flow moving with a parabolic profile, where concentric layers of blood move in parallel along the length of the blood vessel with blood nearest the vessel wall having the lowest velocity (V=0), due to high blood-vessel wall friction [188, 189] .As the blood layers slide past one another moving forward and away from the vessel wall towards the centre of the lumen, they progressively increase in velocity to reach the highest value (V_{max}) at the centreline [188]. Blood velocity can be described as the rate of linear displacement of the blood within the circulatory system and it is inversely proportional to the cross-sectional area of the vessel through which the blood is passing. The high velocity at the centre generates shear forces between adjacent blood layers that progressively becomes maximal towards the vessel walls [188, 189]. Shear rate is defined as the velocity nearest to the vascular wall divided by blood flow distance from the wall, while wall shear stress is the force exerted on the vessel wall by the near-wall fluid [187]. The shear stress is dependent on blood viscosity (blood density) and wall shear rate [187, 188].

Constriction or obstruction of the blood vessel causes narrowing of the lumen, which can be imposed by stenotic, atherosclerotic, or thrombotic lesions. As the streamline blood flow passes, the layer of the blood is disturbed and the parabolic arrangement is disrupted

resulting in turbulent blood flow, where blood is now moving radially and axially with different streams having different velocities. In these conditions, higher physiological shear rates and shear stresses occur, as the relationship is inversely proportional to the cross sectional diameter of the vessel [187, 188]. These principles are outlined simply in Figure 1.5 below.

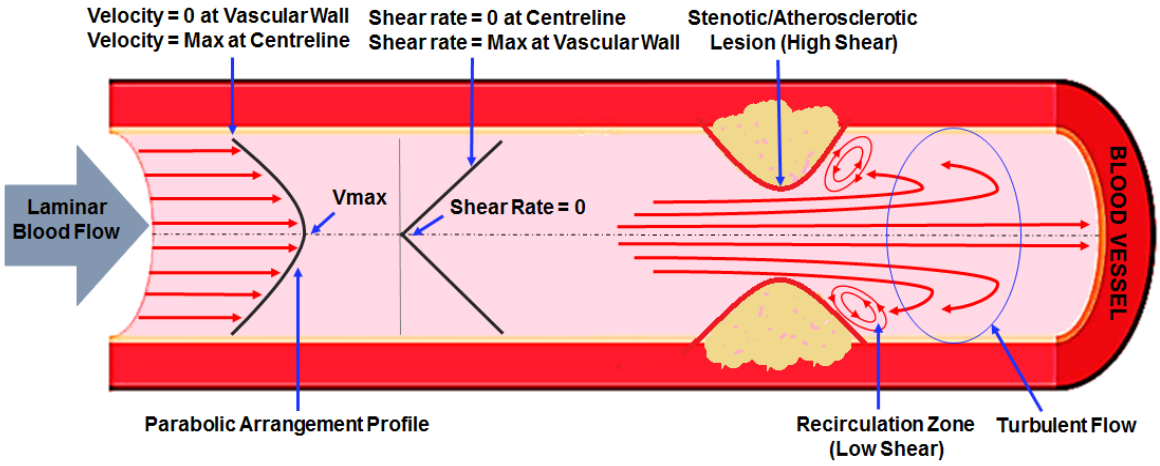

Figure 1.6: Summary of parabolic velocity profile and blood flow properties under physiological and pathological conditions.
Blood flows through the blood vessel in a laminar fashion with a parabolic profile. This results in minimum shear rate and maximum velocity at the centre of blood streamline, progressively changing to maximum shear rate and minimum velocity when it reaches the vessel wall. Blood flow profile changes to become turbulent, generating radial and axial streams that have different velocities, when there is an obstruction within the vessel lumen, such as, stenotic or atherosclerotic lesions. (Original figure modified from [187-189]).

In normal physiological blood flow conditions, vascular wall shear rates range from low values in venous systems, generally between 20-200 s^{-1} (per second), to higher wall values in arterial systems ranging between 300-1600 s^{-1}. However, under pathological flow conditions, such as in case of stenotic or atherosclerotic arteries, vascular wall shear rate can reach up to 40,000 s^{-1} [187, 188, 190]. In AD, the cerebrovasculature is compromised and is shown to have diminished blood flow, resulting in brain hypoperfusion and contributing further to the progression and pathogenesis of AD [191, 192].

Within the circulatory system, red blood cells (RBCs or erythrocytes) dominate the cellular constituents of the blood, comprising 40% of total cell mass. Due to their physical deformation and rotation within the blood stream, they create erratic motion and migrate laterally toward the central axis of the stream causing local stirring of the flow [187, 189, 193]. This mechanism expels and diffuses circulating platelets and white blood cells (leukocytes) away from the blood central streamline in the lumen towards the periphery allowing it to occupy regions near the vessel wall [187, 193]. Consequently, this arrangement allows platelets

to be regulated in close vicinity by healthy endothelial cells and also allows them to perform their physiological role in case of endothelial damage [193].

Mechanisms of Platelet Adhesion, Activation, and Signalling

As the platelets travel throughout the body, they exist in an inactivated state. However, upon encountering exposed ECM, platelets can become activated by binding directly or indirectly to several ECM proteins, as they possess multiple cell-surface adhesion receptors or by exposure to agonists present in the vicinity of exposed ECM [184]. This process can occur at both low and high shear flow conditions, but the mechanism by which platelets adhere to receptor sites is distinct in the two cases [186, 194]. Under low shear rate conditions, such as in veins and large arteries, platelets are able to adhere directly to exposed collagen, fibronectin, and laminin, and become activated forming a monolayer of cells (thrombi) to cover the injury site which contains relatively more trapped RBCs and a fibrin network [195, 196]. On the other hand, under high shear rate conditions, such as in small arteries and stenotic vessels, platelets are unable to bind directly to the injury site, thus their adhesion is predominately facilitated by the interaction of the GPIB-V-IX receptor complex with VWF present in the exposed ECM [195, 197]. Since higher concentrations of platelets are marginalized towards the vessel wall under these conditions, thrombus growth increases rapidly resulting in platelet-rich thrombi “white thrombi” containing less fibrin and are deprived of trapped RBCs [195, 196]. Primary platelet adhesion occurs when circulating VWF binds to exposed collagen at the vascular injury site [195, 196].

Collagen

Collagen is a potent highly thrombogenic platelet activator and the most abundant protein found in the body (abound 30% of total protein mass) [198]. Collagen is considered a main component of ECM and is usually present in a fibrillar form. Collagen is a triple-stranded helical molecule consisting of 3 polypeptide chains twisted together into a helix [199]. The structural orientation is stabilized by electrostatic interactions and hydrogen bonds formed among its characteristic repeating three amino acid motif of proline, hydroxyproline, and glycine [199]. The triple helix strands can assemble into bigger molecular complexes like fibrils, but that depends upon the type of collagen present. Humans carry more than 25 forms of collagen with types I, II, III, IV, V, VI, VIII, XII, XIII and XIV found in the vascular wall

[198, 200, 201]. The most abundant fibrillar collagen types found in the superficial luminal layer of the vascular wall (accounting for 80-90% of total collagen in blood vessels), are type I and type III, while in the deeper layer (subendothelial basement membrane) collagen type IV is found [199, 201, 202]. Platelets express three main receptors that facilitate the interaction with exposed collagen, either indirectly, via its GPIB-V-IX receptor complex that binds to VWF on collagen or directly via integrin α2β1 and immune receptor homologue glycoprotein VI (GPVI) receptors. VWF can adhere to collagen types I, II and VI firmly facilitating GPIB-V-IX interaction, while GPVI and α2β1 binding affinity varies depending on the different regions of exposed collagen fibrils [201, 203]. In general, collagen is a powerful inducer of platelet activation and supports their adhesion and aggregation.

Von Willebrand Factor (VWF) and GPIB-V-IX

VWF is a glycoprotein present in circulating blood that exists as a heterogeneous mixture of multimers varying in size and linked by disulphide bridges [204]. Smaller multimers are constitutively secreted into the plasma by endothelial cells and megakaryocytes, while larger multimers are stored within endothelial cells in organelles known as Weibel-Palade bodies, and in platelets in α-granules [204]. Larger VWF multimers have higher adhesive efficacy and activity than the smaller ones, and thrombogenic effects are maintained and regulated by a proteolytic enzyme called ADAMTS13 (a disintegrin and metalloproteinase with a thrombospondin type 1 motif, member 13) [204]. This enzyme cleaves large VWF multimers into smaller sizes in the blood circulation hence maintaining normal haemostasis. Reduction in the activity of this enzyme can lead to a life-threatening condition called thrombotic thrombocytopenic purpura (TTP), where a patient develops microscopic blood clots throughout their body [205, 206].

VWF amino acid sequence analysis shows distinct repetitive domains identified as Domains A, B, C, and D, which are arranged in the following sequence: D1-D2-D'-D3-A1-A2-A3-D4-B1-B2-B3-C1-C2-CK, with several specific domains serving as binding sites [205]. Domain A1 is a binding site for glycoprotein Ibα (GPIbα or CD42), which is a component of platelet receptor complex GPIB-IX-V, while Domain D'-D3 binds heparin, coagulation factor VIII and possibly P-selectin. Domain A2 serves as a cleavage site for ADAMTS13, with Domain C1 providing a binding site for integrin αIIbβ3 via its peptide motif Arg-Gly-Asp (RGD) sequence, and Domain A3 binding to fibrillar collagen type I and III [205].

The vascular injury site creates local turbulence in the blood flow and brings inactivated platelets close enough to it so that the GPIB-V-IX platelet receptor complex binds to immobilized VWF on collagen [207]. This triggers platelet downstream intercellular stimulation of tyrosine kinases, such as focal adhesion kinase (FAK), and protein tyrosine kinase 2 (Pyk2), and spleen tyrosine kinase (Syk) activation, which is mediated through clustering and phosphorylation of GPIB-V-IX associated with the Fc receptor γ-chain (FcR γ-chain) and the low-affinity receptor for IgG [205, 208-210]. The activation of these tyrosine kinases among other intracellular proteins, such as 14-3-3 proteins (commonly isoform 14-3-3 zeta (ζ)), results in the activation of phospholipase C γ2 (PLCγ2), cytosolic phospholipase A2 (cPLA2), and phosphoinositide 3-kinase (PI3K). Several intracellular messenger molecules are produced, e.g. diacylglycerol (DAG) and inositol 1,4,5-triphosphate (IP3), eliciting multiple signal transduction pathways [205, 208-210].

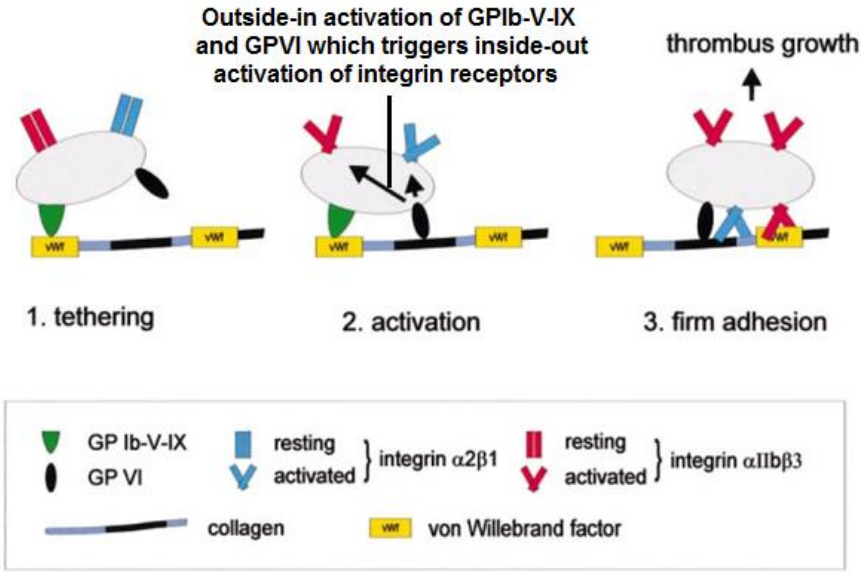

Figure 1.7: Simplified diagram for the process of platelet initial tethering, rolling and firm adhesion and to collagen through VWF and the three main adhesion receptors as shown. (Modified figure from [211])

Ultimately, these signalling pathways cause a transient increase in intracellular calcium ions (Ca^{2+}), inside-out activation of integrin $\alpha_{IIb}\beta3$ (which promotes platelets aggregation), and activation of cytoskeletal and actin-binding proteins, such as filamin, F-actin, talin, and α-actinin [212]. This mediates the attachment of the GPIB-V-IX receptor complex to the cytoskeleton leading to cytoskeleton rearrangement and shape change that includes the extension of filopodia [212, 213]. The rapid initial interaction of VWF with GPIB-V-IX receptor complex is considered reversible [212, 213]. The hydrodynamic drag forces of blood flow causes captured platelets to tether, roll, and translocate along vascular injury site [214]. This process slows down the platelets and allows the engagement of two other main important

adhesion receptors that bind directly to exposed collagen, namely integrin $\alpha_2\beta_1$ (GPIa/IIa) and immune receptor homologue glycoprotein VI (GPVI). This results in irreversible firm cell adhesion [211-213], as shown in Figure 1.7 which simply demonstrates this process of platelet adhesion.

Integrin $\alpha_2\beta_1$ (GPIa/IIa)

Integrin $\alpha_2\beta_1$ is a class-I transmembrane glycoprotein that exists as non-covalently bound heterodimeric complexes of α and β-subunits. Both of these subunits consist of a large N-terminal extracellular domain, a single hydrophobic membrane-spanning region, and a short C-terminal cytoplasmic tail [215]. The extracellular domain of the α_2 subunit harbours a segment containing 191 amino acids called I (inserted)-domain, which serves as a ligand-binding site with the aid of divalent metal ions (e.g. Mg^{2+} and Mn^{2+}), and is considered essential for platelet-collagen binding [215]. The extracellular domain of the β_1 subunit also contains the I-like domain and is thought to regulate α_2 I-domain binding affinity. The β_1 subunit is one of three types of integrins present in platelets, and the others are β_2 and β_3. There are three members that belong to the β_1 family, that are: $\alpha_2\beta_1$ (binds to collagen), $\alpha_6\beta_1$ (binds to laminin), and $\alpha_5\beta_1$ (binds to fibronectin) [216]. $\alpha_L\beta_2$ is the only known member of the β_2 family, and is known as the intracellular adhesion molecule 2 (ICAM-2) that facilitates platelet-leukocyte interaction [217]. Platelets contain two important members of the β_3 family, which are $\alpha_V\beta_3$ and $\alpha_{IIb}\beta_3$ [216, 217]. The $\alpha_V\beta_3$ receptor mediates platelet adhesion by binding to vitronectin, fibrinogen, VWF, prothrombin and thrombospondin, while integrin $\alpha_{IIb}\beta_3$ promotes platelet aggregation by binding to fibrinogen, VWF, fibrin, fibronectin, vitronectin, and thrombospondin [217].

Integrin $\alpha_2\beta_1$ adhesion to collagen has been shown to play a supportive role to strengthen firm adhesion rather than an essential one [218]. The GPVI receptor is considered central to mediating platelet adhesion and activation on collagen and it has been shown to upregulate integrin $\alpha_2\beta_1$ activity via the inside-out activation, through the GPVI–FcRγ chain complex and activation of PLCγ2 [216, 219]. This causes a conformational change of the integrin from the closed bent state of α and β subunits to an open active form, where detachment of transmembrane and cytoplasmic domains of both subunits occur. Activated integrin $\alpha_2\beta_1$ allows FAK binding to its cytoplasmic domain resulting in its phosphorylation, which in turns activates PI3K converting phosphatidylinositol 4,5-bisphosphate (PIP2) to phosphatidylinositol 3,4,5-trisphosphate (PIP3). This then phosphorylates and activates the downstream effector protein kinase B, ultimately resulting in platelet activation. Activated

$\alpha_2\beta_1$ can also activate PLCγ2 generating a second signalling pathway thus amplifying platelet activation [216] [211].

Glycoprotein VI (GPVI)

GPVI is a paired class-I transmembrane glycoprotein that belongs to the immunoglobulin superfamily. It contains two immunoglobulin-like domains and a mucin-like Ser/Thr-rich region which are extracellular, a transmembrane region (with a positively charged arginine residue), and a short intracellular cytoplasmic tail [215, 220]. GPVI is associated with one Fc receptor-γ (FcRγ) chain homodimer via forming a salt bridges between the arginine residue within the GPVI transmembrane region and an aspartic acid residue in the transmembrane region of the FcRγ-chain. The FcRγ-chain contains an immunoreceptor tyrosine-based activation motif (ITAM) that is important in relaying signal transduction [215, 221]. The GPVI/FcRγ-chain complex exhibits high affinity towards collagen and upon binding to it, crosslinking within the receptor complex occurs, inducing GPVI clustering and phosphorylation of ITAM tyrosine residues in the FcRγ cytoplasmic domain by Src-family kinases (SFKs), mainly Lyn and Fyn. Subsequently, this leads to engagement and activation of Syk, via its two Src-homology 2 domains (SH2), initiating a downstream phosphorylation cascade of several adaptor proteins including: transmembrane linker for activation of T cells (LAT), lymphocyte cytosolic protein 2 (SLP-76), Vav, Bruton's tyrosine kinase (Btk) and Tec kinases (Itk). This causes the activation of phosphoinositide 3-kinase (PI3K) and phospholipase C γ2 (PLCγ2) [215, 222].

PLCγ2 cleaves phosphatidylinositol 4,5-bisphosphate in the plasma membrane to generate diacylglycerol (DAG) and inositol 1,4,5-triphosphate (IP3) causing Ca^{2+} mobilisation from intracellular stores and resulting in an increase in cytosolic Ca^{2+} levels and activation of protein kinase C (PKC) [222]. These molecules are key signalling elements that result in platelet response, leading to secretion of the content of granules, arachidonic acid mobilization and thromboxane A2 release (activating platelets in an autocrine and paracrine fashion by binding to its G protein coupled receptor GPCR), exposure of receptors on the platelet surface (e.g. $\alpha_{IIb}\beta3$ expression), membrane phospholipid scrambling, cytoskeletal rearrangement, and coagulation initiation [215, 223]. Figure 1.7 illustrates the main platelet receptors and corresponding agonists involved in activation and downstream signalling.

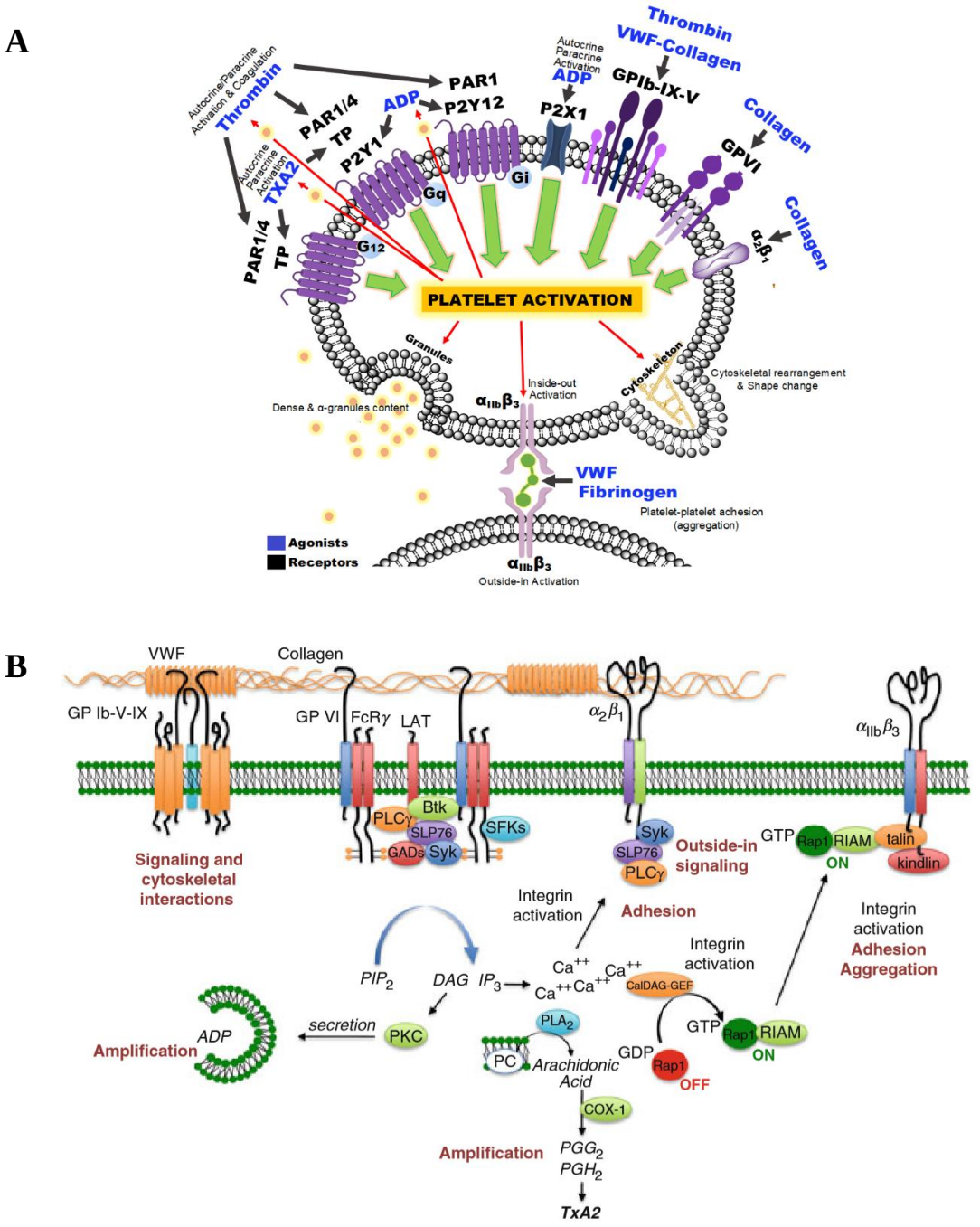

Figure 1.8: Main platelet receptors and their signalling mechanisms involved in initial adhesion and activation to collagen.

(A) Main receptors: both integrins and G-coupled protein receptor (GPCR) with their ligands and the consequence of their activation. (B) Main adhesion receptors signalling involved in platelet adhesion to collagen and the subsequent activation of aggregation receptor $\alpha_{IIb}\beta_3$ (image in A is original, but B is from [224])

Cytoskeleton Rearrangement

In this phase of platelet activation, rearrangement of the internal cytoskeleton occurs transforming platelets from a discoid shape to highly irregular morphologies with multiple filopodial extensions in different directions [175, 225]. This provides an increase in platelet surface area and gives them the ability to physically interlock with and adhere to neighbouring platelets. Resting platelets contain a pool of G-actin monomers that bind to

profilin, forming a G-actin-profilin complex, and F-actin polymers that are capped by capping proteins, such as gelsolin [175, 225]. When platelets are activated, an increase in intracellular Ca^{2+} induces dissociation of actin-profilin complexes freeing actin monomers that then become available for F-actin growth. Ca^{2+} also activates free cytosolic gelsolin to sever longer F-actin filaments and cap them resulting in shorter F-actin chains [224-226].

Signal-mediated PIP2 inactivates F-actin- bound gelsolin and F-actin becomes uncapped causing rapid filament growth. F-actin filaments are then bundled together with some phosphorylated myosin light chain (MLC) and crosslinked by actin bundling proteins, such as, α-actinin. Formation of filopodia, which are finger-like projections, occurs by rapid growth of actin filaments that push the membrane forward. Branching of growing actin filaments is induced by activated PKC that phosphorylates the WAS family of proteins, which in turns activates the ARP2/3 complex that acts as the nucleation and branching point from which new actin filaments can growth and push the plasma membrane forward to form filopodia [227, 228]. Lamellipodia, which are thin-sheet-like structures, are formed when the growing actin filaments start to fill the gaps between projecting filopodia, resulting in a complex network of actin filaments and the observed spreading morphology [224, 226, 227].

Secretion of Granule Contents

The secretion of the platelet granule contents provides concentrated and local delivery of key molecular substances at the injury site that amplify platelet activation, mediate adhesion, promote migration and activation of other cells, and initiate aggregation and thrombus formation [176]. Upon platelet activation, granule centralization occurs concurrently with cytoskeletal rearrangement, which appears to play a role in the movements of granules. The secretion of granule contents to the extracellular domain is mediated by intracellular vesicle fusion with the surface-connected open canalicular system (OCS) in the process of exocytosis. The membrane lipid bilayers of both platelets and granule vesicles contain two lipid components, PIP2 and phosphatidic acid (PA) that serve as protein attachment and signalling sites for membrane fusion [176, 229].

Normally in the unstimulated state, the opposing lipid bilayer membrane can be in close vicinity to one another without fusing. This is due to repulsive electrostatic and hydration forces in between the two membranes that require a certain energy to overcome them. Fusion of opposing membranes can occur with the aid of a distinct family of proteins known as SNARE contained within the lipid bilayers. These membrane-associated proteins are orientated in such a way that most of them are cytosolic. The term SNARE, stands for SNAp

REceptor, where SNAP referred to as Soluble NSF (N-ethylmaleimide-sensitive fusion protein) Attachment Protein [176, 228, 230].

Platelets that contain SNARE proteins are termed vesicle-associated membrane proteins, VAMP 3 and 8, which are concentrated on the membranes of granules membrane, while SNAP-23, and syntaxin 2 (necessary for dense granule release) and syntaxin 4 (necessary for α-granule release) are located in the platelet membrane. Chaperone proteins, such as NFS, Sec1 protein (PSP), Rab proteins and their effectors, are able to bind to and direct the function of SNARE proteins. SNARE proteins present in the platelet membrane are referred to as target or t-SNAREs, and those on the vesicles as v-SNAREs. PSP is associated with regulating the docking of vesicles onto t-SNAREs by binding to syntaxin and blocking its binding to SNAP-23 in t-SNARE, which is itself important for interacting with v-SNAREs. Upon cellular activation, activated PKC can directly phosphorylate certain SNARE proteins and their chaperones, including PSP. Phosphorylation of PSP causes conformational changes and thus the release of Syntaxin [176, 228, 230].

The chaperone molecule Rab may interact with PSP through its effector molecules and play a role in docking the opposing membranes, however, its precise role in exocytosis remains unclear. The N-terminal ends of both t-SNARE and v-SNAREs become closely associated with their respective coiled-coil domains and form a 4-helix bundle ternary complex termed the exocytotic core complex. This complex is capable of overcoming the energy barrier normally present between opposing membranes and results in membrane fusion and the release of granule contents. The process of exocytosis and storage granule release serves to amplify platelet activation at the injury site and recruitment of inactivated platelets in the circulation towards it [176, 228-230].

The bioactive molecules released from alpha and dense granules act in an autocrine and paracrine fashion, thus initiating a positive feedback cascade and promoting rapid platelet aggregation and primary platelet plug formation. Some of the most potent soluble platelet agonists released are adenosine diphosphate (ADP), platelet-derived thromboxane A_2 (TxA_2), and thrombin, which act synergistically to induce full platelet activation and more surface expression of membrane-bound and soluble proteins, e.g. integrin $\alpha_{IIb}\beta_3$, GPVI, platelet endothelial cell adhesion molecule (PECAM), and P-selectin, CD63, fibrinogen, more VWF. The release of adhesion proteins such as fibrinogen and VWF contributes to platelet-platelet adhesion mainly via integrin $\alpha_{IIb}\beta_3$ and contributes to thrombus growth [176, 229]. Table 1.1 summarises the major constituents and bioactive molecules present in platelet granules.

Table 2 | Main bioactive molecules and receptor proteins for platelet granules [231]

GRANULES	MEMBRANE	CONTENTS
Dense	GTP binding proteins Ral1 Glycoproteins GPIb, GPIIbIIIa Granulophysin LIMP1/CD63 LAMP2 Src P-selectin (CD62)	Adenine nucleotide ATP ADP Serotonin (5-HT) Calcium magnesium Pyrophosphate Guanine nucleotides GTP, GDP Histamine
Alpha	GTP binding proteins rab4, GMP33, Rap1 Receptors & antigens P-selectin (CD62) GPIIbIIIa GPIb-XI GPIV (CD36) p24 (CD9) PECAM (CD31) GLUT-3 Vitronectin receptor Osteonectin P-selectin (CD62)	Proteoglycans Platelet specific βTG, PF4. βTG Ag molecules PBP CTAP-III NAP-2 Adhesive glycoproteins Fibronectin Vitronectin VWF Thrombospondin Haemostasis factors & cofactors Fibrinogen, Factors V, VIII, XI, XIII, Kiningens protein S Plasminogen cellular mitogens PDGF TGFβ ECGF EGE VEGF IGF Interleukin β Protease inhibitors α2-macroglobulin α2-antitrypsin PDCI α2-antiplasmin PAI1 TFPI PN-2/APP C1 inhibitor Miscellaneous Immunoglobulins IgG IgA IgM, Albumin, GPIa/multimerin
Lysosomal	LIMP1/CD63 LAMP1, LAMP2	Acid proteases Cathepsins (D, E) Carboxypeptidases (A,B) prolinecarboxypeptidase Collagenase Acid phosphatase Glycohydrolases Heparinase, β-N-acetyl-glucosaminidase α-D-glucosidase α-D-fucosidase

ADP and its Receptors

Adenosine diphosphate (ADP) is an important physiological agonist released from dense platelet granules and damaged endothelial cells. ADP binds and activates three purinergic receptors, P2Y1, P2Y12 and P2X1. P2X1 is a ligand-gated ion channel that mediates early transmembrane calcium flux from the extracellular medium, thus causing a transient increase in intracellular calcium and causing platelets to change shape, however it does not lead to aggregation on its own. Both P2Y1 and P2Y12 are G-coupled protein receptors (GPCRs) and their co-activation is required for ADP-induced platelet aggregation [232].

GPCRs are large tertiary structured membrane protein receptors possessing seven transmembrane helices with three intra- and extracellular loops (which can act as multiple interaction sites), an extracellular N-terminal tail (ligand binding domain), and an intracellular C-terminus (effector domain). The intracellular C-terminus domain is bound to a group of heterotrimeric peptides (α, β, and γ) subunits, called G-coupled proteins, coupled with the energy unit guanosine diphosphate (GDP) or guanosine triphosphate (GTP). The α-subunit has three domains, where two domains are for β and γ subunits, while the third is for GDP or GTP. When G-coupled proteins are inactive, the α-subunit is at a low energy level (bound to GDP), but when activation occurs, the α-subunit loses its GDP and acquires GTP resulting in its detachment from the β and γ subunits (β/γ complex). The released β/γ complex also play a role and can activate downstream effectors [224, 232, 233].

There are four main families of G-proteins that can elicit different signalling pathways termed as, G_i, G_q, G_s, and $G_{12/13}$. The P2Y12 receptor is coupled with G_i while P2Y1 is coupled with G_q. Signalling through P2Y1/G_q mediates the activation of PLC, PIP2, IP3, DAG, calcium, and the PKC signalling pathway, resulting in platelet activation. ADP activation of P2Y12/G_i however, follows a different signalling pathway, and this involves the inhibition of the enzyme adenylyl cyclase (AC), cyclic adenosine monophosphate (cAMP), and cAMP-dependent protein kinase A (PKA), which is generally involved in the inhibition of platelet function [224, 232, 233]. P2Y12/G_i downstream signalling also involves activation of PI3K, Rap1, Akt, and potassium channels leading to platelet activation, aggregation and signal amplification for other agonists. ADP is secreted locally from activated dense platelet granules and acts in an autocrine and paracrine fashion, where it can bind to the same secretory platelets or activate inactivated platelets in its immediate vicinity [224].

Thromboxane A_2 (TxA_2) and its Receptor

Thromboxane A2 (TXA2) is an unstable and short-lived molecule that is diffused from activated platelets, and acts as a potent vasoconstrictor and platelet activator working in an autocrine and paracrine fashion. TXA2 is an example of an eicosanoid, which are an important and diverse group of 20 carbon, polyunsaturated fatty acids that act as signalling molecules. Other examples include prostacyclin (PGI2, which inhibits platelet activation) and prostaglandins. TXA2 is synthesised from arachidonic acid (AA) released from membrane phospholipids by phospholipase A2 (PLA_2) in a multistep process. The cyclooxygenase enzyme, COX1, is involved in converting AA to prostaglandin G2 (PGG2), then into prostaglandin H2 (PGH2), which is then finally converted into TXA2 by thromboxane synthase. The TXA2 receptor (TP) belongs to the GPCR family, and is coupled with G_q which upon binding to TXA2 signals through PLC, PIP2, IP3, DAG, calcium, PKC, PLA_2 (generating more TXA2), with inside-out integrin $\alpha_{IIb}\beta_3$ activation causing platelet activation and aggregation. The generation of more TXA2 creates an amplified platelet activation loop resulting in more platelet activation and aggregation present in its proximity. Activation of signalling by collagen-adhered platelets is powerfully enhanced by the combined effects of TXA2 and ADP [224, 234, 235].

Integrin $\alpha_{IIb}\beta_3$ (GPIIb-IIIa)

Integrin $\alpha_{IIb}\beta_3$ is the most abundantly expressed surface receptor in platelets and is critical in mediating platelet aggregation. This receptor plays an important role in mediating platelet activation and aggregation upon Aβ stimulation, which will be further elaborated on in Chapter 3 and 5, including how it might contribute towards the progression of AD. The structure of $\alpha_{IIb}\beta_3$ is similar to the previously described collagen adhesion receptor, $\alpha_2\beta_1$. Integrin $\alpha_{IIb}\beta_3$ is also a class-I transmembrane glycoprotein that exists in non-covalently bound heterodimeric complexes of α and β subunits. Both of these subunits consist of a large glycosylated N-terminal extracellular domain, a single hydrophobic membrane- spanning region, and a short C-terminal cytoplasmic tail [216, 224, 236-239]. The α_{IIb} subunit consists of 2 chains, a so-called heavy and light chain. The heavy extracellular chain contains 7 homologous repeating segments of around 50 amino acids and it folds into a β-propeller-like structure that offers four cation-binding sites. This heavy extracellular unit that is part of α_{IIb} chain is joined by disulphide bridges to a short light chain consisting of 21 amino acids that occupies the transmembrane region and the cytoplasmic tail, where the C-terminus

contains high-affinity cation binding sites on it. The extracellular domain of the β_3 subunit features a long disulphide loop that folds at the mid-region into a I-domain-like structure with 5-6 α-helices and β-strands containing metal ion-binding motifs, and a middle section composed of cysteine-rich tandom repeats, while the cytoplasmic tail of the β_3 subunit contains tyrosine and threonine phosphorylation sites. The heterodimer subunits are maintained together non-covalently and this is calcium ion dependent. Cations are required to facilitate the binding of ligands, mainly fibrinogen, to $\alpha_{IIb}\beta_3$ in the extracellular region [216, 224, 236-239].

Fibrinogen (Factor I) is a coagulation factor primarily secreted by the liver and is normally present within the blood circulation. Fibrinogen exists as a homodimer with each of the monomers composed of 3 polypeptide chains of Aα, Bβ, and γ that are linked parallel to each other by disulphide bridges [240]. Both monomers form a hexameric complex with the N-terminus of each monomer's polypeptide chains arranged facing each other and forming a central E-domain that extends outwards in a coiled-coil arrangement prior to the C-terminus forming two peripheral globular D-domains. At the D-domain, the end of the 3 polypeptide chains are referred to as αC, βC, and γC. Both βC and γC form the globular region, while αC, being the longest, extends out of the globular region. At the D-domain, a stretch of amino acids are present in γC (KQAGDV) and in αC (RGD) that act as recognition and binding sites for the $\alpha_{IIb}\beta_3$ receptor [240, 241]. Figure 1.8 below further demonstrates the structure of fibrinogen.

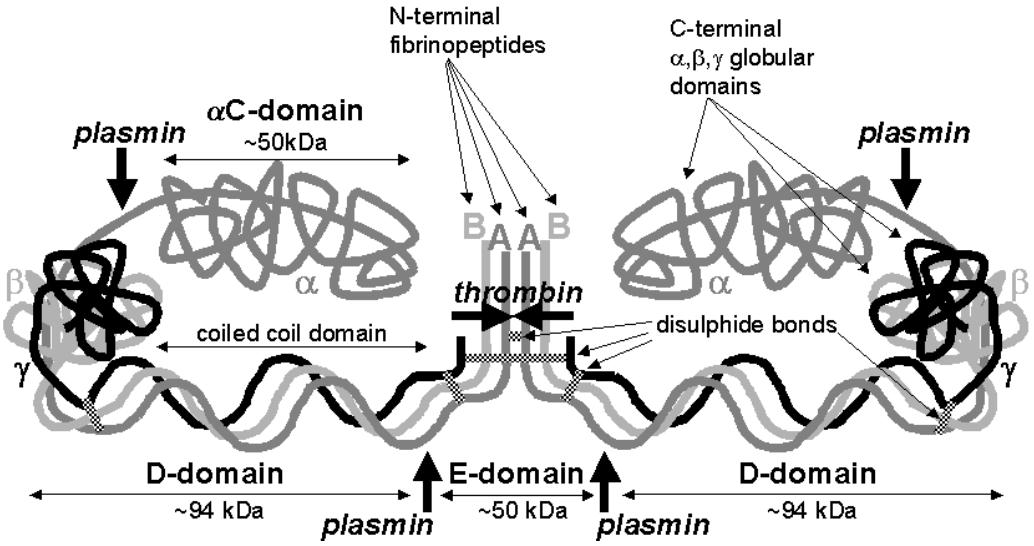

Figure 1.9: Fibrinogen molecular structure. [240]

The fibrinogen E-domain contains thrombin cleavage sites within it on the Aα and Bβ chains. Removal of the N-terminal regions of these chains via proteolytic cleavage by thrombin results in an active E-domain that then binds to the D-domains of other fibrinogen molecules, eventually forming the fibrin network that is required for clot stabilization. Fibrinogen can also be negatively regulated through the binding of plasmin, (a proteolytic enzyme produced from circulating plasminogen by the action of tissue plasminogen activator (tPA) present on ECs), to its specific plasmin cleavage site in the coiled-coil region between E and D-domains, thus limiting fibrin network formation [240, 241].

Despite the presence of a high fibrinogen concentration in the blood, $\alpha_{IIb}\beta_3$ does not interact with it due to its tightly regulated affinity state. Integrin $\alpha_{IIb}\beta_3$ in circulating inactive platelets primarily exists at a low-affinity state preventing its binding to its ligands. Upon activation, $\alpha_{IIb}\beta_3$ transitions from a low- to high-affinity state causing a conformational change within the receptor that thereby allows it to become competent for its ligand binding [241-244]. The importance of integrin $\alpha_{IIb}\beta_3$ activation is due to its bidirectional signalling properties where its activation can occur in an "inside-out" and "outside-in" manner, causing significant platelet activation. The process by which ligands, such as fibrinogen, VWF, fibronectin, and vitronectin, bind to integrin $\alpha_{IIb}\beta_3$ and trigger its activation is termed as "outside-in" signalling, while activation of platelets by other external agonists, such as ADP, TXA2, collagen, and thrombin that results in the activation of $\alpha_{IIb}\beta_3$ via internal signalling pathways is referred to as "inside-out" signalling [241-244].

Platelet activation by agonists, such as ADP, thrombin, TXA2 and collagen, elicits diverse signalling pathways that converge into a common pathway that promotes downstream signalling and a phosphorylation cascade involving PLC, PI3K, Akt, PKC, DAG, Ca^{2+}, and the small GTPase Rap1. Activated Rap1 promotes the recruitment of the cytoplasmic proteins Talin-1 and Kindlin-3 to the β3 subunit cytoplasmic tail of integrin $\alpha_{IIb}\beta_3$ and triggers a conformational change from low to high affinity in an "inside-out" manner. This process now favours the binding of $\alpha_{IIb}\beta_3$ to its ligands and promotes platelet aggregation [243, 245].

Following the inside-out signalling, binding of fibrinogen or VWF to activated $\alpha_{IIb}\beta_3$ triggers another activation signalling pathway (in an outside-in signalling manner) influencing actin dynamics, cytoskeletal reorganization, and initiating platelet morphological changes that support bridging and aggregation between two activated platelets [246]. In a high affinity configuration, the non-receptor tyrosine kinase c-Src becomes associated to an RGT motif of β3 cytoplasmic c-terminal tail via its Src homology 3 (SH3) domain. Outside-in signalling

mediates surface integrin clustering into hetero-oligomers and brings activated c-Src proteins into close proximity, clustering them and thus allowing trans-autophosphorylation. Activated c-Src then supports Syk activation and recruitment to the β_3 tail or to phosphorylated ITAM of the FcRγ-chain [239, 244-246]. Subsequently, this facilitates the assembly and activation of the SLP76/LAT/Btk/Vav complex and initiates a downstream activation signalling cascade involving PLCγ2/ PI3K/ Akt/ DAG/ Ca^{2+}/ α-actinin, and ultimately cytoskeletal reorganisation, granule secretion, spreading, stable adhesion, and clot retraction. It is noteworthy that despite the extensive progress in the platelet field, the exact cellular mechanisms involved in integrin $\alpha_{IIb}\beta_3$ outside-in and inside-out signalling have not yet been fully identified [239, 244, 245].

Thrombin and its Receptors

Thrombin (activated factor II (IIa)) is a potent serine protease agonist for platelet activation and plays a central role in haemostasis and thrombosis. The coagulation cascade is a series of enzymatic conversions of proenzymes (also called zymogens) to activated enzymes (coagulation factors) that culminate in thrombin formation [247]. This results in amplification of platelet activation and ends with the formation of fibrin strands, by the action of thrombin on the newly formed platelet plug. Thrombin is involved in activating several coagulation factors, e.g. factor V, VIII, and XI, and also in stabilizing the new clot and cross linking the fibrin polymer via activating factor XIII. Thrombin possesses two positively charged binding sites, namely Exosite 1 for fibrinogen cleavage and Exosite 2 for heparin and platelet PAR receptors. It also has a catalytic site for coagulation factors [247, 248].

Thrombin activates human platelets mainly through specific protease-activated receptors (PAR1 and PAR4), which are GPCRs (coupled to G_q) [249]. Thrombin binds the extracellular N-terminus of PAR1/4 and cleaves it, causing the newly exposed portion of the receptor to bind to itself and induce a conformational change and receptor activation. Downstream signalling through PAR1/4/G_q mediates the activation of PLC, PIP2, IP3, DAG, calcium, and PKC signalling pathways, resulting in shape change, release of active substances from granules, more thrombin, intra- and extracellularly, exposure of receptors on the surface, and membrane phospholipid scrambling and coagulation initiation [250]. The following Figure 9 shows an overview of the different GPCR intracellular signalling processes upon stimulation with ADP, TXA2 and thrombin [248, 251, 252].

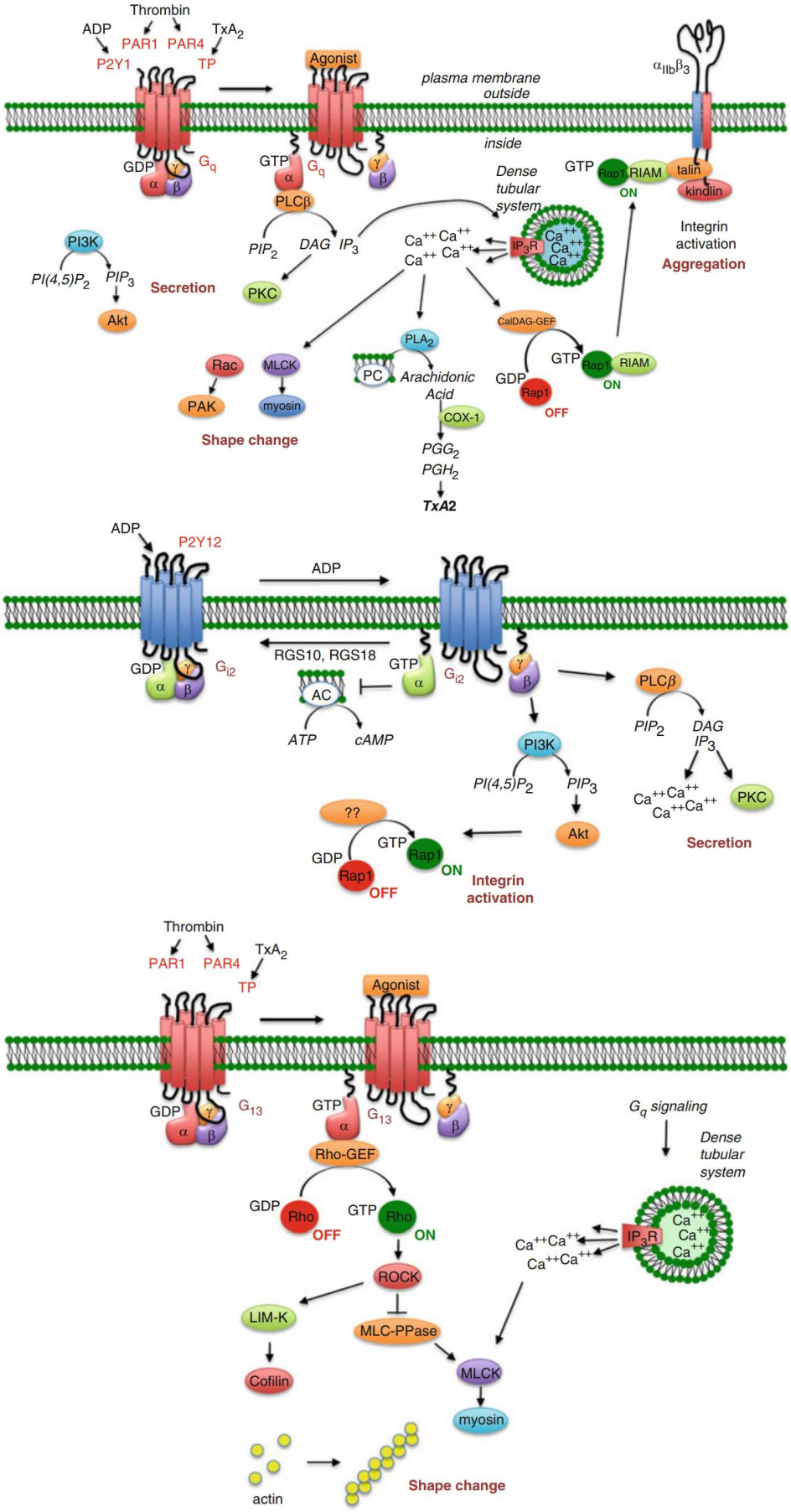

Figure 1.10: Platelet signalling downstream for different GPCRs upon stimulation with its soluble agonists ADP, thrombin, and thromboxane A2. [224]

Secondary Haemostasis

Primary haemostasis entails multifaceted interactions between injured vascular endothelial cells, adhesive proteins, and platelets that ultimately result in platelet adhesion, activation, aggregation, and the formation of a primary platelet plug post-vascular injury [178]. Secondary haemostasis involves a coagulation cascade and the formation of a fibrin mesh (clot) that entraps the loose primary platelet plug resulting in its stabilisation. This process can be initiated spontaneously along with primary haemostasis [178]. The liver produces most of the procoagulants and anticoagulants, with the exception of factor III, IV and VIII, and the former are present in the blood circulation in inactive forms [253]. The majority of coagulation proteins undergo post-translational modification on their glutamic acid residues with the aid of vitamin K to become functional [254], and a suffixing letter "a" is assigned to their Roman numeral depicting their activation. Vitamin K is considered an essential coenzyme in the post-translational modification of several coagulant and anticoagulant proteins including, factor VII, IX, X, II (prothrombin), protein C, and protein [253-255]. It aids in the carboxylation of glutamic acid residues to form γ-carboxyglutamyl residues on these proteins which allows them to become functional and biologically active [254-256].

The γ-carboxyglutamyl residues provide a slight overall negative charge on these proteins and allows the attraction of coagulation factors to the phospholipid membrane surface of platelets [255, 256]. As these factors sit on the platelet membrane surface they may slightly repel each other when they come into contact due to their negative charge. Calcium released from the dense granules of activated platelets can bind to the negatively charged factors resulting in their fixation to each other and activation on the surface of the platelets [257]. The asymmetrically distributed platelet membrane contains phospholipid species that are negatively charged and are predominantly located in the inner membrane leaflet, such as phosphatidylserine (PS) [257, 258]. The increase in intracellular calcium upon platelet activation causes the activation of ATP-independent transmembrane transporter proteins called flippase or scramblase, leading to membrane scrambling and exposure of PS to the outer cell surface, which then acts as a platform for the assembly of coagulation protein complexes [257, 258].

The coagulation cascade is a dynamic series of enzymatic processes that traditionally can be categorised into two distinct pathways known as, the extrinsic and intrinsic pathways, which ultimately converge into a common pathway [247]. This eventually ends with the formation of fibrin strands, termination of the cascade by antithrombotic mechanisms, and finally fibrinolysis to dissolve a clot post-wound healing. The extrinsic pathway is considered the

initial phase, where vascular injury exposes a glycoprotein expressed in vascular adventitia known as tissue factor (TF) [259]. TF binds to circulating factor VII (FVII) and becomes activated (FVIIa) forming a (FVIIa/TF) complex that binds with factor X (FX) on the plasma membrane. This interaction forms a multicomponent complex referred to as extrinsic X-ase or tenase, which in turn activates its substrate, factor X (FXa). Activated factor X (FXa) then binds to activated factor V (FVa) in the presence of calcium and membrane phospholipids on the surface of platelets, forming a multicomponent complex called prothrombinase (FXa/FVa), which binds to and activates prothrombin (FII) to produce thrombin (FIIa). Factor X forms the common link between the extrinsic and intrinsic mechanisms in producing thrombin [247, 253, 259]. Figure 1.10 illustrates a summary of coagulation cascade pathways.

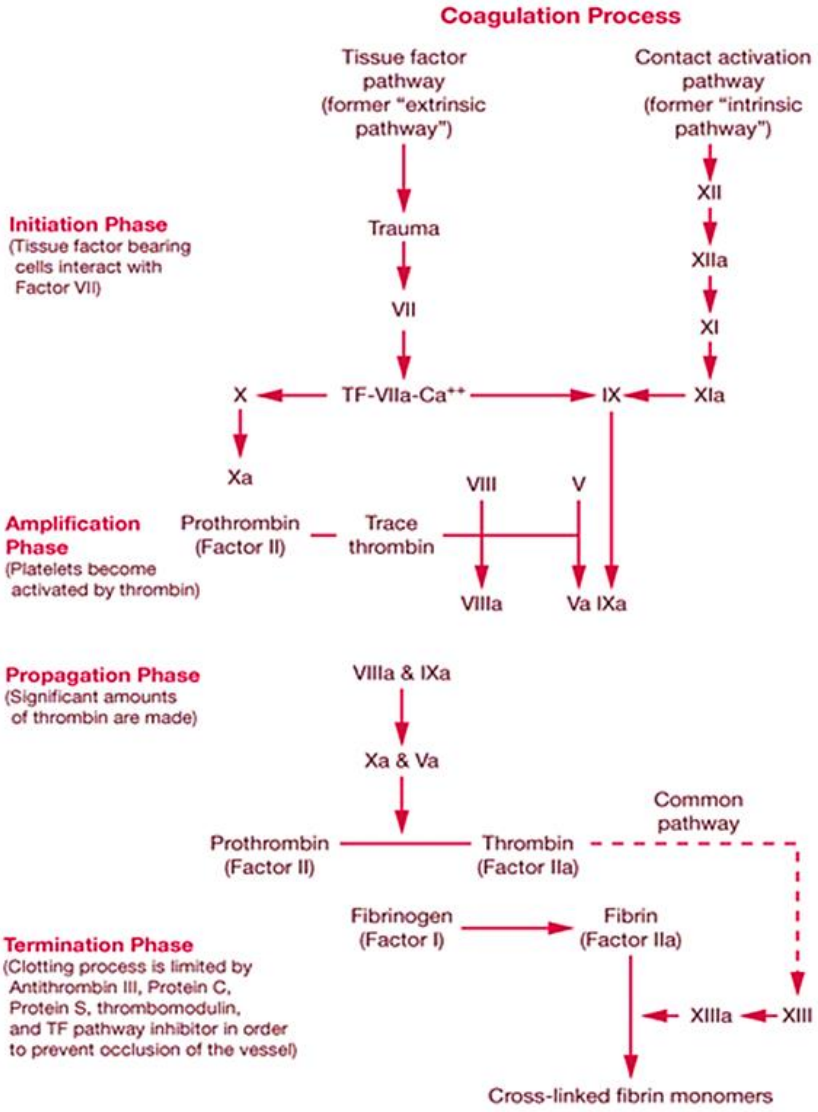

Figure 1.11: Summary of coagulation cascade model (modified from [260])**.**

Factor XII becomes activated (FXIIa) when it comes into contact with exposed collagen from endothelial damage or activated platelets, initiating the intrinsic pathway that runs in parallel with the extrinsic pathway. FXIIa or thrombin can then activate factor XI (FXIa) that binds and activates Factor IX (FIXa) [261]. TF can also activate factor IX. FIXa then binds to activated factor VIII (FVIIIa) in the presence of calcium and membrane phospholipids on the surface of platelets, forming a multicomponent complex (IXa/VIIIa) referred to as (intrinsic X-ase or tenase). This in turn activates its substrate, factor X (FXa), which again results eventually in the formation of thrombin. Thrombin converts fibrinogen that is circulating or that is released from activated platelets to fibrin. The soluble fibrin monomers spontaneously form relatively weak threads, and Factor XIII, which is activated by thrombin to FXIIIa then crosslinks and strengthens the overlapping fibrin strands [247, 253, 262, 263].

The above phases of secondary haemostasis may not alone yield significant amounts of fibrin that then results in a blood clot. Therefore, amplification and propagation process occur, where in this phase the limited amount of thrombin already produced activates local inactive platelets to release the contents of their granules to produce more prothrombin and coagulation factors [264]. Thrombin also activates more coagulation factors present locally including FVa, FVIIIa and FXIa, while the FVIIa/TF complex and activated factor XIa is able to activate factor FIX [263]. Activated FIXa binds to VIIIa (IXa/VIIIa) thus activating X to Xa too. Each activated FXa converts more prothrombin to thrombin, which in turn further accelerates the process [247, 253, 264].

VWF plays a key role in the amplification phase as it binds to circulating inactive FVIII and prolongs its half-life by preventing its premature degradation [265, 266]. The propagation process ensures continuous thrombin generation and the subsequent formation of the fibrin meshwork that is then crosslinked and stabilized by the action of FXIIIa (secondary haemostatic plug) [266]. The 3-dimentional meshwork of fibrin in which RBCs and platelets become trapped represents the final step in the conventional coagulation cascade [247, 253, 266]. Thrombin also activates activatable fibrinolysis inhibitor (TAFI) that protects the fibrin network by cleaving the C-terminal residues that are important for the action of plasmin, thus making fibrin relatively resistant to degradation (fibrinolysis) [267]. Table 3 provides an overview of the Roman numerical nomenclature for coagulation proteins, the coagulation pathways they are involved in, and their physiological functions [253]

Table 3 | Coagulation proteins nomenclature, pathways involved, and function. [253]

umber	Name	Pathway	Function
I	Fibrinogen	Both	Clot formation, cleaved by thrombin to form fibrin monomers.
II	Prothrombin	Both	Activation of I, V, VII, VIII, XI, XIII, protein C, and platelets.
III	Tissue factor (TF)	Extrinsic	Co-factor of VIIa.
IV	Calcium	Both	Facilitate coagulation factor binding to phospholipids.
V	Proacclerin labile factor	Both	Co-factor of X-Prothrombinase complex.
VI	Accelerin	Both	Same as activated factor V.
VII	Stable factor proconvertin	Extrinsic	Activates factors IX and X.
VIII	Antihaemophilic factor A	Intrinsic	Co-factor of IX-tenase complex.
IX	Antihaemophilic factor B Christmas factor	Intrinsic	Activates factor X: forms a tenase complex with factor VIII.
X	Stuart-Prower factor	Both	Prothrombinase complex with factor V and activates factor II.
XI	Plasma thromboplastin antecedent	Intrinsic	Activates factor IX.
XII	Hageman factor	Intrinsic	Activates factor XI, VII and Prekallikerin.
XIII	Fibrin-stabilising factor	Both	Crosslinks fibrin and stabilizes fibrin clot.
XV	Prekallikerin (F Fletcher)	Intrinsic	Serine protease zymogen, functions with factor XV and XII.
XV	HMWK-(F Fitzgerald)	Intrinsic	Co-factor in kallikrein and factor XII activation, necessary in factor XIIa activation of XI.
XVI	Von Willebrand factor		Binds to VIII, mediates platelet adhesion.
XVII	Antithrombin III		Inhibits activated factors II, II, and other proteases.
XVIII	Heparin cofactor II		Inhibits activated factor II.
XIX	Protein C		Inactivates activated factors V and VIII.
XX	Protein S		Co-factor for activated protein C.

In order to prevent spontaneous thrombosis, clot overgrowth, or runaway activation of vascular coagulation proteins, the healthy endothelium expresses and produces a number of anticoagulant and antiplatelet factors that serve to localize procoagulant activity at the injury site, thus maintaining haemostatic balance. These factors include: surface-expressed heparin sulphate, which binds to antithrombin III (a serine protease inhibitor) and inactivates thrombin FVIIa, FIXa, FXa, and FXIa; nitric oxide (NO release vasodilates vessels and inhibits platelet activation and aggregation); ADP dephosphatases (which break down ADP); and prostacyclin (released PGI_2 - binds to platelet receptors and prevents their activation and aggregation) [178, 268, 269]. In addition, the endothelial surface expresses thrombomodulin, which binds to thrombin and induces conformational changes in the presence of a proenzyme called Protein C, thereby altering thrombin's capacity to activate platelets or to convert fibrinogen into fibrin. Activated Protein C is associated with its cofactor Protein S, and inactivates FVa and FVIIIa, and also inhibits the function of prothrombinase and intrinsic tenase complexes.

Tissue factor pathway inhibitor (TFPI) is another molecule with inhibitory effects that circulates in the blood, but is mostly found adhered to the endothelium, and which can reversibly bind and inhibit FVIIa/TF complex and FXa [270]. Fibrinogen in the circulation is also subjected to degradation by endothelial surface-expressed tissue plasminogen activator (tPA) that converts plasminogen to plasmin for fibrin degradation. Plasmin works on crosslinked fibrin essentially by severing the fibrin threads, and then cleaving fibrinogen and other clotting factors at multiple sites resulting in clot dissolution [269]. The processes of primary and secondary haemostasis are mechanistically intertwined and occur spontaneously along with the production of procoagulant physiological inhibitors, thus providing a synergistic action in response to vascular injury and preventing blood loss. Figure 1.11 summarises the stages of haemostasis.

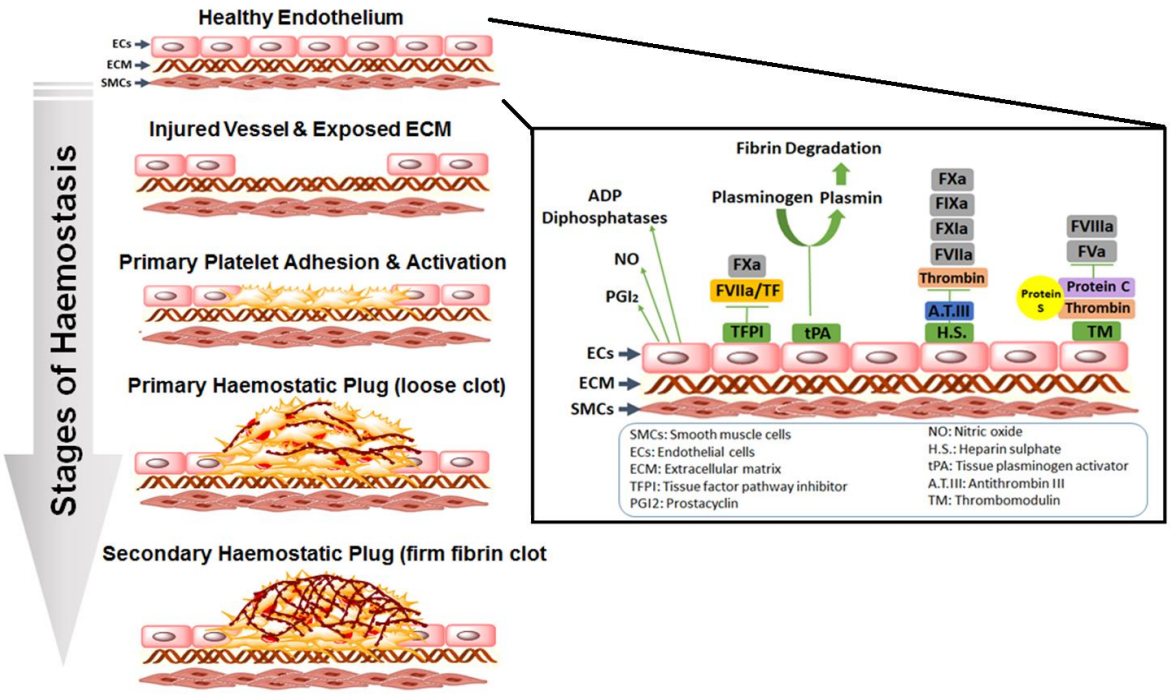

Figure 1.12: Summary of the different stages for maintaining haemostasis, and mechanisms of anticoagulation system involving endothelial cells.

Negative regulatory mechanisms from healthy endothelial cells prevent pathological accumulation of procoagulants within the blood stream thus maintaining blood fluidity and protecting the blood vessel. However, upon vascular injury to the endothelial lining, several repair mechanisms are activated and a coagulation process initiates until the injury is sealed as shown in this Figure. (Original image created from [178, 268, 269])

In a variety of disease states such as Alzheimer's disease, the balance between anticoagulant and prothrombotic mechanisms is altered. Endothelial dysfunction, vascular abnormalities, and compromised blood flow, result which can lead to thrombotic or haemorrhagic

complications [86, 271, 272]. A prothrombotic state and altered coagulation profile have been documented in AD thus predisposing patients to higher risks of cardiovascular disease, microinfarcts and strokes [271]. Several studies showed altered fibrin clots which are resistant to degradation in the presence of Aβ peptides (decreased fibrinolysis) [273]. Aβ peptides were also shown to activate coagulation factor FXII, promoting thrombus generation, and elevated plasma fibrinogen levels were documented resulting in an increase blood viscosity, RBCs aggregation, reduced blood flow, and increased platelet activation [273, 274] .

1.4.4. Platelet Abnormalities in AD

Platelets are considered key contributing players in cerebrovascular pathophysiology, such as, strokes, and cerebral amyloid angiopathy (CAA), associated with AD [275]. Numerous studies have been conducted by different groups to investigate their potential role in AD which have revealed a number of abnormalities present in platelets from AD patients and animal models compared to their age-matched controls [171, 276]. Initially, platelet membrane abnormalities were reported in the 1990s, from membrane fluidity fluorescence studies on platelets from AD patients, and these studies indicated that there is a biophysical alteration of the platelet membrane [277, 278]. Higher intracellular membrane fluidity was observed, which might result in dysregulation of membrane biosynthesis with these alterations being significantly correlated with the severity of the disease [279].

The preliminary work done by Rosenberg's group in 1997 highlighted possible platelet activation in AD patients due to altered processing of APP isoforms [280]. Important work following up on these observations came from Sevush's group in 1998, where they examined unstimulated platelets from AD patients and their age-matched control and reported a significant increase in the percentage of circulating platelet aggregates (39.5%), platelet-leukocyte complexes (53.3%), and an increase in surface expression of p-selectin by 59.3% (a marker of platelet activation and α-granule secretion) [151]. These results strongly indicated that there is an aberrant and chronic pre-activation state of platelets in AD [151]. Further studies by other groups also supported these observations and also showed the activation of integrins $\alpha_{IIb}\beta_3$ on unstimulated platelets from AD subjects [281-283].

In the early stages of AD, a high level of activated platelets called "coated" platelets are present in the blood [284, 285]. This is a platelet subset that retains high concentrations of several procoagulant proteins on its membrane, and expresses high levels of full-length APP, upon dual activation with thrombin and collagen when compared to platelets stimulated with

a single agonist [284]. Platelets from AD patients have shown abnormalities in a host of membrane and cellular proteins including decreased receptor affinity for the neurotransmitter serotonin and impaired serotonin uptake, cytoskeletal abnormalities, cytochrome c oxidase deficiency and increase in monoamine oxidase-B activity in platelet mitochondria, which thus increases oxidative stress, as well as decreased phospholipase C (PLC) activity, and increased cytosolic protein kinase C (PKC) levels [286-291].

Kinetic studies on platelet membrane β-secretase have shown a significant elevation of β-secretase activity (17%) in AD patients compared to age-matched controls, suggesting that elevated platelet β-secretase activity may precede the onset of symptoms [292]. An interesting study documented that, β-secretase activity is modulated by platelet membrane cholesterol content in a biphasic manner, thereby linking dietary effects with AD [293]. Elevation of β-secretase activity in AD patients can result in increased production and release of Aβ peptides into the circulation and thus an increased local concentration [294]. In addition, platelets in transgenic mouse models of AD pathogenesis were also found to display accumulation and activation at vascular Aβ deposition sites in CAA lesion and vascular injury [86, 295]. This can result in the activation of more platelets within the vicinity and the release of more Aβ peptides into circulation, creating a vicious cycle of platelet activation and potential thrombus formation and vessel occlusion at these sites, thus exacerbating and contributing towards the cerebrovascular complications associated with AD [86].

1.4.5. Amyloid β Peptides and Platelet Activation

A number of studies have explored the use of Aβ peptides to understand the effects of their exposure upon platelet activation. Several authors have utilized soluble or fibrillar forms of Aβ1-42, and Aβ1-40, and synthetic Aβ25-35 that retains the biological and toxic properties of the full length Aβ1-42 and Aβ1-40 [295-301]. A preliminary study by Herczenik's group tested the effects of proteins with amyloid properties on human platelet activation, and demonstrated that fibrillar Aβ1-40 does indeed induce platelet activation and aggregation through binding to the scavenger receptor CD36/p83(MAPK)/TXA2 and through GPIbα mediating platelet aggregation [302]. Another study using Aβ25-35, showed that collagen and ADP-induced platelet aggregation was potentiated at concentrations of 1–2 μM, while at higher concentrations (2–10 μM), Aβ25–35 could directly promote aggregation through pathways involving PLCγ2, intracellular calcium mobilisation, and PKC pathway. The PAR1 receptor was also activated initiating a signalling cascade via Ras/Raf, PI3K, Akt, P38 MAPK, cPLA2 and TxA2 formation [296, 297].

Canobbio's group conducted several studies utilizing Aβ25–35 on platelets and revealed that the first event in Aβ-induced platelet activation is the increase of intracellular Ca^{2+} concentration, and also showed the essential role for Ca^{2+} and ADP in platelet activation and thrombus formation [303]. They proposed that an increase of intracellular Ca^{2+} concentration as a result of exposure to Aβ was dependent upon the presence of extracellular calcium, and this first cellular event occurs possibly through the ability of Aβ to form cation-permeable pores in the plasma membranes [303]. The capacity of Aβ molecules to form ion channels was originally proposed in 1993 by the Arispe's group, and their idea was that the Aβ peptide was capable of forming an amphipathic beta-sheet due to presence of alternating polar and nonpolar residues, which could result in channel formation at the membrane. In addition, they showed that calcium-dependent release of ADP is responsible for the activation of the small GTPase Rap1b and inside-out activation of integrin $\alpha_{IIb}\beta_3$, leading to platelet aggregation and increased thrombus formation [304, 305].

Canobbio's group also demonstrated that immobilized Aβ25–35, Aβ1-40, and Aβ1-42 peptides induced platelet adhesion and spreading [300]. They also found that Aβ25–35 accelerated platelet spreading over collagen or fibrinogen and enhanced platelet adhesion to collagen under shear flow, indicating the thrombogenic potential of Aβ peptides at vascular lesions or in CAA [300]. In order to understand the underlying molecular mechanism of Aβ on platelets, Sonkar's group carried out a series of experimental studies on platelets using Aβ25–35 and found that 10-20 μM of the peptide was enough to induce strong platelet aggregation independently, and to a similar extent to that induced by physiological agonists [306]. Furthermore, Aβ25–35 was shown to substantially augment platelet spreading on immobilised fibrinogen and also clot retraction, which is greatly dependent on the engagement of integrin $\alpha_{IIb}\beta_3$. It also enhanced and stabilized platelet adhesion on immobilised collagen under arterial shear flow [306].

Our group's earlier work also highlighted that Aβ25–35-stimulated platelets induce an increase in intracellular Ca^{2+} that mediated dense granule release and ADP secretion as the earliest event taking place [303]. ADP is thus considered a major player in the subsequent propagation and activation of small GTPase Rap1b and consequently integrin $\alpha_{IIb}\beta_3$ in platelets [303]. Moreover, ADP released by platelets stimulated with Aβ25–35, resulted in the phosphorylation and activation of key signalling molecules including, Syk, PKC, PI3K, and p38MAPK and ERK1/2 [303]. In addition, it was suggested that Aβ25–35 might be interacting with GPCR coupled with G_{13} or G_q subunits to initiate a signal, since there was an observation of increased levels of Rho-GTP, Rho-associated coiled-coil protein kinase

(ROCK) and phosphorylation of myosin light chain (MLC) and MLC phosphatase, respectively, thus mediating cytoskeleton reorganisation and actomyosin contraction [303]. Sonkar's group evaluated thrombus formation *in vivo* in the presence of Aβ25–35 using a pulmonary thromboembolism model of Swiss albino mice [306]. The mice exhibited a significant number of thrombi in their pulmonary vessels and shorter bleeding time when compared to the ones treated with collagen plus epinephrine alone [306].

Interestingly, Donner's group, have shown that Aβ1-40 can bind to integrin αIIbβ3 and trigger the release of ADP and clusterin (chaperone molecules), which promoted the formation of Aβ1-40 fibrils and reinforced platelet activation via ADP binding to its P2Y12 receptor [307]. Aβ promotion of platelet activation at an injured carotid artery model *in vivo* was also confirmed by Gowert's group [295]. This group also carried out cerebral vessel wall analysis of APP23 and APP Dutch mice that are known to develop CAA upon aging. These mice displayed platelet accumulation at vascular amyloid plaques over time, showing that sustained platelet recruitment may eventually lead to full vessel occlusion [295].

Recently, it has been demonstrated that mitochondrial respiration is increased in Aβ-stimulated platelets and that cytochrome c oxidase, an enzyme that belongs to the complex IV of the respiratory chain, was diminished in platelets and hippocampal mitochondria of AD patients [308, 309]. This points towards a state of redox stress in AD patients. Several publications have suggested the important role of reactive oxygen species (ROS) as second messengers and as critical signalling modulators in platelet activity, such as in the inhibition of phosphatases, increasing tyrosine phosphorylation, and increasing ADP release and bioavailability [310-312]. However, excess production of ROS, i.e. oxidative stress, can itself lead to oxidative damage and platelet apoptosis [313].

There are many sources of ROS in platelets, such as mitochondrial respiration, NAD(P)H oxidase (NOX), uncoupled endothelial nitric oxide, xanthine oxidase, lipoxygenase, and arachidonic acid-dependent phospholipase [312, 314]. Different ROS species are generated, e.g. superoxide anion radical, hydroxyl radical, hydrogen peroxide, nitric oxide, and peroxynitrite anion. However, NADPH oxidases (NOXs) are considered to have a pivotal role in regulating and modulating platelet haemostasis in response to different stimuli [310, 312, 314-317]. Information gathered from these previous studies suggests the possibility that the stimulatory effects of Aβ on platelet activation are induced by redox stress.

The exact cellular mechanism by which Aβ peptides activate platelets and regulate haemostasis and thrombosis is not well defined. Because of the complexity of the chemistry

of ROS and the great number of regulatory enzymatic sources that are potentially involved, the role of ROS in platelet activation upon Aβ peptide stimulation and a complete picture of the link between Aβ peptides and platelet redox homeostasis is still missing. In particular, the types of ROS generated, their specific significance with respect to platelet activity, and the signalling mechanisms involved have not been determined clearly. Therefore, the present PhD project aimed to investigate the mechanisms underlying Aβ peptide-dependent activation of platelets and the potential role of ROS in this pathophysiological event.

1.5. RESEARCH HYPOTHESIS

Amyloidogenic Aβ peptides within the bloodstream cause cerebrovascular complications associated with Alzheimer's disease via redox-dependent activation of platelets.

1.6. AIMS OF THE STUDY

The overall aim of the presented work is to investigate the mechanisms underlining β-amyloid peptide-dependent regulation of platelets and the potential role of ROS in this pathophysiological event. This can provide new insights in understanding cerebral microthrombosis and impaired blood flow associated with Alzheimer's disease progression.

The project is divided into 3 main phases:

PHASE I

Investigate the effects of Aβ peptides on platelet functional responses, i.e. adhesion, aggregation, and thrombus formation under physiological blood flow conditions

PHASE II

Explore different methodologies to assess oxidative changes in platelets upon treatment with Aβ peptides

PHASE III

Investigate redox- and NADPH oxidase-dependence of platelet functional alterations induced by Aβ peptides

CHAPTER 2

Materials & Methods

2. MATERIALS & METHODS

2.1. EXPERIMENTAL SECTION A: PEPTIDE SYNTHESIS

2.1.1. Aβ25-35 Solid Phase Peptide Synthesis (SPPS)

The SPPS technique involves successive assembly of orthogonally protected amino acids from the C to N terminus to form any desired sequence in a step-wise manner. The basic process of SPPS is initiated by covalently attaching the activated carboxyl function of the first N-α-Fmoc protected amino acid to a polystyrene-based insoluble solid support. The temporary Fmoc amino protecting group is then removed (deprotection) under mild basic conditions and a second activated Fmoc protected amino acid added with the aid of a coupling agent to expand the peptide chain. The procedure of deprotection and addition/coupling of an amino acid is known as a cycle and SPPS consists of a series of repetitive cycles with washes in between allowing the removal of excess reagents, amino acids, and soluble by-products via simple filtration. Once the synthesis is complete, the new peptide is cleaved from the resin into solution under strongly acidic conditions that also remove side chain groups. The nascent peptide is then purified and characterized using high performance liquid chromatography (HPLC) and mass spectroscopy (MS) [318, 319]. Figure 3.1 illustrates the basic steps of SPPS.

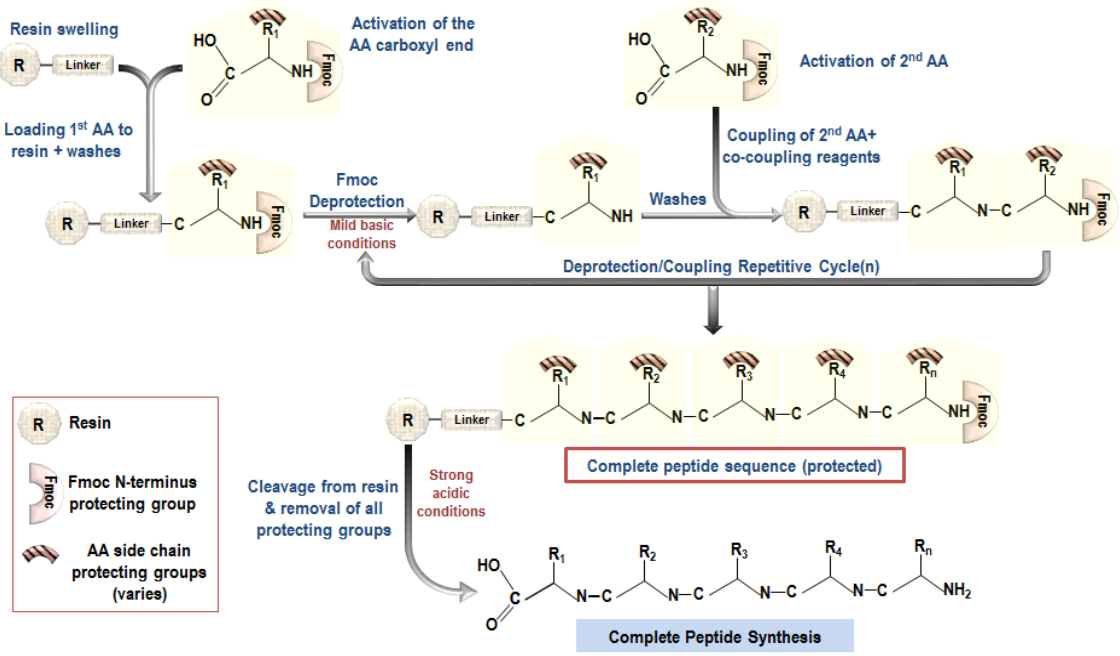

Figure 2.1: Illustration of the basic principles in SPPS.
The first step involves resin swelling and anchoring the C-terminus of the first amino acid to the resin, typically after its activation. Deprotection of the amino acid N-terminus takes place followed by coupling of the second amino acid by its C-terminus to the first one. The cycle is repeated until the desired peptide is completed and finally all protecting groups are removed and the peptide is detached from the resin. (Original figure created from [319, 320])

Materials & Instruments:

Materials and chemical reagents were purchased from Sigma-Aldrich®, Fluka®, Acros Organics®, VWR™ Merck and Novabiochem®. All solvents were reagent grade or HPLC grade (Fisher Scientific®). Anhydrous (dry) dichloromethane (DCM) was obtained via distillation over calcium hydride (CaH_2). Conventional 9-fluorenylmethoxycarbonyl (Fmoc) chemistry protocols were followed using an Activo-P11 automated peptide synthesizer. For the synthesis of Aβ25-35, the following list of Fmoc-protected amino acids from Novabiochem® were utilized as shown in Table 3:

Table 4 | **Fmoc-protected amino acids for synthesis of Aβ25-35**

Fmoc-Met-OH
Fmoc-Leu-OH
Fmoc-Gly-**OH**
Fmoc-Ile-OH
Fmoc-Ile-OH
Fmoc-Ala-OH
Fmoc-Gly-OH
Fmoc-Lys(Boc)-OH
Fmoc-Asn(Trt)-OH
Fmoc-Ser(tBu)-OH
Fmoc-Gly-OH

Analytical Reverse Phase High Performance Liquid Chromatography (RP-HPLC) was performed at 35 ± 0.1 °C on a Dionex UltiMate 3000 HPLC system (Dionex, UK) equipped with a Phenomenex Gemini 5µm C-18 (150 x 4.6 mm) column with a flow rate of 1 mL min^{-1}. Preparative RP-HPLC was performed on a Dionex HPLC system using a Phenomenex Gemini 5µm C-18 (250 x 30 mm) column and a flow rate of 2.5 mL min^{-1}. Mobile phase A was 0.1% TFA in water and mobile phase B was 0.1% TFA in MeCN for both devices.

Analytical HPLC gradient was T= 0.0-10.0 min, B = 5-95%; T= 10.0-15.0 min, B= 95%; T= 15.0–15.1 min, B= 95-5%; T= 15.1–18.0 min, B= 5%.

Preparative HPLC gradient was T= 0.0-6.0 min, B = 5%; T= 6.0-26.0 min, B= 5-95%; T= 26.0–36.0 min, B= 95%.

Mass spectrometry (Bruker Daltonics; Bremen, Germany) was performed using a microTOF instrument in positive-ion mode.

Method:

Coupling of 1st Amino Acid

250 mg of 2-chlorotrityl CTC resin (Bachem, 200-400 mesh, loading 1.4 mmol/g) was weighed into a 10 mL SPPS reaction vessel with bottom filtration. The resin was pre-swollen using 3 mL of dry DCM (~1 mL/100 mg resin) for 15 min twice. The first amino acid was preloaded by dissolving Fmoc-Met-OH (1.2 eq. relative to the resin) and DIEA (4eq. relative to the carboxylic acid) in dry DCM (3 mL). The mixture was then added to the reaction vessel containing the resin and was left on a rotator for 1 hr. The solvent was drained off and the resin was washed 3x3 min in DCM/MeOH/DIEA (17:2:1), 3x3min DCM, 2x3 min DMF, 2x3 min DCM and then left to dry in vacuo overnight.

Determination of Resin Loading

A small amount of dried Fmoc amino acid-resin was accurately weighed (24 mg, approximately 5 µmole with respect to Fmoc) into a 10 mL graduated flask. 2% DBU in DMF (2 mL) was added to the resin and left to agitate gently for 30 min. The solution was then diluted to 10 ml with acetonitrile (MeCN) and mixed. 800 µl of resin solution was transferred carefully to another graduated flask and was further diluted up to 10ml with MeCN. A reference solution was also prepared using the method mentioned previously but without the addition of the resin. The optical density of the resin and reference solutions was measured at 304 nm using a spectrophotometer (Helios Gamma Unicam, 190-1100 n Wavelength). The actual Fmoc loading (0.34 mmol/g) and estimated first residue attachment were obtained by using the following equation: Fmoc loading mmol/g = ($Abs_{sample} - Abs_{reference}$) X16.4/mg of resin. The actual Fmoc loading obtained was used to adjust the required amount of amino acids and chemical reagents (i.e. required weight = resin loading x resin/g x eq. x MW of AA) required in subsequent cycles.

Fmoc Cleavage (Deprotection)

Dried Fmoc amino acid-resin was first washed with DMF (2x 2 min). 20% piperidine in DMF (3 ml) was added to the resin and was placed on the rotator for precisely 2 min. The solution was then drained under reduced pressure and this step was repeated again, but for 15 min. The resin was washed thoroughly with DMF (5x 2 min) and then with DCM (2x 2 min). A Kaiser test [321] was performed to confirm successful deprotection. For the expected

positive result, the resin beads show a colour change to deep blue/purple. Negative results display no colour change.

Automated Peptide Synthesis

The total resin was transferred to the peptide synthesizer reactor vessel which was fitted with a reactor heating jacket. All the remaining amino acids where loaded and coupled using the following Fmoc-based SPPS protocol: 3 eq. of each amino acid; 3 eq. of coupling agent, benzotriazol-1-yl-oxytripyrrolidinophosphonium hexafluorophosphate (PyBOP, 0.15 M in DMF); 6 eq. of the base N,N-diisopropylethylamine (DIEA, 0.48 M in DMF); 25% v/v piperidine in N,N-dimethyl formamide (DMF). The reactor vessel temperature was maintained at 70^{o}C for both coupling and deprotection steps.

Final Peptide Cleavage

After completing the peptide synthesis, the resin was washed with DCM (2x2 min). The resin was then cleaved using a cleavage solution mixture of trifluoroacetic acid (TFA), Triisopropylsilane (TIS), deionised water, and 1,2-ethanedithiol (EDT) (TFA/TIS/H_2O/EDT (94:2.5:2.5:1 v/v/v/v)) for 3 h. The resin solution was then added to diethyl ether (Et_2O) to produce a white precipitate that was collected by centrifugation, and the Et_2O was discarded. The crude peptide was then re-dissolved in MeCN. The solution was filtered using a 0.2 µ PTFE membrane filter. Analytical and preparative HPLC were performed for peptide analysis and purification, while mass spectrometry was used for peptide identification and characterization.

Confirmation of Commercially Synthesized Aβ Peptides (LifeTein) by Liquid chromatography and Mass Spectrometry

Materials & Instruments:

Several Aβ peptides were purchased from LifeTein® (New Jersey, USA) and their details are shown in Table 4.

Table 5 | Sequences and molecular formulae of Life Tein Aβ peptides

NAME	SEQUENCE	FORMULA	M.W.
Scrambled Aβ1-42	DEFAKNIGHHDGVAVHMYKGR QVEFIGSIALVFEDVGSAGLV	$C_{203}H_{311}N_{55}SO_{60}$	4514.07
Aβ1-42	DAEFRHDSGYEVHHQKLVFFAE DVGSNKGAIIGLMVGGVVIA	$C_{203}H_{311}N_{55}SO_{60}$	4514.07
Aβ1-40	DAEFRHDSGYEVHHQKLVFFAE DVGSNKGAIIGLMVGGVV	$C_{194}H_{295}N_{53}SO_{58}$	4329.84
Aβ25-35	GSNKGAIIGLM	$C_{45}H_{81}N_{13}SO_{14}$	1060.28

Samples of these peptides were submitted to the Materials and Chemical Characterisation Facility at the University of Bath for analysis by liquid chromatography (Dionex Acclaim RSLC Polar Advantage II (PA2), 2.2 µm, 120 Å, 2.1 x 50 mm and mass spectrometry using a MaXis HD quadrupole electrospray time-of-flight (ESI-QTOF) instrument (Bruker Daltonik GmbH, Bremen, Germany), operating in ESI positive-ion mode and coupled to a Ultimate 3000 UHPLC (Thermo Fisher Scientific, California, USA). Data were analysed using Analysis software version 4.3 (Bruker Daltonik GmbH, Bremen, Germany).

Method:

Analysis of LifeTein peptides was conducted using a Quadrupole electrospray time-of-flight mass spectrometer (QTOF) coupled with an Ultimate 3000 UHPLC (QTOF-UHPLC) as detailed above. The capillary voltage was set to 4500 V, with the nebulizing gas at 3 bar, and drying gas at 10 L/min at a drying temperature of 210°C. The time-of-flight (TOF) scan range was from 150 – 2200 mass-to-charge ratio (m/z). Liquid chromatography was performed with a flow rate of 0.4 ml/min at 40°C, and an injection volume of 10 µl. Mobile phases A and B consisted of 0.1% v/v formic acid in water, and 0.1% v/v formic acid in MeCN, respectively. Gradient elution was carried out with T= 0.0-10.0 min, B = 5-95%; T= 10.0-15.0 min, B= 95%; T= 15.0–15.1 min, B= 95-5%; T= 15.1–18.0 min, B= 5%. The mass spectrometer was calibrated using a range of sodium formate clusters introduced by 10 µl loop-injection prior to the chromatographic run. The mass calibrant solution consisted of 3 parts of 1 M NaOH to 97 parts of 50:50 water to isopropanol with 0.2% formic acid. The observed mass and isotope pattern perfectly matched the corresponding theoretical values as calculated from the expected elemental formula using analysis software.

2.2. EXPERIMENTAL SECTION B: PLATELET STUDIES

2.2.1. MATERIALS

Most commercially available materials and chemical reagents were purchased from Sigma-Aldrich® and the following are the materials used specifically for the platelet studies.

Table 6 | Platelet Stimuli

Reagent	Source	Catalogue
Arachidonic Acid	Sigma-Aldrich, USA	#A3611
Collagen Related Peptides (CRP)	Collagen Toolkits, University of Cambridge	-
Native Collagen Fibrils (Type I)	Chrono-Log Corporation, USA	#P/N 385
Thrombin from human plasma (Lyophilized powder)	Sigma-Aldrich, USA	#T6884
Low Density Lipoprotein (Oxidized, oxLDL)	Kind gift from Dr. Katie Wraith and Dr. Khalid Naseem, University of York, Hull-York Medical School, UK	-
Low Density Lipoprotein (Normal, nLDL)	Kind gift from Dr. Katie Wraith and Dr. Khalid Naseem, University of York, Hull-York Medical School, UK	-
Hydrogen peroxide solution (contains inhibitor 30 wt. % in H2O, ACS reagent	Sigma-Aldrich, Germany	#216763-M
Fibrinogen from human plasma 50-70% (≥80% of protein clottable)	Sigma-Aldrich, USA	#F3879

Table 7 | Platelet Inhibitors

Reagent	Source	Catalogue
2-Acetylphenothiazine (2-APT)	Sigma Aldrich, USA	#175226
GP91 ds-tat	Anspec Inc, CA	#AS-63818
GP91 ds-tat scrambled	Anspec Inc, CA	#AS-63821
Indomethacin (≥99% (TLC)	Sigma-Aldrich, USA	#I7378
Losartan Potassium	Tocris Bioscience, UK	#3798
ML161 ≥98% (HPLC)	Tocris Bioscience, UK	#4570/10
NOXA1ds scrambled	Kind gift from Professor Patrick Pagano, University of Pittsburgh	-
NOXA1ds	Kind gift from Professor Patrick Pagano, University of Pittsburgh	-
N-Acetyl-L-Cysteine (NAC)	Sigma-Aldrich, China	#A9165
Prostaglandin E_1 (PGE_1; ≥98% (HPLC) synthetic	Sigma-Aldrich, USA	#P5515
Sulfosuccinimidyl Oleate sodium salt (SSO)	Cayman Chemical Company, USA	#11211
VAS2870	Sigma-Aldrich, USA	# SML0273
Citrate Concentrated Solution (4% (w/v)	Sigma-Aldrich, USA	# S5770

Table 8 | Amyloid Peptides β

Reagent	Source	Catalogue
Aβ25-35	LifeTein, USA	#LT1148-6
Aβ1-40	LifeTein, USA	#LT1148-3
Aβ1-42	LifeTein, USA	#LT1148-2
Aβ1-42 Scrambled	LifeTein, USA	#LT1148-5
Aβ1-42 fibrils	Kind gift from Dr. Janet Kumita and Prof. Christopher Dobson, University of Cambridge, UK	-

Table 9 | Antibodies, Molecular & Fluorescent Probes

Reagent	Source	Catalogue
Anti-CD36 antibody [FA6-152]	Abcam, UK	#ab17044
Anti-p-selectin (PE-Cy™5 mouse anti-human CD62P)	BD Biosciences USA	#551142
PAC1 (FITC Mouse Anti-Human PAC-1)	BD Bioscience, USA	#340507
Phalloidin-Tetramethylrhodamine B isothiocyanate (TRITC conjugated)	Sigma-Aldrich, USA	#P1951
Carboxy-H_2DCFDA (6-carboxy-2',7'-dichlorodihydrofluorescein diacetate)	Life Technologies, USA	#C400
Dihydroethidium (DHE)	Life Technologies, USA	#D11347
CMH spin probe (1-hydroxy-3-methoxycarbonyl-2,2,5,5-tetramethylpyrrolidine)	Noxygen GmbH, Germany	# NOX-2.1
DiOC6 (3, 3′-Dihexyloxacarbocyanine iodide)	Sigma-Aldrich, USA	# 318426

Table 10 | Other Reagents

Reagent	Source	Catalogue
Bovine Serum Albumin (BSA; Heat shock fraction, pH 7, ≥98%)	Sigma-Aldrich, USA	#A7906
Bidistilled water (ESR grade water)	Noxygen GmbH, Germany	#NOX-9.1-1L
Deferoxamine methanesulfonate salt (DF)	Noxygen GmbH, Germany	# NOX-9.1
D-(+)-Glucose monohydrate	Sigma-Aldrich, France	#49158
Dimethyl Sulfoxide (DMSO, sterile-filtered, ≥99.7%)	Sigma-Aldrich, USA	#D2650
HEPES (4-(2-Hydroxyethyl) piperazine-1-ethanesulfonic acid)	Sigma-Aldrich, USA	#H4034
Kreb HEPE Buffer (ESR)	Noxygen GmbH, Germany	#NOX-7.6.1-1L
Paraformaldehyde 4 % w/v in PBS	Sigma-Aldrich, USA	#P6148
Thioflavin T	Sigma-Aldrich, India	#T3516
Triton-x100 SigmaUltra	Sigma-Aldrich, Germany	# T9284
VECTASHIELD Mounting medium for Fluorescence	VCTOR Laboratories, Burlingame, CA	-

Table 11 | Instruments & Software

Instruments
490D Aggregometer (Chrono-Log Corporation, Havertown, PA)
Centrifuge (Thermo Scientific Heraeus™ Megafuge™)
Ibidi Vena8 Fluoro+ microchips (Ibidi GmbH, Martinsried, Germany)
Electron Paramagnetic Resonance (EPR) MS200spectrometer (Magnettech, Berlin, Germany)
Exigo pump (Cellix Microfluidics Solutions, Dublin, Ireland).
EVOS Fl microscope (Thermo Fisher Scientifics, Waltham, MA US)
Flow Cytometry (BD FACSAria™ III, Becton Dickinson, Wokingham, UK)
Leica Microsystems DM4000 B LED Fluorescence Microscope
Microplate reader (FLUOstar Omega BMG Labtech)
Platelet counter (Z1 Series Beckman Coulter Particle Counter)
Software
AGGRO/LINK software
BD FACSDiva software
GraphPad Prism 5 for Windows Version 5.04
Image J (Version 1.47 and 1.52e, Wayne Rasband, NIH)
Leica Microsystems Application Suite X

2.2.2. METHODOLOGY

2.2.2.1. Platelet Isolation

Human blood was drawn from healthy volunteers (both genders) by median cubital vein venepuncture under local ethics committee approval, either following University of Bath or Royal Devon and Exeter NHS Foundation Trust Code of Ethics and Research Conduct. Warm sodium citrate solution (4% w/v) was used as anti-coagulant at a ratio of 1:7 to blood (approximately 0.6% w/v). Platelet rich plasma (PRP) was then isolated from whole blood by first centrifugation at 200 xg for 20 min. PRP was then subjected to a second centrifugation at 500 xg for 10 min in the presence of indomethacin (10 μM) and PGE1 (40 ng/ml) to isolate platelets. Once platelets were isolated, they were resuspended in warm Tyrode buffer (37 °C) at a density of 2 x 10^8 platelets/ml ready for further experiments. In most of the following experiments this was the standard platelet isolation protocol.

2.2.2.2. Adhesion Assay

Coating preparations: Round coverslips (22 mm) were placed in a clear bottom flat 6-well plate and then coated overnight at 4 °C with 10 μM Aβ1-42, Aβ1-40, Aβ25-35, scrambled Aβ1-42, or 5 mg/ml BSA, all diluted in PBS.

Platelets adhesion assay: The platelet isolation method was followed, and after the first centrifugation, PRP was subjected to a second centrifugation at 200 xg for 20 min to remove any remaining erythrocytes before the final centrifugation at 500 xg for 10 min. PPP was discarded and the platelet pellet was re-suspended carefully in warm (37 °C) modified Tyrode's HEPES buffer (145 mM NaCl, 2.9 mM KCl, 10 mM HEPES, 1 mM MgCl2, pH 7.3; 5 mM D-glucose was added before use) at a density of 2 x 10^7 platelets/ml. Platelets were then left to rest for 30 min in a 37°C warm water bath. Excess solutions from coverslips were then gently removed and the coverslips were blocked with 5 mg/ml BSA in PBS for 1 h at room temperature. The coated dishes were then washed gently and carefully with PBS, and platelets were added (0.5ml) and incubated for 30 min at 37°C. In case where inhibitors were used, after platelets were rested, they were incubated with different inhibitors for 10 min prior to adding onto coated slides. Non-adherent platelets were discarded and the adherent ones were gently washed with PBS and then fixed with 4% paraformaldehyde for 10 min at RT. The coated coverslips were then washed carefully with 3 x PBS, then 50 mM ammonium chloride/PBS was added for 10 min. 0.1% Triton-x100/PBS was added to

permeabilized platelets after 3 x gentle washing with PBS. After 5 min, 0.1% Triton-x100/PBS was removed and the coated coverslips were washed gently 3 x with PBS and then blocked with 5 mg/ml BSA in PBS for 30 min. The fixed platelets were then stained with TRITC-conjugated phalloidin for 1 hour at RT and then washed with 3 x PBS, and each coverslip was mounted onto a microscope slide using Vectashield. Evaluation of platelet adhesion and spreading was performed using a Leica LED Fluorescence Microscope, and digital images were acquired at 10 x and 100 x magnification.

2.2.2.3. Platelet Aggregation Assay by Suspension Turbidimetry

Human platelets were isolated and suspended in modified HEPES Tyrode with glucose at physiological density (2 x 10^8/ml) and rested in a water bath (37°C) for 30 min. Aggregation experiments were performed by either by adding agonists directly to platelets or pre-incubating with ROS inhibitors/scavengers prior to adding agonists with continuous stirring at 800 RPM over 10 min measured by turbidimetry at 37°C using a 490D aggregometer. These agonists included thrombin (0.1, 0.05 and 0.03 units/ml), collagen (3 and10 μg/ml), Aβ peptides (20 μM, with scrambled Aβ1–42 as a control), CRP (3 μg/ml), or arachidonic Acid (AA, 30 μM). The ROS scavenger used was NAC (3 mM), and inhibitors were VAS2870 (10 μM), indomethacin (10 μM), NOXA1ds (10 μM), with scrambled NOXA1ds as control), or NOX2ds-TAT (10 μM, with scrambled NOX2ds-TAT as control).

2.2.2.4. Thrombus Formation Assay under Physiological Flow

Human platelets were isolated and fluorescently labelled by incubation with 1 μM DiOC6 (green fluorescent dye in DMSO) for 10 min. Ibidi Vena8 Fluoro+ microchips were coated with 10 μM Aβ peptides or 0.1 mg/ml fibrillary collagen for 2 hours. Non-specific binding sites were saturated with 0.1% w/v BSA. Physiological flow conditions (200-1000 s^{-1}) were applied using an Exigo pump and images of the thrombi after 10 min of flow were obtained with an EVOS Fl microscope. Platelet coverage was then measured using Image J (Version 1.52e).

2.2.2.5. Platelet α-Degranulation and αIIbβ3 Activation by Flow cytometry

Human platelets were isolated and suspended in modified HEPES Tyrode with glucose at physiological density (2 x 10^8/ml) as described previously. Platelets were stimulated in suspension with Aβ1-42, Aβ1-40, Aβ25-35, scrambled Aβ1-42 (5-10 µM) or thrombin (0.5 unit/ml) for 10 min at 37 °C. Platelets were then incubated for a further 10 min with PAC1 and anti-P-selectin antibodies (1 in 1000) conjugated to FITC and PE-Cy5. After 1 in 10 dilution with Tyrode's buffer, surface fluorescence was assessed using a flow cytometer. A minimum of 3 experiments were performed with 3 repeats per condition and an average of 50,000 events/sample were recorded. Data were obtained by BD FACSDiva software. Gate selection was performed using logarithmic side and forward scattering (SSC & FSC).

2.2.2.6. Detection of Platelet binding to FITC-labelled Aβ Peptides

FITC-Labelling of β-amyloid peptides was carried out by Dr. Abhishek Upadhyay and Dr. Mareike Posner in the Department of Biology and Biochemistry at the University of Bath. The following method was used.

Preparation of FITC-labelled Amyloid peptides β: Stock solutions of FITC and β-amyloid peptides β (scAβ1-42 and Aβ1-42) were separately prepared in anhydrous DMSO at 1 mg/ml. For each 1 ml of peptide solution, 50 µl of FITC solution was added very slowly in 5 µl aliquots while gently and continuously stirring the peptide solution. After the required amount of FITC had been added, the reaction was incubated in the dark for 8 hours at room temperature (20 °C). Ammonium chloride was added to a final concentration of 50 mM and the reaction mixture was further incubated for 2 hours at 20 °C. Excess or unreacted FITC was removed by dialysis against DMSO using a ready dialysis kit (Pur-A-Lyzer™ Mega Dialysis Kit). Briefly, the sample was loading into the Pur-A-Lyzer tube and sealed using a cap provided in the kit. The Pur-A-Lyzer tube was then placed in the supplied floating rack and left in a measuring cylinder containing a 25-fold excess of DMSO. The dialysis buffer was changed 4 times. The samples were then pipetted out carefully from the Pur-A-Lyzer tube to a clean tube and frozen in aliquots and stored at -20°C until further use.

Binding of FITC-labelled Amyloid peptides to platelets by flow cytometry: Isolated human platelets in suspension (at a density of 2 x 10^8 platelets/ml) were rested in a water bath (37°C) for 30 min before being incubated with FITC-Aβ peptides (10 µM) or FITC-Aβ peptides

with thrombin at (0.03 and 0.1 units/ml) for 30 min. Samples were diluted (1:10) with room temperature modified HEPES Tyrode and analysed immediately by flow cytometry.

2.2.2.7. Detection of ROS by Microplate Reader

Platelet rich plasma (PRP) was isolated from whole blood following the method above, and afterthe first centrifugation at 200 xg for 20 min. PRP was carefully collected in a single tube and placed in a 37°C water bath. The molecular probe carboxy-H2DCFDA (10 μM) was added to PRP and incubated for 45 min in a water bath (working in the dark from this point forward). Carboxy-H2DCFDA (pre-incubated with PRP) was then centrifuged at 500 xg for 10 min in the presence of PGE1 (0.1 μg/mL) and indomethacin (10 μmol/L) to obtain an isolated platelet pellet. Platelet-poor plasma (PPP) was discarded and the platelet pellet was resuspended in half PRP volume of modified Tyrode's-HEPES buffer (145 mM NaCl, 2.9 mM KCl, 10 mM HEPES, 1 mM MgCl2, pH 7.3; 5 mM D-glucose was added before use). Platelets were then rested for 15 min in a 37°C water bath. The platelet suspension was divided into sections to provide positive and negative controls. For negative controls, platelets were incubated with 1 and 30 mM ROS scavenger N-acetyl-L-cysteine (NAC) for 10 min. Different stimuli (H_2O_2, Aβ25-35, Aβ1-40, and Aβ1-42; 20 μM) were then added and incubated for another 10 min, then 200 μl of each condition were transferred to a 96-well plate and samples were analysed for dichlorofluorescein (DCF) using a microplate reader at excitation/emission wavelengths 485/530 nm.

2.2.2.8. Detection of Intracellular ROS in Platelets by Flow Cytometry

Following the platelet isolation method above, after the second centrifugation, the platelet pellet was resuspended in modified Tyrode's-HEPES buffer with glucose at a density of 2 $x10^8$ cells/ml and rested for 30 min in a 37°C water bath. Working in the dark, carboxy-H2DCFDA (10 μM) was added to the platelet suspension which was incubated for a further 30 min in the water bath. Where the ROS scavenger, NAC, was used, platelets were incubated with NAC prior to adding any stimulus. The effects of different concentrations of different stimuli on ROS generation in platelets were tested for 30 min. The samples were then further diluted with 1 ml cold Tyrode (4°C), placed on ice, and analysed by flow cytometry immediately. A minimum of 3 experiments were performed with 3 repeats per

condition, and an average of 10,000 events/sample were recorded. Data were obtained by BD FACSDiva software. Gate selection was performed using logarithmic side and forward scattering (SSC & FSC) with the gain set at 40 and 220 mV, respectively. Fluorescence excitation was at 485 nm, and emission was detected at 535 nm. The baseline for unstimulated samples was set at 100 relative fluorescence units. Statistical analysis of the data was performed using GraphPad Prism.

2.2.2.9. Detection of Superoxide Anion in Platelets by Flow Cytometry

Following the platelet isolation method above, after the second centrifugation, the platelet pellet was resuspended in modified Tyrode's-HEPES buffer with glucose at a density of 2 $x10^8$ cells/ml and rested for 30 min in a 37°C water bath. Working in the dark, DHE (5 μM) was added to the platelet suspension which was incubated for a further 15 min in the water bath. Platelets were then stimulated for 15 min with different physiological stimuli. Where ROS scavenger or NOX inhibitor was used, they were added to the platelets for 10 min prior to stimulation of the platelets with agonists. At the end of the incubation time, platelet suspensions were diluted 1:10 in cold modified Tyrode's-HEPES buffer and samples were then analysed immediately by flow cytometry using a 85 μ nozzle at low flow rate 3 (corresponds to approximately 10–80 μL/min). A minimum of 3 experiments were performed with 3 repeats per condition and an average of 10,000 events/sample were recorded. Data were obtained by BD FACSDiva software. Gate selection was performed using logarithmic side and forward scattering (SSC & FSC) with the gain set at 40 and 220 mV, respectively. Fluorescence excitation was with a violet laser at 405 nm and emission was collected at 580 nm with a LP600 filter. The baseline for unstimulated samples was set at 200 relative fluorescence units.

2.2.2.10. Detection of Superoxide Anion by Electron Paramagnetic Resonance (EPR)

Blood collection and platelet isolation, for these studies was carried out with the assistance of Dr. Dina Vara, Department of Pharmacy & Pharmacology, University of Bath. Detection of of superoxide anion using EPR was carried out by Dr. Dina Vara.

Preparation of EPR materials: Stock solutions of CMH spin probe (10 mM) for detection of superoxide anion were freshly prepared for each set of experiments in Tyrode-HEPES buffer

prepared with EPR grade water, containing 25 μM DF salt and 5 μM DETC. The solution was kept under argon on ice to keep an oxygen-free atmosphere.

Detection assay: Following the platelet isolation method described previously, platelet suspensions were prepared at physiological density of 2 x 10^8 platelets/ml then they were stimulated in the presence of 200 μM CMH with Aβ peptides (20 μM) with or without the NOX inhibitors (10 μM VAS2870, 0.5 μM 2-APT, scrambled NOXA1ds and NOXA1ds (10 μM), and scrambled NOX2ds-TAT and NOX2ds-TAT (10 μM). Inhibitors were pre-incubated for 10 min prior to stimulation using an aggregometer for platelet activation. After 10 min of stimulation, platelets were removed by a quick spin on a table top centrifuge and exactly 50 μl of supernatant was immediately transferred into the Hirschmann precision micropipettes and read using the e-scan. EPR spectra were recorded using the following EPR settings: field sweep, 80 G; microwave frequency, 9.39 GHz; microwave power, 2 mW; modulation amplitude, 5 G; conversion time, 327.68 ms; time constant, 5242.88 ms; 512 points resolution and receiver gain, 1×10^4. Samples for calibration curves were obtained from a 10 mM stock solution of a standard CM* solved in Tyrode-HEPES, and diluted to concentrations of typically 5, 10, 25, 50, 100 and 500 μM. The EPR signal from samples was expressed in CMH oxidation rate (femtomoles per platelet per minute) from the platelet density.

2.2.2.11. Amyloid Peptide β Fibrillation in Real Time Using Thioflavin T Assay

Based on the BMG LABTECH protocol, aggregation buffer was prepared (50 mM phosphate and 150 mM NaCl) and warmed in a water bath at 37 °C. 20 μM Thioflavin T was then added to the buffer and 200 μl of the Thioflavin T solution was transferred to a 96-well plate to make 3 replicates per condition. All β-amyloid peptides were then added at 100 μM and the well-plate was sealed and then immediately placed in the microplate reader for measurements. The fluorescence increase was measured continuously every 30 min from the bottom of the well with prior plate shaking (double-orbit mode) for 30 s at 500 rpm. The instrument settings were as follows: detection mode (fluorescence intensity, plate mode kinetics), optic (bottom optic), orbital averaging (activated, 4 mm diameter), filters (excitation: 440-10 and emission: 480-10), number of cycles (90), cycle time (1800 sec), number of flashes (10), instrument temperature (37 °C). Raw data was obtained and analysed using MARS Data analysis software and GraphPad Prism.

CHAPTER 3

Effects of Aβ Peptides on Platelet Functional Responses

3. RESULTS

3.1. BACKGROUND

Vascular pathologies and AD are age-related diseases that share significant overlaps in their pathophysiological mechanisms, including vascular dysfunction, atherothrombosis and blood hypoperfusion [81]. Hypoperfusion is particularly important in dementia (including AD), as it affects numerous cellular functions, such as glucose uptake, oxygen delivery, and regulation of cellular waste metabolites and toxins, which leads to chronic localised inflammation and oxidative stress [49, 322-326]. Hypoperfusion also interferes with Aβ elimination from the brain parenchyma resulting in its pathological accumulation in the brain and within the cerebrovasculature [327].

Platelets are considered major players in vascular diseases and a number of studies have revealed considerable abnormalities in platelets of AD patients or animal models of this disease. These include altered APP processing and APP isoform ratios that correlated with cognitive decline [280, 292, 328], aberrant pre-activation state [151], altered membrane fluidity [171, 279], cytochrome c oxidase deficiency [309], increased platelet mitochondrial respiration, and oxidative stress [289, 309, 329-331], enhanced platelet adhesion, and accumulation of vascular Aβ deposition [295]. The observation of platelet adhesion to vascular Aβ deposition sites raised the question of how Aβ may modify haemostasis and thrombosis. An increasing number of studies have consequently investigated the relationship between Aβ and platelet activation and their contribution to cerebrovascular complications associated with AD and CAA progression [153, 275, 295, 298, 306, 307, 332-334].

Platelets are considered to be a major contributor of Aβ in the blood as they express large amounts of APP with all the enzymatic and machineries for its metabolism [154, 155]. Upon platelet activation, they release stored Aβ peptides from their α-granules [335] along with other potent platelet agonists into the blood to activate other platelets within its vicinity. Since vascular Aβ deposits have been shown to recruit platelets to the site of cerebrovascular injury and lead to their activation, the accumulation of Aβ may represent a positive feedback mechanism inducing platelet activation on one hand, and stimulating further Aβ deposition on the other [295, 298].

In AD, platelets are in an aberrant pre-activated state [151],which creates a highly prothrombotic environment within the cerebrovascular system, but the mechanism by which Aβ triggers platelet activation is not well understood. In one study it was shown that the fibrillar form of Aβ1-40 induced platelet aggregation in a concentration-dependent manner,

and when antibodies were used against integrin $\alpha_{IIb}\beta_3$, it blocked platelet adhesion to fibrillar Aβ1-40 but no direct peptide interaction with purified integrin $\alpha_{IIb}\beta_3$ was detected [336]. These observations suggested that the interaction of fibrillar Aβ1-40 with platelets is mediated by integrins with the indirect involvement of GPIIb/IIIa (i.e. integrin $\alpha_{IIb}\beta_3$), possibly through fibrinogen [336].

A more recent study demonstrated that fibrillar Aβ1-40 does indeed induce platelet activation and aggregation through two pathways. One of these is a GPIbα-dependent pathway, where GPIbα is a VWF receptor and a component of platelet receptor complex GPIB-IX-V [302]. GPIB-IX-V activation triggers a downstream intercellular stimulation of tyrosine kinases, such as FAK and Pyk2 that mediates clustering and phosphorylation of ITAM tyrosine residues in the FcRγ cytoplasmic domain by Src-family kinases (SFKs) [337]. Subsequently, this leads to the engagement and activation of Syk, and downstream signalling activation of PI3K/PLCγ2/DAG/IP3/Ca^{2+}/PKC causing platelet granule secretion, inside-out activation of integrin $\alpha_{IIb}\beta_3$, arachidonic acid mobilization and TXA2 release, thus mediating platelet aggregation [302, 338, 339]. The second is where fibrillar Aβ1-40 was shown to induce platelet aggregation through a second pathway where it binds to a scavenger receptor CD36-dependent cascade following p38MAPK/COX1 activation pathway and results in TXA2 release [302].

A number of studies have explored the use of the synthetic Aβ25-35 peptide, which retains the biological and toxic properties of the full length Aβ1-42 and Aβ1-40, in order to understand the effects of the endogenous peptides on platelets [296, 297, 300, 301, 303, 306, 340]. Aβ25-35 induced abnormal changes in intracellular calcium in normal human platelets [301]. In two studies, the authors mentioned that they carried out pilot work that was not published, where they compared the effects of Aβ25-35 and Aβ1-40 in inducing platelet activation. They stated that their initial experimental work showed that these two peptides had equal potencies in exerting their effects on platelets, hence they chose to use Aβ25-35 for their subsequent experiments in their publications [296, 297].

The authors demonstrated that Aβ25-35 induces platelet activation through thrombin receptor PAR1 and activates platelets through Ras-PI3K-Akt-p38 MAPK-cPLA2 signalling pathway resulting in TXA2 release. Aβ25-35 also affected platelets in a dose-dependent manner, where at lower concentrations (0.5–2 μM), it potentiated agonist-induced platelet aggregation (collagen and ADP), while at higher concentrations (2–10 μM), it directly activated the aggregatory responses without the presence of co-agonists. Immunoblotting analysis revealed that Aβ25-35 at 2–10 μM produced marked phosphorylation of PLCγ2 and

platelet activation, suggesting that Aβ stimulation of platelet aggregation is, at least partly, mediated by the PLCγ2-PKC signalling pathway [296, 297].

A previous study done in our laboratory tested the effects of Aβ25-35 on platelet activation and signal transduction and showed that Aβ25-35 promotes an increase in intracellular Ca^{2+}, dense granule mobilization, and ADP release that can act in an autocrine/paracrine fashion to activate platelets [303]. Aβ25-35 induced platelet aggregation was shown to be dependent on endogenous ADP release and immunoblotting analysis revealed time-dependent phosphorylation of several key signalling molecules involving Syk-PI3K/Akt-MAPkinases/PKC substrate pleckstrin [303]. Another group, showed that Aβ25-35 increased platelet adhesion to collagen under flow conditions, and at 10 – 20 μM, it elicited similar effects to physiological agonists and induced strong platelet aggregation and integrin activation. Furthermore, at 20 μM, Aβ25-35 modulated cytoskeletal reorganization through RhoA/ROCK/MLC and its phosphatase (MYPT1); RhoA/Rap1b activation and inside-out integrin $\alpha_{IIb}\beta_3$ expression [306].

In the same year, a different group explored the effects and cellular mechanisms triggered by Aβ1-40 on platelets and highlighted additional important aspects of platelet signalling in response to these peptides [295]. The authors showed that exposure to Aβ1-40 induces ROS generation, membrane scrambling and phosphatidylserine exposure, mitochondrial depolarization, and activation of caspase-3. In addition, platelets were shown to mediate the organisation of soluble Aβ1-40 into a fibrillar form in a time and concentration-dependent manner [295]. A recent supporting study showed that soluble Aβ1-40 was able to bind to integrin $\alpha_{IIb}\beta_3$ via its RHDS amino acid motif and this stimulated the secretion of ADP and the chaperone protein clusterin [307].

Clusterin promoted the formation of fibrillar Aβ1-40 aggregates, while ADP acted through its receptors P2Y1 and P2Y12 on platelets and enhanced the outside-in activation of integrin $\alpha_{IIb}\beta_3$, reinforcing the secretion of more clusterin and Aβ1-40 binding to platelets [307]. However, a follow up study showed that the RHDS amino acid motif of Aβ is important for integrin binding but not sufficient for binding Aβ to it and it requires other recognition or binding motifs for platelet-mediated fibril formation [341]. Another study showed that Aβ1-40 enhanced platelet adhesion under static and dynamic flow conditions, and showed platelet localization at Aβ vascular deposit sites of the cerebral vessel wall in APP Dutch and APP23 transgenic mice [295].

These previously mentioned studies highlight the potential role of Aβ peptides in platelet dysfunction associated with CAA and AD. However, several aspects of the effects of Aβ peptides on platelets remain unclear. There is no previous study that has compared the effects of the different peptides side-by-side in a systematic manner, and the majority of these studies utilized Aβ25-35 as a representative peptide. Even though Aβ25-35 is known to represent the biologically active region that mediates full length Aβ toxicity, its effects do not entirely represent the effects of the full length Aβ1-40 and Aβ1-42. Therefore, the present study aimed at investigating the effects of such Aβ peptides (i.e. Aβ1-40, Aβ1-42, Aβ25-35, and scrambled Aβ1-42 as control) on platelets in order to understand the potential mechanisms involved in platelet recruitment to the vascular Aβ deposit sites in AD. Understanding the molecular mechanisms underlying the ability of Aβ peptides to modulate haemostasis and thrombosis may represent an additional therapeutic avenue in the treatment of AD.

3.2. AIMS & OBJECTIVES

- Determine the effects of Aβ peptides i.e. Aβ25-35, Aβ1-40, Aβ1-42, and scrambled Aβ1-42 as control, on platelet adhesion, activation, and spreading using adhesion assay under static conditions.
- Determine the effects of Aβ peptides as agonists or co-agonists on platelet aggregation using turbidimetric aggregometry.
- Determine the effects of Aβ peptides on platelet adhesion under physiological shear stress using microfluidic pump.
- Determine Aβ peptide-induced platelet activation by measuring P-selectin expression and integrin $\alpha_{IIb}\beta_3$ activation using flow cytometry.

3.3. RESULTS

3.3.1. Aβ25-35 solid phase peptide synthesis (SPPS)

The initial aim was to synthesize a range of different Aβ peptides i.e. Aβ25-35, Aβ1-40, Aβ1-42, and scrambled Aβ1-42 as control. Full-length Aβ peptides have been typically regarded as 'difficult sequences' to synthesize by SPPS, like many peptides of > 30-50 amino acids. The quality and yield of such peptides may often be dramatically decreased due to incomplete coupling and deprotection reactions as a result of the formation of secondary structures and aggregation during the synthesis.

Recent advances in SPPS methods, particularly the application of microwave activation, have allowed these problems to be overcome allowing the successful production of longer Aβ peptides [342]. By comparison, Aβ25-35 is a short peptide, which should not pose significant problems, and it was successfully and easily synthesised and characterised by mass spectrometry and HPLC as shown in Figure 3.1. Due to time constraints and the inherent synthetic challenges for the longer peptides, these peptides were obtained from commercial sources as they were required only as tools and their synthesis was not one of the main aims of this project.

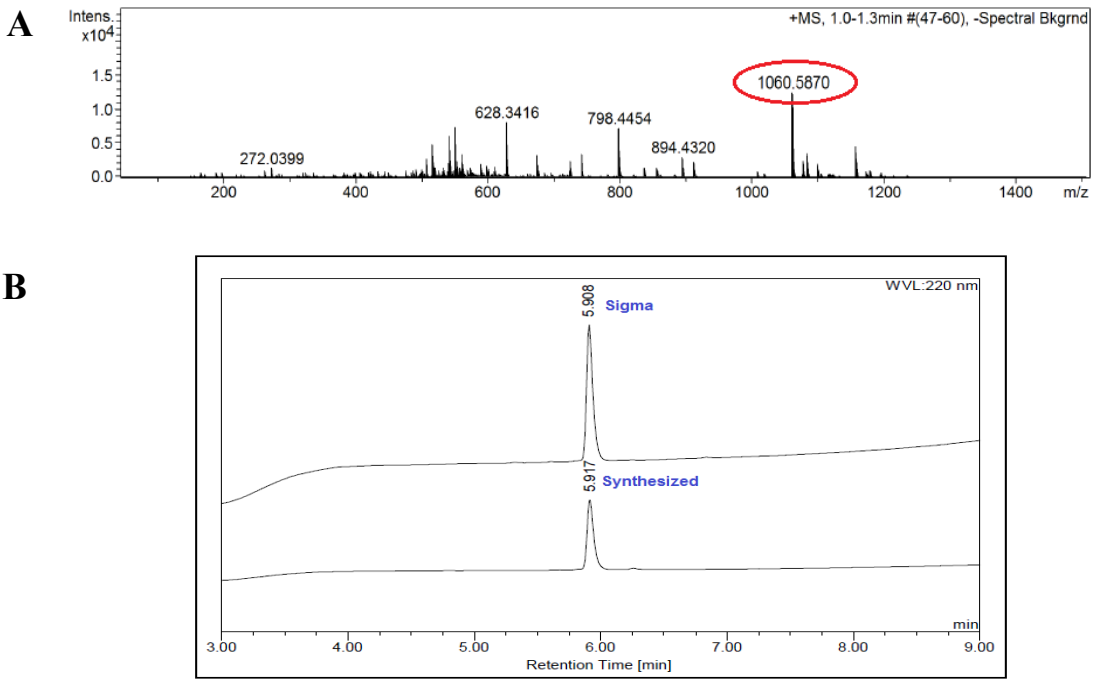

Figure 3.1: Aβ25-35 peptide synthesis.
(A) MS analysis of synthesized Aβ25-35; Expected formula = $C_{45}H_{81}N_{13}O_{14}S$, Theoretical m/z = 1059.5746; found ESI = 1060.5870 $[M+H]^+$. (B) RP-HPLC analysis between in-house synthesized Aβ25-35 and commercially available Aβ25-35 (Sigma), with t_R = 5.917 min and t_R = 5.908 min respectively.

3.3.2. Aβ peptides support platelet adhesion under static conditions

In order to determine the effects of Aβ peptides on platelet adhesion and morphological changes, collagen type I and fibrinogen, which are potent thrombogenic proteins that promotes platelets activation and aggregation, were used as positive controls in the present study. This allows the evaluation of platelet adhesion and spreading when compared to the effects of Aβ peptides on platelets. Platelet adhesion to collagen or fibrinogen was assessed under static conditions using an adhesion assay mentioned previously in Chapter 2.

Briefly, isolated human platelets in suspension (2×10^7 platelets/ml) were allowed to adhere over collagen type I (25 µg/ml), fibrinogen (100 µg/ml), or BSA (5 mg/ml)-coated surfaces under static conditions for 30 min. Non-adhering platelets were washed off, then platelets were fixed with 4% paraformaldehyde (PFA), permeabilized with 0.1% Triton-x100/PBS, and stained with TRITC-conjugated phalloidin, then mounted on to a microscope slide using Vectashield. Digital images were taken of platelet adhesion and spreading area and analysed at 10x and 100x magnification. Representative images of platelet adhesion and spreading area for each of the conditions are shown in Figure 3.2 (A and B).

Quantification and analysis of the average number of adhered platelets and spreading area are shown in Figure 3.2 (C and D). Both collagen and fibrinogen significantly induced platelet adhesion and spreading compared to BSA (P-value<0.05 and P-value<0.01 respectively) in our experimental conditions. Morphological changes associated with platelet activation displayed in images (A and B), show different stages of platelet shape change. Some of the adhered platelets display round shapes morphology as shown with BSA, while others have irregular shapes with filopodia and lamellipodia (full spreading) with collagen or fibrinogen.

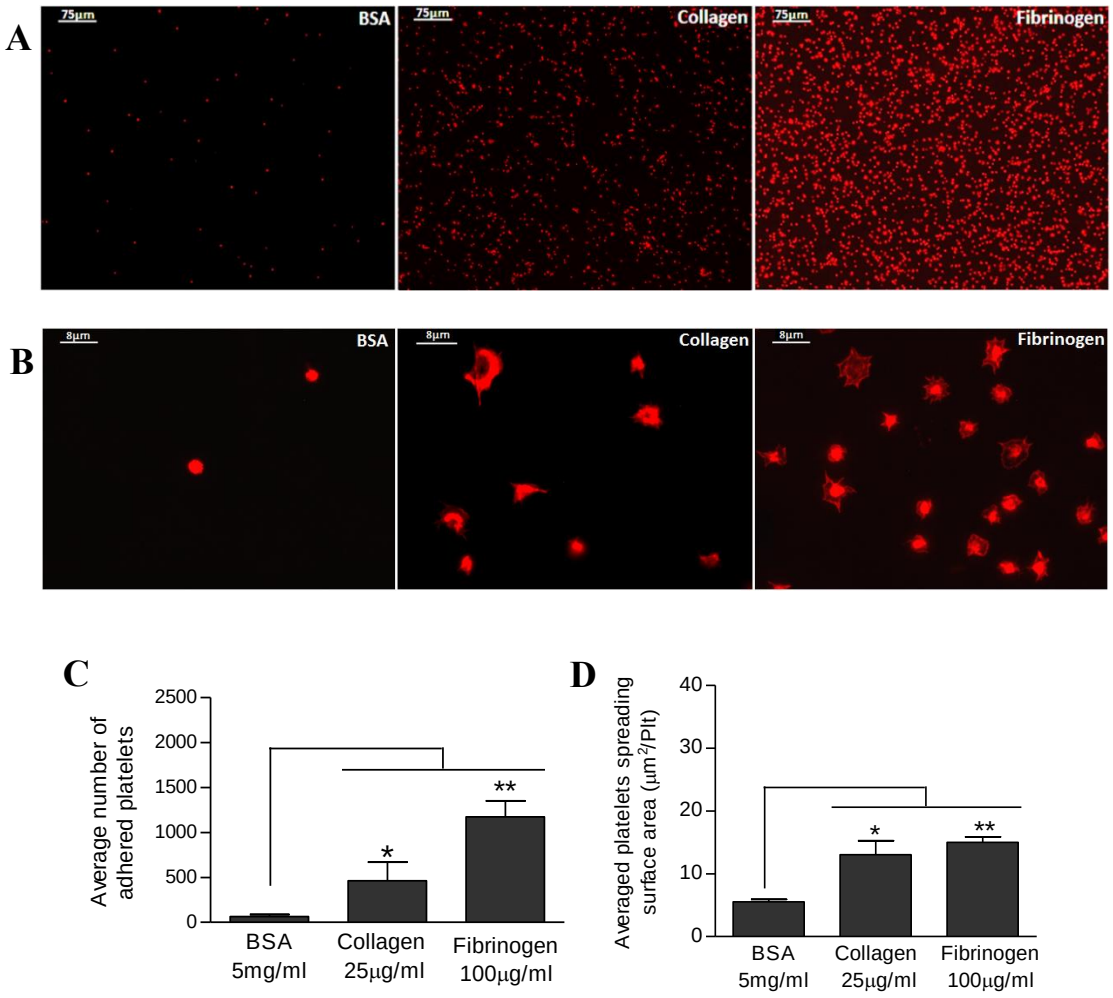

Figure 3.2: Platelet adhesion and spreading area over collagen or fibrinogen-coated surfaces under static conditions.

(A-B) Representative images of platelets that were allowed to adhere onto glass coverslips coated with BSA (5 mg/ml), collagen type I (25 µg/ml), or fibrinogen (100 µg/ml). Platelets were then fixed, stained, then visualized under the fluorescence microscope and images were taken at 10x and 100x magnification. (C-D) Quantification and evaluation of the mean number of adhered platelets and mean spreading area per optical field from at least 4 independent experiments. Both collagen and fibrinogen show significant increase in the mean number of adhered platelets and spreading area when compared to BSA. Statistical significance was assessed using one-way ANOVA with Bonferroni post-test; P-value < 0.05 (*), and P-value <0.01 (**). Error bars represent mean ± SEM.

Normally, circulating plasma Aβ peptides are present at concentrations of around (mean±SD: 84.7±19.6 pg/ml for Aβ1-40, and 14.2±4.5 pg/ml for Aβ1-42) [343]. However, in order to carry out experiments *in vitro*, much higher concentrations were utilized in previous studies to measure an effect on platelets, as mentioned previously. With regards to physiological relevance, the effects of using higher Aβ concentrations may reflect and correlate to the levels of vascular Aβ deposits that have been shown to accumulate in atherosclerotic lesions and AD cerebrovasculature, and their ability to recruit platelets to the site of cerebrovascular injury and lead to their activation, enhancing thrombus formation at the site, which may eventually lead to full vessel occlusion [295].

In order to assess the effects of Aβ peptides on platelet adhesion and morphological changes, adhesion assays were carried out as described in Chapter 2 (Methodology). Representative images for platelet adhesion and spreading area are shown in Figure 3.3 (A and B). The average numbers of adhered platelets and mean spreading area were quantified and represented in Figure 3.3 (C and D).

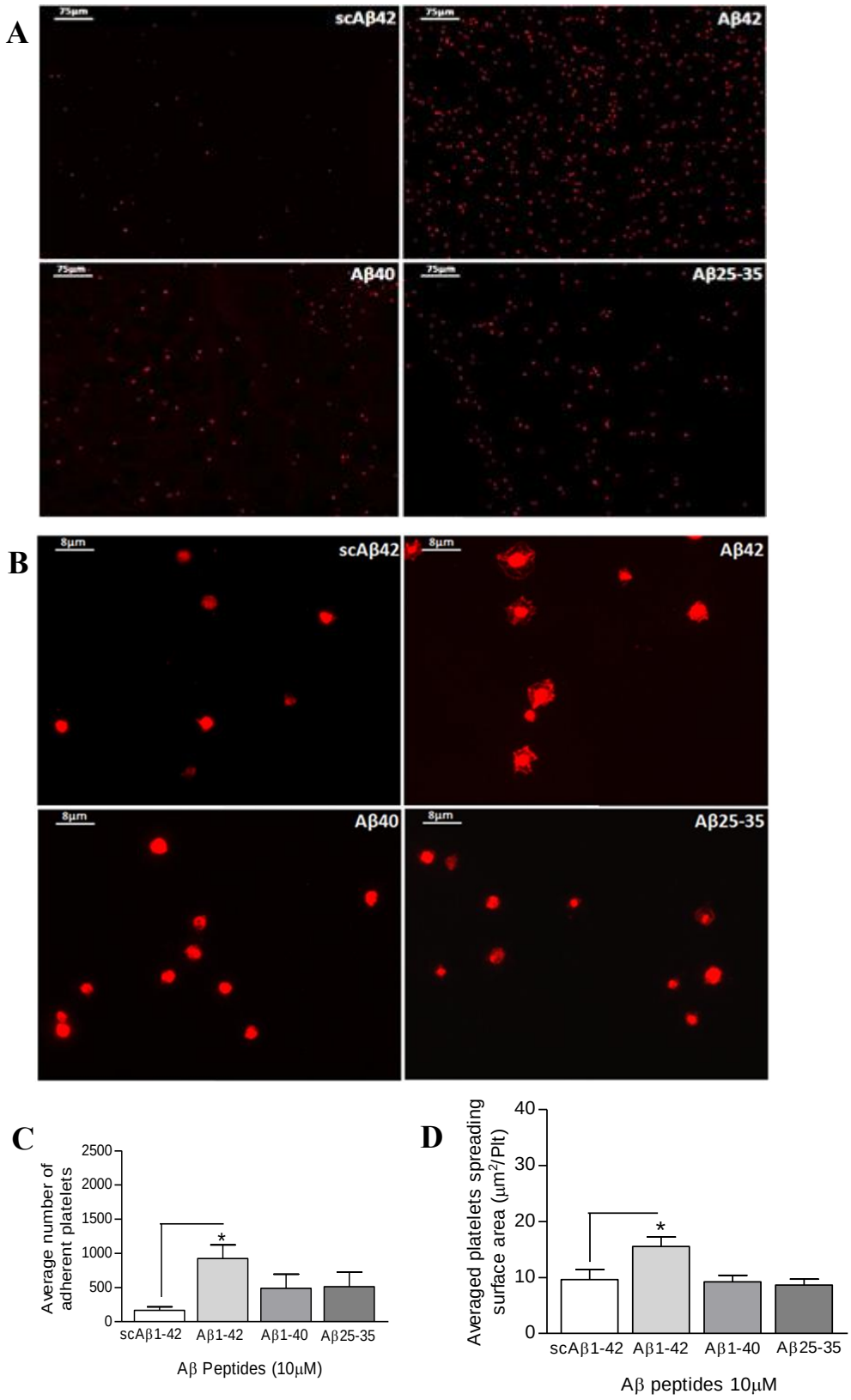

Figure 3.3: Aβ peptides support platelet adhesion under static conditions.
(A-B) Representative images of platelets that were allowed to adhere onto glass coverslips coated with 10 μM Aβ peptides (scrambled Aβ1-42 as control, Aβ1-42, Aβ1-40 and Aβ25-35). Platelets were then fixed, stained, then visualized under the fluorescence microscope and images were taken at 10x and 100x magnification. (C-D) Quantification and evaluation of the mean number of adhered platelets and mean spreading area per optical field from at least 4 independent experiments. Only Aβ1-42 show significant increase in the mean number of adhered platelets and spreading area when compared to scrambled control. Statistical significance was assessed using one-way ANOVA with Bonferroni post-test; P-value < 0.05 (*). Error bars represent mean ± SEM.

Interestingly, only Aβ1-42 shows a significantly higher number of adhered platelets and increased spreading area (P-value <0.05) compared to the scrambled Aβ1-42 control and the other two peptides. With that being said, this study also shows moderate adhesion of platelets to Aβ1-40 and Aβ25-35 compared to scrambled control. To understand the thrombogenic potential of Aβ peptides and determine their ability to exacerbate vascular dysfunction within neurovascular lesions associated with CAA, this study also examined the concomitant presence of Aβ peptides with collagen or fibrinogen under static conditions following the adhesion assay mentioned previously.

Representative images of platelet adhesion and spreading area are shown in Figure 3.4 (A and B) for collagen and Figure 3.5 (A and B) for fibrinogen. The average number of adhered platelets and mean spreading area were quantified and represented in Figure 3.4 (C and D) for collagen and Figure 3.5 (C and D) for fibrinogen. Aβ1-42 with collagen appears to induce similar effects on platelet adhesion compared to Aβ1-42 without collagen, as do the other peptides under our experimental conditions. However, while it is evident that the effects of Aβ peptides moderately enhanced platelets spreading, no statistical significance was obtained when compared to scrambled control.

Previous studies have reported that platelets have shown strong integrin activation, degranulation, and spreading kinetics over fibrinogen in AD transgenic mice (APP23) [298]. Therefore, the effects of Aβ peptides with fibrinogen on platelets were also examined. The results show enhanced platelet adhesion to all the peptides, especially Aβ1-42, but not much change in terms of spreading area. The results in this study are in agreement with previous studies and show enhanced platelet adhesion. However, the results are not statistically significant and further experiments are required to obtain it.

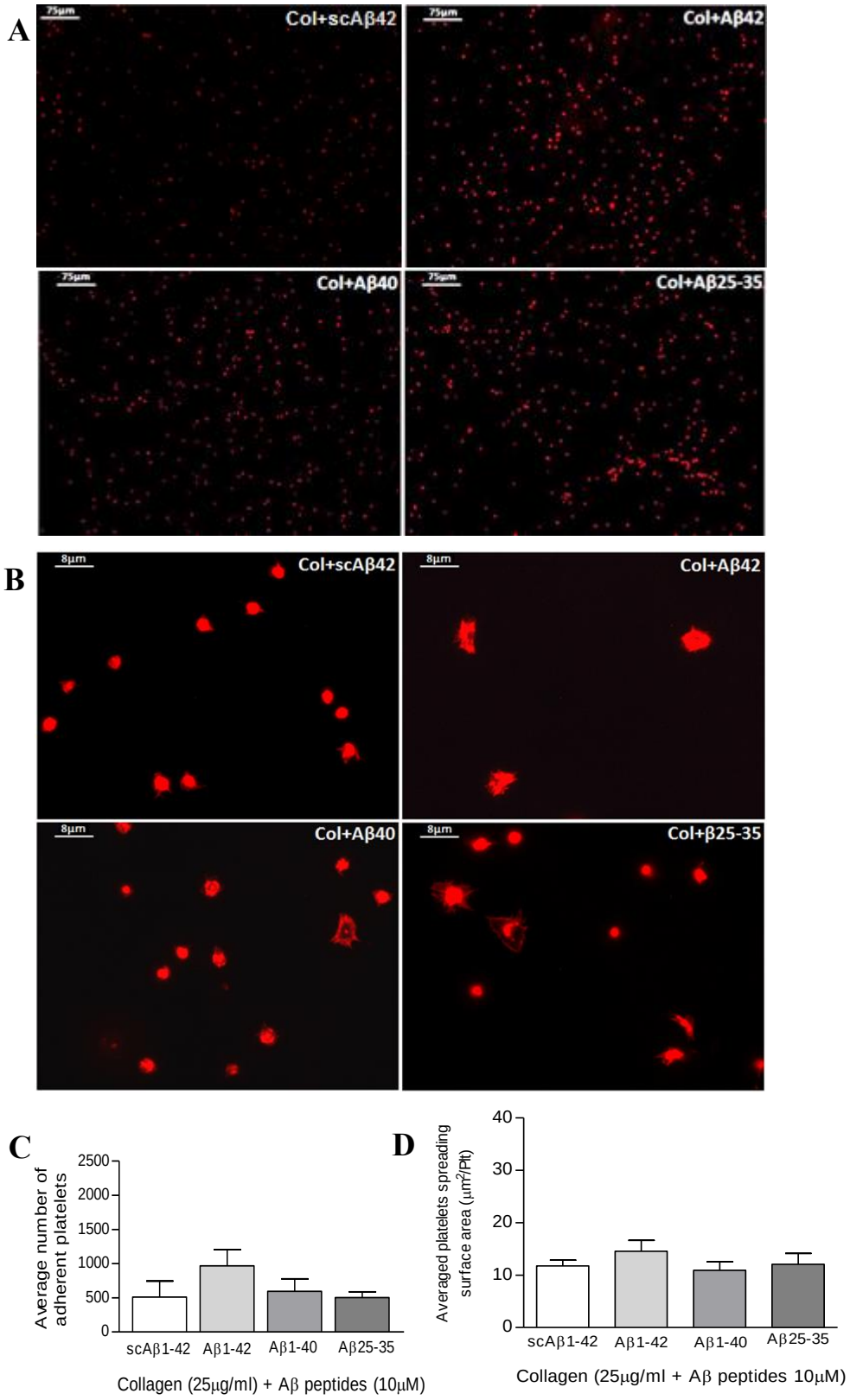

Figure 3.4: Platelet adhesion and spreading onto dual coated surfaces with collagen and Aβ peptides under static conditions.

(A-B) Representative images of platelets that were allowed to adhere onto glass coverslips coated with 25 μg/ml collagen type I and 10 μM Aβ peptides (scrambles Aβ1-42 as control, Aβ1-42, Aβ1-40 or Aβ25-35). Platelets were then fixed, stained, then visualized under fluorescence microscope and images were taken at 10x and 100x magnification. (C-D) Quantification and evaluation of the mean number of adhered platelets per optical field from at least 4 independent experiments. No statistical significance was shown compared to scrambled control using one-way ANOVA with Bonferroni post-test. Error bars represent mean ± SEM.

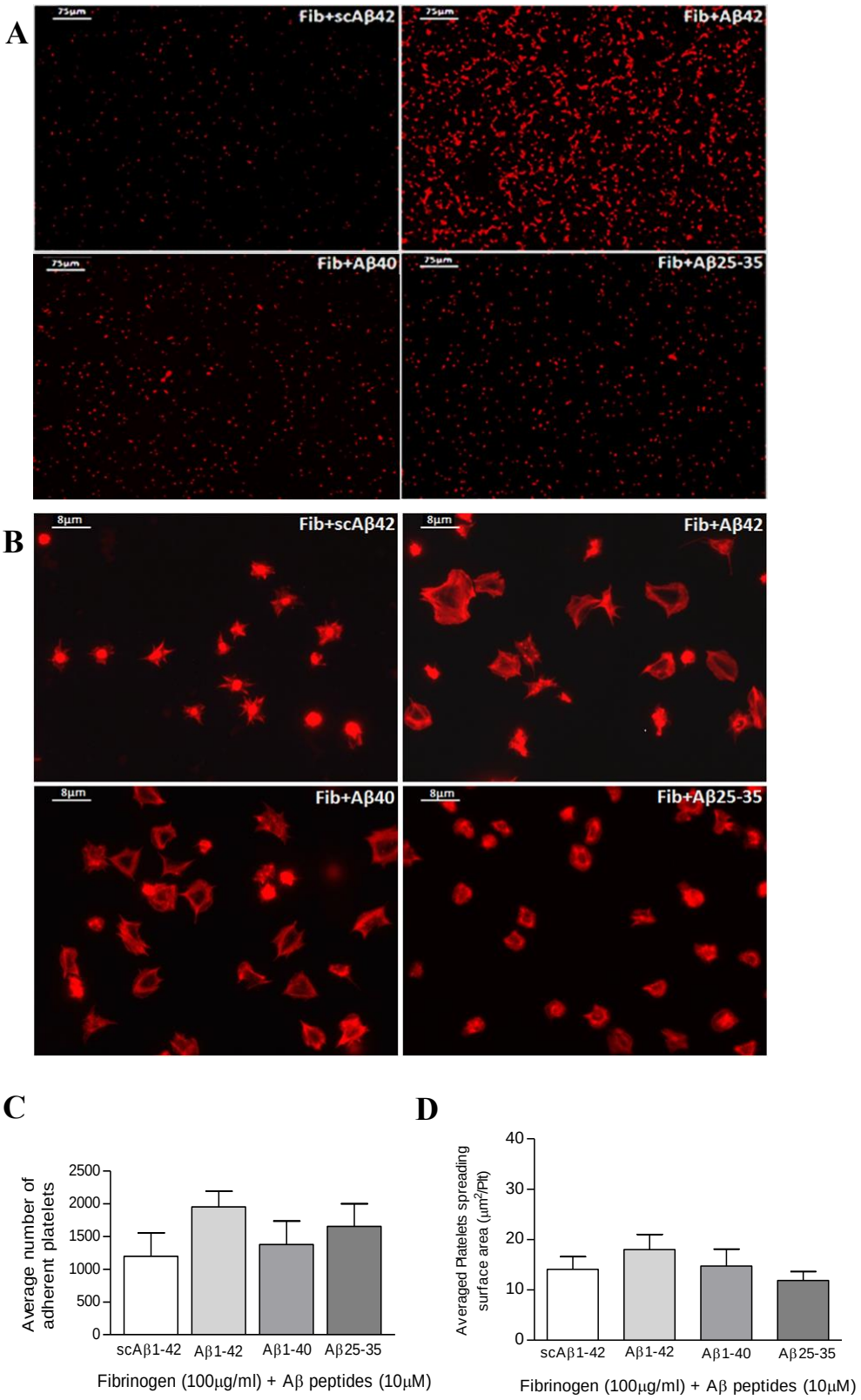

Figure 3.5: Aβ peptides potentially enhance platelet adhesion in the presence of fibrinogen.
(A-B) Representative images of platelets that were allowed to adhere onto glass coverslips coated with 100 µg/ml fibrinogen and 10 µM Aβ peptides (scrambles Aβ1-42 as control, Aβ1-42, Aβ1-40, or Aβ25-35). Platelets were then fixed, stained, then visualized under fluorescence microscope and images were taken at 10x and 100x magnification. (C-D) Quantification and evaluation of the mean number of adhered platelets and mean spreading are per optical field from at least 4 independent experiments. No statistical significance was shown compared to scrambled control using one-way ANOVA with Bonferroni post-test. Error bars represent mean $\pm$ SEM.

3.3.3. Effects of Aβ peptides as agonists or co-agonists on platelet aggregation

Since Aβ peptides had been shown to affect platelet adhesion and activation under static conditions, a series of experiments were carried out to examine the level of platelet aggregation in response Aβ peptides as agonists or co-agonists with two potent physiological platelet stimuli, thrombin or collagen. Initially, experiments were conducted to examine the level of platelet aggregation in response to thrombin at concentrations of 0.05 and 0.1 unit/ml, and collagen at concentrations of 3 and 10 µg/ml, measured by turbidimetric aggregometer (see Chapter 2 for methodology). This allowed the confirmation of the agonists' ability to stimulate platelets under the chosen experimental conditions. Both thrombin and collagen were found to induce significant platelet aggregation to varying degrees at different concentrations as shown in Figure 3.6.

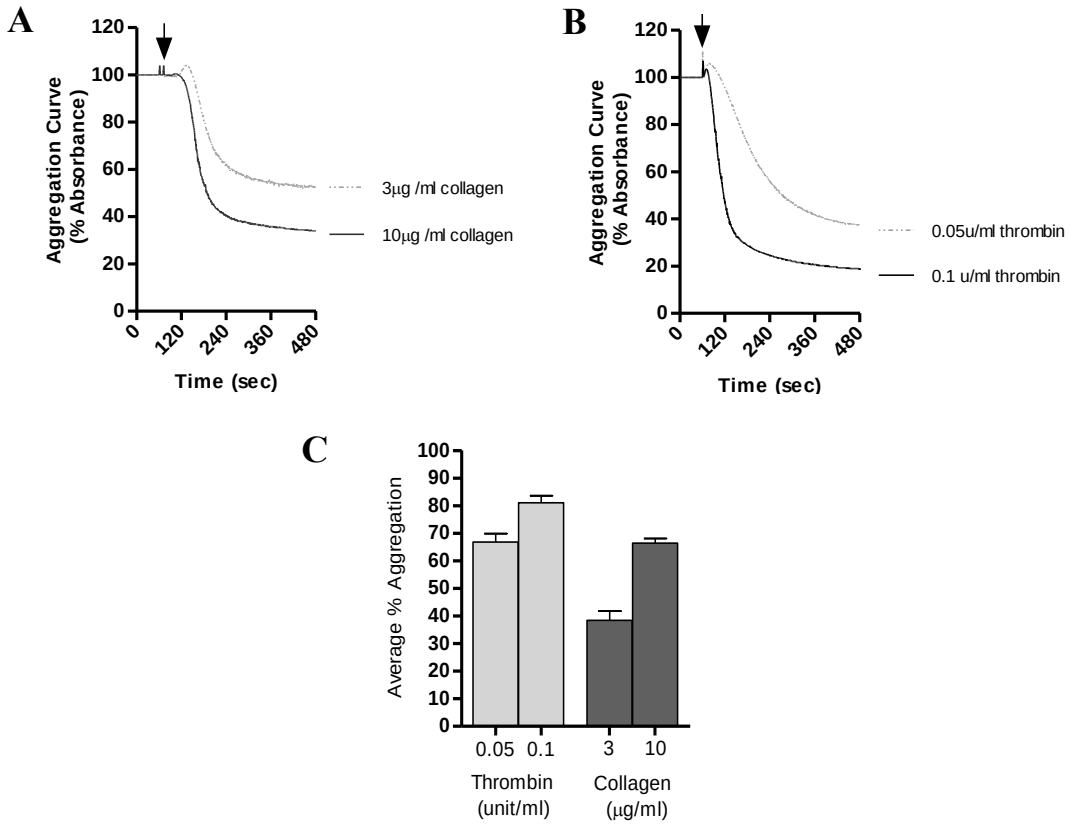

Figure 3.6: Platelet aggregation in response to thrombin or collagen.
Platelet aggregation experiments were performed using a 490D aggregometer. (A) Representative aggregation curves induced by two collagen concentrations (3 and 10 µg/ml). (B) Representative aggregation curves induced by two thrombin concentrations (0.05 and 0.1 units/ml). (C) Average percentage aggregation quantified from 4 independent experiments. Error bars represent mean ± SEM.

With regards to the physiological relevance of thrombin in blood, no diagnostic assay is currently available that enables the direct measurement of thrombin concentrations, and its presence in healthy individuals can trigger clot formation in circulating blood, However,

prothrombin (thrombin precursor) was reported to circulate at around 1.4 µM [344]. Representative aggregation curves are shown in Figure 3.6 (A and B), while the average percentage aggregation that was quantified from 4 independent experiments is shown in Figure 3.6 (C).The effects of Aβ peptides as agonists on platelet aggregation were assessed next following the previously indicated aggregation methodology and the results are shown in Figure 3.7. Representative aggregation curves are shown in Figure 3.7 (A-C), while the average percentage aggregation is shown in Figure 3.7 (D). Only Aβ1-42 showed statistical significance (P-value < 0.05) at a concentration of 20 µM (the most common *in vitro* concentration used in previous studies) and moderate platelet aggregation compared to scrambled peptide control while the other peptides did not.

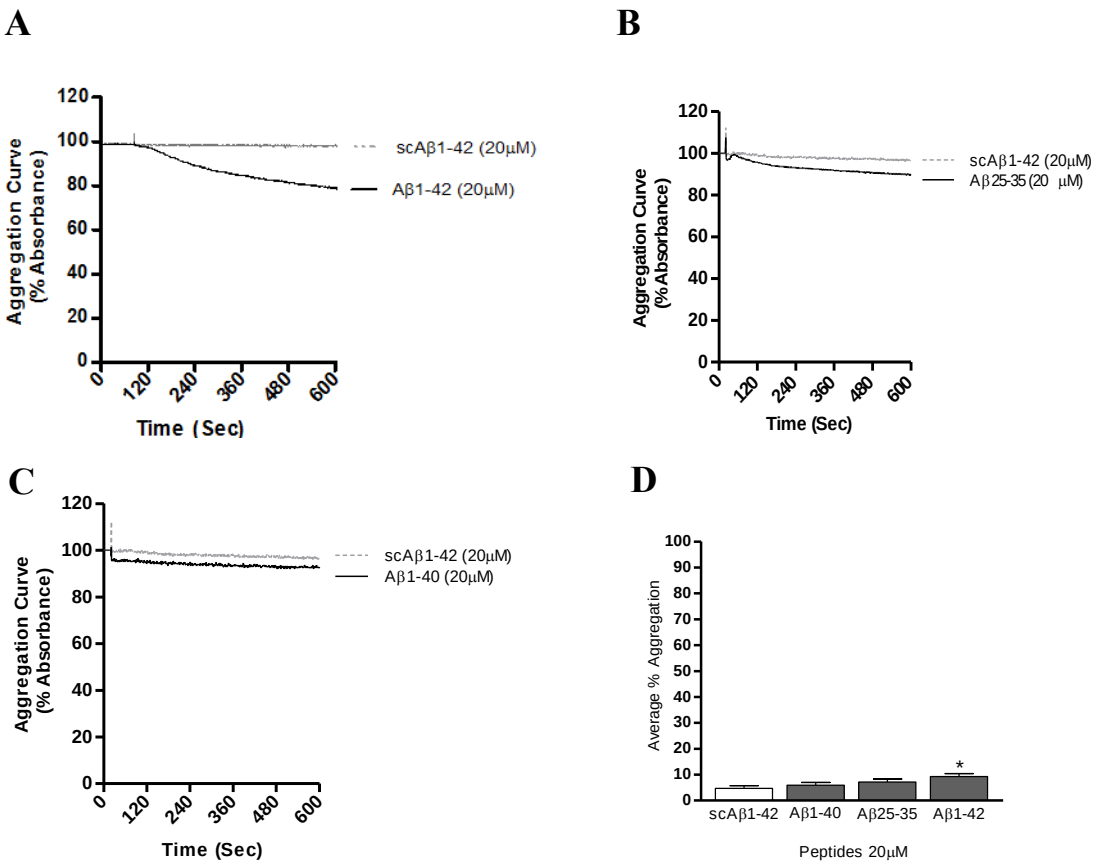

Figure 3.7: Examining platelet aggregation in response to amyloid peptides as agonists.
Platelet aggregation experiments were performed using a 490D aggregometer. (A-C) Representative aggregation curves induced by 20 µM of scrambled Aβ1-42 as control and, Aβ1-42 (A), Aβ25-35 (B), or Aβ1-40 (C). (D) Average percentage aggregation quantified from 4 independent experiments. Only Aβ1-42 show significant increase in percentage aggregation compared to scrambled control. Statistical significance was analysed using one-way ANOVA with Bonferroni post-test; P-value < 0.05 (*). Error bars represent mean ± SEM.

Further experiments were conducted to determine the effects of Aβ peptides on platelet aggregation upon co-stimulation with a submaximal concentration (assessed previously from Figure 3.6) of 3 µg/ml collagen type I and 0.05 units/ml thrombin. Representative

aggregation curves are shown in Figure 3.8 (A-C) for co-stimulation with collagen and Figure 3.9 (A-C) for co-stimulation with thrombin. Average percentage aggregation is shown in Figure 3.6 (D) for collagen and Figure 3.9 (D) for thrombin.

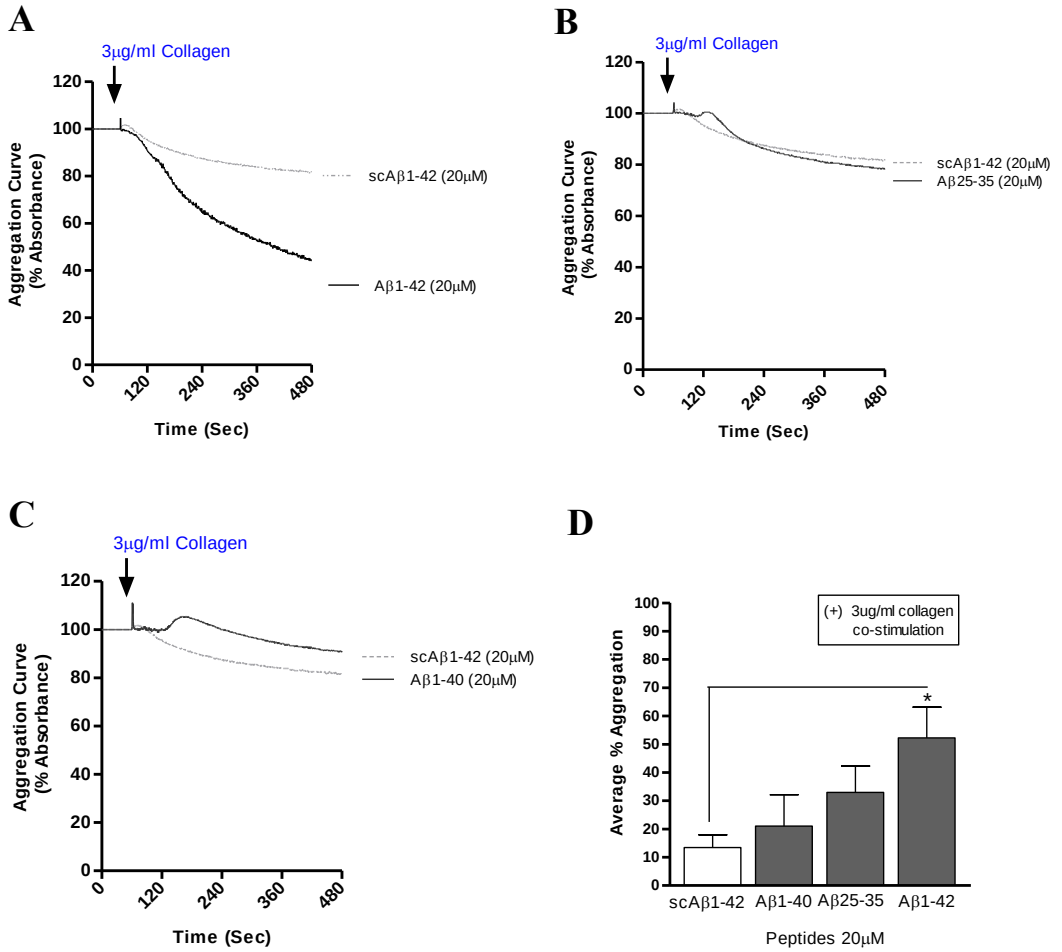

Figure 3.8: Potentiation of platelet aggregation in response to amyloid peptides with collagen.
Platelet aggregation experiments were performed using a 490D aggregometer. (A-C) Representative aggregation curves induced by collagen 3 µg/ml and 20 µM of scrambled Aβ1-42 as control and, Aβ1-42 (A), Aβ25-35 (B), or Aβ1-40 (C). (D) Average percentage aggregation quantified from 4 independent experiments. Only Aβ1-42 potentiated significant increase in in average percentage aggregation compared to scrambled control in the presence of collagen. Statistical significance was analysed using one-way ANOVA with Bonferroni post-test; P-value < 0.05 (*). Error bars represent mean ± SEM.

Looking at the results in Figure 3.8, only Aβ1-42 in the presence of collagen potentiated a significant aggregation response compared to scrambled control. Other peptides did not induce significant aggregation response when compare scrambled control. Similarly, only Aβ1-42 in the presence of thrombin potentiated a strong and significant aggregation response compared to scrambled control as shown in Figure 3.9. In addition, Figure 3.9 (A) shows a secondary potentiation phase, which could indicate the release of secondary agonists, e.g. ADP, as mentioned in a previous study conducted in our laboratory [303].

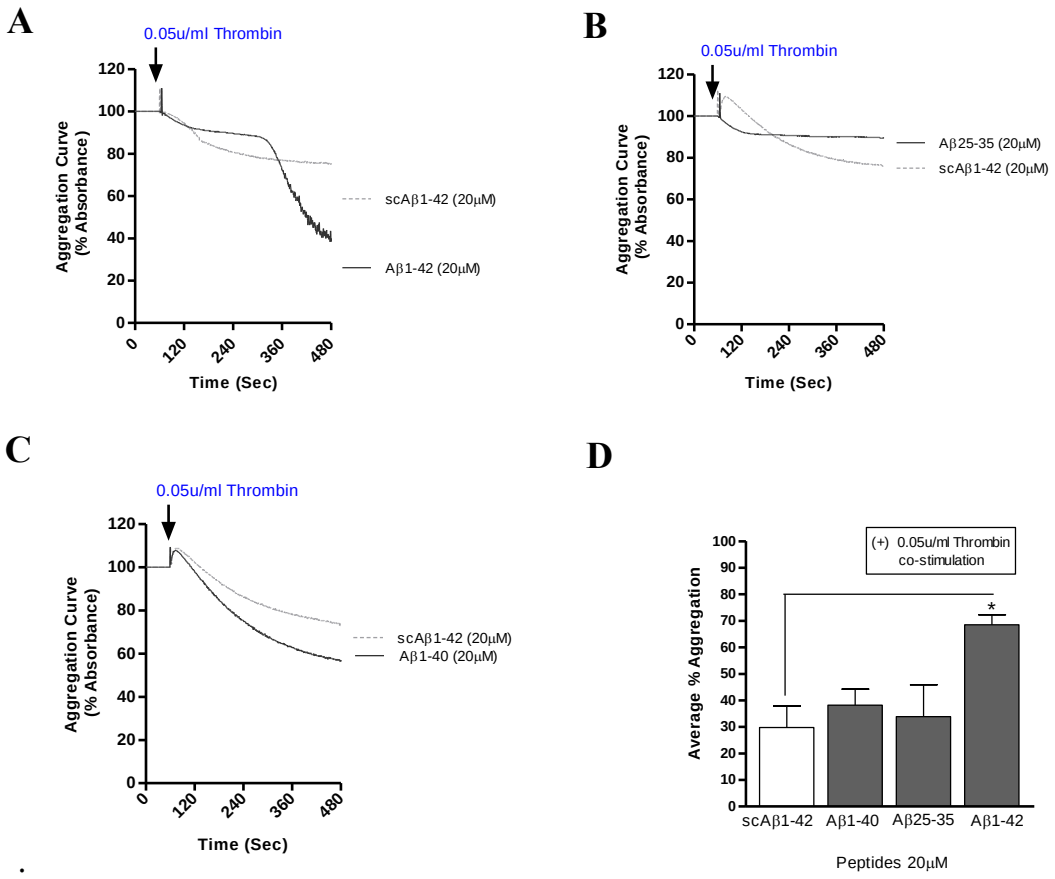

Figure 3.9: Potentiation of platelet aggregation in response to amyloid peptides with thrombin. Platelet aggregation experiments were performed using a 490D aggregometer. (A-C) Representative aggregation curves induced by thrombin 0.05 u/ml and 20 μM of scrambled Aβ1-42 as control and, Aβ1-42 (A), Aβ25-35 (B), or Aβ1-40 (C). (D) Average percentage aggregation quantified from 4 independent experiments. Only Aβ1-42 potentiated significant increase in in average percentage aggregation compared to scrambled control in the presence of thrombin. Statistical significance was analysed using one-way ANOVA with Bonferroni post-test; P-value < 0.05 (*). Error bars represent mean ± SEM.

3.3.4. Aβ1-42 increases thrombus formation in whole blood under physiological venous flow conditions

The previous adhesion assays showed that Aβ peptides, especially Aβ1-42, support platelet adhesion under static conditions, induce moderate platelet aggregation as agonists, and potentiate platelet aggregation in the presence of other physiological agonists (i.e. collagen or thrombin). Therefore, platelet adhesion and thrombus formation under physiological shear stress in vitro was next examined for Aβ1-42 using a microfluidic pump, as this resembles normal human physiological blood flow conditions within the systemic circulation. Platelet adhesion was tested using human whole blood at an arterial shear rate of 1,000 sec^{-1} and a venous shear rate of 200 sec^{-1}. In the present study, Aβ1-42 peptide was also found to be sufficient by itself to induce thrombus formation under venous flow compared to scrambled Aβ1-42, Aβ1-40, and Aβ25-35 as shown in Figure 3.10. Representative images of platelet

adhesion under flow are shown in Figure 3.10 (A-F). The surface area coverage was quantified and analysed and the results are shown in Figure 3.10 (G). Aβ1-42 peptide had a remarkable and significant (P-value <0.0001 (****)) ability to induce platelet adhesion under venous flow compared to scrambled control and the other peptides.

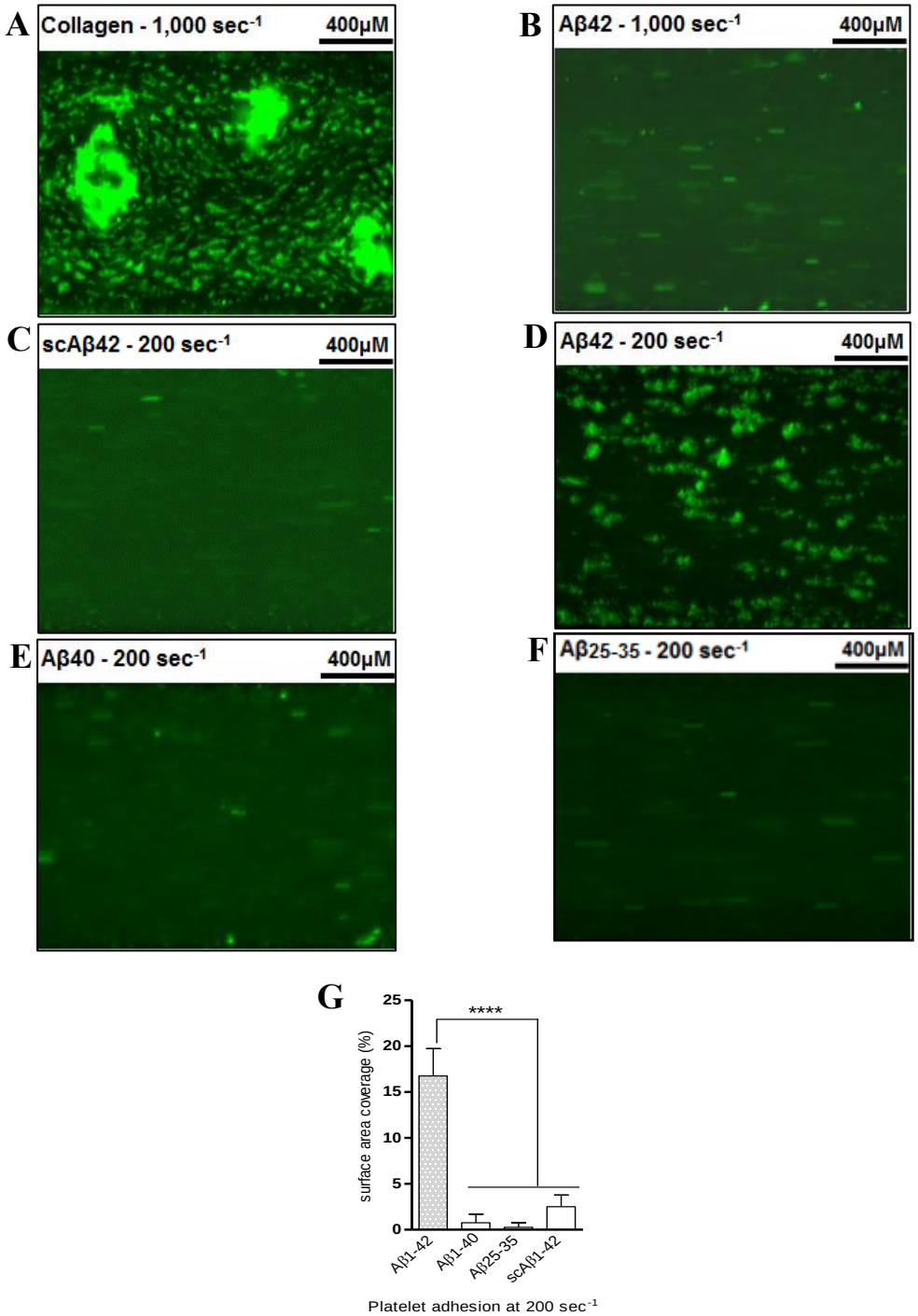

Figure 3.10: Platelet adhesion to amyloid peptides under physiological shear stress.
Vena 8 Fluoro microchips were coated with 10 μM Aβ peptides or 0.1 mg/ml fibrillary collagen. Platelet adhesion was tested in human whole blood at shear rates 1,000 sec^{-1} and 200 sec^{-1} using an ExiGo pump and images were obtained and shown in (A-E). (F) Surface area coverage was quantified from 3 independent experiments using Image J. Only Aβ1-42 induced significant increase in the percentage of surface area coverage with platelets compared to scrambled control. Statistical significance was analysed using one-way ANOVA with Bonferroni post-test; P-value < 0.0001 (****). Error bars represents mean ± SEM.

3.3.5. Aβ1-42 induces platelet activation and expression of integrin $\alpha_{IIb}\beta_3$

Aβ peptide-induced platelet activation was next assessed by measuring P-selectin surface expression and integrin $\alpha_{IIb}\beta_3$ activation using flow cytometry and the results are presented in Figure 3.11. Integrin $\alpha_{IIb}\beta_3$ was significantly activated by Aβ1-42 (but not by Aβ1-40, Aβ25-35 or scrambled Aβ1-42 - see Figure 3.11 (F)). This reflects the profound ability of 20 μM Aβ1-42 to induce signalling and activation in platelets under our experimental conditions. However, despite the ability of Aβ1-42 to induce integrin $\alpha_{IIb}\beta_3$ activation, platelet degranulation and P-selectin expression was not detected (see Figure 3.11 (G)). This indicates that Aβ1-42 has a partial role in stimulating platelets without inducing full activation. Thrombin was used as positive control in the experiments.

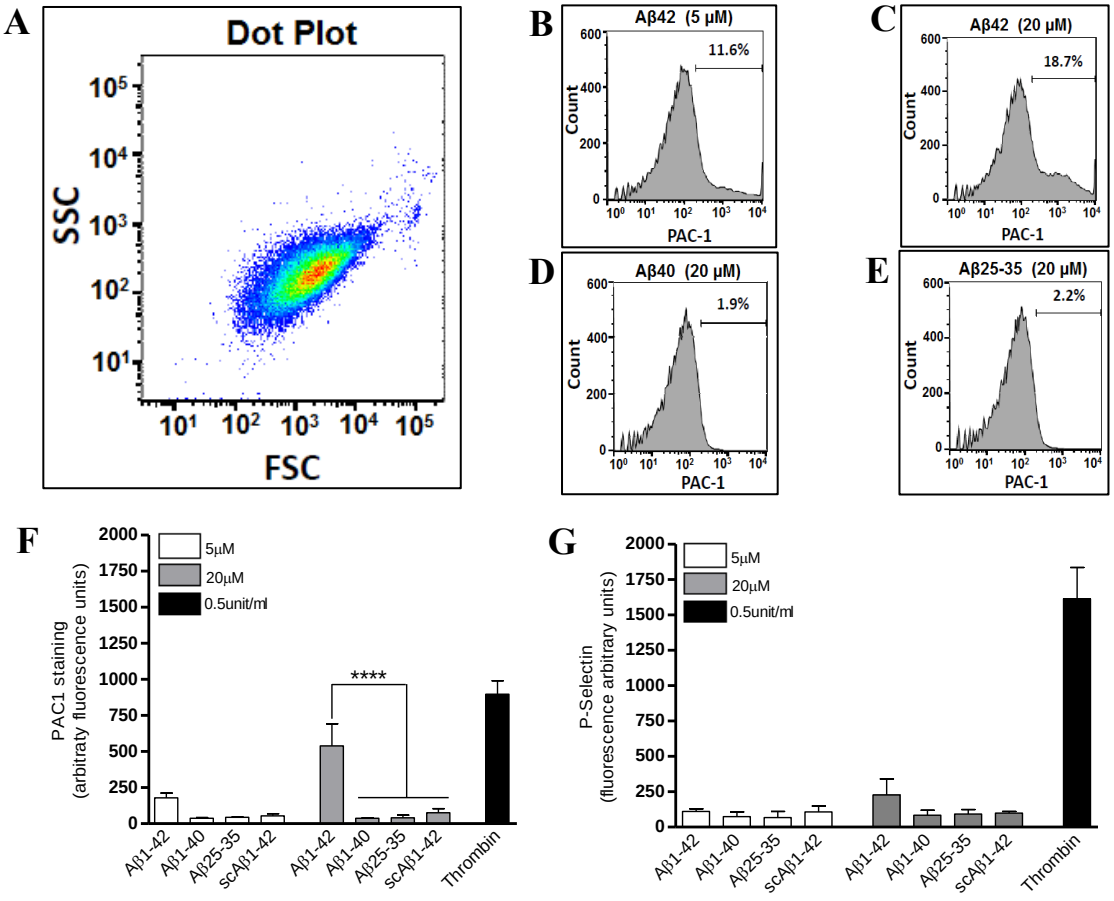

Figure 3.11: Activation of integrin $\alpha_{IIb}\beta_3$ by Aβ1-42.
Isolated human platelets in suspension were stimulated with Aβ1-42, Aβ1-40, Aβ25-35, scrambled Aβ1-42 or 0.5 unit/ml thrombin for 10 min and then labelled with FITC-PAC1 or PE-Cy5-P-selectin for further 10 minutes. (A) Side scattering (SSC) / forward scattering (FSC) dot plot suggests high purity of the platelet preparation. (B-E) Representative histograms for the intensity of PAC1 staining in the different conditions. (F and G) evaluation of fluorescence detected for P-selectin expression or integrin $\alpha_{IIb}\beta_3$ activation from 3 independent experiments. Significant fluorescence was detected with PAC1 staining for Aβ1-42 compared to scrambled control and the other peptides as shown in (F). However, no P-selectin surfaced expression was detected on platelets when stimulated with any of the Aβ peptides. Statistical significance was analysed using one-way ANOVA with Bonferroni post-test; P-value < 0.0001 (****). Error bars represent mean ± SEM.

Since Aβ1-42 was shown to be the most active peptide in our experimental conditions, as it activated platelet adhesion receptors and promoted moderate platelet aggregation, a further confirmatory study was carried out using only FITC-labelled Aβ1-42 and scrambled Aβ1-42 (provided by Dr. Upadhyay and Dr. Posner, University of Bath) to visualise its ability to bind to platelets as an agonist or in the presence of another physiological agonist thrombin at two different concentrations (0.03 and 0.1 unit/ml). The results in Figure 3.12, show enhanced binding of Aβ1-42 to platelets in the presence of the secondary physiological agonist in a concentration dependent manner. Therefore, these results could possibly shed light on the ability of Aβ at vascular lesions or in CAA to support thrombus formation at an accelerated rate and further supports previous studies.

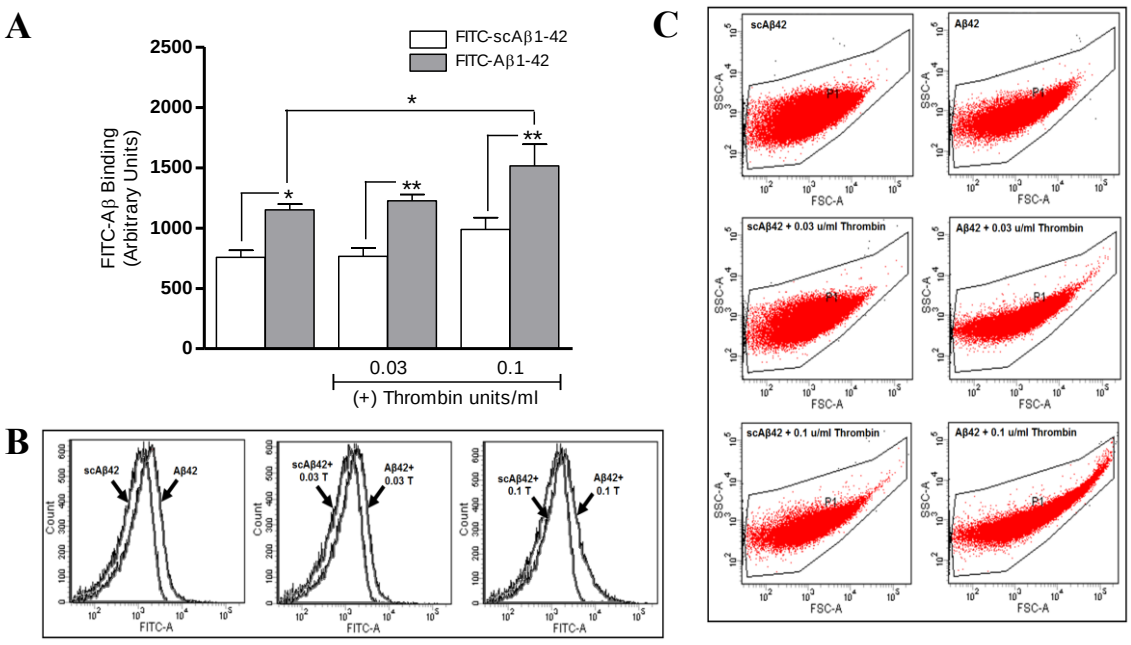

Figure 3.12: Binding of FITC-labelled Amyloid peptides to platelets.
(A) Shows significant level of FITC-labelled Aβ1-42 binding to platelets alone or in the presence or physiological stimuli thrombin at two different concentrations. Isolated human platelets in suspension (at a density of 2 x 10^8 platelets/ml) were resting in water bath (37°C) for 20 min before incubated with FITC-Aβ peptides (10µM) or FITC-Aβ peptides with thrombin at (0.03 and 0.1 units/ml) for 30 min. Samples were diluted (1:10) with room temperature modified HEPES Tyrode and read immediately with flow cytometry. (B) Representative histograms of mean fluorescence intensity. (C) Representative dot plot figures of flow cytometry gating of detected platelets population (P1) shown in a forward (FSC) vs side scattering (SSC) plot. Y-axis is a logarithmic scale. FITC-labelled Aβ1-42 show significant binding ability to platelets when compared to scrambled control and this binding was enhanced in the presence of thrombin in a concentration dependent manner. Statistical significance was analysed using one-way ANOVA with Bonferroni post-test; P-value < 0.01 (**) and P-value < 0.05 (*). Error bars represent mean ± SEM.

3.4. SUMMARY OF RESULTS

- Aβ peptides support platelet adhesion.
- Aβ1-42 induced significant platelet adhesion and spreading under static conditions compared to the other peptides.
- Aβ1-42 enhances platelet adhesion in the presence of fibrinogen but not collagen.
- Aβ1-42 can directly bind to platelets in suspension and the bind is enhanced in the presence of secondary platelet agonist.
- Aβ1-42 moderately induces platelet aggregation and potentiates aggregation in the presence of submaximal concentrations of collagen or thrombin.
- Aβ1-42 increases thrombus formation in whole blood under physiological venous flow conditions.
- Aβ1-42 induces integrin $\alpha_{IIb}\beta_3$ expression and platelet activation but not degranulation.

3.5. DISCUSSION

The thrombogenic potential of Aβ peptides has been reported to exacerbate vascular dysfunction and neurovascular lesions associated with CAA and AD and has been shown to enhance thrombus formation at these sites [295, 306]. Several studies highlighted the important role of Aβ peptides in mediating platelet adhesion and spreading [295, 300, 306, 307, 336]. However, these studies lacked consistency in their methodology and the forms of peptides used, which made their precise effects on platelets unclear. Therefore, the effects of different Aβ peptides on platelets were examined side-by-side in a systematic manner. The present study of the effects of Aβ peptides on platelet adhesion, activation, and spreading under static conditions were initially investigated, as they can provide an insight into how these peptides affect platelet adhesion and recruitment to vascular Aβ deposit sites.

The results demonstrated that platelets preferentially adhered to Aβ1-42 compared to other Aβ peptides, and noticeable platelet spreading was also observed over Aβ1-42. This suggested that only Aβ1-42 activates platelet signalling under our experimental conditions. However, closer investigation of the static adhesion results for the Aβ1-40 and Aβ25-35-coated surfaces compared to the scrambled Aβ1-42 showed noticeable increases in platelet adhesion from 200 to 500 platelets/optical field, while Aβ1-42 reached over 900 adhered platelets/optical field. Evaluation of adhered platelet spreading at higher magnification revealed that Aβ1-40 and Aβ25-35 did not induce extensive platelet spreading and most adhered platelets displayed spherical morphology and modest filopodia formation, which are indicative of partial activation.

These data therefore suggest that Aβ25-35 and Aβ1-40 possess some ability to induce platelet adhesion but are not able to induce full activation. On the other hand, platelet adhesion and spreading with extensive lamellipodia formation was very noticeable over Aβ1-42 indicating that this peptide induces platelet intracellular signalling. These results on Aβ peptides did not show the expected level of adhesion and spreading as observed in Canobbio's study [300], when their methodology was followed. The slight modifications carried out in our study with their protocol, is most likely the cause behind the differences in the results obtained in this study.

These modifications involved the preparation of platelet suspensions, where platelets were not washed with PIPES buffer before resuspension in HEPES Tyrode, which also lacked 1 mM $CaCl_2$. In addition, the coating of glass coverslips with two co-stimuli (i.e. Aβ peptides + collagen or fibrinogen) was not done separately (i.e. coating and incubating with collagen

or fibrinogen first, removing excess solution then coating with Aβ), but rather Aβ + stimuli were resuspended together and the coverslips were coated directly. The incubation time of platelets for the different conditions was also shorter (30 min instead of 60 min).

The dual surface coating experiments with Aβ peptides and collagen or fibrinogen were carried out to investigate for different Aβ peptides the potential augmentation of platelet recruitment, activation and thrombus formation at the site of CAA. Aβ1-42 with collagen appears to cause platelet adhesion with a similar potency to Aβ1-42 alone without collagen, as do the other peptides. These results suggest that Aβ1-42 may induce platelet adhesion via an independent mechanism to collagen that is potentially mediated through a different receptor.

However, a recent study in 2018 demonstrated the ability of Aβ1-42 to act as a ligand for GPVI, which is one of the main adhesion receptors for collagen [345]. Therefore, it is tempting to suggest that Aβ1-42 might possibly be competing with collagen for the same receptor. Further experiments testing inhibition of different receptors that are potentially involved in the presence of Aβ1-42 might be useful to gain more insight and additional experiments are required to detect potential phosphorylation of key signalling proteins, e.g. PKC or PI3K, with phosphoimmunoblotting to validate the effects of these peptides on platelets.

The thrombogenic potential of Aβ peptides was also examined in the presence of fibrinogen, and the results showed enhanced levels of adhesion when compared to fibrinogen alone. These results are in agreement with those of other authors [273, 306]. These authors also showed that co-localisation of Aβ and fibrinogen results in fibrinogen binding to Aβ *in vitro* enhancing fibrinogen aggregation and Aβ fibrillization, which also confirmed earlier in vitro studies [346]. These studies could explain the enhanced adhesion levels of platelets to Aβ1-42 and fibrinogen demonstrated in this study.

Integrin $\alpha_{IIb}\beta_3$ is a known main receptor for fibrinogen but recent studies showed that immobilized fibrinogen does not only act through integrin $\alpha_{IIb}\beta_3$ but also through GPVI-dimer D-domains and thus promoting platelet adhesion, activation and thrombus formation [347, 348]. Since co-localisation with fibrinogen shown to enhance Aβ fibrillization [346], Aβ1-42 may act in a similar manner to fibrillar collagen and activate GPVI and other adjacent GPVI receptors and cause receptor dimerization [349, 350], that initiates and induces effective intracellular signalling in platelets leading to "inside-out" activation of integrin $\alpha_{IIb}\beta_3$. This can then lead to fibrinogen also binding to $\alpha_{IIb}\beta_3$ and causing "outside-in" activation and

enhancing cellular signalling, and eventually causing full platelet activation, adhesion and spreading [351].

Interestingly, Aβ1-40 did not potentiate platelet adhesion in the presence of fibrinogen in our experimental conditions. Since fibrinogen promotes platelet aggregation and activation mainly through integrin $\alpha_{IIb}\beta_3$, it is tempting to suggest that Aβ1-40 and fibrinogen might also be competing for the same receptor as soluble Aβ1-40 has previously been shown to bind to integrin $\alpha_{IIb}\beta_3$ [307]. In order to fully understand the binding regulation of Aβ peptides to platelets and the discrepancies found between this study and previous studies, further experiments are required, such as, protein-receptor co-immunoprecipitation or radioligand binding studies in order to provide a better explanation. The results of the present study reveals more information on the potential role of Aβ1-42 that accumulates in the perivascular space and vessel wall, or migrates into the bloodstream, on platelet activation. Aβ1-42 was shown to activate platelets, enhance their adhesion, and potentiate thrombus formation, which can create a vicious cycle of platelet hyperactivity within the bloodstream, and possibly contributing to the microthrombosis observed in AD neurovasculature.

The second aim of this study was to investigate the effects of Aβ peptides as agonists or co-agonists on platelet aggregation using turbidimetry. Only Aβ1-42 at 20 μM shown to induce significant moderate aggregation of around 10% compared to the other peptides and in the presence of another physiological agonist, i.e. collagen or thrombin, it potentiated platelet aggregation to around 70%. This highlights the potent role of Aβ1-42 in promoting platelet aggregation. A secondary potentiation phase was also observed when Aβ1-42 co-stimulated platelet with thrombin. This can be an indicator of platelet degranulation, and the release of secondary agonists, e.g. ADP, as noted in a previous study conducted in our laboratory [303].

However, the aggregation results with Aβ25-35 do not support our laboratory's previously published work [303] that highlighted the important role of Ca^{2+} and ADP in platelet aggregation upon activation with Aβ25-35 that mediated integrin activation and endogenous ADP release in the presence of extracellular calcium. The lack of platelet responses observed with Aβ peptides might be due to the different buffer used during the aggregation assays, as our buffer did not contain Ca^{2+}, and also 1mM extracellular Ca^{2+} was not added prior to aggregation unlike the previous work [303]. These differences points towards the potential important role of extracellular calcium in inducing platelet aggregation. Therefore additional future experiments are required to study the effects of extracellular calcium on Aβ peptide-induced platelet activation and aggregation with our peptides.

Upon examination of the effects of Aβ peptides on platelet adhesion and thrombus formation under physiological shear stress, Aβ1-42 demonstrated evident platelet adhesion and thrombus formation under venous blood flow condition, while the other peptides did not. This study therefore, presents the first evidence that Aβ1-42 alone is sufficient to induce thrombus formation under physiological flow. Our previous study [303] showed that Aβ25-35 alone was unable to induce thrombus formation under flow conditions, and the present results are also support of these observations. Aβ1-42 was shown to have a negligible effect on platelets under high shear stress or arterial blood flow, while it appears to potentially have a greater influence upon inducing thrombus formation under venous flow. The present data are supportive of previously published observations with CAA on how larger arteries are less affected in severity to CAA than arterioles or capillaries [142]. Therefore, Aβ1-42 that accumulates within the microvasculature is most likely to contribute towards the thromboembolic complications observed in AD.

The present study also revealed that Aβ1-42, but not Aβ1-40, Aβ25-35, or scrambled Aβ1-42, induced integrin $\alpha_{IIb}\beta_3$ activation, which is a marker of platelet activation, but did not caused α-degranulation associated with full platelet activation. This highlights the profound biological effects of Aβ1-42 on platelets. It also suggests that Aβ1-42 induces partial platelet activation that involves platelet adhesion, but not degranulation and content release. The lack of Aβ1-40 and Aβ25-35 peptides efficiency in activating of integrin $\alpha_{IIb}\beta_3$ in this study, is partially in contrast with other previously published work, which showed the ability of these peptides to induce platelet activation, enhanced intracellular signalling, and phosphorylation of key signalling proteins [303, 307, 341].

Some limitations should be acknowledged in the work presented, which also suggest areas for future additional investigations. For example, the monomeric form of Aβ peptides received from manufacturers was not verified using TEM microscopy, although a second in-house analysis was conducted on Aβ peptides using HPLC and MS to verify the composition of the compounds received. Also, despite the extra precautions taken during the preparation of Aβ stock solutions in DMSO, potential formation of Aβ dimers or oligomers theoretically can occur. DMSO is a commonly used solvent that prevents β-sheet formation and maintains the monomeric form of Aβ in stock solutions. However, if there are existing pre-formed dimers, tetramers, or oligomers, then DMSO cannot reverse them back to their monomeric forms. The FITC-labelled Aβ peptides in this study were used only to visualize the ability of Aβ peptide to bind to platelets using flow cytometry, however, this fluorescence labelling technique does not reveal which part of the peptide sequence binds to platelets. Identifying

the Aβ binding sequence or the portion of the peptide that binds to platelets would therefore be important in future studies. Finally, platelets in blood circulation have a different age, maturation state, size, and density, and they vary greatly within an individual, where some platelets have a more procoagulant and reactive capability compared to others [352]. These different features of platelets creates what is referred to as, platelet subpopulations, that carry out different biological functions [352]. In this research project however, platelet subpopulations were not investigated and how relevant the effects of Aβ on these subpopulations and their level of adhesion is not clear, but can potentially be investigated in a future research project.

Overall, the present study highlights the profound biological activity of Aβ1-42 on platelet adhesion, activation, and aggregation. However, the receptor responsible for the initial engagement of Aβ1-42 to platelets still remains unclear. The engagement of many receptors has been now demonstrated with Aβ1-40 and Aβ25-35 in previous studies, including PAR1, CD36, GPIbα, integrin $\alpha_{IIb}\beta_3$, and partially APP [296, 302, 307, 341, 353, 354]. The most recent study last year by Elaskalani's group [345], also demonstrated the ability of Aβ1-42 to act as a ligand for GPVI. This could explain the observations obtained from the experiment with thrombus formation under venous flow. The present study does not solve the question of which receptor may be involves in the interactions with Aβ1-42 and further studies are required. However, this study sheds a new light on the abilities of Aβ1-42 to support thrombus formation at vascular lesions or CAA at an accelerated rate, and further supports previous studies of the effects of Aβ peptides on platelets.

CHAPTER 4

Redox Changes in Platelets upon Aβ Peptide Stimulation

4. RESULTS

4.1. BACKGROUND

Platelets are critical for the regulation of haemostasis and play a key role in cardiovascular pathologies. Understanding their intracellular physiological regulation is thus of great importance. Activation of platelets elicits an intricate physiological response leading to its adhesion, activation, aggregation, and secretion of a large range of biologically active substances that profoundly affect different cells and molecules within its vicinity. An important aspect of this response is, the ability of platelets to generate endogenous reactive oxygen species (ROS). Several studies have now shown that ROS are critically involved in platelet intracellular signal transduction pathways and subsequent amplification of platelet responses and agonist release [355-359].

ROS are considered secondary cellular signalling molecules that modulate the activity of a number of protein kinases as well as protein phosphatases [360, 361]. Ligand-induced activation and ROS generation can result in protein tyrosine phosphorylation, and also catalytic inactivation of PTP enzymes by oxidation. Decrease of intracellular ROS concentrations allows the recovery of PTP enzymatic activity, thus resulting in dephosphorylation of phosphorylated protein and signal termination. Therefore, ROS are considered critical regulators of platelet activation and thrombosis [361-363].

ROS are short-lived diffusible molecules, typically possess one or more unpaired electrons that are generated by oxygen reduction or from oxygen-derived free radicals [316]. There are several sources of ROS identified in platelets including, mitochondrial respiration, NADPH oxidase, xanthine oxidase, lipoxygenases, cyclooxygenase, arachidonic acid-dependent phospholipase, and uncoupled endothelial nitric oxide synthase [317]. Several species of reactive oxygen are produced and they include superoxide anion ($O_2^{-}\bullet$), hydroxyl radical ($OH\bullet$), Hydrogen peroxide (H_2O_2), and peroxynitrite ($ONOO^{-}\bullet$) [312]. Platelets also contain an endogenous antioxidant system or are affected by exogenous antioxidants that counteract the damaging effects of these radical species to maintain redox homeostasis, such as glutathione reductase and peroxidase, superoxide dismutase (SOD), catalase, α-lipoic acid, vitamin E and C, and minerals, such as, Zn, Mn, Cu, Se…etc [364-366].

Superoxide anion ($O_2^{-}\bullet$) is considered central to ROS chemistry and can act as a precursor for many other ROS species, due to its highly reactive nature [314]. Superoxide anion generated by xanthine oxidase, NADPH oxidase, or mitochondrial activities, can rapidly

interact with nitric oxide (NO) and produce highly reactive nitrogen species, such as peroxynitrite ($ONOO^-$•), which in turn gives rise to hydroxyl radical and nitrogen dioxide (NO2) that damages cells when protonated [87, 367-369]. Alternatively, O_2^-• can be converted to hydrogen peroxide (H_2O_2) by the enzymatic action of superoxide dismutase (SOD), and it is more stable and membrane-permeable than superoxide anion [315]. H_2O_2 is most efficiently scavenged by the enzymatic action of glutathione peroxidase, which utilizes glutathione (GSH active and reduced form) to produce water and glutathione disulfide (GSSG, inactive and oxidised form). The oxidised GSSG is then reduced back to GSH by the enzyme glutathione reductase, which utilizes NADPH as an electron donor. H_2O_2 can also be degraded by the enzymatic action of catalase into water and oxygen. Some transition metals such as Fe^{2+} or Cu^+, are able to breakdown H_2O_2 into the reactive hydroxyl radical that is extremely damaging to the cell in a reaction known as Fenton reaction [366].

Normally, the intracellular redox environment of platelets is balanced and maintained at an equilibrium between the presence of oxidant agents (e.g. reactive oxygen species (ROS) and reactive nitrogen species (RNS)) and anti-oxidant systems e.g. glutathione and vitamins, that is crucial for the cell physiological functions [370]. However, if ROS generation is not counter-balanced by the antioxidant system of the cell, oxidative stress is induced that modifies cell physiology and potentially damages proteins, cell membrane lipids, and nucleic acids. Oxidative stress can be caused by environmental agents, such as, pollution or radiation, and it also accompanies many pathological conditions, such as cancer, cardiovascular and neurodegenerative diseases, diabetes, and also ageing [370-378]. A summary of the sources of platelet ROS, free radicals, and antioxidants are represented in Figure 4.1.

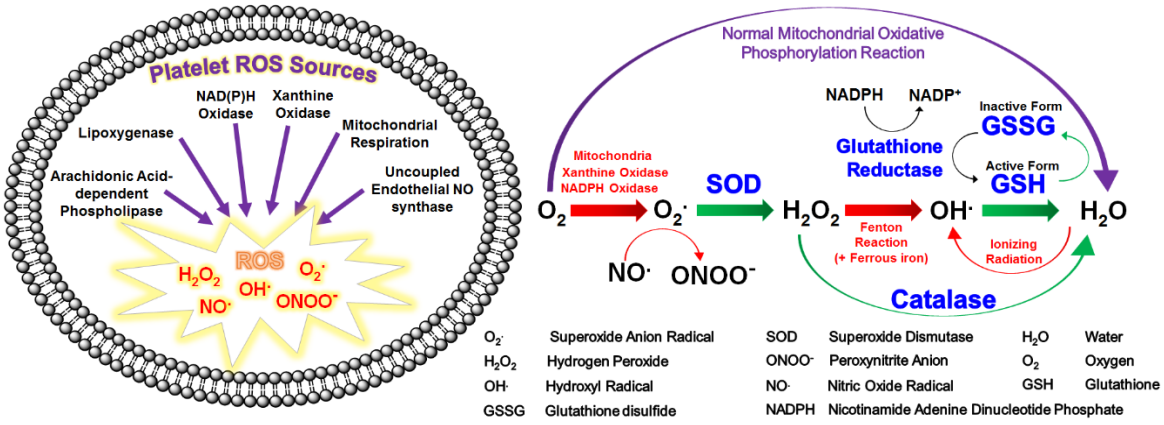

Figure 4.1: Summary of platelet sources of ROS, free radical formation, and antioxidant enzymes. (Original figure created from [312, 317, 366]).

Superoxide anion is considered an important source of oxidative stress since it is central to ROS chemistry. One of the main sources of superoxide anion generation in platelets, are NADPH oxidases (NOXs), with their sole function is superoxide generation [367]. NADPH oxidases (NOXs) are complex multiunit enzymatic systems that are able to transfer an electron to oxygen resulting in superoxide anion formation [379, 380]. The constituents of this multi-protein complexes are comprised of a catalytic subunit, which contains a conserved six transmembrane-spanning regions of α-helices with cytosolic N- and C-termini, and several regulatory subunits that are localized in both the cytoplasm and cell membrane [381].

Seven NOX family members have been reported, i.e. NOX1, NOX2, NOX3, NOX4, NOX5, Dual oxidase 1 (Duox1), and Dual oxidase 2 (Duox2), with NOX1 and NOX2 isoforms being shown to be expressed in mouse and human platelets [357, 382, 383]. NOX1 activation occurs when NOX1 binds to associated membrane protein $P22^{phox}$ with their cytosolic subunits NOX organizer 1 (NOXO1; analogue to $p47^{phox}$), NOX activator 1 (NOXA1; analogue to $p67^{phox}$), and small GTPase Rac, forming multicomponent protein complex [384]. NOX1 has also been shown to be able to utilize $p47^{phox}$ and $p67^{phox}$ subunits [385]. Similarly, NOX2 ($gp91^{phox}$) binds to associated membrane protein $P22^{phox}$ with their cytosolic subunits $p47^{phox}$, $p67^{phox}$, and $p40^{phox}$, and small GTPase Rac1/2 [384]. A representative diagram of NOX1 and NOX2 structures is shown below in Figure 4.2.

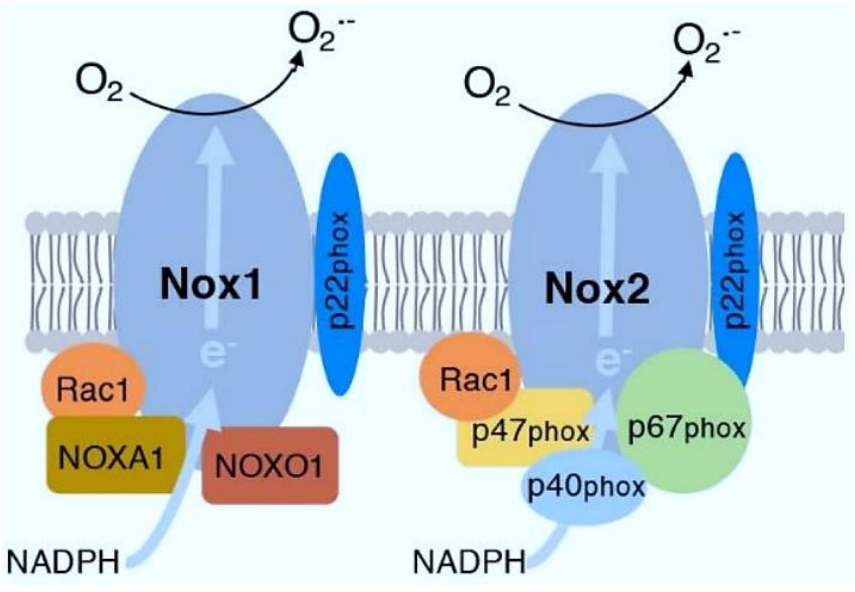

Figure 4.2: Schematic representation of structure of NADPH oxidase enzymes (1 and 2) and assembly of subunits. (Modified from [386])

Several studies have demonstrated the critical role of ROS in regulating platelet activity. This includes the ability of O_2^-• to increase ADP release and bioavailability, which leads to

increased recruitment and activation of additional platelets [314]. Platelet stimulation with thrombin, collagen, or thromboxane has been shown to activate NOXs resulting in the generation of ROS, which modulated the activation of integrin $\alpha_{IIb}\beta_3$ that is independent of the NO/cGMP signalling pathway [387, 388]. Human and mouse platelets have also been shown to express both NOX1 and NOX2, and NOX1 inhibition using the NOX1-selective inhibitor 2-acetylphenothiazine (2-APT), was found to significantly attenuate superoxide anion formation but not overall ROS generation when simulated with collagen [383]. NOX1 but not NOX2 was also shown to be involved in GPVI-induced ROS generation that was required for p38 MAPK signalling activation and subsequent release of TXA2 in platelets [389], while thrombin-induced ROS generation via GPIbα and PAR4 (but not PAR1) receptors was shown to be mediated via NOX1 and FAK proteins [357]. Finally, platelet activation and signalling through the scavenger receptor CD36 by oxidised low density lipoprotein (oxLDL) has been shown to involve NOX2-derived ROS generation and a PKC dependent pathway [390], while NOX1 and NOX2 knockout mice revealed a differential role for these NOXs in different platelet activation pathways and thrombus formation with their ROS involving Syk/PLCγ2/calcium signalling to promote platelet activation [391].

In previous studies, the inhibition of platelets and anti-thrombotic effects of antioxidants have demonstrated the dependency of platelet activation on ROS generation [392, 393]. However, few studies have reported the formation of ROS upon Aβ peptides stimulation of platelets. Aβ1-40 has been shown to induce ROS generation, mitochondrial depolarization, and increased cytosolic calcium in platelets [295], while another study used the ROS detection method known as electron spin resonance (ESR), to show that 2-10 μM of Aβ25-35 triggers hydroxyl radical formation [297]. An additional study showed that Aβ25-35 increased cytosolic calcium and ROS generation in platelets [340]. Information gathered from these studies suggests the possibility of Aβ peptide involvement in activating platelets via induction of redox stress. However, the exact cellular mechanism by which Aβ peptides activate platelets and regulate haemostasis and thrombosis remains to be defined.

Redox-dependent regulation of platelets remains challenging due to the complexity of ROS biochemistry and the lack of a reliable and easily accessible ROS detection methodology in the platelets field [394, 395]. Understanding oxidants regulation in platelets relevant to Aβ peptides effects, can provide important insights into the mechanisms relating to its roles in haemostasis and thrombosis, both in health and disease. This information can be utilized for future development of pharmacological and antithrombotic treatments based on regulating ROS generation and platelet activation. The present study aimed to investigate the

mechanisms underlying Aβ peptide-dependent activation of platelets and the potential role of ROS in this pathophysiological event. The challenging aspect of ROS detection methodology in the platelets field, prompted the exploration and utilization of different ROS detection techniques. The study in this chapter aimed to explore and assess oxidative changes in platelets upon stimulation with Aβ peptides (Aβ25-35, Aβ1-40, Aβ1-42, and scrambled Aβ1-42 as control.

4.2. AIMS & OBJECTIVES

- Determine whether the molecular probe DCFDA (6-carboxy-2',7'-dichlorodihydrofluorescein diacetate) allows the reliable detection of intracellular ROS in platelets using both physiological agonists and amyloid peptides as stimuli.
- Determine whether the molecular probe DHE (Dihydroethidium) allows the reliable detection of intracellular superoxide anion in platelets using both physiological agonists and amyloid peptides as stimuli.
- Determine the source of ROS produced upon Aβ peptide-induced platelet activation using ROS and NOX inhibitors.
- Quantitative confirmation of Aβ peptide-induced platelet ROS using electron paramagnetic resonance (EPR).

4.3. RESULTS

4.3.1. ROS detection in platelet using DCFDA

Subcellular detection and localization of ROS is crucial in understanding cellular redox status, therefore, the use of reliable ROS detection methods is important. The initial approach in this study was to utilize the wildly reported fluorescent molecular probe carboxy-H2DCFDA (6-carboxy-2',7'-dichlorodihydrofluorescein diacetate; Life Technologies) to measure oxidative stress in platelets [357, 383, 387-390]. H2DCFDA has the ability to permeate the cell membrane into the cytosol as a non-fluorescent molecule, where it is then becomes subject to hydrolysis by cellular esterases into H2DCF carboxylate anion (non-fluorescent). H2DCF can be oxidised by hydroxyl radical, carbonate radical, and nitrogen dioxide, as well as by thiyl radicals resulting from thiol oxidation. This results in H2DCF forming a DCF radical that is then further oxidised into fluorescent DCF [395-397]. Figure 4.3 (A) briefly demonstrates the conversion of H2DCFDA to fluorescent DCF. There are certain limitations associated with any ROS detection assay, therefore caution should always be taken, as artefacts can be generated in *in vitro* conditions that are not usually encountered *in vivo*.

A pilot study was conducted where platelet rich plasma (PRP) was incubated with 10 μM carboxy-H2DCFDA for 45 min then centrifuged to isolate platelets in the presence of indomethacin and PGE1 to avoid mechanical stress-induced platelet activation. Platelets were then resuspended in modified Tyrode's-HEPES buffer and tested in 96-well microplates using a fluorescence microplate reader at excitation/emission wavelengths 485/530 nm. The results are shown in Figure 4.3 (B). H_2O_2 (20 μM) was used as a platelet stimulus and positive control when testing the effects of monomeric Aβ25-35, Aβ1-40, and Aβ1-42 (20 μM). ROS scavenger N-acetyl-L-cysteine (NAC) at 1 and 30 mM was used as a negative control. N-acetyl-L-cysteine (NAC) is an aminothiol that functions as a precursor for the intracellular antioxidants glutathione (GSH) and cysteine, which in turn act as substrates for ROS scavenging enzymes and play a pivotal role in apoptosis regulation [398, 399]. Neither oxidative stress induced by H_2O_2 nor the antioxidant activity of NAC could be detected with this method, as shown by the lack of statistical significance of the data shown in Figure 4.3 (B).

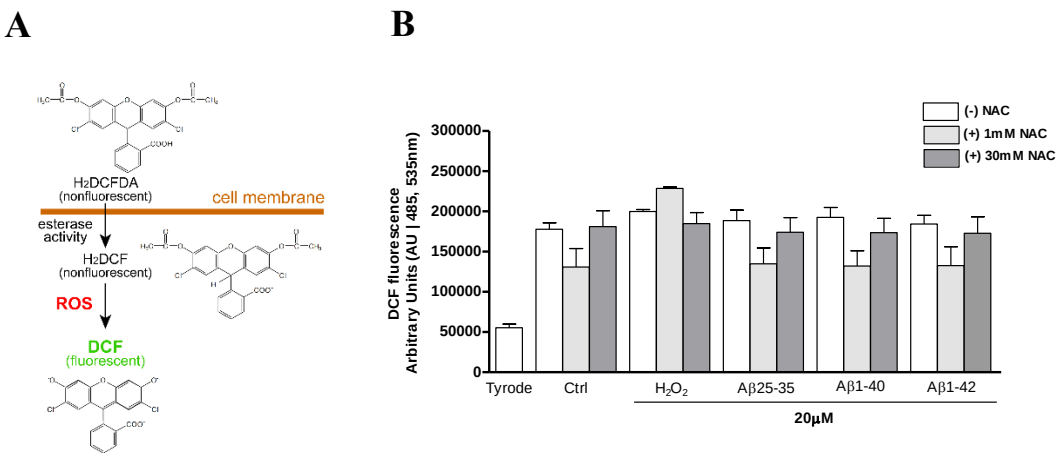

Figure 4.3: Preliminary study on ROS generation in live platelet suspension using microplate reader. (A) Summary of the formation of fluorescent compound DCF by ROS (Image was obtained from bio-protocol.org). (B) DCF fluorescence levels detected in platelets that are tested with different stimuli (H_2O_2, Aβ25-35, Aβ1-40, and Aβ1-42; 20 μM). The effects of the ROS scavenger, N-acetyl-L-cysteine (NAC) at 2 different concentrations (1 and 30 mM) on stimulated platelets are also shown. Statistical significance was analysed from 3 independent experiments using one-way ANOVA with Bonferroni post-test. Error bars represent mean ± SEM.

The results displayed high basal saturation levels causing inaccurate ROS readings. Several follow up experimental attempts (data not shown) exploring different concentration and incubation times were also a failure and generated varied and inconsistent results. Therefore, the idea of using the microplate reader was discarded and detection using flow cytometry was the next step followed to investigate ROS generation in live platelets. Adopting a previously published DCFDA protocol [387], several platelet agonists were investigated to assess the validity of this ROS detection method, including thrombin, collagen, collagen related peptides (CRP), arachidonic acid (AA), oxidised low density lipoprotein (oxLDL), or adenosine diphosphate (ADP). DCF fluorescence was detected by flow cytometry and the results obtained appeared to be more promising as shown in Figure 4.4. The results from the present study show significant ROS generation upon stimulation with collagen, thrombin, and CRP compared to resting platelets, but AA, ADP, and oxLDL did not induce ROS at the tested concentrations in this assay as shown in Figure 4.4 (E-F)).

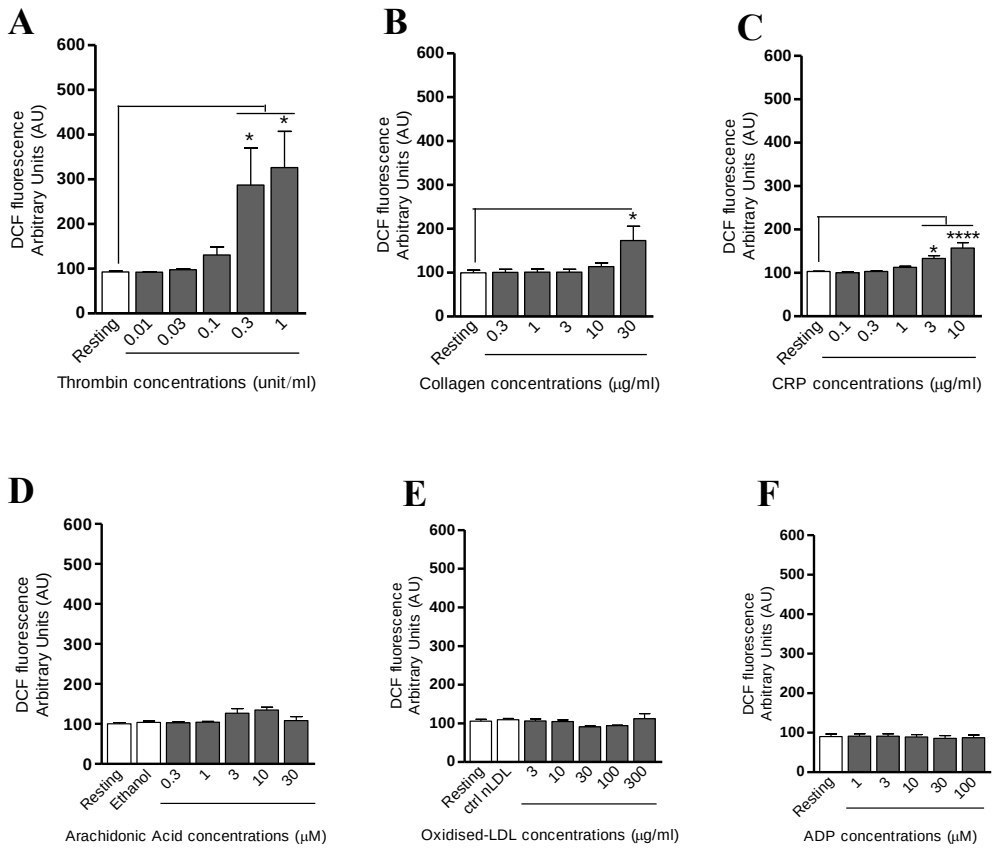

Figure 4.4: Determination of optimum concentrations for 6 different stimuli to detect ROS generation in live platelet suspensions by flow cytometry.
Platelets were stimulated with different agonists for 30 min. (A) Different concentrations of thrombin (1 and 0.3 unit/ml) showing statistical significance compared to resting. (B) Different concentrations of collagen with only 30 μg/ml showing statistical significance compared to resting. (C) Different concentrations of collagen-related peptide (CRP) with (3 and 10 μg/ml) showing statistical significance compared to resting. (D-F) Different concentrations of arachidonic acid, of oxidised low-density lipoprotein (oxLDL), and adenosine diphosphate (ADP) show no statistical significance ROS generation compared to their controls (i.e. ethanol, ctrl nLDL, or resting platelets respectively). Statistical significance was analysed using one-way ANOVA with Bonferroni post-test; P-value < 0.0001 (****), P-value <0.01 (**), and P-value <0.05 (*). Error bars represent mean ± SEM.

In order to validate ROS detection in this assay, the effects of the ROS scavenger NAC at different concentrations (3 and 30 mM) and different pre-incubation times (3 and 30 min) were assessed before adding collagen (30 μg/ml) as a platelet agonist and the results are shown in Figure 4.5. Both collagen and thrombin were shown to have significant effects on platelet ROS generation, however, since thrombin had greater variability in results with DCFDA (error bars) compared to collagen, collagen was used in this experiment as positive control, and to also test the effect of NAC in scavenging collagen-stimulated ROS generation in platelets. Pre-incubation with 3 mM NAC showed a slight decrease in ROS, while 30 mM NAC at 3 and 30 min both show a marked decrease in DCF fluorescence.

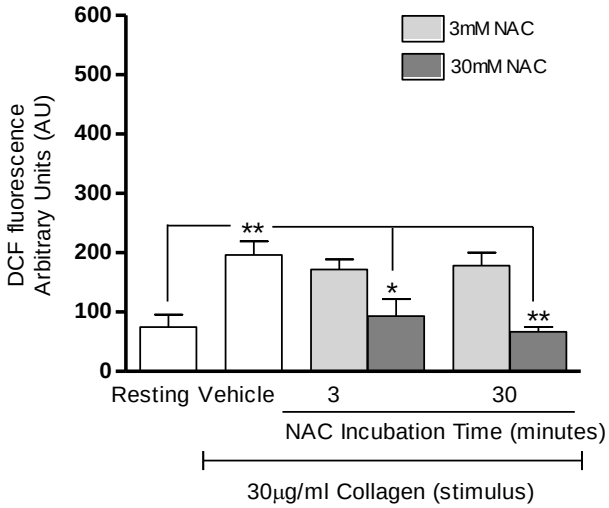

Figure 4.5: Optimum time and concentration for use of NAC as ROS scavenger on stimulated platelet suspensions.
Different NAC concentrations were tested with pre-incubation periods of 3 and 30 min before adding collagen to stimulate ROS generation. 30 mM NAC shows decreased DCF fluorescence to almost control level (resting) but not 3 mM NAC. Statistical significance was analysed using one-way ANOVA with Bonferroni post-test. Error bars represent mean ± SEM.

The effects of Aβ peptides on platelet ROS generation were assessed next and the results are shown in Figure 4.6. Aβ25-35 shows significant levels of DCF fluorescence when compared to resting platelets, but these are not significant when compared to scrambled Aβ1-42. Aβ1-40 and Aβ1-42 did not show significant DCF fluorescence.

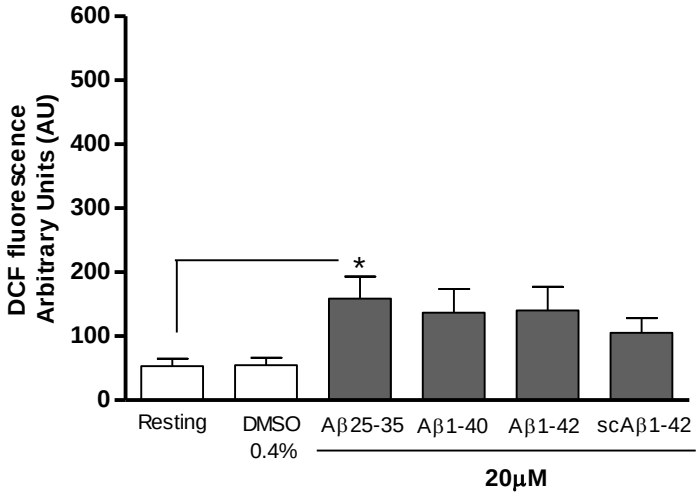

Figure 4.6: Effects of different Aβ peptides on ROS generation in live platelet suspensions detected by flow cytometry.
Aβ25-35 shows significant levels of DCF fluorescence when compared to resting platelets, but was not significant when compared to scrambled Aβ1-42. Aβ1-40 and Aβ1-42 did not show significant DCF fluorescence compared to resting or scrambled Aβ1-42. Aβ peptides were dissolved in DMSO 0.4%, so DMSO alone was also tested to check that it did not have any effects on platelets at that dose. Statistical significance was analysed using one-way ANOVA with Bonferroni post-test; P-value <0.05 (*). Error bars represent mean ± SEM.

Looking at the overall results with DCFDA, DCF fluorescence values seem insufficient or diminished for the different physiological agonist used, as the concentrations to obtain a detectable response are too high compared to normal concentrations used *in vitro*. Therefore a second molecular probe for the detection of ROS, in particular superoxide anion, was investigated next.

4.3.2. Superoxide detection in platelets using Dihydroethidium

Dihydroethidium (DHE; Life Technologies) has been suggested as an accurate and non-problematic molecular probe for intracellular superoxide anion detection [400]. When DHE enters the cell and interacts with ROS, it forms one of two detectable molecules that are retained within the cells known as, 2-hydroxy-ethidium (2OH-Et+), which is formed when DHE interacts with superoxide anion, or ethidium, which is when DHE interacts with other oxidants [395]. 2OH-Et+ absorbs light at 405nm and 480nm with emission at 580nm, while ethidium absorbs light only at 480nm with emission at 580nm. Therefore, fluorescence measurements at 405/580 ex/em enables the assessment of 2OH-Et+ generation, which is directly proportional to the amount of superoxide anion interacting with DHE. This dye can therefore be used to reliably determine the level of intracellular superoxide anion by flow cytometry. Figure 4.7 (A) shows the structural and spectral properties of DHE and its two oxidation products ethidium and 2-hydroxy-ethidium (2OH-Et+).

A study was initially carried out to determine the optimum incubation time with DHE in our experimental conditions using the potent platelet agonist, thrombin, and the results are shown in Figure 4.7 (D). Since thrombin has previously been shown to have the greatest impact in generating ROS in platelets and because a new intracellular molecular probe (DHE) was being used to detect superoxide anion generation, thrombin was chosen as a positive control to test. In addition, not many studies on platelets have used DHE, and therefore, it was necessary to determine the ideal incubation time with DHE for the detection of superoxide anion under our experimental conditions. According to the results in Figure 4.7 (D), 15 min incubation with DHE yielded the highest detectable fluorescence when platelets were stimulated with thrombin, and thus, all subsequent experiments were carried out with DHE at that incubation time.

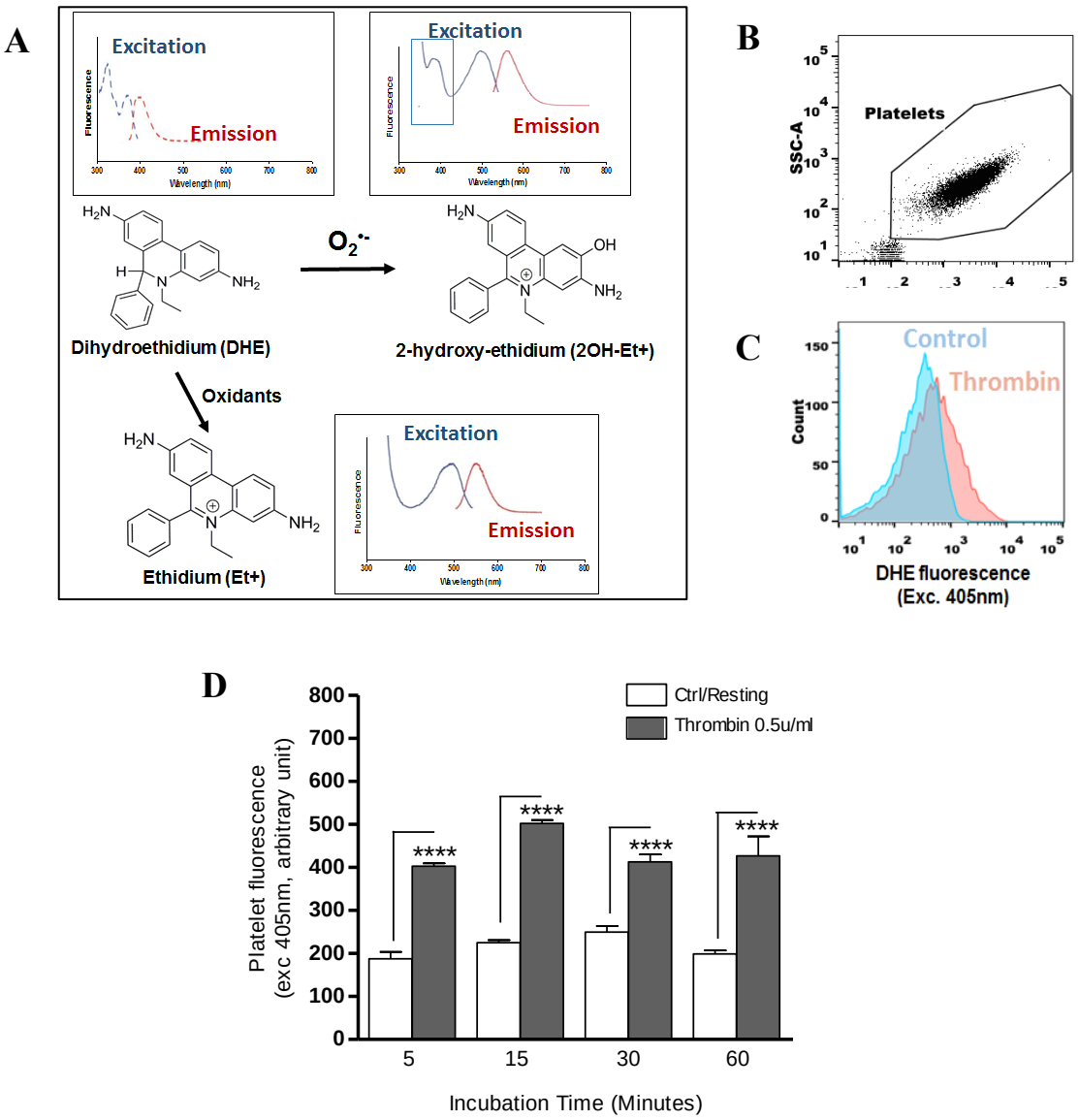

Figure 4.7: Use of DHE to detect superoxide anion formation in platelets.
(A) Structural and spectral properties of DHE and its two oxidation products, ethidium and 2-hydroxy-ethidium (2OH-Et+). The excitation peak at 405 nm specific for 2OH-Et+ is highlighted with a blue rectangle [401]. (B) Flow cytometry gating shown in a forward (FSC) vs side scattering (SSC) plot. (C) Representative example of the fluorescence shift by thrombin-dependent stimulation of platelets in the 2OH-Et+ fluorescence (405/580 nm ex/em). (D) Platelet suspensions were rested for 30 min at 37°C before incubation with 5 µM DHE for 15 min. Platelets were then stimulated with physiological stimulus thrombin (0.5 unit/ml) at different time points to determine optimal stimulation time. The optimal stimulation time of platelet using DHE shown to be at 15 min. Statistical significance was analysed from 4 independent experiments using one-way ANOVA with Bonferroni post-test; P-value < 0.0001 (****). Error bars represent mean ± SEM.

In order to examine the new optimised methodology with DHE, further tests on superoxide generation in platelets were carried out using varying concentrations of different physiological stimuli, i.e. thrombin, collagen, CRP, AA, oxLDL, and ADP. The results in Figure 4.8 (A-E) show statistically significant superoxide anion generation with thrombin (0.1, 0.3, 1 u/ml), collagen (30 µg/ml), CRP (3 and 10 µg/ml), AA (10 and 30 µM), and

oxidised LDL (30, 100, and 300 µg/ml), but not ADP compared to resting platelets (Figure 4.8 (F)).

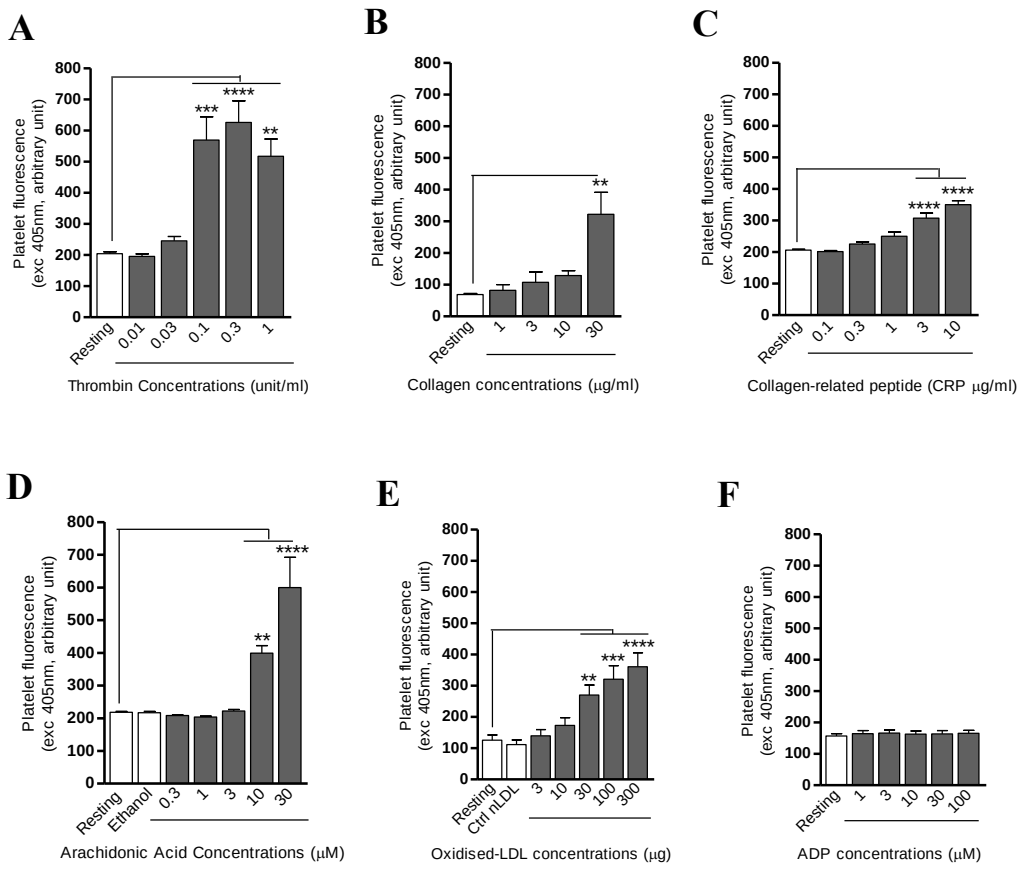

Figure 4.8: Determination of the concentration dependence of superoxide anion generation for 6 different stimuli.
Platelets were stimulated with different agonists for 15 min. (A) Different concentrations of thrombin 0.1, 0.3, and 1 unit/ml showing statistical significance compared to resting platelets. (B) Different concentrations of collagen with only 30 µg/ml showing statistical significance compared to resting platelets. (C) Different concentrations of collagen-related peptide (CRP) with 3 and 10 µg/ml showing statistical significance compared to resting platelets. (D) Different concentrations of arachidonic acid with 10 µM and 30 µM showing statistical significance compared to ethanol stimulated and resting platelets. (E) Different concentrations of oxidised low-density lipoprotein (oxLDL) with 30, 100 and 300 µg/ml showing statistical significance compared to nLDL stimulated and resting platelets. (F) Different concentrations of adenosine diphosphate (ADP) show no statistical significance compared to resting platelets. Statistical significance was analysed from 4 independent experiments using one-way ANOVA with Bonferroni post-test; P-value < 0.0001 (****), P-value < 0.001 (***), and P-value <0.01 (**). Error bars represent mean ± SEM.

The new optimised method with DHE was further validated with using ROS scavenger NAC and NOX inhibitors. NAC concentration-dependent experiments were carried out using thrombin (0.3 unit/ml) as a physiological stimulus to determine the optimal concentration of NAC to be used in future experiments for DHE. The results are shown in Figure 4.9 (A). NAC concentrations of 3 mM, 100 µM, 30 µM, and 10 µM, significantly decreased superoxide anion generated by thrombin. NAC at 3 mM seems to ideally abolish ROS and

bring the fluorescence values of platelets down to basal level similar to the resting state. Therefore, another set of experiments were also carried out testing its efficiency with other physiological stimuli and the results are show in Figure 4.9 (B). 3 mM NAC significantly reduced superoxide generated by CRP (3 µg/ml), and oxLDL (30 µg/ml) but not platelets stimulated with AA.

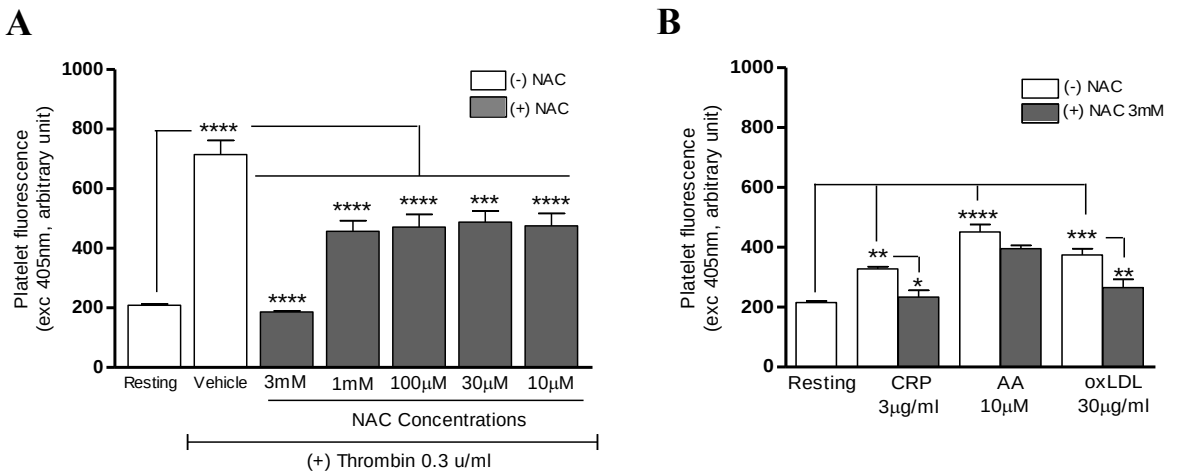

Figure 4.9: Investigation of the effects of the ROS scavenger NAC at different concentrations on platelet superoxide anions formation by different physiological stimuli.
After platelets were isolated and resting for 30 min in water baths, 5 µM DHE was added for 15 min. (A) Different concentrations of NAC were pre-incubated with platelets for 10 min before adding 0.3 u/ml thrombin to investigate optimal NAC concentration to be used. At the end of the incubation time, platelet suspensions were diluted 1:10 in cold modified Tyrode's-HEPES buffer and samples were analysed immediately by flow cytometry. All the different concentration of NAC (3 mM, 1 mM, 100 µM, 30 µM, and 10 µM) shown statistical significance. (B) Other stimuli (collagen related peptide (CRP, 3 µg/ml), arachidonic acid (AA, 10 µM), and oxidised low density lipoprotein (oxLDL, 30 µg/ml)) were tested with 3 mM NAC (which seemed to be ideal concentration based on results in (A)) and both CRP and oxLDL showed statistical significance with NAC but not AA. Statistical significance was analysed using one-way ANOVA with Bonferroni post-test; P-value < 0.0001 (****), P-value < 0.001 (***), P-value <0.01 (**), and P-value <0.05 (*). Error bars represent mean ± SEM.

Different NOX inhibitors were assessed next on platelets stimulated with thrombin (0.3 u/ml) including NOX inhibitor VAS2870 (10 µM), NOXA1ds (10 µM), and scrambled NOXA1ds (control). The results are presented in Figure 4.10 and showed that only the NOX inhibitor VAS2870 significantly eliminated the generation of superoxide anion, which suggests that thrombin-stimulated superoxide anion generation is mainly NOX-dependent. When NOX1 inhibitor (NOXA1ds) was used, no significant decrease in the fluorescence was observed when compared to vehicle or scrambled NOXA1ds (control), indicating that thrombin is NOX1-independent.

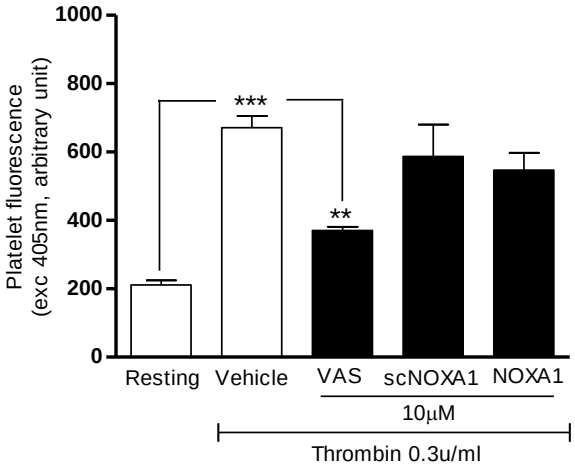

Figure 4.10: The effects of NOXs inhibition in platelets stimulated by thrombin. After platelets were isolated and rested for 30 min in a water bath, 5 μM DHE was added for 15 min. The following inhibitors were used (10 μM NOX inhibitor VAS2870, 10 μM scrambled NOXA1ds control for NOXA1. These inhibitors were incubated with platelets for 10 min before being stimulated with thrombin (0.3 unit/ml) for another 15 min. At the end of the incubation time, platelets were diluted 1:10 in cold modified Tyrode's-HEPES buffer and samples were analysed immediately by flow cytometry. VAS2870 significantly abolished superoxide anion produced by thrombin when compared to thrombin alone (Vehicle). Statistical significance was analysed from 4 independent experiments using one-way ANOVA with Bonferroni post-test; P-value < 0.0001 (****) and P-value <0.01 (**). Error bars represent mean ± SEM.

From these results, both NAC at 3 mM and VAS2870 at 10 μM inhibited ROS and superoxide anion generation respectively in our experimental conditions, and thus were utilized at those concentrations in future experiments. Since superoxide detection assay with DHE was optimised, the effects of Aβ peptides on platelet redox homeostasis was finally tested and the results are shown in Figure 4.11. Only Aβ1–42 (20 μM) had a significant effects on superoxide generation compared to resting platelets and scrambled Aβ1–42 as control (Figure 4.11).

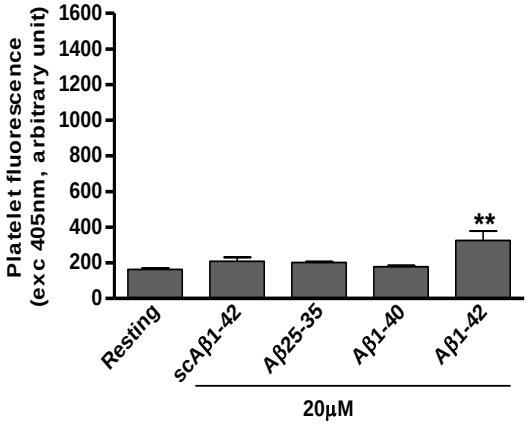

Figure 4.11: Superoxide anion formation induced by Aβ peptides. Superoxide anion formation was measured as described in previous figures using DHE in response to 20 μM Aβ1–40, Aβ1–42, scrambled Aβ1–42 or Aβ25-35. Only Aβ1–42 showed a significant statistical increase in superoxide anion formation compared to scramble control and the other peptides. Statistical significance was analysed using one-way ANOVA with Bonferroni post-test; P-value <0.01 (**). Error bars representing mean ± SEM.

Since Aβ1-42 peptide had shown significant superoxide generation, a concentration-response study was carried out to find the optimum and minimum concentration of Aβ1-42 peptide that could be used in our experimental conditions, and the results are shown in Figure 4.12 (A). The results showed, a pronounced increase in superoxide anion generation with concentrations of Aβ1-42 greater than 10 μM. Since NAC (3 mM) and NOX inhibitor VAS2870 (10 μM) had been shown to be effective at abolishing ROS as seen previously with thrombin, CRP, and oxLDL, these concentrations were also tested with Aβ1-42 stimulated platelets. Both the ROS scavenger NAC and the NOX inhibitor VAS2870 significantly reduced Aβ1-42 peptide-dependent increase in superoxide anion formation as shown in Figure 4.12 (B). These results show that Aβ1-42-stimulated ROS generation in platelets is NOX-dependent.

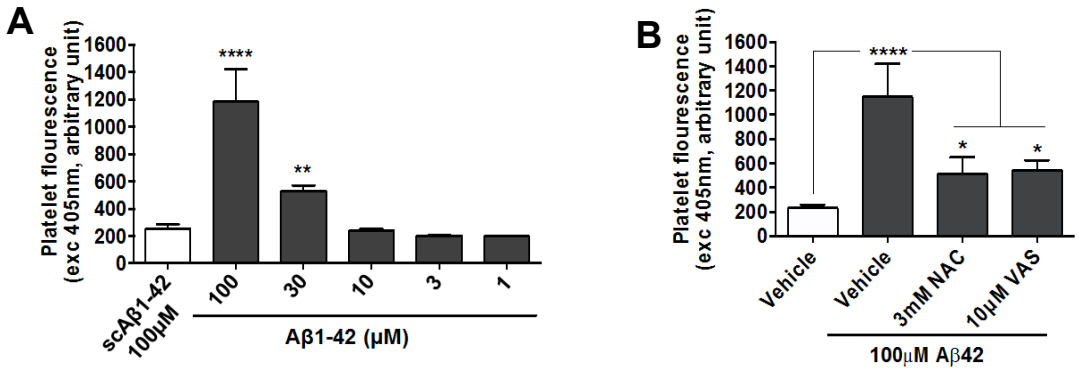

Figure 4.12: Aβ1-42 concentration-dependent response of superoxide anion formation and the effects of ROS inhibition. Superoxide anion formation was measured as described in previous figures using DHE. (A) Different concentrations of Aβ1–42 (1–100 μM). (C) Superoxide anion formed after stimulation by Aβ1–42 (100 μM) and inhibited by 10 min pre-incubation with ROS scavenger NAC (3 mM) or NOX inhibitor VAS2870 (10 μM). Statistical significance was analysed from 4 independent experiments using one-way ANOVA with Bonferroni post-test; P-value <0.05 (*), P-value <0.01 (**) and P-value < 0.0001 (****). Error bars representing mean ± SEM.

The new optimised methodology with DHE is easily accessible and promising, and the exciting results obtained with regards to the effects of Aβ peptides on platelet redox behaviour, prompted the use of another ROS detection methodology to confirm these observations.

4.3.3. Superoxide detection in platelet using electron paramagnetic resonance (EPR)

To confirm and further determine Aβ peptides-induced superoxide generation in platelets, electron paramagnetic resonance (EPR) experiments were carried out in collaboration with the EPR expert in our group, Dr. Dina Vara. Electron spin or paramagnetic resonance (ESR or EPR) spectroscopy is considered the "gold standard" technique among quantitative ROS detection assays in terms of accuracy and reliability [402, 403]. Generation of superoxide anion can be detected using the cell-permeable cyclic hydroxylamine spin probe, known as 1-hydroxy-3 methoxycarbonyl-2, 2, 5, 5-tetramethylpyrrolidine (CMH). CMH is specific for the detection of intracellular superoxide anions and is resistant to auto-oxidation.

When CMH crosses the plasma membrane and enters the cells, it can interact with oxygen radicals and form more stable radicals (nitroxide radical CM•) that last several hours and are detectable by EPR [395, 404, 405]. EPR operates by exciting transitions of unpaired electrons in a sample placed in an applied magnetic field through the absorption of microwave energy. The number of unpaired electrons present in the sample is proportional to the strength or amplitude of the EPR signal detected. The rate of (O_2^-•) generated is measured as the rate of CMH oxidation and is represented as amplitude strength signal detected by EPR [251, 402, 406]. Using this technique, superoxide anion formed in platelets stimulated by scrambled Aβ1-42, Aβ25-35, Aβ1-42 and Aβ1-40 at 20 μM was assessed and the results are shown in Figure 4.13.

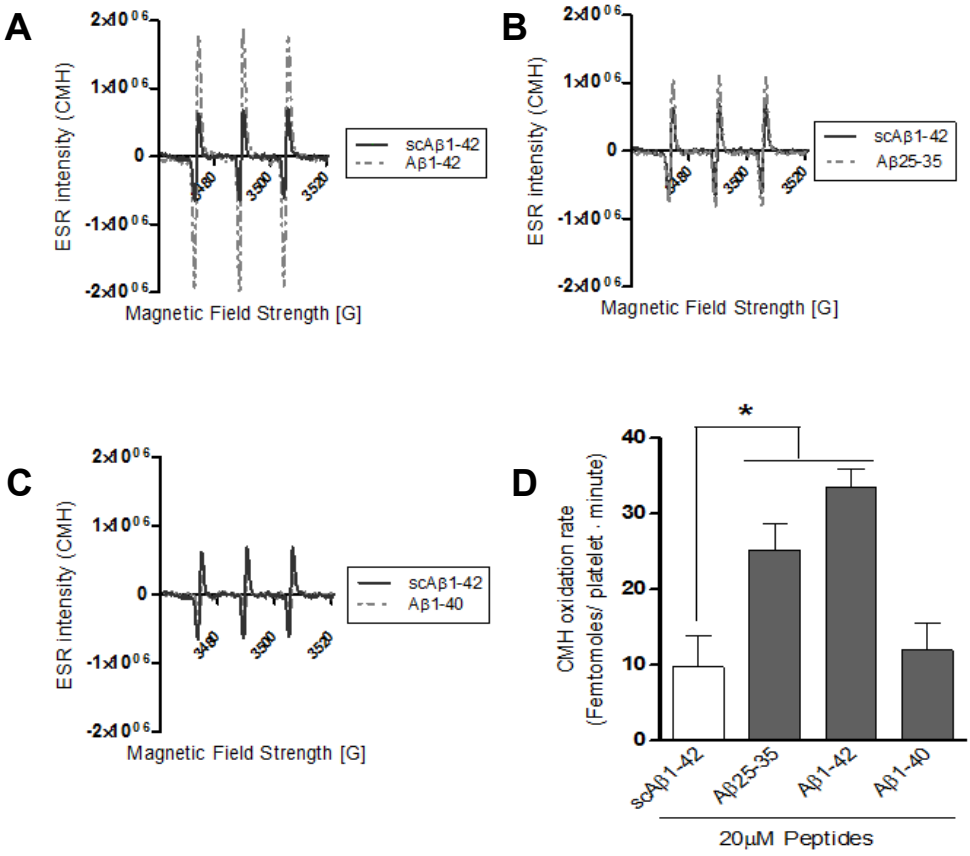

Figure 4.13: Detection of superoxide anion generated in response to Aβ peptide stimulation of platelets using EPR. (A-C) Different magnitude of EPR spectral peaks generated by the level of superoxide anion formed in platelets stimulated by scrambled Aβ1-42, Aβ25-35, Aβ1-42 and Aβ1-40 at 20 μM for 10 min. (D) Quantification and analysis of CMH oxidation rate from 3 or more independent experiments. Aβ1-42 and Aβ25-35 induced platelet activation show significant CMH oxidation rate compared to scrambled Aβ1-42 (control) Statistical significance was analysed using one-way ANOVA with Bonferroni post-test; P-value <0.05 (*). Error bars representing mean ± SEM.

In support of the previous results with DHE methodology, Aβ1-42 induced significant superoxide anion generation compared to scrambled Aβ1-42. However, not only did Aβ1-42 induce significant superoxide anion generation, but so did Aβ25-35 as shown in the results in Figure 4.13 (D). Therefore, the effects of Aβ1-42 and Aβ25-35-induced superoxide generation were further probed using NOX inhibitors to potentially identify the types of NOX involved. A series of EPR experiments were conducted testing several NOX inhibitors at 10 μM. These NOX inhibitors included: VAS2870, which is a commercially available triazolo pyrimidine derivative that is a selective NADPH oxidase inhibitor but not isoform specific [381, 407]; 2-APT (2-acetylphenothiazine), a NOX1-selective inhibitor [383]; scrambled NOXA1ds (control); and NOXA1ds (also known as NOXA1 docking system), which is a cell-permeable peptide that exhibit selectivity for NOX1 and prevents the binding of the NOX activator 1 subunit [408, 409]; scrambled NOX2ds-TAT (control), and NOX2ds-TAT

(also known as NOX2 docking sequence TAT or gp91ds-TAT) that is a peptide designed to inhibit the interaction between NOX2 and $p47^{phox}$.

The TAT portion of the last two inhibitors mentioned corresponds to 9 amino acids that facilitate cell membrane entry and internalization of the peptide [408, 410]. EPR results using all of the NOX inhibitors with Aβ1-42 and Aβ25-35 are shown in Figures 4.14 and 4.15 respectively. Stimulated platelets revealed noticeable and statistically significant superoxide inhibition for both NOXs. These results confirm that superoxide generation from Aβ1-42 and Aβ25-35-induced platelet activation is NOX-dependent and highlights the underlying platelet activation dependency on ROS upon Aβ peptides.

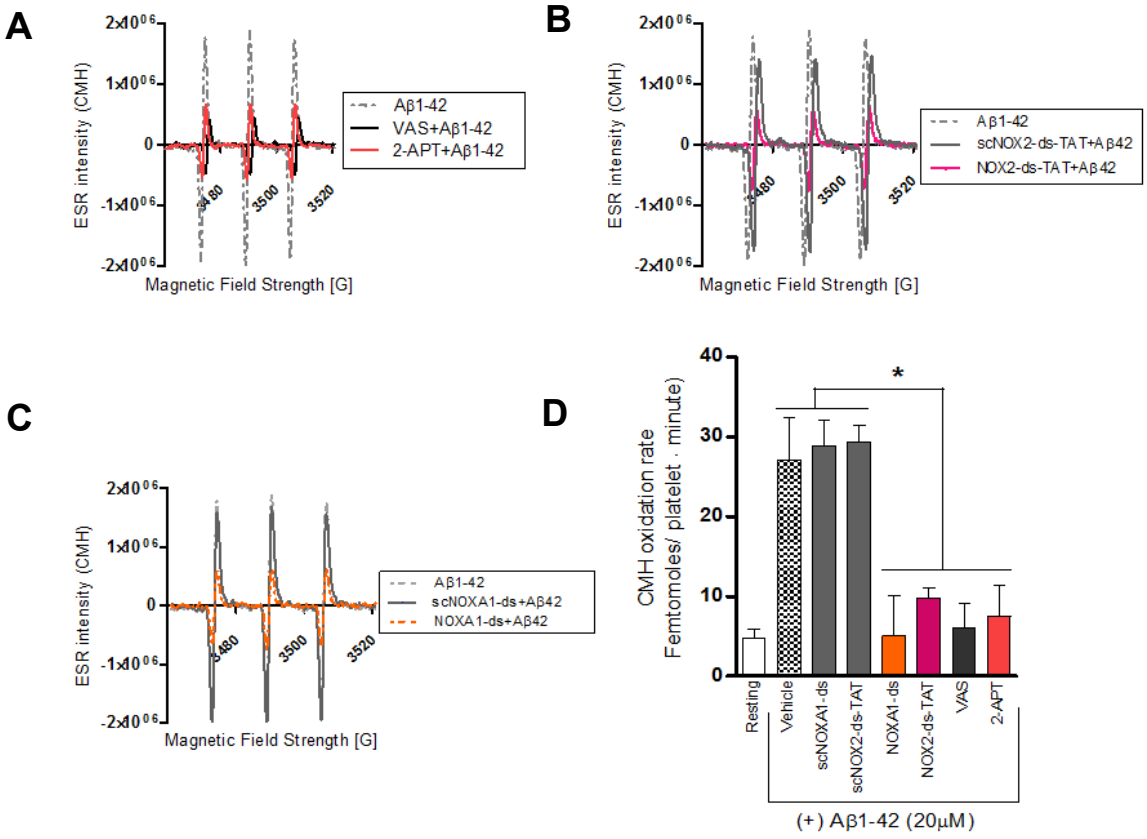

Figure 4.14: Aβ1-42 induced superoxide anion generation in platelets is NOX dependent. (A-C) Different magnitude of EPR spectral peaks generated by the level of superoxide anion formed in platelets upon Aβ1-42 (20 μM) stimulation in the presence or absence of VAS2870 (10 μM), 2-APT (0.5 μM), scrambled NOX2ds-TAT (control), NOX2ds-TAT (10 μM), scrambled NOXA1ds (control) and NOXA1 (10 μM). (D) Quantification and analysis of CMH oxidation rate from 3 or more independent experiments. Inhibition of either NOXs significantly abolished superoxide generation in platelets stimulated with Aβ1-42 compared to controls. Statistical significance was analysed using one-way ANOVA with Bonferroni post-test; P-value <0.05 (*). Error bars representing mean ± SEM.

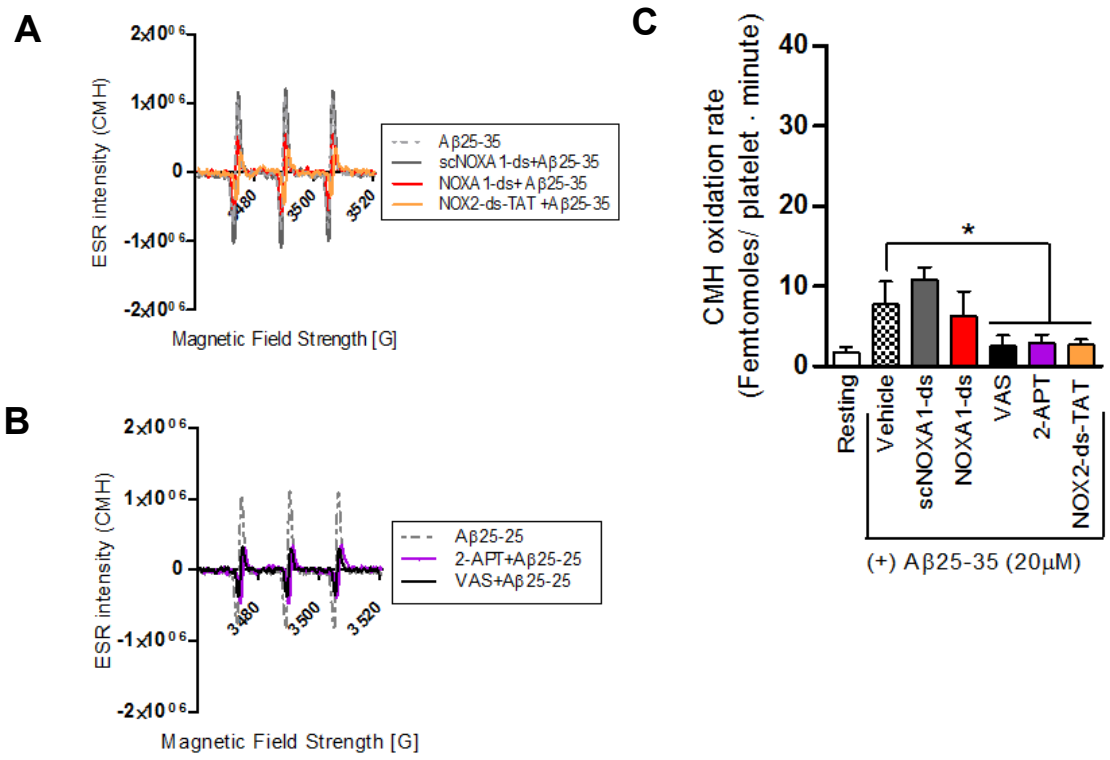

Figure 4.15: Identifying sources of Aβ25-35-induced superoxide anion generation in platelets using different NOX inhibitors with EPR. (A-B) Different magnitude of EPR spectral peaks generated by the level of superoxide anion formed in platelets upon Aβ25-35 (20 μM) stimulation in the presence or absence of VAS2870 (10 μM), 2-APT (0.5 μM), scrambled NOX2ds-TAT (control), NOX2ds-TAT (10 μM), scrambled NOXA1ds (control) and NOXA1 (10 μM). (D) Quantification and analysis of CMH oxidation rate from 3 or more independent experiments. Inhibition of either NOXs significantly abolished superoxide generation in platelets stimulated with Aβ25-35 compared to controls Statistical significance was analysed using one-way ANOVA with Bonferroni post-test; P-value <0.05 (*). Error bars representing mean ± SEM.

The fibrillar form of Aβ peptides has previously been reported to have significant effects on platelet activation and aggregation [302, 307, 336, 345, 353]. For example, it has been shown that the fibrillar form of Aβ1-40 induced platelet aggregation in a time-dependent manner and Aβ1-40 fibrils could activate platelets through scavenger receptor CD36/P38 MAPK/ TXA2 release, and also through GPIbα-mediated aggregation [302]. In addition, strong evidence for platelet contribution to CAA was shown by modulation of soluble Aβ1-40 into the fibrillar form, which facilitated platelet adhesion at vascular Aβ deposition sites [295, 307]. Furthermore, fibrillar Aβ1-40 and Aβ1-42 have been previously demonstrated to bind to APP on neurons at a concentration range of 5-20 μM [353]. APP and its homologues have been shown to be able to homo- or heterodimerize and form cell surface receptor-like complexes that are able to modulate signalling events and facilitate integrin-mediated cell adhesion [411, 412].

This notion has been recently supported by our group with APP KO mice, where it has been demonstrated that adhesion on immobilized Aβ peptides Aβ1–40, Aβ1–42 and Aβ25–35 was completely abolished in platelets lacking APP, but did not affect their aggregation. It also showed that Aβ-promoted potentiation of thrombus formation under flow and APP may facilitate an early step in thrombus formation [354]. These studies demonstrated the importance of understanding the effects of the fibrillar forms of Aβ peptides on platelets.

However, there is a lack of studies on the effects of fibrillar Aβ peptide-induced platelet activation on ROS generation. Therefore, since soluble Aβ peptides, particularly Aβ1-42, had been shown to induce ROS production, an assessment to test ROS generation in platelets induced with fibrillar form of Aβ peptides was desirable. A pilot study was therefore first carried out for the fibrillization of Aβ peptides using the Thioflavin T (ThT) assay following the BMG LABTECH handbook protocol (see below). Aβ fibrils are naturally large, insoluble, non-crystalline, and resistant to degradation, and their formation usually occurs from normal soluble proteins. Structural studies using X-ray diffraction, electron microscopy (EM), and solid-state nuclear magnetic resonance (NMR) [413-415] have revealed that Aβ fibrils are composed of a β‑sheet structure, where the β-strands are arranged perpendicular to the fibrillar axis. The β-sheet strand edges are unstable, and can grow by interacting with any other β-strands they encounter [416]. Due to the repetitive nature of peptide self-assembly, recurrent side-chain interactions arise that run across β-strands within a β-sheet layer, parallel to the long axis of the fibril. This specific arrangement of side chains is called the "cross strand ladder" [413-415, 417].

The most convincing theoretical model of fibril formation is known as the "nucleation-dependent polymerization model", where the fibrillation process consists of three distinct stages known as nucleation, elongation, and equilibrium, leading to a sigmoid-shaped profile [418, 419] as shown in Figure 4.16 (A). The hydrophobic and fibrillogenic nature of amyloid peptides, especially Aβ1-42, allows them to undergo fibrillation in a self-propagating manner. It starts with a relatively long lag-phase (nucleation phase), where oligomeric nucleus 'seeds' are formed, which then allows further addition of monomers in a fast propagation phase (elongation phase), ultimately resulting in the formation of amyloidogenic β-sheet fibrils that are stabilized (equilibrium phase) [418]. Thioflavin T (ThT) is a benzothiazole dye that binds along the surface side-chain grooves of β-sheet fibrils and becomes fluorescent, thus allowing the monitoring of amyloid fibrillization [417].

Using the ThT assay, 100 μM Aβ peptides (scrambled Aβ1-42, Aβ1-42, Aβ1-40, and Aβ25-35) were added to a well-plate containing aggregation buffer and ThT, and their fluorescence

was measured under agitation for 40 hours by microplate reader. The results in Figure 4.16 (B) show fluorescence intensity endpoints and high fibrillization profiles for Aβ1-42, Aβ25-35, and Aβ1-40, compared to scrambled Aβ1-42. However, the fibrillization of these peptides were not statistically significant when compared to control, possibly due to the high error bars. Samples of these fibrils were tested on platelets for superoxide detection with DHE at 5 μM (data not shown) but no response was detected and these results suggested that the protocol required further optimisation and characterisation of peptide fibrils with transmission electron microscopy (TEM) before testing on platelets.

Since these fibrils were to be mainly used as tools in this project, we collaborated with experts in misfolded protein chemistry, Dr. Janet Kumita and Prof. Christopher Dobson, from the University of Cambridge. They were able to provide us with a small sample of only fibrillar Aβ1-42, but not the other peptides. Flash-frozen fibril samples were prepared in Cambridge from 100 μM monomeric Aβ1-42 with 4% DMSO in PBS, and were stored at -20 °C. The effect of Aβ1-42 fibrils upon platelet superoxide anion generation was then tested in our laboratory in Bath. Platelets were stimulated with scrambled Aβ1-42, soluble Aβ1-42, and fibrillar Aβ1-42 in the presence of DHE, and the results showed that both soluble and fibrillar Aβ1-42 induced significant superoxide generation in platelets as displayed in Figure 4.16 (C).

Since fibrillar Aβ1-42 had been shown to induce superoxide anion generation, a follow up aggregation experiments were carried out to test the ability of this form of the peptide to promote platelet aggregation. Fibrillar Aβ1-42 was tested as an agonist alone or as a co-agonist with either 0.05 unit/ml thrombin or 3 μg/ml collagen. The aggregation results are presented in Figure 4.16 (D, E and F). Surprisingly, fibrillar Aβ1-42 did not induce even moderate platelet aggregation at a concentration of 1 μM, but platelet aggregation was slightly potentiated in the presence of collagen or thrombin. These results suggest that higher concentrations of fibrillar Aβ1-42 might be needed to induce significant platelet aggregation.

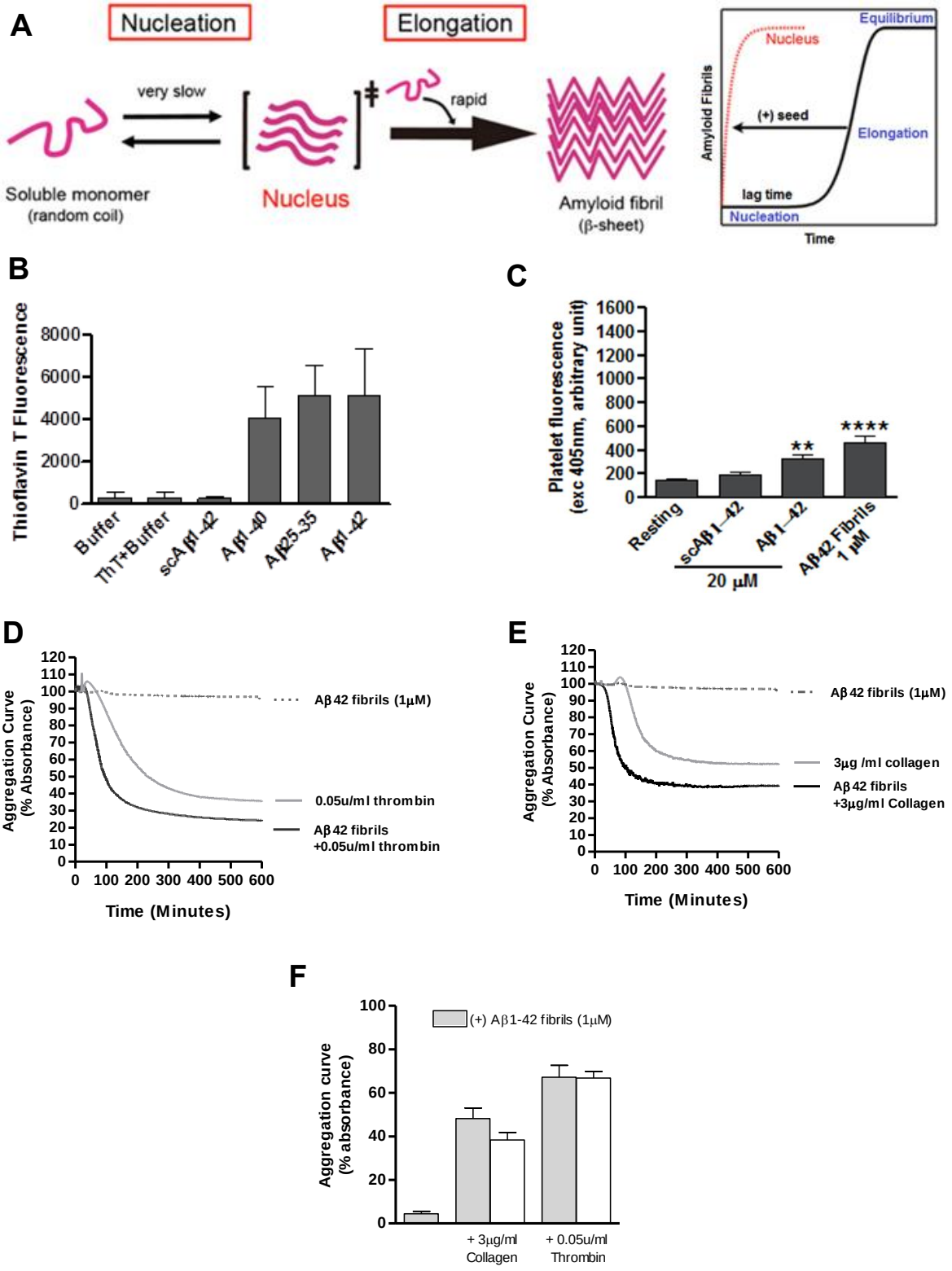

Figure 4.16: Effects of Aβ1-42 fibrils on superoxide anion formation and platelet aggregation.
(A) Nucleation dependent polymerization model for predicted amyloid fibril formation (modified from [418]. (B) Fluorescence intensity endpoints were quantified and analysed from 3 independent experiments for Aβ1-42, Aβ25-35, and Aβ1-40 and scrambled Aβ1-42 as control. (C) Superoxide anion formation upon fibrillar Aβ1-42 stimulation that was measured as described in previous figures using DHE. (D-E) Representative aggregation curves induced solely by 1 μM Aβ1-42 fibrils or co-stimulated with 0.05 u/ml thrombin (D) or collagen 3 μg/ml (E). (F) Quantification of average percentage aggregation of fibrillar Aβ1-42 stimulated platelet from 4 independent experiments. Statistical significance was analysed using one-way ANOVA with Bonferroni post-test; P-value <0.01 (**) and P-value < 0.0001 (****). Error bars represent mean ± SEM.

4.4. SUMMARY OF RESULTS

- The use of DCFDA for the detection of ROS appears promising as it showed ROS generation in platelets upon stimulation with thrombin (0.3 and 1 unit/ml), collagen (30 µg/ml), CRP (10 µg/ml), and Aβ25-35 (20 µM) but not Aβ1-40 or Aβ1-42. However, overall DCF fluorescence values and responses detected were quite low in spite of using high concentrations of different physiological agonists compared to normal concentrations used *in vitro*.
- A novel and reliable method was developed using DHE as a molecular probe for the detection of superoxide anion. Superoxide anion was significantly detected upon stimulation with thrombin (0.1, 0.3, and 1 unit/ml), collagen (30 µg/ml); CRP (3 and 10 µg/ml), arachidonic acid (10 and 30 µM), oxidised LDL (30, 100, 300 µg/ml) when compared to resting platelets; and also Aβ1-42 (20 µM), but not Aβ1-40 or Aβ25-35 when compared to scrambled control.
- 3 mM NAC and 10 µM VAS2870 were sufficient to abolish ROS or superoxide generation in Aβ1-42 stimulated platelets
- Thrombin-induced superoxide generation was abolished in the presence of VAS2870 but not in the presence of NOX1 inhibitors indicating that thrombin-induced superoxide generation might potentially be NOX1-independent
- Aβ1-42 shown to induce superoxide anion in platelets with DHE, while Aβ25-35 shown to induce ROS using DCFDA.
- Quantitative analysis with EPR confirmed the results obtained with the optimised DHE assay and showed that both Aβ1-42 and Aβ25-35 (to a lesser extent) induced superoxide anion generation in platelets. Superoxide generation in platelets stimulated with Aβ1-42 or Aβ25-35 is NOX-dependent.
- Fibrillar Aβ1-42 induced superoxide anion formation in platelets, but did not result in platelet aggregation at 1 µM as an agonist alone. However, fibrillar Aβ1-42 potentiated platelet aggregation in the presence of collagen or thrombin. This suggests that low concentration of fibrillar Aβ1-42 can result in partial activation of platelets through ROS generation but requires the presence of a secondary agonist to potentiate full platelet activation.

4.5. DISCUSSION

Several publications have now shown the important role of reactive oxygen species (ROS) as second messengers and as critical intracellular signalling modulators of platelet activities in health and disease for the subsequent amplification of platelet responses and agonist release [355-359]. Under pathological conditions, such as ischemia, hypercholesterolemia, cardiovascular diseases, and AD, studies have shown platelets to be altered or hyperactive with prominent involvement of ROS that may lead to excess clot formation and pro-thromboembolic complications associated with these diseases [312, 364, 370, 420]. Few studies have reported the formation of ROS upon Aβ peptides stimulation of platelets [295, 297, 340], and therefore, the present study assessed redox changes in platelets upon Aβ peptides stimulation using different ROS detection methodologies.

At the initial stages of this study, the molecular probe DCFDA was used for the detection of ROS generation in platelets, mainly for H_2O_2 [421]. The pilot study for the detection of DCF fluorescence using a microplate reader displayed high basal saturation levels causing inaccurate ROS readings. The high basal saturation levels were thought to be due to the long incubation with DCFDA or potential artificial amplification of the fluorescence signal intensity due to certain limitations associated with DCFDA [395, 421, 422]. The idea of using microplate reader was discarded after several follow up failed experiments. The use of flow cytometry for ROS measurement was the next step followed, since positive results were reported previously [357, 387, 423]. Our results obtained with flow cytometry appeared to be more promising in terms of ROS detection. Several platelet agonists were investigated to assess the validity of this ROS detection method, including collagen, thrombin, CRP, arachidonic acid, ADP, and oxidised LDL. The results from the present study are in agreement with previous publications in terms of ROS generation upon stimulation with collagen, thrombin, and CRP [310, 314, 357]. The ROS scavenger NAC was used to validate the results of this study with regards to the detected ROS at different concentrations and incubation time, and 30 mM NAC was able to bring down ROS to basal level of resting platelets upon collagen stimulation.

When the effects of Aβ peptides on platelet ROS generation were then tested, Aβ25-35 showed statistical significance compared to resting platelets, but not to scrambled Aβ1-42 (control). The effects of Aβ25-35 on ROS generation in platelets in this study are in agreement with previously published work [296, 340], however, previous studies showed that Aβ1-40 also induced ROS generation in platelets, which we could not replicate in this study using DCFDA [295, 307]. Overall, DCF fluorescence seemed insufficient when looking at the

results of different physiological agonists used as the concentrations to obtain a detectable response were too high compared to normal concentrations used *in vitro*. In addition, the NAC concentration needed to scavenge ROS was high compared to the ones used in other studies [153, 399, 424, 425]. Since superoxide anion (O_2^{-}•) is considered central to ROS chemistry and platelet have been shown to mainly produce this species [312, 426], a second molecular probe dihydroethidium (DHE), was utilized.

DHE was chosen as another detection fluoroprobe to further investigate the oxidative state in live platelets, and its use was optimised with flow cytometry. Several agonists were tested, the same ones previously mentioned with DCFDA experiments, and our results were in agreement with previous studies when using thrombin [387, 388], collagen (and CRP) [383, 389], arachidonic acid [380], oxidised LDL [390], and shown to induce superoxide anion generation in platelets. The results also indicate that ADP alone as an agonist did not trigger superoxide generation in platelets, which suggests that ADP-mediated platelet activation is independent of NOX activity and ROS generation. To validate the results obtained, NAC concentration-dependent experiments were carried out using thrombin as a physiological stimulus to determine the optimal concentration of NAC to be used in future experiments. NAC at 3 mM seemed to ideally abolish ROS and bring the fluorescence values of platelets down to basal levels similar to the ones in the resting state. Therefore, another set of experiments were also carried out testing its efficiency with other physiological stimuli including arachidonic acid (AA), oxLDL and CRP. Both CRP and oxLDL showed significant reduction in the superoxide detected, but this was not observed for platelets stimulated with AA.

To further investigate and validate sources of superoxide anion generated in platelets, NOX inhibitors (VAS2870 and NOX1 inhibitor) were used in platelets stimulated with thrombin. Superoxide generation was significantly inhibited with VAS2870 but not with NOX1 inhibitor, which might suggests that superoxide generated from thrombin is NOX1-independent. This result with thrombin is not consistent with Delaney's study [391] that highlighted the essential involvement of NOX1 in thrombin stimulation and it is most likely due to the experimental conditions used, but other previous studies are in agreement with our data [357, 383]. In addition, our most recent published work using EPR and transgenic mice, demonstrated that thrombin stimulation of platelets is NOX2-dependent [427], which further validates this result.

Finally, Aβ peptide-induced superoxide anion generation in platelets was assessed. Interestingly, only soluble Aβ1–42 (20 μM) had a significant effect on superoxide generation, but not Aβ1–40 or Aβ25-35 when compared to the scrambled Aβ1-42 control.

The ability of this peptide to produce these kind of responses in platelets compared to Aβ1-40, is potentially associated with its more highly hydrophobic nature. This study revealed for the first time that Aβ1-42 peptide induced significant superoxide anion generation in live platelets. The concentration-response study with Aβ1-42 showed that concentrations greater than 10 μM induced significant increases in superoxide anion generation using the newly optimised protocol, and that this was significantly inhibited with previously determined concentrations of VAS2870 and NAC. These results demonstrated that Aβ1-42 induces platelet activation and superoxide generation in a NOX-dependent manner and these findings were published in 2017 [401].

When EPR became accessible in our laboratories, further experiments were conducted on Aβ peptides to confirm and further investigate the sources of superoxide anions generated. Since EPR has high quantitative accuracy for ROS detection, it not only confirmed Aβ1-42 effects on platelet superoxide generation but also showed that Aβ25-35 is able to moderately induce superoxide generation in platelets, which can explain some of the ROS results previously reported in the literature with this peptide [297, 340], and in our earlier work using DCFDA.

To further examine the sources of superoxide generated with these peptides, pharmacological NOX inhibitors for NOX1 and NOX2 were used. Aβ1-42 and Aβ25-35 stimulated platelets revealed significant abolishment of superoxide when either NOXs were inhibited, which suggests that both NOXs are essential for superoxide generation in platelets stimulated by these peptides. Our group's recent published work investigated the effects of Aβ1-42 on platelets using EPR, aggregation assays, and transgenic mice, and confirmed that both NOXs are important in Aβ1-42 induced platelet activation [427]. These results highlights the central importance of ROS in platelet activation by Aβ peptides, with the exception of Aβ1-40.

Since soluble Aβ1-42 induced significant superoxide generation, the fibrillar form of Aβ1-42 was also tested and the results showed significant superoxide generation at 1 μM by fibrillar Aβ1-42 and was at a higher level than superoxide generation by 20 μM soluble Aβ1-42. This might be due to the highly hydrophobic nature of this form of the peptide and cytotoxicity associated with it. The N-terminus of Aβ1-42 peptide is thought to be important for initiating the conformational switching from α-helical (monomer) to β-sheet structure (oligomer), and the peptide shows enhanced susceptibility for self-aggregation to oligomers and fibrillar β-sheet structures, due to intermolecular interactions between its hydrophobic regions [428-430].

The formation of these oligomers and fibrils has been markedly connected with cell toxicity [431], and are shown to be protease-resistant with oligomers being were reported to form Ca^{2+}-permeable Aβ channels and elevating intracellular Ca^{2+} [432]. Since soluble Aβ1-42 had been shown previously to induce moderate platelet aggregation and potentiation as an agonist or co-agonist in the presence of another physiological agonist, the effects of fibrillar Aβ1-42 on platelet aggregation were also assessed.

Surprisingly, fibrillar Aβ1-42 did not induce platelet aggregation as an agonist nor potentiated aggregation as a co-agonist in the presence of thrombin (0.05 u/ml) or collagen (3 µg/ml), despite its profound effects in generating superoxide anion in platelets. An explanation for these results might be due to the low concentration of Aβ1-42 (1 µM) used as other studies using the fibrillar form of Aβ have been reported to use higher initial concentrations [302, 345, 353]. The very recent Elaskalani's study [345], demonstrated that Aβ1-42 fibrils does induce platelet activation in a concentration-dependent manner (5, 10, and 20 µM). However, they also used Tyrode buffer containing 1.8 mM $CaCl_2$ while ours was Ca^{2+} free.

The difference between our methodology and that used by the Elaskalani's group is the buffer composition and fibril concentrations used, which could explain the lack of strong platelet aggregation observed in our experiments upon Aβ fibril stimulation. Nonetheless, fibrillar Aβ1-42 potentiated platelet aggregation in the presence of collagen or thrombin which suggests that low concentrations of fibrillar Aβ1-42 can result in partial activation, and in the presence of a secondary agonist can potentiate full platelet activation. This may reflect on the effects of fibrillar forms of Aβ peptides that accumulation in the cerebrovasculature of AD patients, and future experiments for platelet aggregation with higher fibril concentrations are therefore worth investigating to further understand their underlying mechanism of action.

One limitation in the study here was that time and cost constraints did not permit the potential exploration of various other ROS or RNS. The detection of such species both intra- and extracellularly in platelets using EPR and the effect of using other effective pharmacological inhibitors of ROS is an area which may be investigated further. The lack of availability of fibrillar Aβ1-40 also did not allow its effect on platelet adhesion and aggregation to be investigated in this study, and similarly the effects of both fibrillar Aβ1-40 and Aβ1-42 on platelets under flow conditions. Structural characterization of fibrillar Aβ (e.g. using TEM imaging) that was indicated by the ThT assay could also have been carried out to elaborate further on the aggregation results obtained with fibrillar Aβ1-42 and platelets.

In summary, the present study proposes a novel flow cytometry-based assay for the detection of superoxide formation using DHE in live platelets that is reliable and easily accessible in academic institutions and clinical laboratories. Even though EPR is considered the ideal standard method for the detection of intracellular ROS, it requires highly specialised equipment and dedicated specialist personnel to handle procedural complexities and lengthy data analysis, which makes its usage limited to only certain research and clinical institutions that can meet these demands. Therefore, the development of a widely available, cost effective, and reliable ROS detection methodology was desired and here we have proposed a novel alternative methodology that can be utilized in haemostasis and thrombosis studies.

In addition, the results of this study highlight the importance of NADPH oxidase enzymes and oxygen radical formation in platelet function and activation in response to Aβ peptides, especially Aβ1-42. Moreover, this study confirms the association of ROS generation with platelets stimulated with physiological stimuli such as collagen, thrombin and arachidonic acid, and is consistent with previously published studies. Furthermore, the current study also reveals that ADP-mediated platelet activation is independent of NOX activity and ROS generation and shows that thrombin induces superoxide anion generation in a NOX1-independent manner. Aβ1-42 was demonstrated to induce superoxide generation in platelets in a NOX-dependent manner. These findings suggest that NADPH oxidases can potentially be used as therapeutic targets to address the effects of Aβ peptides on platelet activation and their prothrombotic activities associated with Alzheimer’s disease and its complications.

CHAPTER 5

Redox-Dependent Changes in Platelet Functional Responses Induced by Aβ Peptides

5. RESULTS

5.1. BACKGROUND

It has becoming increasingly evident that the role of oxidant in platelet function and biology is critical and that the balance between oxidants and antioxidants regulation systems can be affected in health and disease [433]. Dysregulation in platelet activation and function can lead to thrombogenesis and death by cardiovascular diseases [177]. The effects of oxidants on platelet activation and aggregation from both exogenous and endogenous sources have been documented by several studies. For example, some studies have documented that exposure of platelets to H_2O_2 showed inhibitory effects on platelet function [434-436], while other studies showed enhanced aggregation and involvement of superoxide radicals [437, 438]. Much of the discrepancies between the studies on whether oxidants enhanced or inhibited platelet aggregation are usually attributed to the differences in experimental protocols followed.

In recent years several studies have highlighted the importance role of endogenous oxidants in regulating platelet activity and signalling upon stimulation with physiological agonists, such as collagen, TXA2, thrombin, and arachidonic acid [357, 358, 383, 387-391, 427, 439], Endogenous ROS generation and release from platelets whether stimulated or unstimulated were reported and indicate their role in facilitating platelet activation in an autocrine or paracrine fashion with similar effects to exogenous ROS [358, 440]. Platelets have been shown to be in a hyperactive state in many pathological conditions, such as, in AD, and diabetes mellitus [151, 441, 442], which creates a highly prothrombotic environment. Inhibition of platelets and anti-thrombotic effects of antioxidants in previous studies have demonstrated the dependency of platelet activation on ROS generation.

Several studies have reported the involvement of Aβ in platelet activation, adhesion and aggregation and their supportive role in thrombus formation at vascular lesions or CAA [295-298, 300, 302, 303, 306, 307], and while fewer studies have reported the formation of ROS upon stimulation of platelets by Aβ peptides [295, 296]. However, several aspects of the effects of Aβ peptides on platelets remain unclear and the exact cellular mechanism by which Aβ peptides activate platelets and regulate haemostasis and thrombosis remains to be defined.

Therefore, the main aims of the previous Chapters 3 and 4 in this project, were to determine the effects of Aβ peptides i.e. Aβ25-35, Aβ1-40, Aβ1-42, and scrambled Aβ1-42 as control, on platelet adhesion, activation, and aggregation under static and flow conditions, and assess their effects on redox changes in platelets. The findings in these studies revealed that, Aβ peptides support platelet adhesion, particularly with Aβ1-42, where it induced significant

platelet adhesion and spreading under static condition. It also induced and potentiated platelet aggregation, increased thrombus formation in whole blood under physiological venous flow conditions, and induced significant superoxide anion generation in live platelets in a NOX-dependent manner. Since Aβ1-42 appeared to be the most active peptide in our experimental conditions, the present Chapter aimed to investigate redox-dependent changes in platelet functional responses upon stimulation with Aβ1-42 peptide, and the potential receptors that might be involved.

5.2. AIMS & OBJECTIVES

- Determine the effects of ROS and NOX inhibition on platelet adhesion and spreading to Aβ1-42 peptide using adhesion assay under static conditions.
- Determine the effects of NOX inhibition on platelet adhesion to Aβ1-42 under physiological shear stress.
- Determine whether integrin αIIbβ3 activation by Aβ1-42 is NOX-dependent.
- Determine the effects of NOX inhibition on Aβ1-42 stimulated platelet aggregation and potentially which NOX isoform is involved.
- Determine the effects of Aβ1-42 on platelet intracellular signalling activation using phosphospecific immunoblotting.
- Determine the effects of PAR1, CD36, and GPVI receptors inhibition on platelet adhesion and spreading to Aβ1-42 peptide under static conditions.

5.2. RESULTS

5.2.1. Effects of ROS inhibition on Aβ1-42-induced platelet adhesion and spreading under static conditions

The initial aim of this study was to examine the effects of redox changes on platelet functional responses in terms of adhesion, activation, and aggregation. A series of experiments were carried out using an adhesion assay (see Chapter 2 for methodology) to determine the effects of ROS inhibition on platelet adhesion and spreading on Aβ1-42, Aβ1-42 with collagen, or Aβ1-42 with fibrinogen. This was due to the profound effects of Aβ1-42 on platelet adhesion and spreading compared to the other peptides, as demonstrated in Chapter 3. Previously determined concentrations of ROS scavenger NAC (3 mM), and NOX inhibitor VAS2870 (10 μM) (from Chapter 4) were used.

The results for ROS inhibition with NAC are presented in Figures 5.1, 5.2, and 5.3, while results for NOX inhibitor VAS2870 are presented in Figure 5.4, 5.5, and 5.6. Panels A-B for all these figures are representative images of platelet adhesion and spreading for each of the conditions, while panels C-D show quantitative analysis of adhesion and spreading area. Unexpectedly, the presence of NAC produced an increased platelet adhesion and spreading area onto Aβ1-42 but this was not statistically significant when compared to Aβ1-42 without NAC (see Figure 5.1 (C and D)).

Platelet adhesion and spreading onto Aβ1-42 with collagen (Figure 5.2 (C and D)) was not inhibited with NAC compared to BSA, but a noticeable decrease was observed (Figure 5.3 (C and D)) on Aβ1-42 with fibrinogen. Interestingly, BSA showed increased platelet adhesion and spreading area in the presence of NAC when compared to experiments without. Overall, ROS inhibition with NAC at 3 mM was not sufficient to prevent Aβ1-42-induced platelet adhesion and spreading with or without the presence of collagen or fibrinogen under static conditions. Further NAC concentration-dependent future experiments on platelet adhesion should be explored. In addition, error bars in these previously mentioned figures with NAC show large variability in the repeats, which indicates that additional repeat experiments are required.

On the other hand, the NOX inhibitor VAS2870, strongly impaired both platelet adhesion and spreading onto Aβ1-42, alone or in the presence of collagen or fibrinogen but the number of adhering platelets was not completely abolished as shown in Figures 5.4, 5.5, and 5.6. These results indicate the importance of NOXs in mediating platelet adhesion and activation.

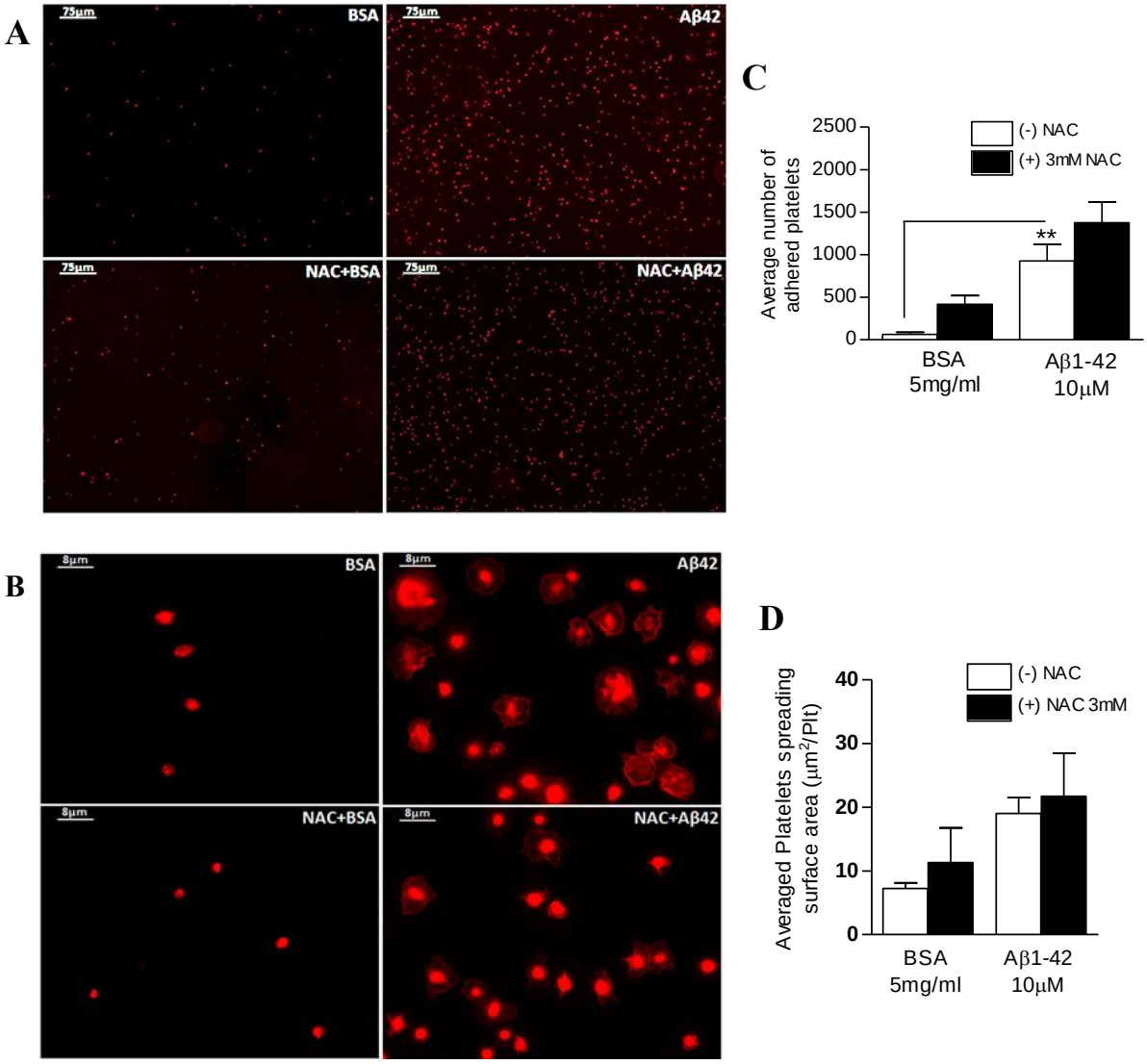

Figure 5.1: Effects of ROS inhibition with NAC on platelet adhesion and spreading over Aβ1-42-coated surfaces.

(A-B) Representative images of platelets with or without NAC presence that were allowed to adhere onto glass coverslips coated with 10 µM Aβ1-42 or BSA 5mg/ml. Platelets were then fixed, stained, then visualized under the fluorescence microscope and images were taken at 10x and 100x magnification. (C-D) Quantification and evaluation of the mean number of adhered platelets and mean spreading area per optical field from at least 4 independent experiments. Statistical significance was analysed using one-way ANOVA with Bonferroni post-test; P-value < 0.01 (**) refers to significance in the mean number of adhered platelets to Aβ1-42 compared to BSA (control). Error bars represent mean ± SEM.

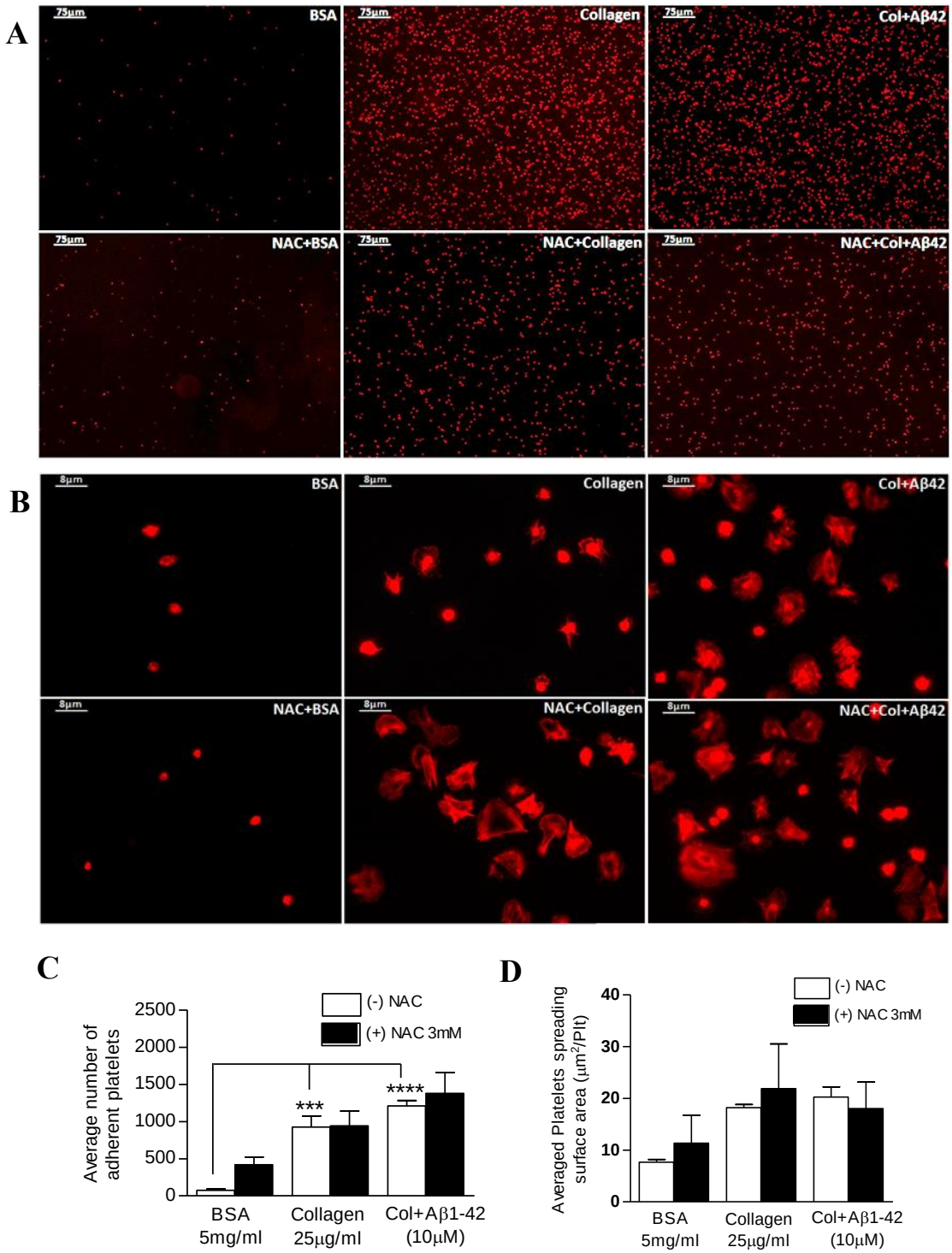

Figure 5.2: Effects of ROS inhibition with NAC on platelet adhesion and spreading over dual coated surfaces with collagen and Aβ1-42.
(A-B) Representative images of platelets with or without NAC presence that were allowed to adhere onto glass coverslips coated with bovine serum albumin (BSA, 5 mg/ml), collagen (25 µg/ml), or collagen with Aβ1-42 peptide (10 µM). Platelets were then fixed, stained, then visualized under the fluorescence microscope and images were taken at 10x and 100x magnification. (C-D) Quantification and evaluation of the mean number of adhered platelets and spreading area per optical field from at least 4 independent experiments. Statistical significance was analysed using one-way ANOVA with Bonferroni post-test; P-value < 0.001 (***) and P-value < 0.0001 (****) refers to significance in the mean number of adhered platelets to either collagen or collagen with Aβ1-42 compared to BSA (control). Error bars represent mean ± SEM.

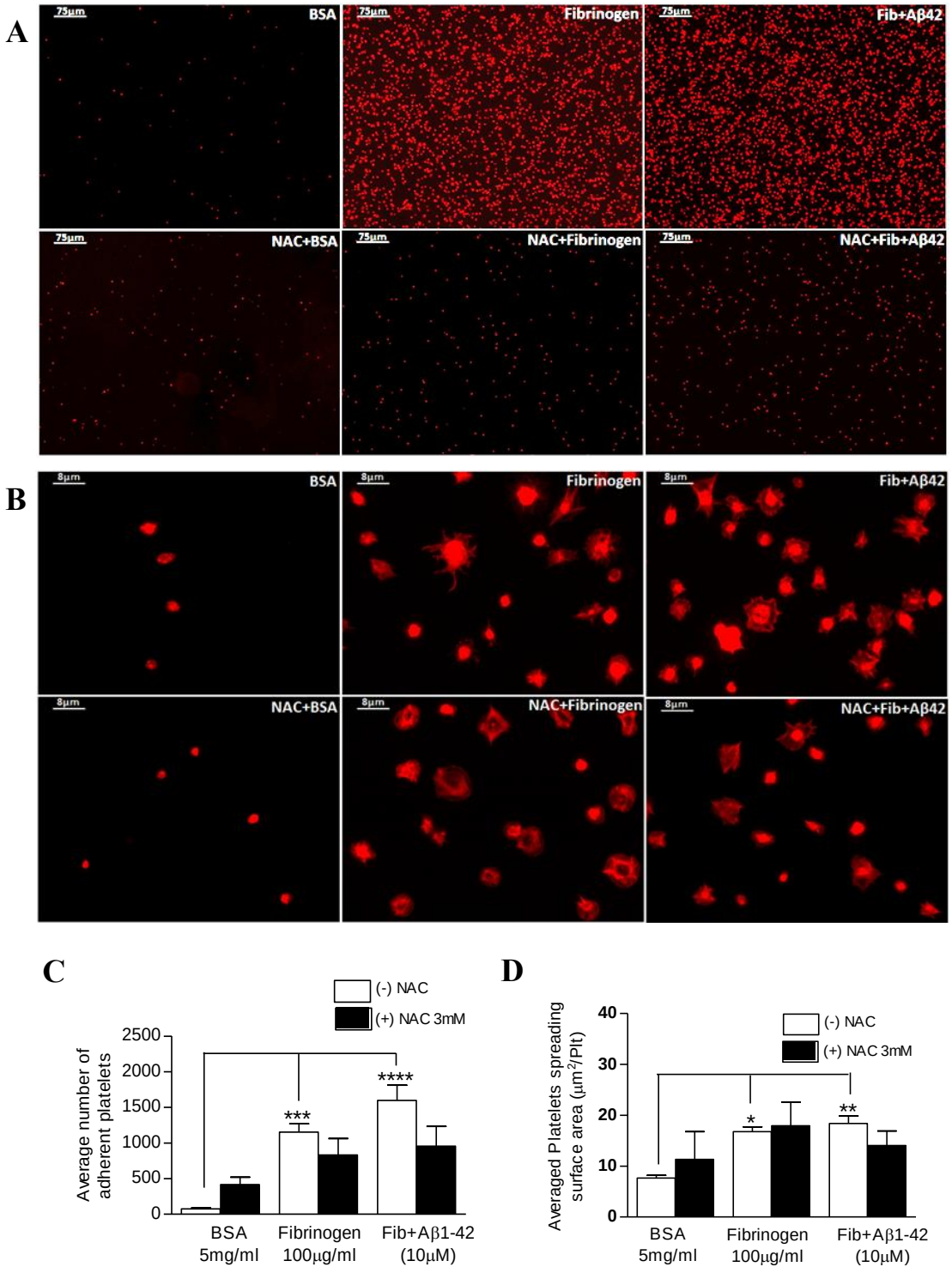

Figure 5.3: Effects of ROS inhibition with NAC on platelet adhesion and spreading area over dual coated surfaces with fibrinogen and Aβ1-42.

(A-B) Representative images of platelets with or without NAC that were allowed to adhere onto glass coverslips coated with bovine serum albumin (BSA, 5 mg/ml), fibrinogen (100 µg/ml), or fibrinogen with Aβ1-42 peptide (10 µM). Platelets were then fixed, stained, then visualized under the fluorescence microscope and images were taken at 10x and 100x magnification. (B) Quantification and evaluation of the mean number of adhered platelets and spreading area per optical field from at least 4 independent experiments. Statistical significance was analysed using one-way ANOVA with Bonferroni post-test; P-value < 0.05 (*), P-value < 0.01 (**), P-value < 0.001 (***) and P-value < 0.0001 (****) refers to significance in the mean number of adhered platelets and spreading area to either fibrinogen or fibrinogen with Aβ1-42 compared to BSA (control). Error bars represent mean ± SEM.

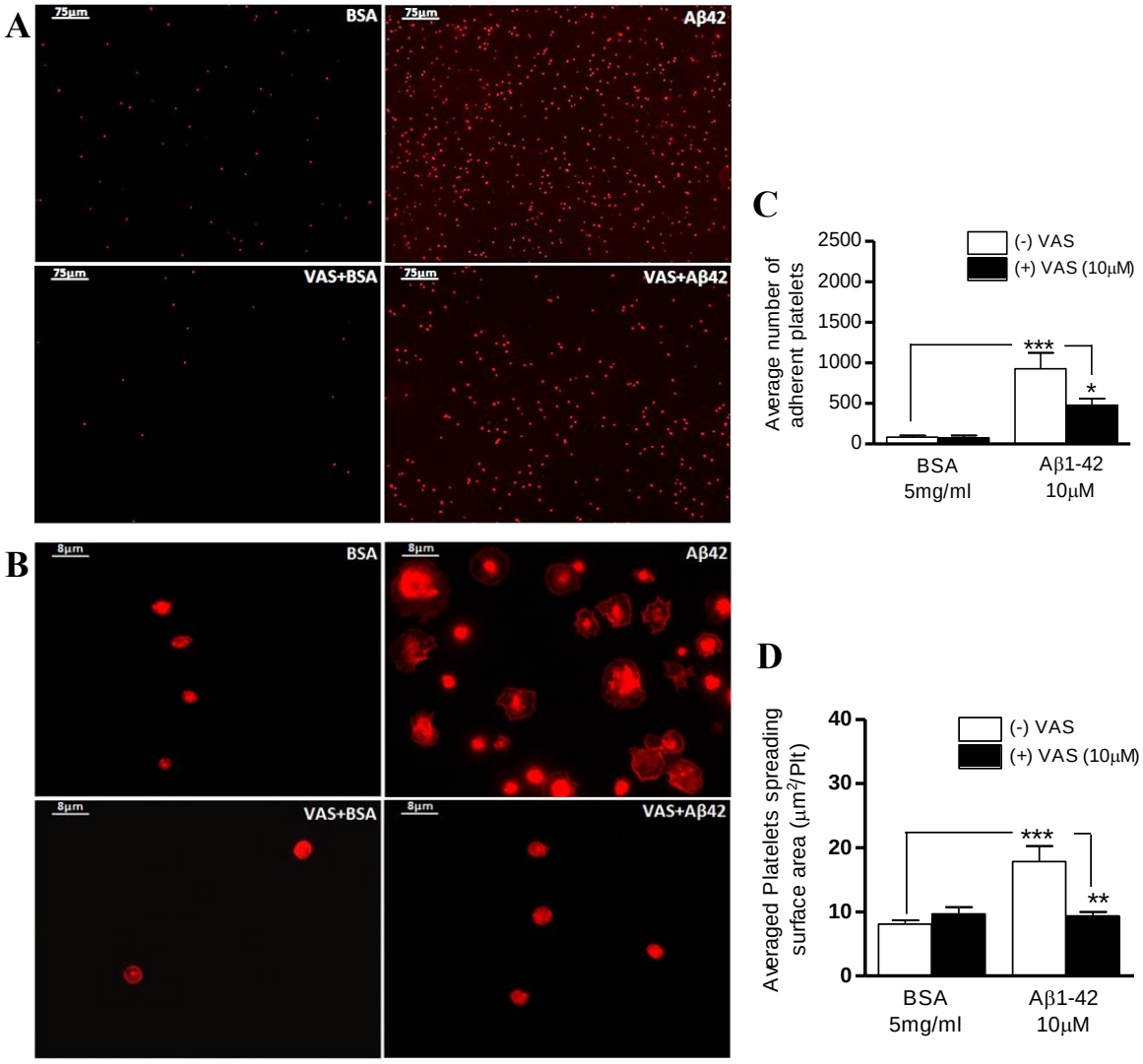

Figure 5.4: Aβ1-42 induces NOX-dependent platelet adhesion and spreading under static conditions. (A-B) Representative images of platelets with or without NOX inhibitor VAS2870 (10 µM) that were allowed to adhere onto glass coverslips coated with 10 µM Aβ1-42 or BSA 5mg/ml. Platelets were then fixed, stained, then visualized under the fluorescence microscope and images were taken at 10x and 100x magnification. (C-D) Quantification and evaluation of the mean number of adhered platelets and spreading area per optical field from at least 4 independent experiments. Statistical significance was analysed using one-way ANOVA with Bonferroni post-test; P-value < 0.05 (*), P-value < 0.01 (**), and P-value < 0.001 (***) refers to significance in the mean number of adhered platelets and spreading area to Aβ1-42 compared to BSA (control) and also the decrease in the mean number of adhered platelets and spreading area upon treatment with NOX inhibitor VAS2870 (+) compared to the ones without the inhibitor (-). Error bars represent mean ± SEM.

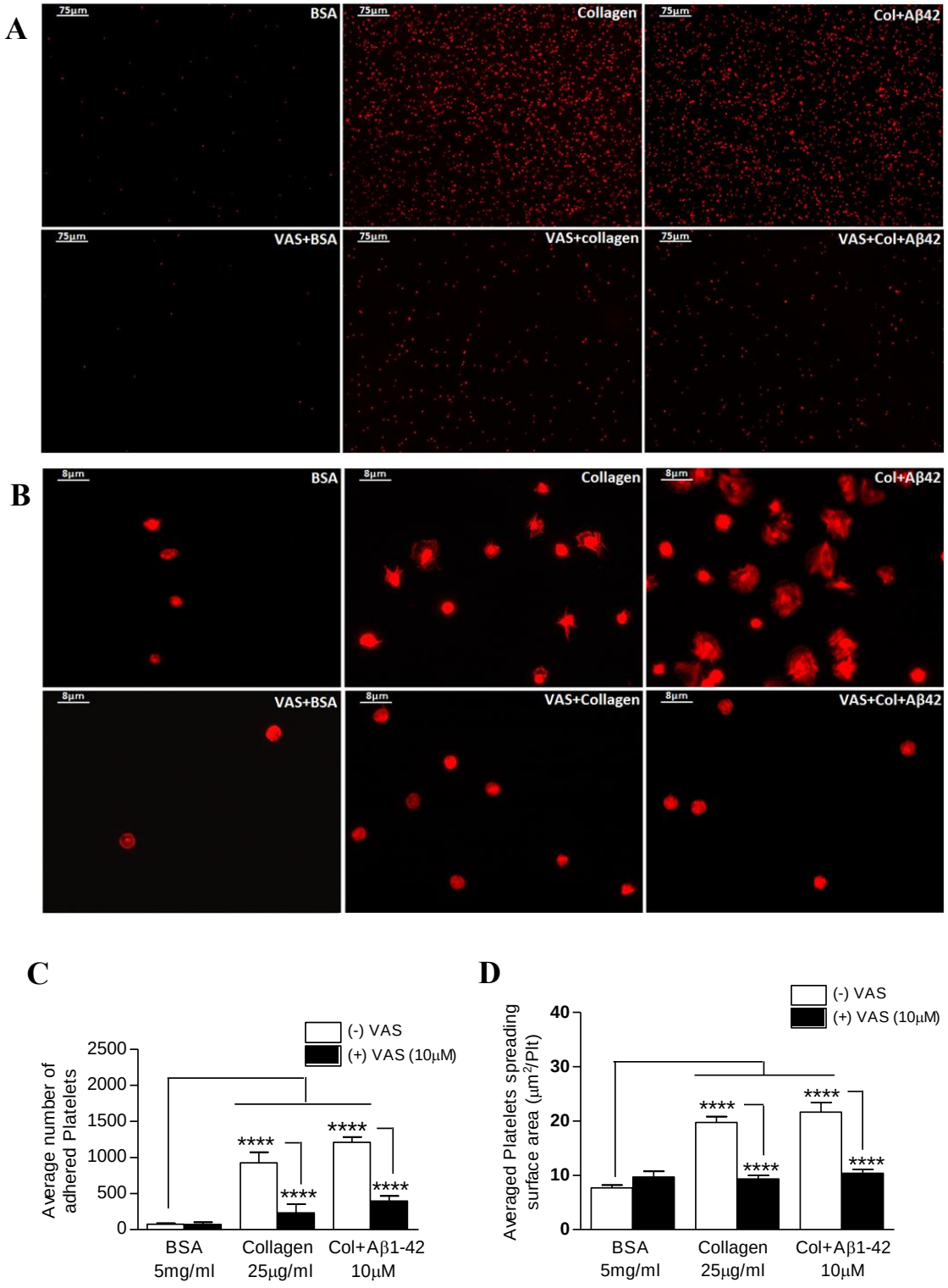

Figure 5.5: NOX-dependent inhibition of platelet adhesion and spreading over dual coated surfaces with collagen and Aβ1-42.

(A-B) Representative images of platelets with or without NOX inhibitor VAS2870 (10 µM) that were allowed to adhere onto glass coverslips coated with bovine serum albumin (BSA, 5 mg/ml), collagen (25 µg/ml), or collagen with Aβ1-42 peptide (10 µM). Platelets were then fixed, stained, then visualized under the fluorescence microscope and images were taken at 10x and 100x magnification. (C-D) Quantification and evaluation of the mean number of adhered platelets and spreading area per optical field from at least 4 independent experiments. Statistical significance was analysed using one-way ANOVA with Bonferroni post-test; P-value < 0.0001 (****) refers to significance in the mean number of adhered platelets and spreading area to collagen or Aβ1-42 with collagen compared to BSA (control) and also the decrease in the mean number of adhered platelets and spreading area upon treatment with NOX inhibitor VAS2870 (+) compared to the ones without the inhibitor (-). Error bars represent mean ± SEM.

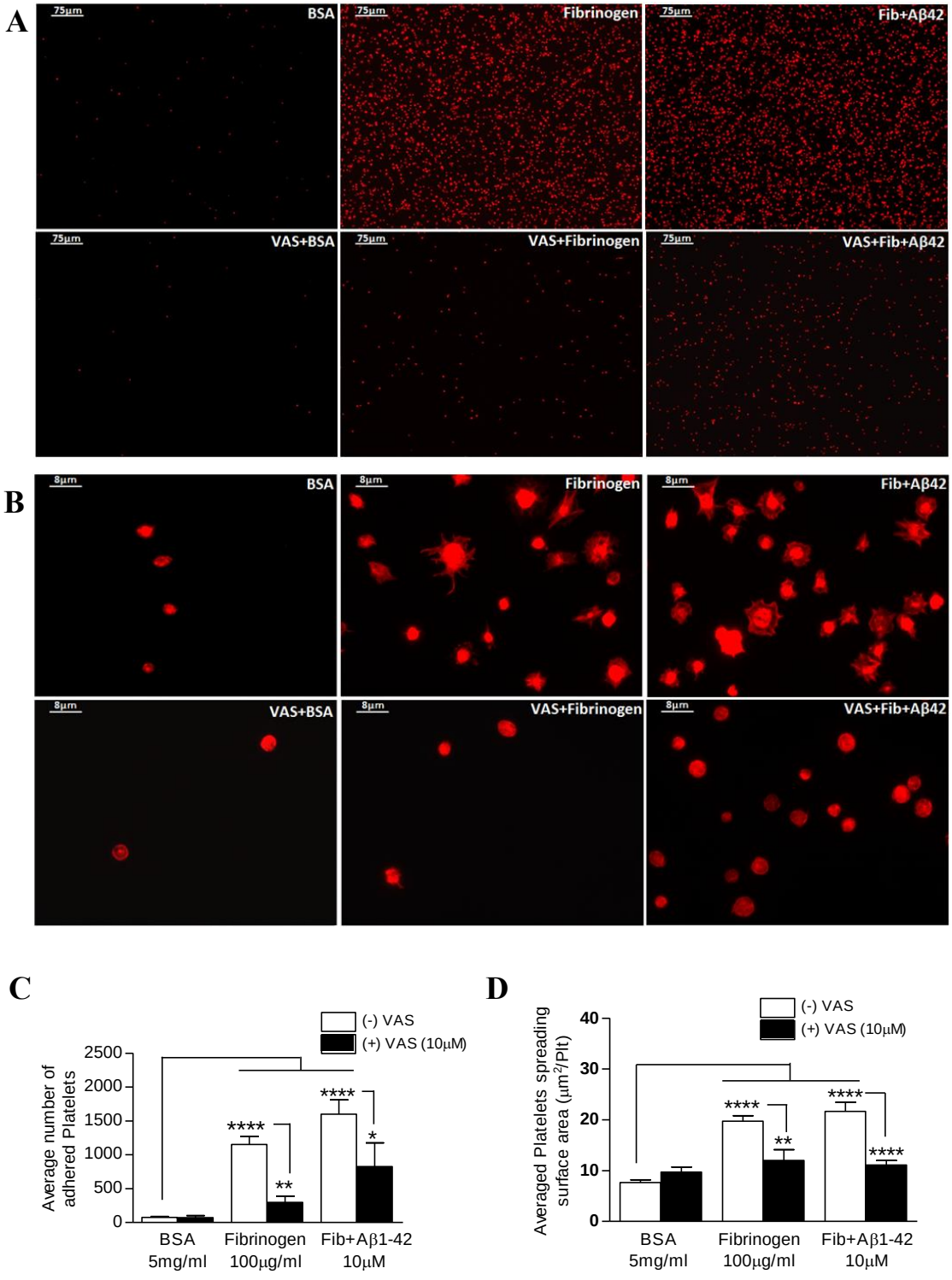

Figure 5.6: NOX-dependent inhibition of platelet adhesion and spreading over dual coated surfaces with fibrinogen and Aβ1-42.

(A-B) Representative images of platelets with or without NOX inhibitor VAS2870 (10 µM) that were allowed to adhere onto glass coverslips coated with bovine serum albumin (BSA, 5 mg/ml), fibrinogen (100 µg/ml), or fibrinogen with Aβ1-42 peptide (10 µM). Platelets were then fixed, stained, then visualized under the fluorescence microscope and images were taken at 10x and 100x magnification. (C-D) Quantification and evaluation of the mean number of adhered platelets and spreading area per optical field from at least 4 independent experiments. Statistical significance was analysed using one-way ANOVA with Bonferroni post-test; P-value < 0.05 (*), P-value < 0.01 (**), and P-value < 0.0001 (****) refers to significance in the mean number of adhered platelets and spreading area to fibrinogen or Aβ1-42 with fibrinogen compared to BSA (control) and also the decrease in the mean number of adhered platelets and spreading area upon treatment with NOX inhibitor VAS2870 (+) compared to the ones without the inhibitor (-). Error bars represent mean ± SEM.

5.2.2. NOX inhibition attenuated thrombus formation potentiated by Aβ1-42 under physiological venous flow conditions

In order to examine the effects of NOX inhibition on Aβ1-42-stimulated platelet adhesion and thrombus formation under physiological shear stress *in vitro*, an experiment was carried out using an ExiGo microfluidic pump (see Chapter 2 for methodology). Platelet adhesion on 10 μM Aβ1-42, scrambled Aβ1-42, or 0.1 mg/ml fibrillary collagen were tested in human whole blood at arterial shear rates of 1,000 sec^{-1} and a venous shear rate of 200 sec^{-1} and the results are shown in Figure 5.7. Representative images of platelet surface area coverage are shown in Figure 5.7 (A-E), while quantification and analysis of surface area coverage is shown in Figure 5.7 (F). NOX inhibitor VAS2870 significantly inhibited platelet adhesion to Aβ1-42 peptide under venous flow.

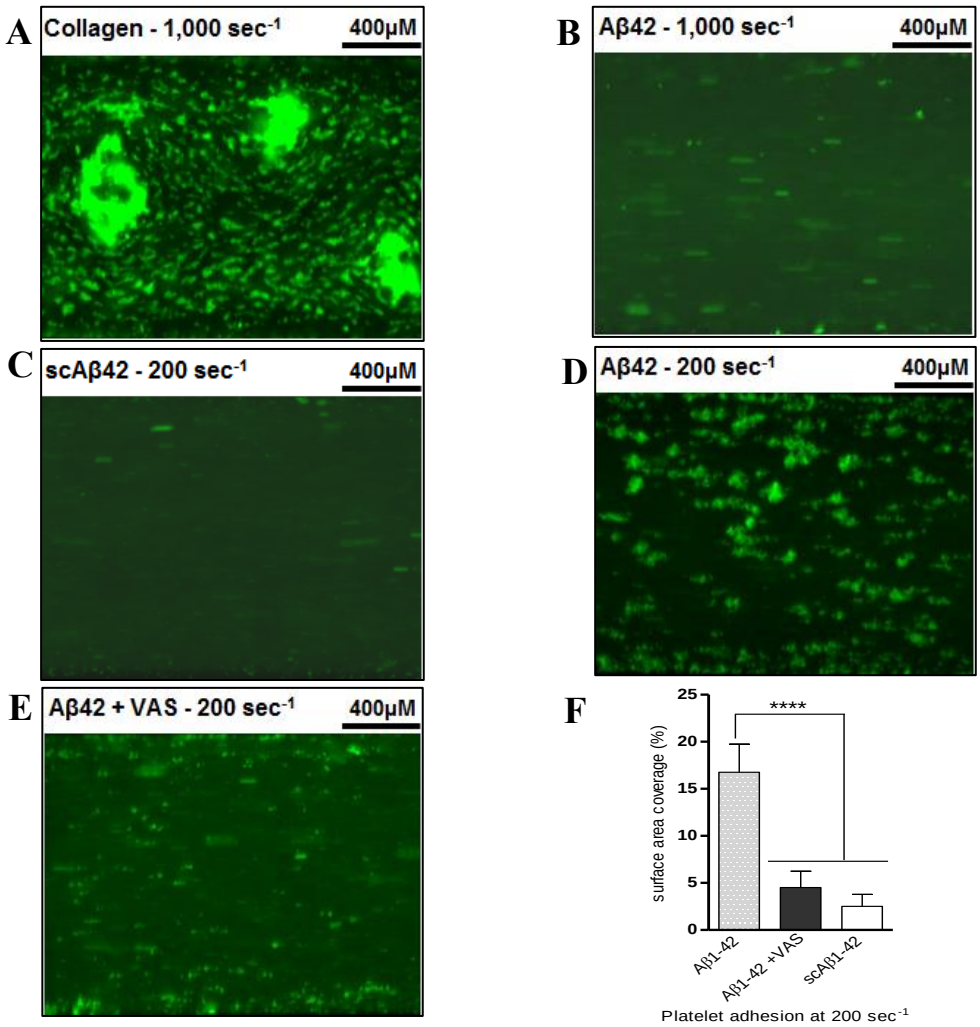

Figure 5.7: Effects of NOX inhibition on platelet adhesion to Aβ1-42 under physiological shear stress. Vena 8 Fluoro microchips were coated with 10 μM Aβ peptides or 0.1 mg/ml fibrillary collagen. Platelet adhesion with or without NOX inhibitor VAS2870 was tested in human whole blood at shear rates 1,000 sec^{-1} and 200 sec^{-1} using an ExigGo pump and images were obtained and shown in (A-E). (F) Quantification and analysis of surface area coverage from 3 independent experiments using Image J. Statistical significance was analysed using one-way ANOVA with Bonferroni post-test; P-value < 0.0001 (****) refers to significant decrease in the surface area coverage with adhered platelets to Aβ1-42 upon treatment with VAS2870. Error bars represents mean ± SEM.

5.2.3. Aβ1-42 stimulated platelets induce $\alpha_{IIb}\beta_3$ activation in a NOX-dependent manner

In Chapter 3, Aβ1-42 had been shown to support platelet adhesion under static conditions and under venous flow, promote and potentiate platelet aggregation, and integrin $\alpha_{IIb}\beta_3$ activation. Aβ1-42-induced integrin $\alpha_{IIb}\beta_3$ activation and P-selectin expression was next assessed in the presence of 10 μM NOX inhibitor VAS2870. NOX inhibition abolished Aβ1-42-induced $\alpha_{IIb}\beta_3$ activation as shown in Figure 5.8 (E). Aβ1-42 effects on platelet degranulation and translocation of P-selectin to the surface membrane of the platelets was also investigated in the presence of VAS2870. Aβ1-42 was not able to effectively induce platelet degranulation on its own but there is a noticeable decrease in the intensity of PAC1 staining in the presence of VAS2870, although the results are not significant compared to control. Figure 5.8 (A) shows side scattering (SSC) and forward scattering (FSC) dot plot of platelets detected and suggests high purity for the platelet preparation. (B-D) are representative histograms for the intensity of PAC1 staining in the different conditions.

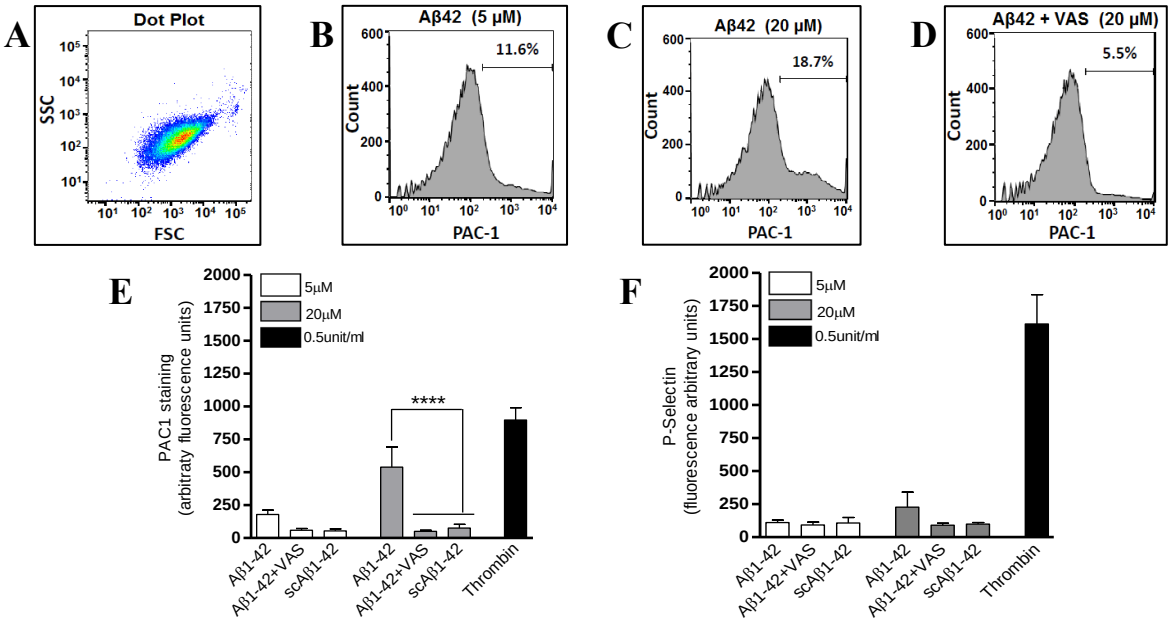

Figure 5.8: Activation of integrin αIIbβ3 by Aβ1-42 is NOX-dependent.
Isolated human platelets in suspension were stimulated with Aβ1-42 and scrambled Aβ1-42 or 0.5 unit/ml thrombin in the presence or absence of VAS2870 for 10 minutes and then labelled with FITC-PAC1 or PE-Cy5-P-selectin for further 10 minutes. (A) Side scattering (SSC) / forward scattering (FSC) dot plot suggests high purity for the platelet preparation. (B-D) Representative histograms for the intensity of PAC1 staining in the different conditions. (E-F) Quantification and statistical analyses of 3 independent experiments for the detection of P-selectin expression or integrin $\alpha_{IIb}\beta_3$ activation using one-way ANOVA with Bonferroni post-test; P-value < 0.0001 (****) refers to significance in fluorescence with PAC1 staining for Aβ1-42 compared to scrambled Aβ1-42 and significant inhibition in the presence of VAS2870. Error bars represent mean ± SEM.

Thrombin was used as positive control in the experiments. (E-F) shows quantification and statistical analysis for P-selectin expression or integrin $\alpha_{IIb}\beta_3$ activation. The results indicate the important role of NOX in integrin $\alpha_{IIb}\beta_3$ activation in platelets when stimulated with Aβ1-42 and thus suggesting that Aβ1-42-induced integrin $\alpha_{IIb}\beta_3$ activation is NOX-dependent.

In order to examine the effects of Aβ1-42 on redox changes in platelet functional responses in terms of aggregation, three agonists were initially used: thrombin, CRP, and arachidonic acid (AA). These agonists previously induced ROS generation in platelets as reported in Chapter 4. Therefore the present study investigated the effects of ROS inhibition on platelet aggregation stimulated by these agonists. This also allowed the confirmation of the activity of these peptides under our experimental conditions before examining the effects of ROS inhibition in Aβ1-42-stimulated platelet aggregation. The source of superoxide anion generated in response to 0.1 units/ml thrombin and 3 μg/ml CRP was investigated using NOX inhibitor VAS2870, since both agonists showed ROS inhibition with 3 mM NAC previously in Chapter 4.

The results are presented in Figure 5.9 (A), which shows representative aggregation curves induced by collagen (3 μg/ml) or thrombin (0.1 u/ml) in the presence or absence of NOX inhibitor VAS2870. Figure 5.9 (B) presents quantification analysis of average percentage absorbance. VAS2870 significantly inhibited platelet aggregation indicating that platelet stimulation with thrombin or CRP is NOX-dependent. The effect of ROS inhibition on platelet aggregation stimulated with 30 μM AA was also examined and the results are shown in Figure 5.9 (C and D). Interestingly, superoxide generated by AA seem to be NOX-independent with VAS2870, and was partially inhibited with 3 mM NAC, while the cyclooxygenase inhibitor indomethacin (Indo.), completely abolished AA induced platelet aggregation. This highlights the importance of cyclooxygenases in converting AA to prostaglandin H2, where thromboxane synthase then converts it into TXA2.

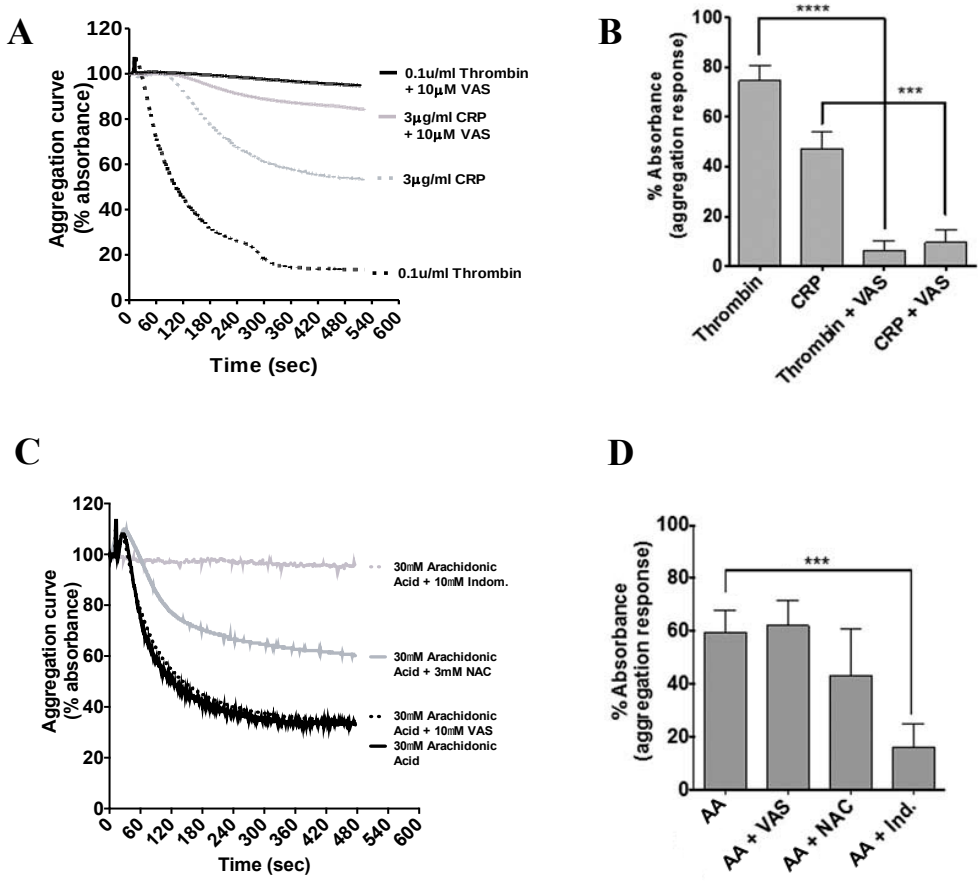

Figure 5.9: Effects of NOX inhibition on platelet aggregation stimulated by physiological agonists. Platelet aggregation experiments were performed using a 490D aggregometer. (A) Representative aggregation curves induced by collagen (3 μg/ml) or thrombin (0.1 u/ml) in the presence or absence of NOX inhibitor VAS2870. (B) Quantification of average percentage absorbance from 4 independent experiments. (C) Representative aggregation curves induced by arachidonic acid (AA) (30 μM) in the presence or absence of ROS scavenger NAC, NOX inhibitor VAS2870, or cyclooxygenase inhibitor, indomethacin (Indo.). (D) Quantification of average percentage absorbance quantified from 4 independent experiments. Statistical significance analysed by one-way ANOVA with Bonferroni post-test; P-value < 0.001 (***), and P-value < 0.0001 (****) refers to significant decrease in the percentage platelet aggregation in the presence of inhibitors. Error bars represent mean ± SEM.

5.2.4. Aβ1-42-induced platelet aggregation is NOX-dependent

The effect of NOX inhibition on Aβ1-42-stimulated platelet aggregation was finally examined, since Aβ1-42 was shown to induce superoxide generation in platelets and it was NOX-dependent as previously demonstrated with the DHE assay and EPR in Chapter 4. Aβ1-42 was also shown previously to significantly potentiate platelet aggregation in the presence of a physiological agonist. Since AA had been shown to induce platelet aggregation in a NOX-independent manner, it was used as a second physiological agonist with Aβ1-42. 10 μM AA only induced around 30% aggregation, but the aggregation increased to almost

80% in the presence of 20 μM Aβ1-42 peptide. The effect of Aβ1-42 with AA on platelet aggregation was significantly attenuated in the presence VAS2870 from 80% to 40% percentage absorbance as shown in Figure 5.10. These results suggest that NOX activity is necessary for the effect of Aβ peptides on human platelet aggregation and functional responses.

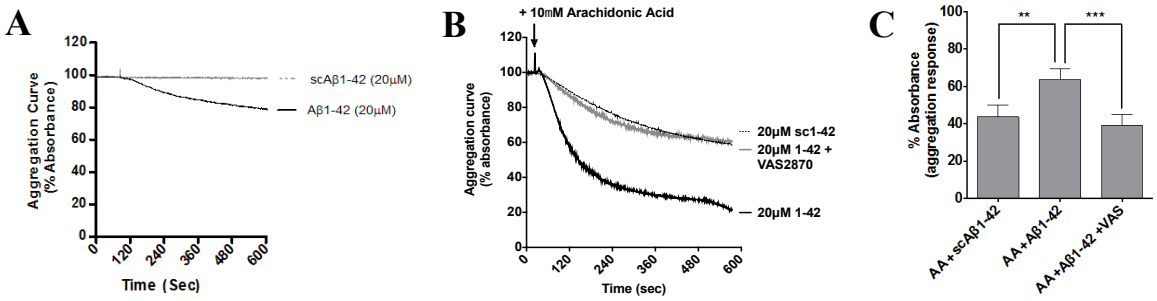

Figure 5.10: Aβ1-42 induced platelet aggregation is NOX-dependent.
Platelet aggregation experiments were performed using a 490D aggregometer. (A) Representative aggregation curves induced by 20 μM Aβ1-42 or Aβ1-42 as control. (B) Representative aggregation curves induced by 10 μM arachidonic acid (AA) with 20 μM Aβ1-42 or Aβ1-42 as control in the presence or absence of NOX inhibitor VAS2870. (C) Quantification of average percentage absorbance from 4 independent experiments. Statistical significance analysed by one-way ANOVA with Bonferroni post-test; P-value < 0.01 (**), and P-value < 0.001 (***). Error bars represent mean ± SEM.

Since there are two NOX isoforms that have been discovered in human platelets, the next step was to identify which of the NOXs is involved upon Aβ1-42-induced platelet aggregation. NOX1 (NOXA1ds) and NOX2 (NOX2ds-TAT) inhibitors (both 10 μM) were used in the following aggregation assay. Representative aggregation curves induced by 20 μM Aβ1-42 or Aβ1-42 as control in the presence of NOXA1ds or NOX2ds-TAT are shown in Figure 5.11 (A-B). Quantitative analysis showed statistically significant inhibition of both NOXs as shown in (C). This suggests that either of the NOXs are needed for Aβ1-42 induced platelet aggregation.

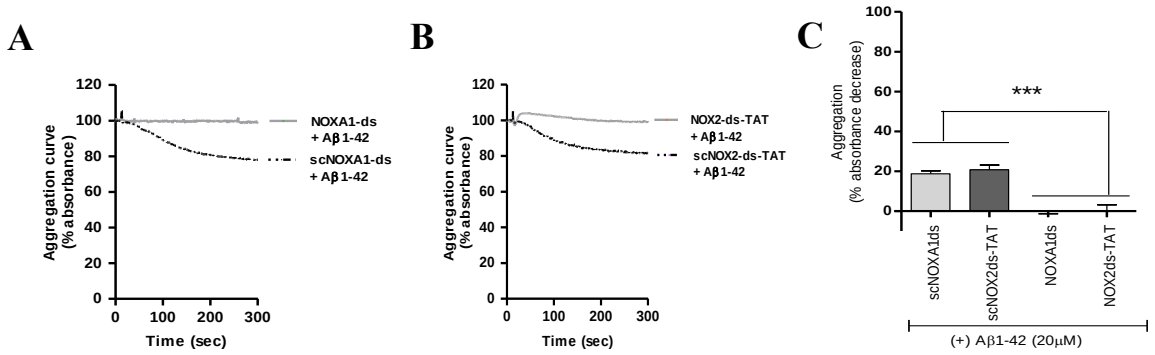

Figure 5.11: NOX1 and NOX2 inhibition attenuated by Aβ1-42-induced platelet aggregation.
Platelet aggregation experiments were performed using a 490D aggregometer. (A-B) Representative aggregation curves induced by 20 μM Aβ1-42 or Aβ1-42 in the presence of 10 μM NOX inhibitors scrambled NOX2ds-TAT (control), NOX2ds-TAT, scrambled NOXA1ds (control) and NOXA1. (C) Quantification of average percentage absorbance from 3 independent experiments. Statistical significance analysed by one-way ANOVA with Bonferroni post-test; P-value < 0.001 (***). Error bars represent mean ± SEM.

Aβ1-42 peptide had been shown to affect platelet functional responses in a redox-dependent manner, and in order to investigate its effect on platelet intracellular signalling, a phosphospecific immunoblotting was carried out in collaboration with Canobbio's group (refer to publication for methodology [351]). Both unstimulated and Aβ1-42-stimulated human platelets were treated with either DMSO (control) or VAS2870. They were then lysed, and their protein extracts were separated by SDS-PAGE. Antibodies against phosphorylated PKC substrates, tyrosine protein substrates, and pleckstrin (which is used as a loading control), were used to detect the activation of tyrosine phosphorylation cascades and PKC substrate phosphorylation upon Aβ1-42 treatment. The results of this immunoblotting analysis, shown in Figure 5.12, only provides a qualitative evidence of signalling activation and not target identification in the phosphorylation events.

This can however be provided as a proof that Aβ1-42 induces platelet signalling activation since tyrosine phosphorylation is one of the pivotal events that occurs upon platelet activation. Figure 5.12 (A) shows the tyrosine phosphorylation profile for unstimulated and Aβ1-42-stimulated human platelets treated with either DMSO as control or VAS2870. Several bands are observed in Figure 5.12 (A) upon stimulation with Aβ1-42 compared to DMSO-treated controls and the pre-treatment with NOX inhibitor VAS2870 obliterated tyrosine phosphorylation in response to Aβ1-42. The generation of tyrosine-phosphorylated protein substrates suggests that Aβ1-42 activates tyrosine kinase-dependent pathways, and that the activity of NADPH oxidases is necessary for the Aβ1-42 peptide signalling in platelets.

PKC is one of the main essential intracellular protein kinase enzymes associated with platelet activation and thrombus formation that is activated by DAG and increased intracellular Ca^{2+} resulting in the phosphorylation of regulatory serine/threonine residues in PKC substrate proteins [443, 444]. Upon immunoblot profile analysis for the phosphorylation of PKC substrates shown in Figure 5.12 (B), several intense bands corresponding to different substrate proteins for PKC can be seen upon Aβ1-42 stimulation compared to DMSO (control). In addition, the pre-treatment of VAS2870 abolished phospho-PKC immunostaining indicating that Aβ1-42-dependent platelet signalling requires NOX activation and it leads to PKC activation.

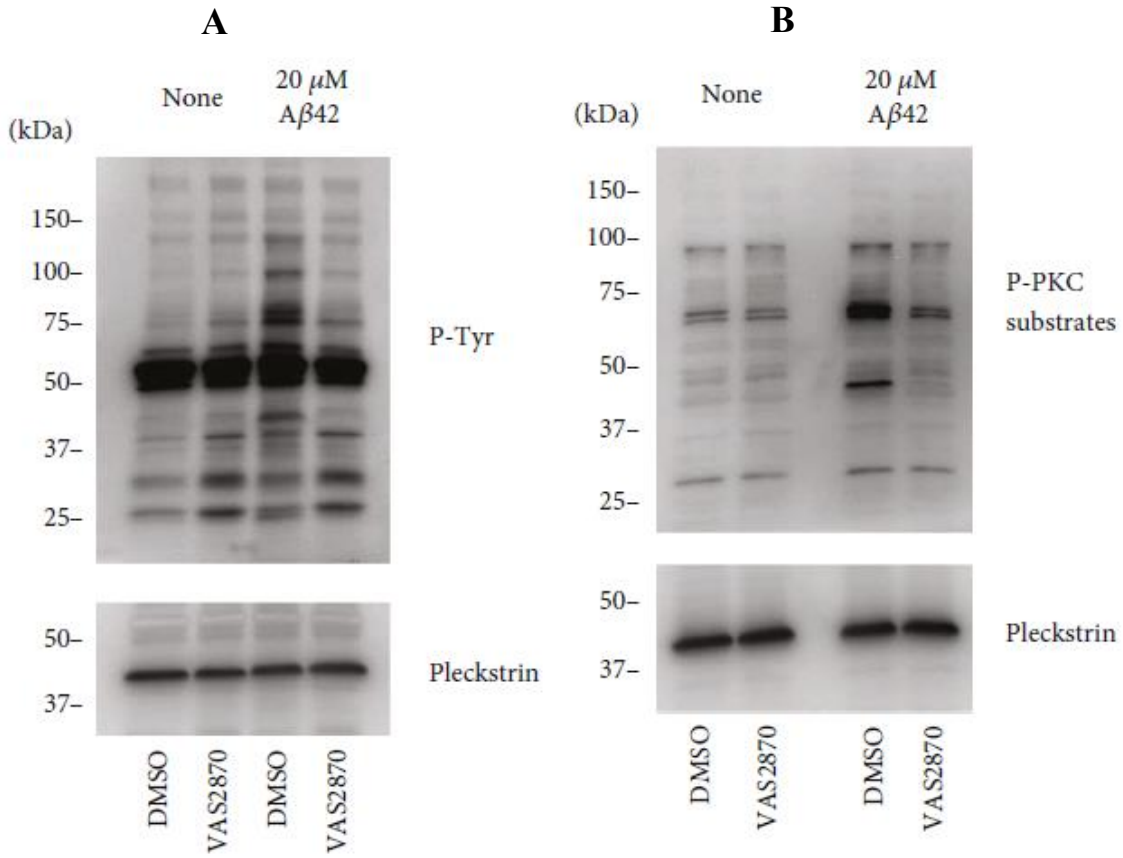

Figure 5.12: Aβ1-42 induced signalling in platelets.
Unstimulated and Aβ1-42-stimulated human platelets were treated with either DMSO (control) or VAS2870, lysed, and their protein extracts were separated by SDS-PAGE. Protein phosphorylation was analysed by immunoblotting with the indicated antibodies: (a) anti-p-Tyr and anti-pleckstrin antibody, and (b) anti-PKC phospho-substrate and anti-pleckstrin antibody. The figure represents blots from three independents (from [351])

5.2.5. Identification of potential platelet receptors involved in binding to Aβ1-42 using inhibitors

Several studies have investigated the engagement of many receptors for Aβ peptides on platelets and demonstrated the involvement of PAR1, CD36, GPIbα, integrin $\alpha_{IIb}\beta_3$, APP (partially), and most recently GPVI [296, 302, 307, 341, 345, 353, 354]. However, the receptor responsible for the initial engagement of Aβ1-42 to platelets still remains unclear. In order to assess PAR1, CD36, and GPVI involvement in platelet adhesion and activation induced by Aβ1-42, the following receptor inhibitors were used: ML161, sulfosuccinimidyl oleate (SSO), and losartan were used.

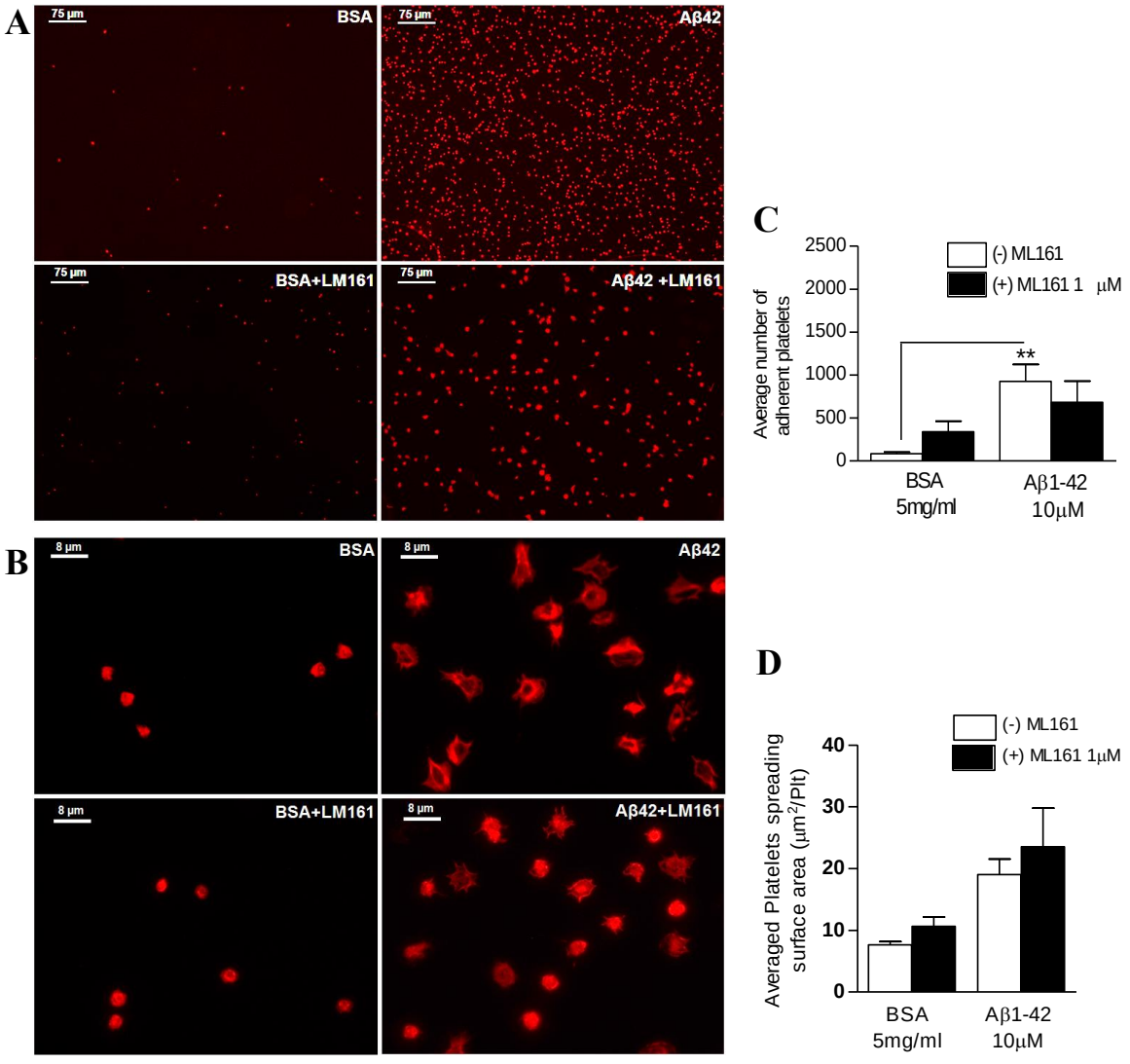

Figure 5.13: Effects of PAR1 inhibition on platelet adhesion and spreading over Aβ1-42 under static conditions.
(A-B) Representative images of platelets with or without PAR1 antagonist ML161 that were allowed to adhere onto glass coverslips coated with 10 µM Aβ1-42 or BSA 5mg/ml. Platelets were then fixed, stained, then visualized under the fluorescence microscope and images were taken at 10x and 100x magnification. (C-D) Quantification and evaluation of the mean number of adhered platelets and spreading area per optical field from at least 4 independent experiments. Statistical significance was analysed using one-way ANOVA with Bonferroni post-test; P-value < 0.01 (**) refers to significance in the mean number of adhered platelets to Aβ1-42 compared to BSA (control). Error bars represent mean ± SEM.

The allosteric inhibitor, ML161, for the thrombin receptor, PAR1, was used to test the effect of PAR1 inhibition on Aβ1-42-induced platelet adhesion and spreading and the results are shown in Figures 5.13, 5.14, and 5.15. PAR1 inhibition with ML161 noticeably reduced the number of adhered platelets onto Aβ1-42 (Figure 5.13 (C)); Aβ1-42 with collagen (Figure 5.14 (C)), and with statistical significance onto Aβ1-42 with fibrinogen (Figure 5.15 (C)). However, no significant spreading area was observed when compared to control with all the ML161 experiments.

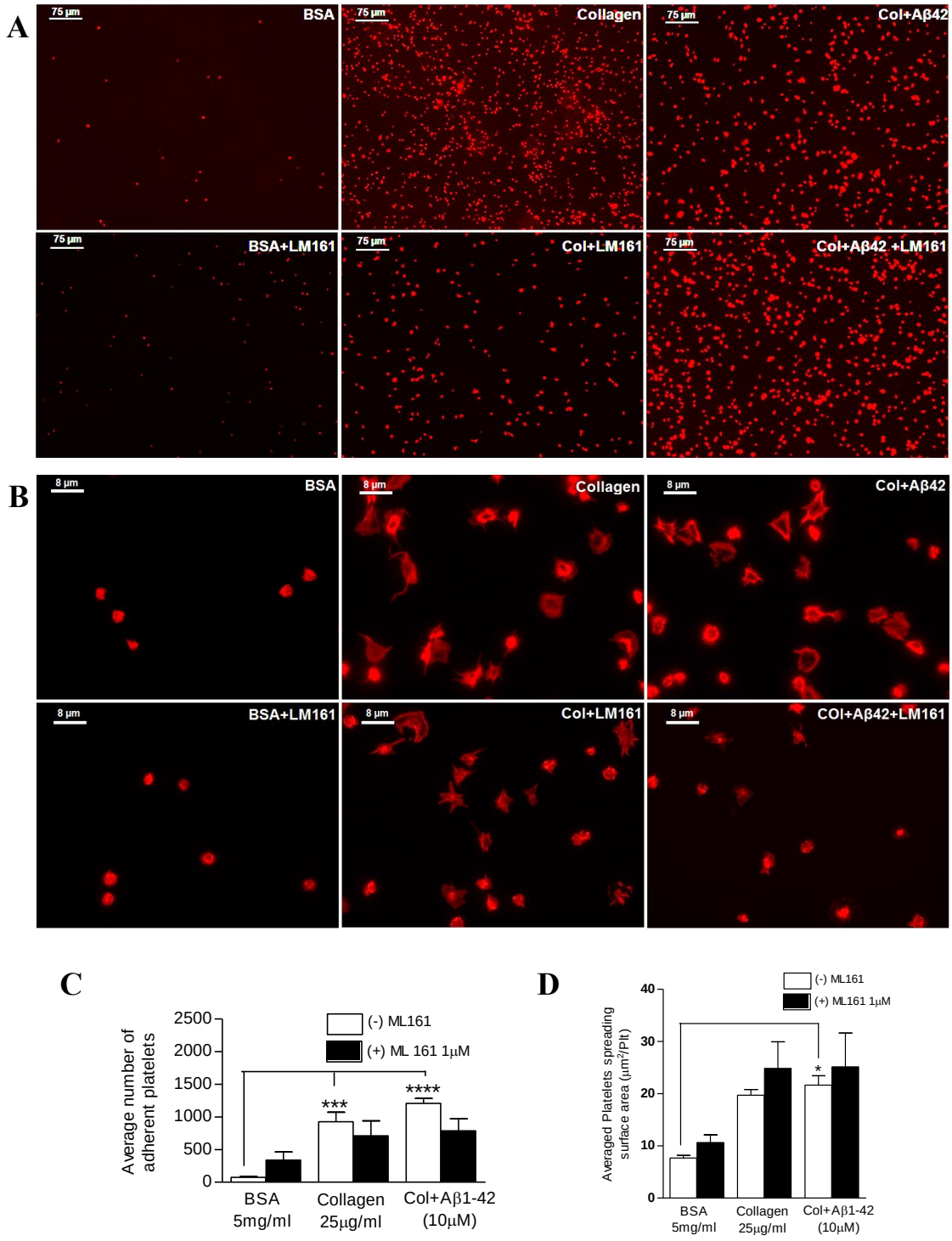

Figure 5.14: Effects of PAR1 inhibition on platelet adhesion and spreading over dual coated surfaces with Aβ1-42 and collagen.

(A-B) Representative images of platelets with or without PAR1 antagonist ML161 that were allowed to adhere onto glass coverslips coated with bovine serum albumin (BSA, 5 mg/ml), collagen (25 µg/ml), or collagen with Aβ1-42 peptide (10 µM). Platelets were then fixed, stained, then visualized under the fluorescence microscope and images were taken at 10x and 100x magnification. (C-D) Quantification and evaluation of the mean number of adhered platelets and spreading area per optical field from at least 4 independent experiments. Statistical significance was analysed using one-way ANOVA with Bonferroni post-test; P-value < 0.05 (*), P-value < 0.001 (***) and P-value < 0.0001 (****) refers to significance in the mean number of adhered platelets and spreading area to either collagen or collagen with Aβ1-42 compared to BSA (control). Error bars represent mean ± SEM.

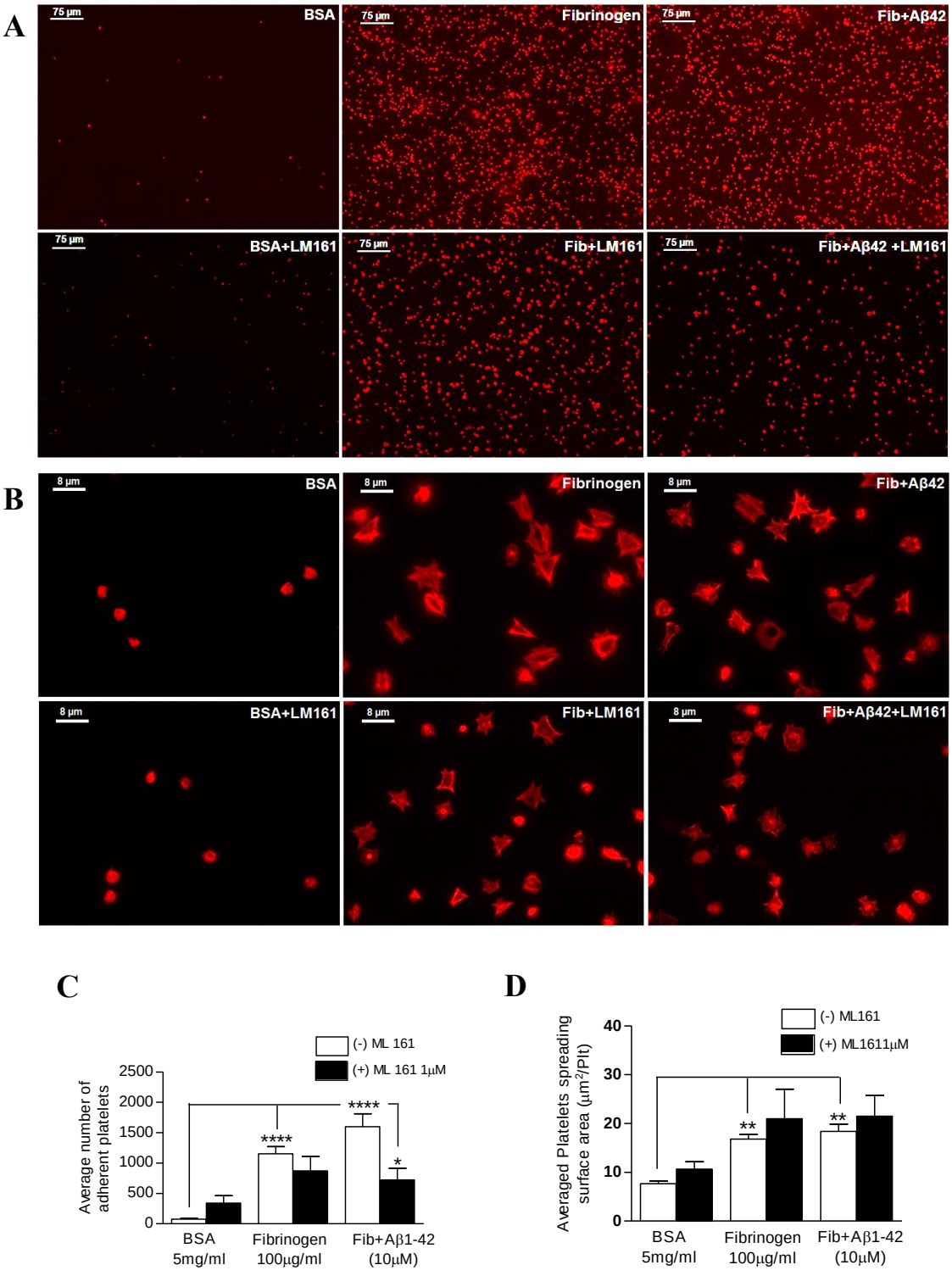

Figure 5.15: Effects of PAR1 inhibition on platelet adhesion and spreading over dual coated surfaces with Aβ1-42 and fibrinogen.
(A-B) Representative images of platelets with or without PAR1 antagonist ML161 that were allowed to adhere onto glass coverslips coated with bovine serum albumin (BSA, 5 mg/ml), fibrinogen (100 µg/ml), or fibrinogen with Aβ1-42 peptide (10 µM). Platelets were then fixed, stained, then visualized under the fluorescence microscope and images were taken at 10x and 100x magnification. (C-D) Quantification and evaluation of the mean number of adhered platelets and spreading area per optical field from at least 4 independent experiments. Statistical significance was analysed using one-way ANOVA with Bonferroni post-test; P-value < 0.05 (*), P-value < 0.01 (**), and P-value < 0.0001 (****) refers to significance in the mean number of adhered platelets and spreading area to either fibrinogen or fibrinogen with Aβ1-42 compared to BSA (control) in the presence (+) or absence (-) of ML161. Error bars represent mean ± SEM

Next, inhibition of scavenger receptor CD36 was investigated using an irreversible CD36 inhibitor SSO, and the results are shown in Figures 5.16, 5.17, and 5.18. Inhibition of CD36 with SSO significantly impeded Aβ1-42 induced platelet adhesion and spreading, as shown in Figure 5.16 (C and D). There was a significant decrease in spreading area of platelets adhering to Aβ1-42 in the presence of collagen (Figure 5.17 (D)) or fibrinogen (Figure 5.18 (D)). There was a noticeable decrease in the number of platelets adhering to collagen or Aβ1-42 with collagen (Figure 5.17 (C)) but a significant decrease was observed on Aβ1-42 with fibrinogen, as shown in Figure 5.18 (C). These results are interesting, as the irreversible inhibition of CD36 apparently affected fibrinogen interaction with the integrin $\alpha_{IIb}\beta_3$ receptor or GPVI on platelets and prevented full platelet activation. An alternative explanation could be that SSO may have cytotoxic effects on platelets at the concentration studied and further experiments with other CD36 inhibitors might therefore be needed.

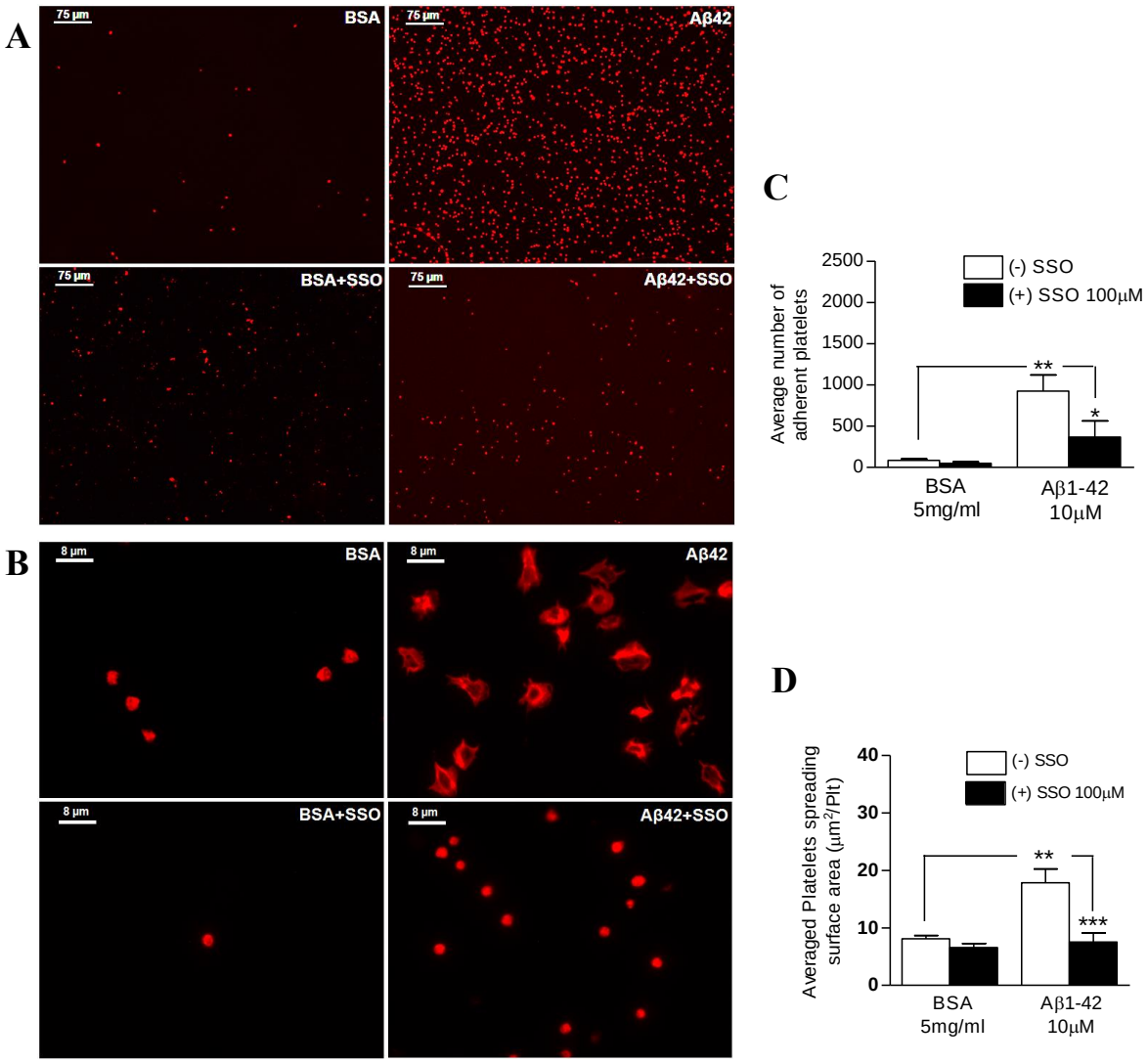

Figure 5.16: Effects of CD36 inhibition on platelet adhesion and spreading over Aβ1-42 under static conditions.

(A-B) Representative images of platelets with or without CD36 inhibitor SSO (100 µM) that were allowed to adhere onto glass coverslips coated with 10 µM Aβ1-42 or BSA 5mg/ml. Platelets were then fixed, stained, then visualized under the fluorescence microscope and images were taken at 10x and 100x magnification. (C-D) Quantification and evaluation of the mean number of adhered platelets and spreading area per optical field from at least 4 independent experiments. Statistical significance was analysed using one-way ANOVA with Bonferroni post-test; P-value < 0.05 (*), P-value < 0.01 (**); and P-value < 0.001 (***) refers to significance in the mean number of adhered platelets and spreading area to Aβ1-42 compared to BSA (control) and also the decrease in the mean number of adhered platelets and spreading area upon treatment with CD36 inhibitor SSO (+) compared to the ones without the inhibitor (-). Error bars represent mean ± SEM.

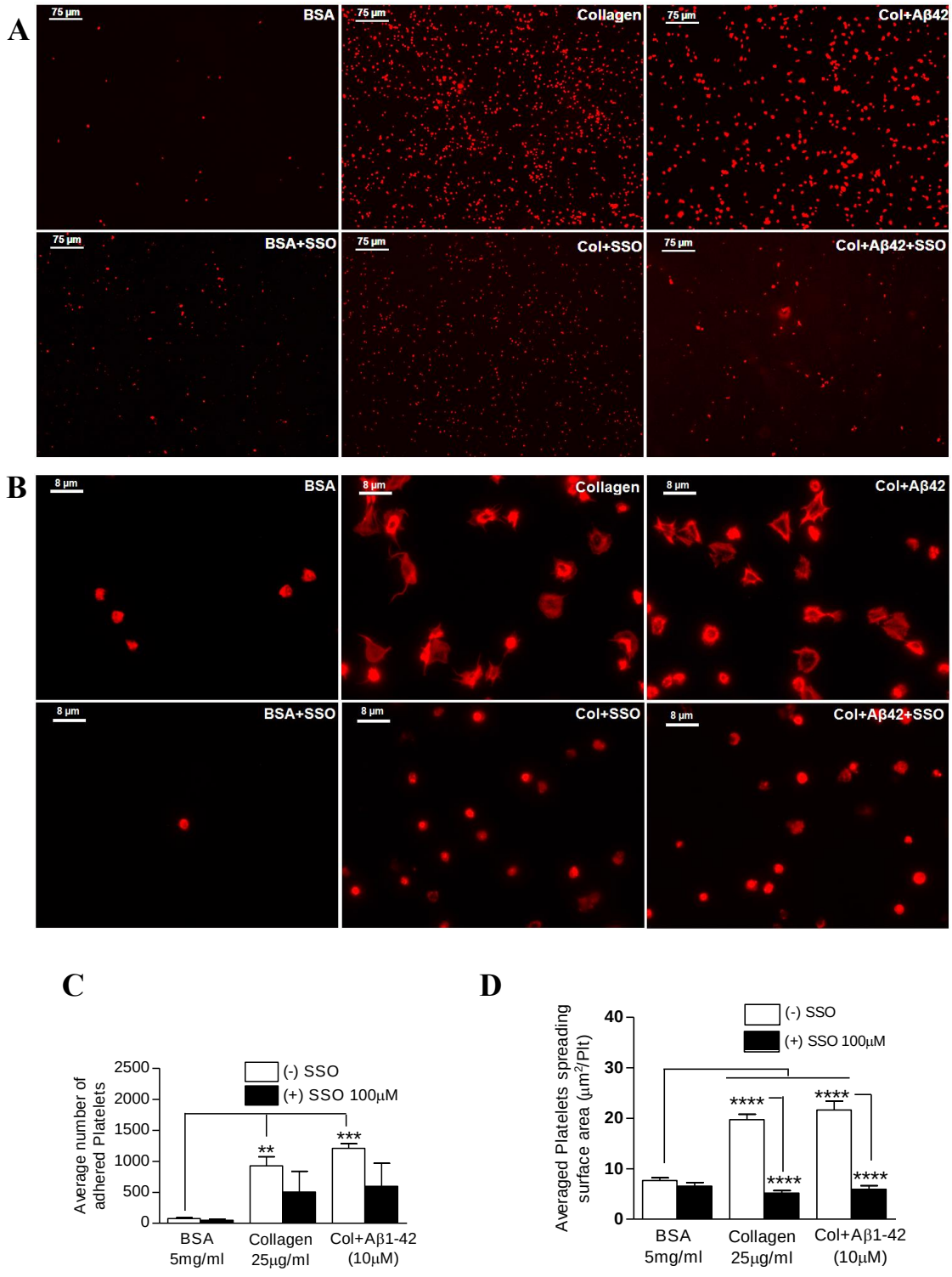

Figure 5.17: Effects of CD36 inhibition on platelet adhesion and spreading over dual coated surfaces with Aβ1-42 and collagen.

(A-B) Representative images of platelets with or without CD36 inhibitor SSO (100 µM) that were allowed to adhere onto glass coverslips coated with bovine serum albumin (BSA, 5 mg/ml), collagen (25 µg/ml), or collagen with Aβ1-42 peptide (10 µM). Platelets were then fixed, stained, then visualized under the fluorescence microscope and images were taken at 10x and 100x magnification. (C-D) Quantification and evaluation of the mean number of adhered platelets and spreading area per optical field from at least 4 independent experiments. Statistical significance was analysed using one-way ANOVA with Bonferroni post-test; P-value < 0.01 (**); and P-value < 0.001 (***); and P-value < 0.0001 (****) refers to significance in the mean number of adhered platelets and spreading area to collagen or collagen with Aβ1-42 compared to BSA (control) and also the decrease in the mean platelet spreading area upon treatment with CD36 inhibitor SSO (+) compared to the ones without the inhibitor (-). Error bars represent mean ± SEM.

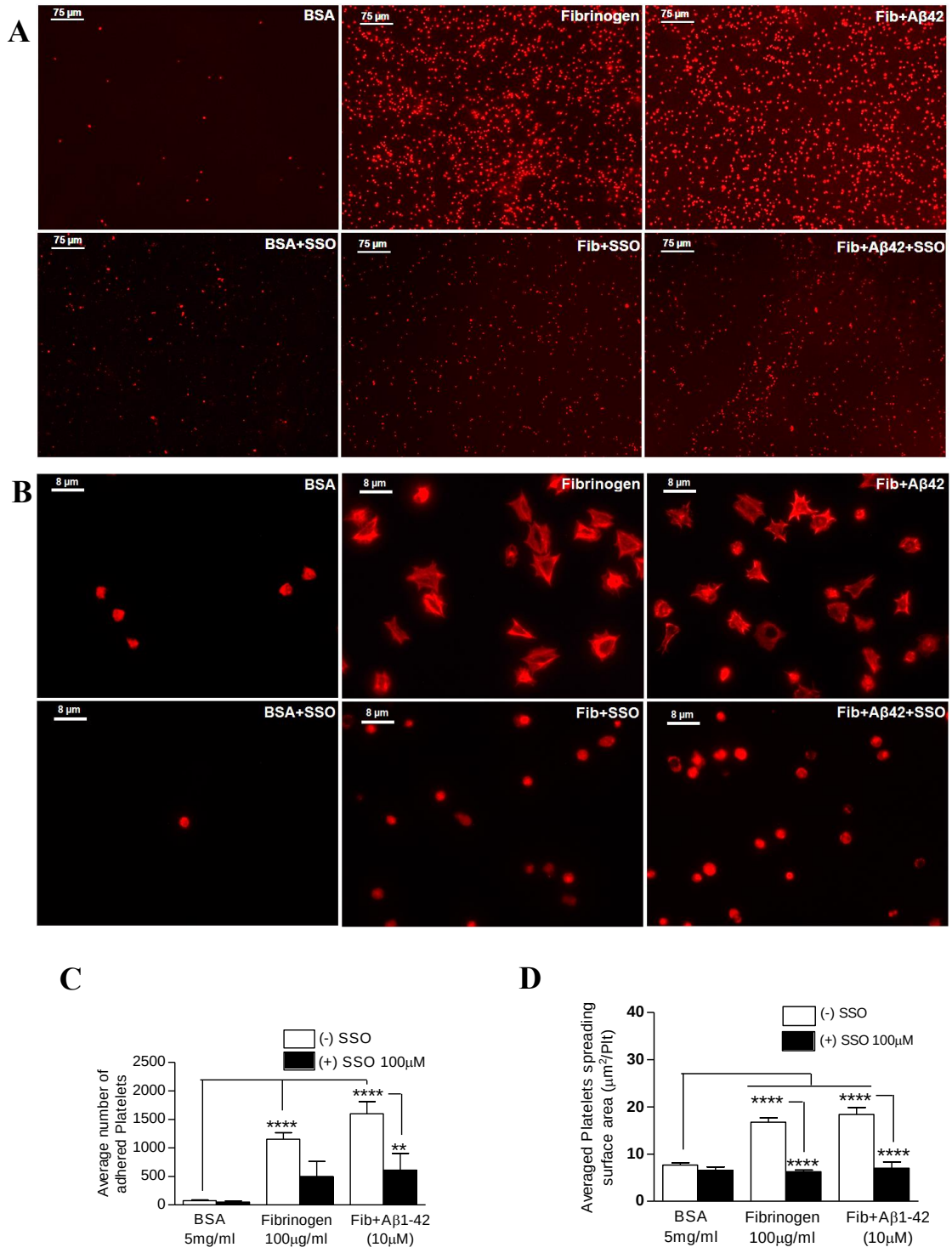

Figure 5.18: Effects of CD36 inhibition on platelet adhesion and spreading over dual coated surfaces with Aβ1-42 and fibrinogen.

(A-B) Representative images of platelets with or without CD36 inhibitor SSO (100 µM) that were allowed to adhere onto glass coverslips coated with bovine serum albumin (BSA, 5 mg/ml), fibrinogen (100 µg/ml), or fibrinogen with Aβ1-42 peptide (10 µM). Platelets were then fixed, stained, then visualized under the fluorescence microscope and images were taken at 10x and 100x magnification. (C-D) Quantification and evaluation of the mean number of adhered platelets and spreading area per optical field from at least 4 independent experiments. Statistical significance was analysed using one-way ANOVA with Bonferroni post-test; P-value < 0.01 (**), and P-value < 0.0001 (****) refers to significance in the mean number of adhered platelets and spreading area to fibrinogen or fibrinogen with Aβ1-42 compared to BSA (control) and also the decrease in the mean adhered platelet and spreading area upon treatment with CD36 inhibitor SSO (+) compared to the ones without the inhibitor (-). Error bars represent mean ± SEM.

The effects of GPVI receptor inhibition with losartan on platelet adhesion and spreading induced by Aβ1-42 was also examined, either with Aβ1-42 alone, or in the presence of collagen or fibrinogen. The results are shown in Figures 5.19, 5.20, and 5.21. Losartan is an angiotensin II (Ang II) type I receptor (AT1R) antagonist shown to inhibit thromboxane A2 (TXA2) receptor (TP) and GPVI in a selective, competitive, and dose-dependent manner [445]. The results show a significant decrease in the spreading area of adhered platelets induced by Aβ1-42 (Figure 5.19 (D)), collagen or Aβ1-42 with collagen (Figure 5.20 (D)), but not with fibrinogen or Aβ1-42 with fibrinogen (Figure 5.21 (D)). Losartan also significantly reduced the number of adhered platelets with Aβ1-42 (Figure 5.19 (C)), collagen, and Aβ1-42 with collagen (Figure 5.20 (C)). There is an overall decreasing trend regarding the effect of losartan on platelet adhesion and spreading in this study. Panels A-B for all these figures are representative images of platelet adhesion and spreading for each of the conditions, while panels C-D show quantitative analysis of adhesion and spreading area.

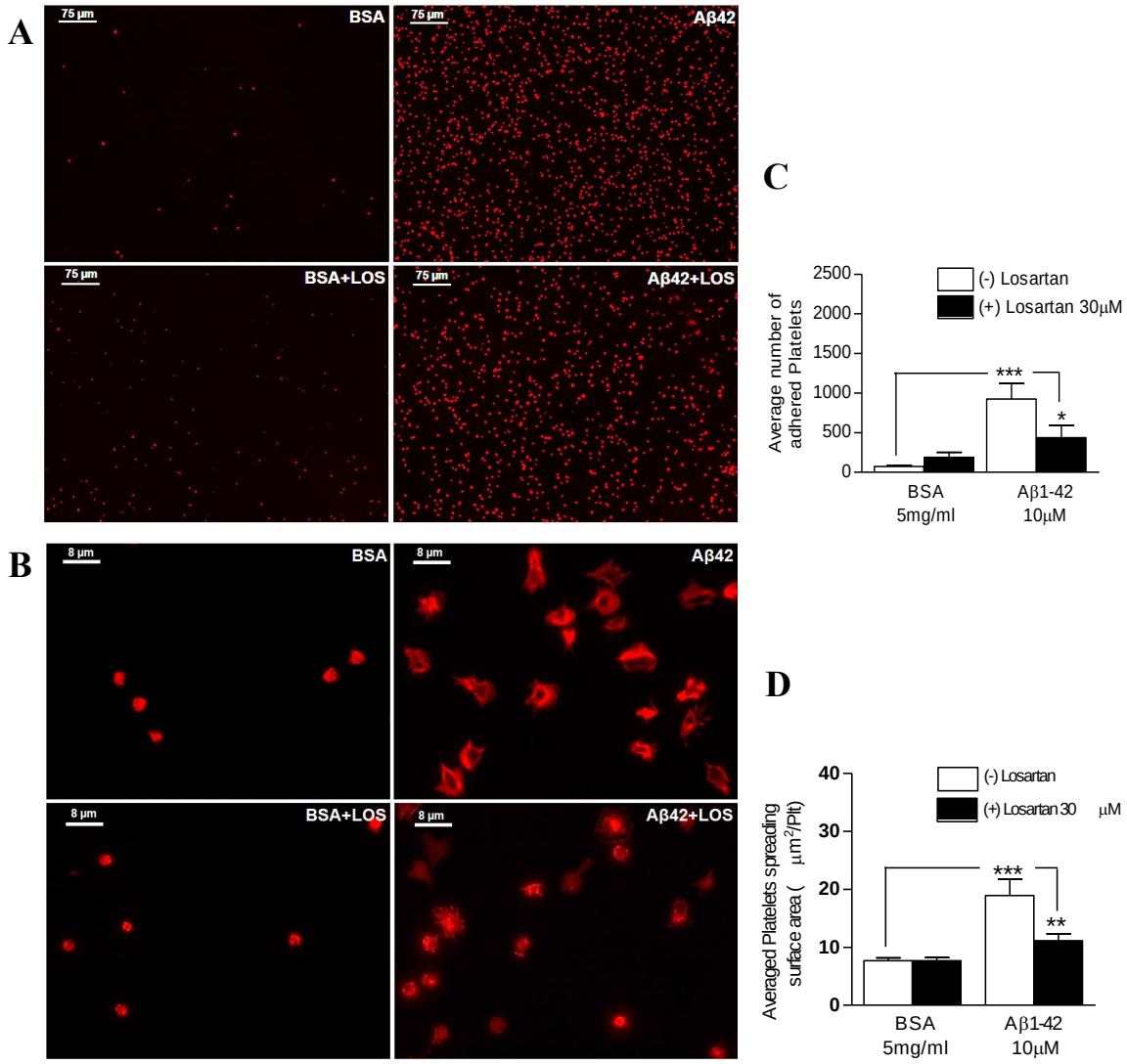

Figure 5.19: Effects of GPVI inhibition by losartan on Aβ1-42 induces platelet adhesion and spreading under static conditions.

(A-B) Representative images of platelets with or without GPVI inhibitor losartan (30 µM) that were allowed to adhere onto glass coverslips coated with 10 µM Aβ1-42 or BSA 5mg/ml. Platelets were then fixed, stained, then visualized under the fluorescence microscope and images were taken at 10x and 100x magnification. (C-D) Quantification and evaluation of the mean number of adhered platelets and spreading area per optical field from at least 4 independent experiments. Statistical significance was analysed using one-way ANOVA with Bonferroni post-test; P-value < 0.05 (*), P-value < 0.01 (**) and P-value < 0.001 (***) refers to significance in the mean number of adhered platelets and spreading area to Aβ1-42 compared to BSA (control) and also the decrease in the mean platelet spreading area upon treatment with GPVI inhibitor losartan (+) compared to the ones without the inhibitor (-). Error bars represent mean ± SEM.

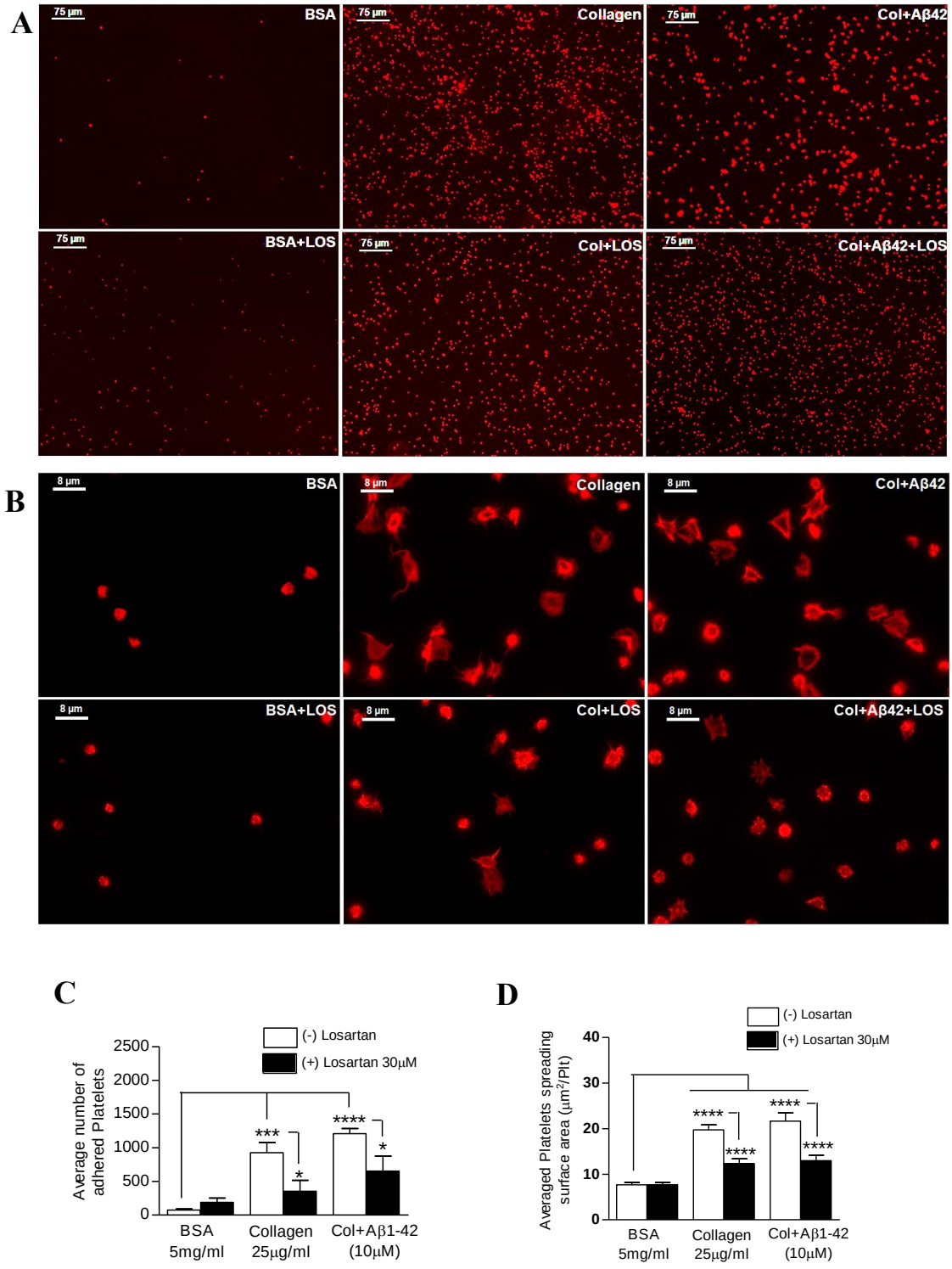

Figure 5.20: Effects of GPVI inhibition by losartan on platelet adhesion and spreading over dual coated surfaces with Aβ1-42 and collagen.

(A-B) Representative images of platelets with or without GPVI inhibitor losartan (30 µM) that were allowed to adhere onto glass coverslips coated with bovine serum albumin (BSA, 5 mg/ml), collagen (25 µg/ml), or collagen with Aβ1-42 peptide (10 µM). Platelets were then fixed, stained, then visualized under the fluorescence microscope and images were taken at 10x and 100x magnification. (C-D) Quantification and evaluation of the mean number of adhered platelets and spreading area per optical field from at least 4 independent experiments. Statistical significance was analysed using one-way ANOVA with Bonferroni post-test; P-value < 0.01 (**), P-value < 0.001 (***), and P-value < 0.0001 (****) refers to significance in the mean number of adhered platelets and spreading area to collagen or collagen with Aβ1-42 compared to BSA (control) and also the decrease in the mean platelet spreading area upon treatment with GPVI inhibitor losartan (+) compared to the ones without the inhibitor (-). Error bars represent mean ± SEM.

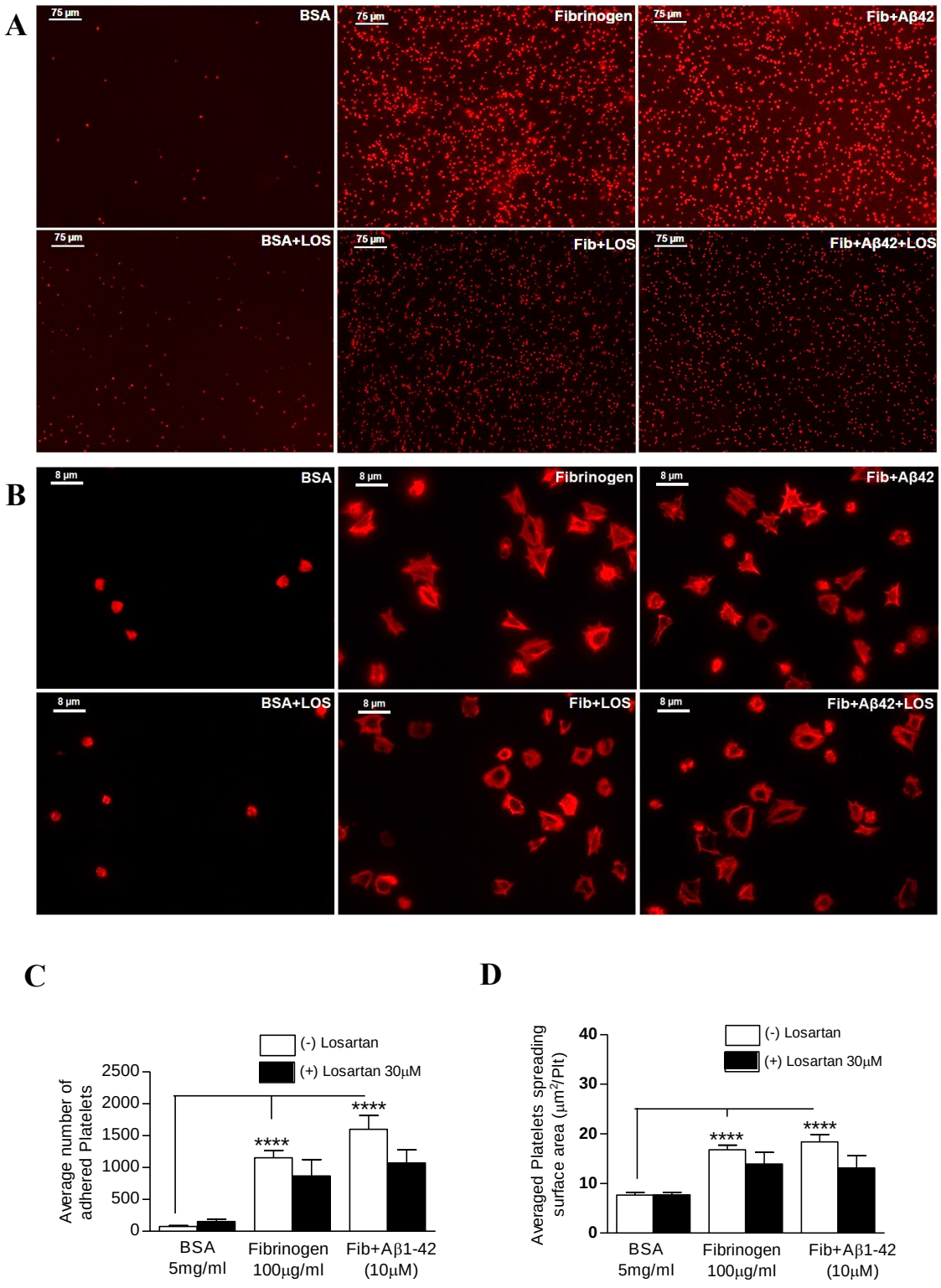

Figure 5.21: Effects of GPVI inhibition by losartan on platelet adhesion and spreading over dual coated surfaces with Aβ1-42 and fibrinogen.

(A-B) Representative images of platelets with or without GPVI inhibitor losartan (30 µM) that were allowed to adhere onto glass coverslips coated with bovine serum albumin (BSA, 5 mg/ml), fibrinogen (100 µg/ml), or fibrinogen with Aβ1-42 peptide (10 µM). Platelets were then fixed, stained, then visualized under the fluorescence microscope and images were taken at 10x and 100x magnification. (C-D) Quantification and evaluation of the mean number of adhered platelets and spreading area per optical field from at least 4 independent experiments. Statistical significance was analysed using one-way ANOVA with Bonferroni post-test; P-value < 0.01 (**), and P-value < 0.0001 (****) refers to significance in the mean number of adhered platelets and spreading area to fibrinogen or fibrinogen with Aβ1-42 compared to BSA (control). Error bars represent mean ± SEM.

5.3. SUMMARY OF RESULTS

- Aβ1-42-induced platelet adhesion and spreading is mediated via NOX activation under static conditions.
- NOX inhibition also attenuated fibrinogen or collagen platelet adhesion and spreading with or without the presence of Aβ1-42 under static conditions.
- Aβ1-42-stimulated platelets induced αIIbβ3 activation in a NOX-dependent manner but did not affect platelet degranulation and P-selectin surface membrane translocation
- Arachidonic acid induces superoxide anion generation in a NOX-independent manner
- Aggregation of Aβ1-42-stimulated platelets is NOX-dependent.
- Inhibition of either NOX1 or NOX2 attenuated Aβ1-42-induced platelet aggregation suggesting a differential role of these NOXs in Aβ1-42 induced platelet aggregation
- Aβ1-42 induced platelet signalling activation and required NOX activation, it also lead to PKC activation.
- PAR1 inhibition with ML161 significantly inhibited platelet adhesion over Aβ1-42 with fibrinogen only. However, there is an observable decrease in the number of platelets adhering to Aβ1-42 with or without the presence of fibrinogen or collagen.
- CD36 inhibition with SSO profoundly abolished the number of platelets adhering and spreading area over Aβ1-42 coated surfaces and also impaired platelet spreading area over collagen and fibrinogen alone or in the presence of Aβ1-42 peptide.
- GPVI inhibition with losartan significantly impaired platelet adhesion and spreading to Aβ1-42, collagen, and Aβ1-42 with collagen.

5.4. DISCUSSION

In the previous Chapters of 3 and 4, Aβ1-42 showed a high activation profile in our experimental conditions compared to Aβ25-35 and Aβ1-40. The disparity in Aβ peptides influence on platelet responses in terms of adhesion and aggregation is quite intriguing. Our results on the effects Aβ25-35 and Aβ1-40 on platelet adhesion and spreading under static conditions disagree partially with previously published work and is most likely due to modifications in the experimental conditions, such as platelet density, Ca^{2+} presence in HEPES Tyrode, incubation time, or the form of peptides used [300, 306, 307, 333, 336, 341]. On the other hand, our Aβ1-42 peptides demonstrated a profound ability to induce platelet adhesion and spreading under static condition, potentiate platelet aggregation, and increase thrombus formation in whole blood under physiological venous flow conditions.

In the present study Aβ1-42-induced platelet adhesion and spreading revealed to be mediated via NOX activation under static conditions and that inhibition of NOX, attenuated platelet adhesion and spreading over fibrinogen or collagen with or without the presence of Aβ1-42. This indicates the important role of NOX and ROS-dependent platelet activation, adhesion and spreading on different extracellular proteins. In Chapter 3, Aβ1-42 showed profound ability to induce platelet adhesion and thrombus formation by itself under venous flow. In this study, NOX inhibition attenuated thrombus formation potentiated by Aβ1-42 under physiological venous flow conditions and also showed that Aβ1-42-stimulated platelets induced "inside-out" $\alpha_{IIb}\beta_3$ activation in a NOX-dependent manner. The most recent publication by our group has confirmed that both NOXs are important in Aβ1-42-induced platelet activation using EPR, aggregation, and transgenic mice, and that only platelet adhesion to Aβ1-42 under low shear seemed exclusively NOX1-dependent [427].

Aβ1-42 induction of ROS generation and integrin activation without platelet degranulation or full activation, indicates a distinct signalling pathway. However, the underlying activation mechanisms remain difficult to explain due to the variability in the peptides used in various previous studies that involved different receptors and signalling pathways and led to discrepancies in the results obtained. However, looking back at the overall results in this study, Aβ1-42-induced platelet activation has consistently shown the importance of either NOX1 or NOX2 in platelet functional responses in terms of adhesion and activation under both static and venous flow conditions. The effects of Aβ1-42 on redox changes in platelet functional responses in terms of aggregation showed that aggregation of Aβ1-42-stimulated platelets is also NOX-dependent. In addition, inhibition of either NOX1 or NOX2 attenuated Aβ1-42-induced platelet aggregation suggesting a differential role for these NOXs.

Aβ1-42-induced platelet signalling activation was confirmed using phosphospecific immunoblotting analysis. The results showed that Aβ1-42-dependent platelet signalling requires NOX activation, and it leads to PKC activation, which is central and common signalling molecule upon stimulation with most platelet agonists [220, 446]. PKC can also directly become activated in the presence of oxidants [447]. This highlights the important role of NOX in mediating Aβ1-42-induced platelet activation. Different forms of Aβ peptides have previously reported to activate the platelet receptors PAR1 [296], GPIbα and CD36 [302], integrin $\alpha_{IIb}\beta_3$ [307], and most recently GPVI [345]. Therefore, the present study investigated the potential involvement of PAR1, GPVI, and scavenger receptor CD36 in Aβ1-42-induced platelet adhesion and spreading.

Inhibition of GPVI receptor by losartan significantly impaired platelet adhesion and spreading over Aβ1-42, collagen, and Aβ1-42 with collagen but not in the presence of fibrinogen. These results suggest that Aβ1-42 induces platelet adhesion and spreading potentially via the GPVI receptor, which supports the recently published work of Elaskalani' group [345]. Due to the hydrophobic nature of Aβ1-42 and its high tendency to self-aggregate and form fibrils, it might act in a similar manner to fibrillar collagen and activate GPVI and other adjacent receptors causing receptor dimerization and initiation of signalling activation.

Previous studies have shown that co-localisation of Aβ and fibrinogen can lead to fibrinogen binding to Aβ enhancing fibrinogen aggregation and Aβ fibrillization [273, 306, 346], which explains the enhancement of adhesion and spreading of platelets to dual coated surfaces of Aβ with fibrinogen in our studies. This suggests that if GPVI preferentially binds to substrates in a fibrillary form, then there should be a significant decrease in platelet adhesion and spreading when GPVI was inhibited with losartan. On the contrary, our results showed no significant decrease in the number of adhered platelets and spreading area with GPVI inhibition in the presence of Aβ1-42 with fibrinogen. This suggests that different forms of Aβ1-42 (particularly fibrillar form) may act through receptors other than GPVI or bind to multiple ones.

A previous study showed that fibrillar Aβ peptides can bind to a complex formed by CD36, CD47 and $\alpha_6\beta_1$ integrin receptors on the surface of microglial cells resulting in the activation of intracellular signal transduction cascades [448]. This signalling transduction cascade involves the activation of specific Src family kinases (Lyn, Fyn or Syk) that phosphorylates Vav which in turn acts as a guanine nucleotide exchange factor for Rac-1, which is an essential component NADPH oxidase, leading to NADPH oxidase-mediated generation of reactive oxygen species [449, 450]. CD36 shown to activate different intracellular signalling

pathways depending on the ligand, co-receptor, and cell type [451]. However, the downstream signalling mechanisms that link CD36 to classical platelet activation pathways are unclear. The importance of scavenger CD36 activation lies upon its multiple functions and assembly with other pattern recognition receptors, and it has been implicated in a variety of pathologies including atherosclerosis and thrombotic complications previously highlighted [390, 451, 452]. Fibrillar Aβ1-40 shown to induce platelet aggregation through the activation of CD36/p38MAPK/TXA2 release [302], thus its potential involvement with Aβ1-42 was investigated in the present study using the CD36 irreversible inhibitor, SSO.

CD36 inhibition with SSO profoundly abolished the number of platelets adhering and spreading area over Aβ1-42 coated surfaces, and also impaired platelet spreading area over collagen and fibrinogen alone or in the presence of Aβ1-42 peptide. These results are interesting, as SSO affected the fibrinogen interaction with its receptors on platelets and prevented full platelet activation. These results may suggest some cytotoxic effects on platelets at that concentration and further experiments with lower SSO concentrations or other CD36 inhibitors might be needed to further test Aβ1-42 effects on CD36. Both GPVI and CD36 seems to be key receptors for Aβ1-42 and further confirmatory future experiments with regards to these two receptors are required.

The involvement of thrombin receptor PAR1 (using ML161 inhibitor) in Aβ1-42 induced platelet adhesion and spreading was also examined. ML161 is an allosteric inhibitor that selectively blocks part of the receptor-mediated response [453]. Our results show an observable decrease in the number of platelets adhering to Aβ1-42 with or without the presence of collagen, and the only significant decrease in the number of adhered platelets was over Aβ1-42 with fibrinogen. These results suggest that fibrillar form of Aβ1-42 can potentially activate PAR1, but when looking at the overall results of PAR1 inhibition with ML161, the large error bars make these data inconclusive and further inhibition studies of this receptor are required.

Putting these findings together, it is possible to hypothesize that Aβ1-42 activates platelets through GPVI and NOX1 under low flow conditions, and other receptors such as CD36 may also be potentially involved, but further work is required to gain more insight. The present study sheds a new light on the importance of NADPH oxidase activation and platelet prothrombotic responses induced by Aβ1-42 that accumulates in the brain of Alzheimer's and cerebral amyloid angiopathy (CAA) patients. Interestingly on another note, human platelets also express the angiotensin II (Ang-II) receptor (AT1R), which is a main target for angiotensin II receptor blockers

(ARBs), such as losartan, used in the treatment of hypertension [454]. It is tempting to investigate the potential binding of Aβ peptides to AT1R especially when this receptor has been shown to activate platelets via NOX activation upon stimulation with Ang-II [455]. Early phase clinical trials are currently investigating the effects of anti-hypertensive drugs on reducing and intervening in the development of AD [456]. However, the effects of these drugs on platelets in AD patients may have been overlooked. Therefore, the effects of losartan on platelets adhesion to Aβ peptides in this study appears promising and it provides an additional avenue to explore potential treatment options for AD patients, since antiplatelet drugs, such as aspirin or clopidogrel, which are used to prevent stroke are also associated with an increased risk of cerebral haemorrhage [457]. Using an alternative treatment option, such as anti-hypertensive drugs, to also target platelets can potentially modify and reduce the pre-activated state in platelets and their contribution towards the thromboembolic events associated with AD.

In order to extend the current work, it would be necessary to address some limitations accompanying the use of the adhesion assay. For instance, the concentration of agonists remaining on the coated coverslips after wash remains unknown. Therefore, it is difficult to accurately determine their relevant effects in the body at a particular concentration. Additional experiments are also needed to confirm the identified Aβ receptors in platelets with knockout mice and accurately identify the signaling mechanisms involved so that the receptors can be used as potential therapeutic targets. In this work, time and cost constraints did not permit the potential exploration of various other pharmacological inhibitors, which would be interesting as some of the inhibitors used for the identification of potential receptors involved with Aβ, might not be as effective. Drugs available in the market to treat hypertension and hypercholesterolemia may also have additional involvement with platelet receptors associated with Aβ and thus should be further explored.

CHAPTER 6

General Conclusions & Future Work

6. GENERAL CONCLUSIONS

The overall aim of this research project was to test the hypothesis as to whether amyloidogenic Aβ peptides within the blood stream cause cerebrovascular complications associated with Alzheimer's disease via redox-dependent activation of platelets. Despite several studies highlighting the important role of Aβ peptides on platelet activation, these studies lacked consistency in their methodology and the forms of peptides used, which made the precise effects of Aβ peptides on platelets unclear. There is no previous study that has compared the effects of the different peptides side-by-side in a systematic manner. Therefore, a series of experiments were carried out utilizing several Aβ peptides, i.e. Aβ1-40, Aβ1-42, and Aβ25-35 and scrambled Aβ1-42 (as control) to investigate their effects on human platelets.

In the first phase of this project, the effects of Aβ peptides on platelet functional responses, i.e. adhesion, aggregation, and thrombus formation under static and physiological flow conditions were investigated. The study revealed that all Aβ peptides (i.e. Aβ1-40, Aβ1-42, and Aβ25-35) support platelet adhesion under static conditions, but with substantial preferential adhesion to Aβ1-42 compared to the other Aβ peptides. Aβ1-42 was shown to significantly promote platelet adhesion and spreading with extensive lamellipodia formation indicating that this peptide induces platelet intracellular signaling. Adhesion experiments in the presence of another physiological stimulus such as collagen with Aβ1-42, revealed similar potency in terms of the number of adhered platelets with Aβ1-42 without collagen suggesting that Aβ1-42 may induce platelet adhesion via an independent mechanism to collagen that is potentially mediated through a different receptor.

Aβ1-42 may also potentially be competing with collagen for the same receptor, i.e. GPVI. On the other hand, the presence of fibrinogen with Aβ1-42 enhanced platelet adhesion and full activation. This may reflect the potential augmentation of platelet recruitment, activation and thrombus formation at the site of CAA. The effect of Aβ peptides on platelet aggregation as an agonist revealed that Aβ1-42 induced moderate aggregation compared to the other peptides and potentiated aggregation in the presence of other physiological agonists, collagen or thrombin. In addition, Aβ1-42 induced partial platelet activation, but not granule release, as assessed by the expression of surface P-selectin and integrin αIIbβ3 activation. Furthermore, Aβ1-42 was shown to have a negligible effect on platelets under high shear stress or arterial blood flow, while it appears to potentially have a greater influence upon induced thrombus formation under venous flow. These results highlight the profound biological effects of Aβ1-42 on platelets.

In the second line of investigation, oxidative changes in platelets upon treatment with Aβ peptides was assessed by exploring different ROS detection methodologies. Aβ25-35 showed significant ROS generation using DCFDA, but the other peptides did not produce the same effects. The lack of strong detectable DCF signal in this assay under our experimental conditions despite the high concentrations of physiological agonists used, prompted an initial ROS detection assay optimization. A novel easy and accessible flow cytometry assay using DHE was developed that detected significant superoxide generation in platelets upon Aβ1-42 stimulation (including fibrillar Aβ1-42), but not with the other peptides. Further investigations of oxidative state in live platelets using the DHE assay revealed for the first time that superoxide anion generation in platelets by Aβ1-42 is NOX-dependent, and this finding was published in 2017 [401]. In addition, generation of superoxide anion in platelets by thrombin stimulation was shown to be NOX1 independent, and ADP-mediated platelet activation was independent of NOX activity and ROS generation.

Follow-up studies using EPR, confirmed that not only superoxide anion was generated by Aβ1-42, but was also moderately generated by Aβ25-35, which can explain some of the ROS results previously reported. Additionally, further examination using NOX1 and NOX2 inhibitors revealed that both NOXs are essential for the generation of superoxide anion in platelets stimulated by either Aβ1-42 or Aβ25-35 peptides. These results greatly highlights the central underlying relationship between ROS and human platelet activation upon Aβ peptide stimulation, and provides a novel alternative methodology that can easily and reliably be utilized in haemostasis and thrombosis studies.

Since Aβ1-42 appeared to be the most active peptide in our experimental conditions, the final phase of this project focused on investigating the redox-dependent changes in platelets and functional responses upon stimulation with Aβ1-42 peptide, and the potential receptors that might be involved. The results from adhesion studies revealed that Aβ1-42 induced platelet adhesion is mediated via NOX activation under static conditions and under physiological venous flow. In addition, Aβ1-42 induces platelet adhesion and spreading most likely via the GPVI receptor and potentially involves the CD36 receptor, but further experimental validations are required for this receptor. Aβ1-42-stimulated platelets induced "inside-out" αIIbβ3 activation and platelet aggregation in a NOX-dependent manner.

Moreover, inhibition of either NOX1 or NOX2 attenuated platelet aggregation and thus highlights the important role of NOX in mediating Aβ1-42 induced platelet activation, adhesion and aggregation. Since several control physiological agonists were tested alongside Aβ1-42 for the effects of NOX inhibition on platelet aggregation, this study reports for the

first time that superoxide anion generated by arachidonic acid was NOX-independent and these results were also published in 2017. Finally, phosphospecific immunoblotting analysis revealed that Aβ1-42-dependent platelet signaling requires NOX activation and this signaling also leads to PKC activation, which is known to be involved in mediating a range of intracellular events leading to platelet activation.

The work done in this project sheds a new and important light on the significance of NADPH oxidase activation and platelet prothrombotic responses induced by Aβ1-42 that accumulates in the brain of Alzheimer's and cerebral amyloid angiopathy (CAA) patients. Aβ1-42 was shown to activate platelets, enhance their adhesion, and potentiate the responses of low levels physiological agonists, which can trigger unwanted hemostatic response and create a vicious cycle with feed-forward loop of platelet hyperactivity within the bloodstream. This supports, thrombus formation at vascular lesions or CAA at an accelerated rate, and possibly contribute to the microthrombosis in neurovasculature and cardiovascular complications observed in AD. Taken together these results and data from previous studies on how platelets contributes to the overall picture of the pathogenesis of AD, a model is proposed in support of the vascular hypothesis as the main contributor to the etiopathogenesis of AD. As summarized in Figure 6.1, this starts from childhood and this figure also shows the potential causative role of pre-activated state of platelets found in AD patients.

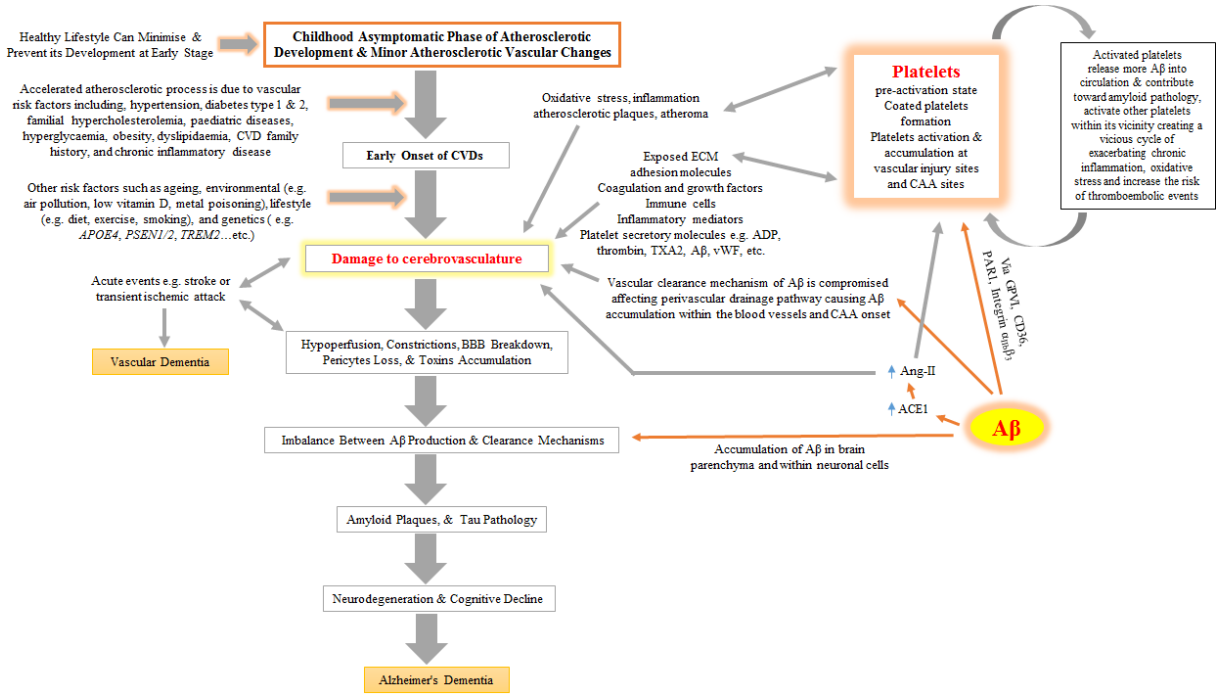

Figure 6.1: Proposed model for the etiopathogenesis of AD and the role of platelets.

The process of atherosclerosis often starts in childhood as fatty streaks and it is usually a long asymptomatic phase of development with minor vascular changes that can be minimized following a healthy lifestyle [458]. However, with increased risk factors or disease during development, it initiates early onset of cardiovascular diseases (CVDs) [458]. Over time, the development of atherosclerotic plaques, causes chronic inflammation, oxidative stress, and vascular changes with increased risk of hypertension, perivascular diseases, and thrombotic events, such as transient ischemic attack or stroke. Acute thrombotic events can cause or be a result of cerebrovascular damage and contributes to the onset of vascular dementia [129]. Cerebrovascular damage can lead to blood vessel constriction, hypoperfusion, compromised BBB barrier, pericytes loss, and the accumulation of toxins including Aβ in brain parenchyma and within the cerebral vessel wall [23, 129].

Compromised blood vessels influences the balance between Aβ production and clearance mechanisms causing its accumulation within the blood vessels and the onset of CAA. Aβ peptides have been shown to support platelet adhesion and activation at vascular injury and CAA sites. This allows the secretion of potent molecules and Aβ from platelets into the circulation that promotes the activation of other platelets within their vicinity creating a highly thrombotic environment. Aβ shown to increase the activity of ACE-1 that results in the increase of Ang-II (potent vasoconstrictor) affecting blood vessels and also activating platelets through AT1R contributing to further activation of platelets in the blood [454]. The presence of inflammatory mediators, coagulation and growth factors, activated immune cells, platelet secretory molecules, Ang-II, adhesion molecules, Aβ, exposed ECM, and oxidative stress, are strong candidate for the formation of the pre-activated state in platelets and coated platelets [459]. As these events feeds into progressive cerebrovascular damage cycle, it eventually leads BBB breakdown and to the accumulation of toxins and Aβ in the brain parenchyma and neuronal cells and resulting the formation of amyloid plaques, tau pathology, neurodegeneration, cognitive decline and ultimately Alzheimer's dementia [23, 460].

The results of this project suggests a potential therapeutic avenue aiming at limiting the vascular component contributing to Alzheimer's disease by targeting potential hypertensive drugs that affect platelet activation, develop antiplatelet drugs selectively targeting specific NADPH oxidase isoenzyme activities and developing relative pharmacotherapy, and finally developing efficient screening systems for identifying children at risk for atherosclerosis to provide an early intervention or delay the progression of atherosclerosis and CVDs as a preventative method.

FUTURE WORK

When looking at the larger picture from all the work accomplished during this project, there are still several gaps that provides new avenues to be explored in future work regarding this topic and some are listed in the following:

- Aβ1-42 induced platelet adhesion in the presence of new CD36 inhibitors and CD36 knockout mice, PAR1 inhibitors, selective GPVI inhibitors, GPIbα inhibitor, $\alpha_{IIb}\beta_3$ inhibitors, and $\alpha_2\beta_1$ inhibitors
- Conduct adhesion assay experiments to investigate the effect of other anti-hypertensive drugs, such as Telmisartan, Candesartan, and Irbesartan (potent and selective to AT1R), on platelet adhesion to amyloid peptides under both static and flow conditions
- Conduct protein-receptor co-immunoprecipitation or radioligand binding studies in order to provide a better explanation and understanding of the receptors involved with Aβ peptides.
- Assess the effect of fibrillar Aβ1-40 on platelet adhesion and aggregation and ROS generation.
- Assess the effects of fibrillar Aβ1-42 and Aβ1-40 under physiological flow conditions and whether they are NOX dependent or not.
- Explore other types of ROS and RNS that might be involved in Aβ stimulated platelets using EPR.
- Conduct a concentration dependent experiments for with regards to fibrillar Aβ1-42 with regards to platelet aggregation.
- Investigate the effect of extracellular calcium on Aβ stimulated platelet adhesion, aggregation, and ROS generation with EPR.
- Conduct signaling studies such as targeted phosphoimmunoblotting of potential key signaling molecules involved in Aβ stimulated platelets to understand their underlying signaling mechanisms.

REFERENCES

1. Qiu, C., M. Kivipelto, and E.V. Strauss, *Epidemiology of Alzheimer's disease: occurrence, determinants, and strategies toward intervention.* Dialogues in Clinical Neuroscience, 2009. **11**(2): p. 111-129.
2. Garand, L. and K.C. Buckwalter, *The biological basis of behavioural symptoms in dementia* Issues in Mental Health Nursing, 2000. **21**(1): p. 91-107.
3. Association, A.s., *Alzheimer's disease facts and figures*, in *Alzheimers Dement*. 2018. p. 367-429.
4. UK, A.s.R. *Cost and projections in the UK and globally*. 2018 [cited 2018 05/11/2018]; Available from: https://www.dementiastatistics.org/statistics/cost-and-projections-in-the-uk-and-globally/.
5. Duong, S., T. Patel, and F. Chang, *Dementia: What pharmacists need to know.* Canadian Pharmacists Journal/Revue des pharmaciens du Canada, 2017. **150**(2): p. 118-129.
6. Hippius, H. and G. Neundörfer, *The discovery of Alzheimer's disease.* Dialogues in Clinical Neuroscience 2003. **5**(1).
7. Perl, D.P., *Neuropathology of Alzheimer's disease.* Mount Sinai Journal of Medicine, 2010. **77**(1): p. 32-42.
8. Maurer, K., S. Volk, and H. Gerbaldo, *Auguste D and Alzheimer's disease.* The Lancet, 1997. **349**(9064): p. 1546-1549.
9. Serrano-Pozo, A., et al., *Neuropathological alterations in Alzheimer disease.* Cold Spring Harb Perspect Med, 2011. **1**(1): p. a006189.
10. Medeiros, R., D. Baglietto-Vargas, and F.M. LaFerla, *The role of tau in Alzheimer's disease and related disorders.* CNS Neuroscience & Therapeutics 2011. **17**(5): p. 514-24.
11. Johnson, G.V. and W.H. Stoothoff, *Tau phosphorylation in neuronal cell function and dysfunction.* Journal of Cell Science, 2004. **117**(Pt 24): p. 5721-9.
12. Kolarova, M., et al., *Structure and pathology of tau protein in Alzheimer disease.* International Journal of Alzheimer's Disease, 2012. **2012**: p. 731526.
13. Brion, J.P., et al., *Neurofibrillary tangles and tau phosphorylation.* Biochemical Society Symposium, 2001(67): p. 81-8.
14. Murphy, M.P. and H. LeVine, 3rd, *Alzheimer's disease and the amyloid-beta peptide.* Journal of Alzheimer's Disease, 2010. **19**(1): p. 311-23.
15. Soto, C. and L.D. Estrada, *Protein Misfolding and Neurodegeneration.* Archives of Neurology, 2008. **65**(2): p. 184-189.
16. D'Andrea, M.R. and R.G. Nagele, *Morphologically distinct types of amyloid plaques point the way to a better understanding of Alzheimer's disease pathogenesis.* Biotechnic & Histochemistry, 2010. **85**(2): p. 133-147.
17. Rak, M., et al., *Dense-core and diffuse Abeta plaques in TgCRND8 mice studied with synchrotron FTIR microspectroscopy.* Biopolymers, 2007. **87**(4): p. 207-17.
18. Schupf, N., et al., *Peripheral Aβ subspecies as risk biomarkers of Alzheimer's disease.* Proceedings of the National Academy of Sciences, 2008. **105**(37): p. 14052-14057.
19. Roher, A.E., et al., *Cortical and leptomeningeal cerebrovascular amyloid and white matter pathology in Alzheimer's disease.* Molecular Medicine, 2003. **9**(3-4): p. 112-22.
20. Smith, E.E. and S.M. Greenberg, *Beta-amyloid, blood vessels, and brain function.* Stroke, 2009. **40**(7): p. 2601-6.

21. Weller, R.O., et al., *Cerebral amyloid angiopathy - amyloid beta accumulates in putative interstitial fluid drainage pathways in Alzheimer's disease.* American Journal ofPathology, 1998. **153**(3): p. 725-733.
22. Greenberg, S.M. and A. Charidimou, *Diagnosis of Cerebral Amyloid Angiopathy.* Stroke, 2018. **49**(2): p. 491-497.
23. Montagne, A., Z. Zhao, and B.V. Zlokovic, *Alzheimer's disease: A matter of blood–brain barrier dysfunction?* The Journal of Experimental Medicine, 2017. **214**(11): p. 3151-3169.
24. de Vries, H.E., et al., *Inflammatory events at blood-brain barrier in neuroinflammatory and neurodegenerative disorders: implications for clinical disease.* Epilepsia, 2012. **53 Suppl 6**(Suppl 6): p. 45-52.
25. Hartz, A.M., et al., *Amyloid-β contributes to blood-brain barrier leakage in transgenic human amyloid precursor protein mice and in humans with cerebral amyloid angiopathy.* Stroke, 2012. **43**(2): p. 514-23.
26. Eng, J.A., et al., *Clinical manifestations of cerebral amyloid angiopathy–related inflammation.* Annals of Neurology: Official Journal of the American Neurological Association and the Child Neurology Society, 2004. **55**(2): p. 250-256.
27. Love, S., *Contribution of cerebral amyloid angiopathy to Alzheimer's disease.* J Neurol Neurosurg Psychiatry, 2004. **75**: p. 1–4.
28. Brion, J.P., *Neurofibrillary tangles and Alzheimer's disease.* Eur Neurol, 1998. **40**(3): p. 130-40.
29. Bagad, M., D. Chowdhury, and Z.A. Khan, *Towards understanding Alzheimer's Disease: An Overview.* Research Journal of Pharmaceutical, Biological and Chemical Sciences, 2013. **4**(4): p. 286-298.
30. O'Brien, R.J. and P.C. Wong, *Amyloid precursor protein processing and Alzheimer's disease.* Annual Review of Neuroscience, 2011. **34**: p. 185-204.
31. Rockenstein, E.M., et al., *Levels and Alternative Splicing of Amyloid b Protein Precursor (APP) Transcripts in Brains of APP Transgenic Mice and Humans with Alzheimer's Disease.* THE JOURNAL OF BIOLOGICAL CHEMISTRY, 1995. **270**(24): p. 28257–28267.
32. Vignini, A., et al., *Platelet amyloid precursor protein isoform expression in Alzheimer's disease: evidence for peripheral marker.* International Journal of Immunopathology and Pharmacology, 2011. **24**(2): p. 529-534.
33. Puig, K.L. and C.K. Combs, *Expression and function of APP and its metabolites outside the central nervous system.* Experimental Gerontology, 2013. **48**(7): p. 608-11.
34. Chow, V.W., et al., *An overview of APP processing enzymes and products.* Neuromolecular Medicine, 2010. **12**(1): p. 1-12.
35. Zimbron, H.L. and S. Rivas-Arancibia, *Deciphering an interplay of proteins associated with amyloid β 1-42 peptide and molecular mechanisms of Alzheimer's disease.* Reviews in the Neurosciences, 2014. **25**.
36. Pauwels, K., et al., *Structural basis for increased toxicity of pathological abeta42:abeta40 ratios in Alzheimer disease.* The Journal of Biological Chemistry, 2012. **287**(8): p. 5650-60.
37. Li, R., et al., *Amyloid β peptide load is correlated with increased β-secretase activity in sporadic Alzheimer's disease patients.* Proceedings of the National Academy of Sciences of the United States of America, 2004. **101**(10): p. 3632-3637.
38. Marshall, K.E., et al., *A critical role for the self-assembly of Amyloid-β1-42 in neurodegeneration.* Scientific Reports, 2016. **6**: p. 30182.
39. Verma, M., A. Vats, and V. Taneja, *Toxic species in amyloid disorders: Oligomers or mature fibrils.* Annals of Indian Academy of Neurology, 2015. **18**(2): p. 138-145.
40. Zheng, H. and E.H. Koo, *Biology and pathophysiology of the amyloid precursor protein.* Mol Neurodegener, 2011. **6**(1): p. 27.

41. Turner, P.R., et al., *Roles of amyloid precursor protein and its fragments in regulating neural activity, plasticity and memory.* Progress in Neurobiology, 2003. **70**(1): p. 1-32.
42. Haass, C., et al., *Trafficking and proteolytic processing of APP.* Cold Spring Harbor Perspective in Medicine, 2012. **2**(5): p. a006270.
43. Pearson, H.A. and C. Peers, *Physiological roles for amyloid beta peptides.* The Journal of Physiology, 2006. **575**(Pt 1): p. 5-10.
44. Morris, G.P., I.A. Clark, and B. Vissel, *Inconsistencies and controversies surrounding the amyloid hypothesis of Alzheimer's disease.* Acta Neuropathologica Communications, 2014. **2**: p. 135.
45. Tarasoff-Conway, J.M., et al., *Clearance systems in the brain-implications for Alzheimer disease.* Nature Reviews Neurology, 2015. **11**(8): p. 457-70.
46. Ries, M. and M. Sastre, *Mechanisms of Aβ Clearance and Degradation by Glial Cells.* Frontiers in Aging Neuroscience, 2016. **8**: p. 160.
47. Piccini, A., et al., *beta-amyloid is different in normal aging and in Alzheimer disease.* The Journal of Biological Chemistry, 2005. **280**(40): p. 34186-92.
48. Wang, J., et al., *A systemic view of Alzheimer disease - insights from amyloid-beta metabolism beyond the brain.* Nat Rev Neurol, 2017. **13**(10): p. 612-623.
49. Ramanathan, A., et al., *Impaired vascular-mediated clearance of brain amyloid beta in Alzheimer's disease: the role, regulation and restoration of LRP1.* Front Aging Neurosci, 2015. **7**: p. 136.
50. Qi, X.M. and J.F. Ma, *The role of amyloid beta clearance in cerebral amyloid angiopathy: more potential therapeutic targets.* Translational Neurodegeneration, 2017. **6**: p. 22.
51. Hersh, L.B. and D.W. Rodgers, *Neprilysin and amyloid beta peptide degradation.* Current Alzheimer Research, 2008. **5**(2): p. 225-231.
52. Nalivaeva, N.N., et al., *The Alzheimer's amyloid-degrading peptidase, neprilysin: can we control it?* International Journal of Alzheimers Disease 2012. **2012**: p. 383796.
53. Wang, D.S., D.W. Dickson, and J.S. Malter, *Beta-amyloid degradation and Alzheimer's disease.* Journal of Biomedicine & Biotechnology, 2006. **2006**(3): p. 58406-58406.
54. Qiu, W.Q. and M.F. Folstein, *Insulin, insulin-degrading enzyme and amyloid-beta peptide in Alzheimer's disease: review and hypothesis.* Neurobiology of Aging, 2006. **27**(2): p. 190-198.
55. Bayes-Genis, A. and J. Lupón, *Neprilysin: Indications, Expectations, and Challenges.* Revista Española de Cardiología (English Edition), 2016. **69**(7): p. 647-649.
56. Hu, J., et al., *Angiotensin-converting Enzyme Degrades Alzheimer Amyloid β-Peptide (Aβ); Retards Aβ Aggregation, Deposition, Fibril Formation; and Inhibits Cytotoxicity.* Journal of Biological Chemistry, 2001. **276**(51): p. 47863-47868.
57. Saido, T. and M.A. Leissring, *Proteolytic degradation of amyloid β-protein.* Cold Spring Harbor Perspectives in Medicine, 2012. **2**(6): p. a006379.
58. Wang, D.S., D.W. Dickson, and J.S. Malter, *beta-Amyloid degradation and Alzheimer's disease.* Journal of Biomedicine & Biotechnology, 2006. **2006**(3): p. 58406.
59. Baranello, R.J., et al., *Amyloid-beta protein clearance and degradation (ABCD) pathways and their role in Alzheimer's disease.* Current Alzheimer Research, 2015. **12**(1): p. 32-46.
60. Deane, R., et al., *Clearance of amyloid-beta peptide across the blood-brain barrier: implication for therapies in Alzheimer's disease.* CNS & Neurological Disorders Drug Targets, 2009. **8**(1): p. 16-30.

61. Bohrmann, B., et al., *Endogenous proteins controlling amyloid beta-peptide polymerization. Possible implications for beta-amyloid formation in the central nervous system and in peripheral tissues.* The Journal of Biological Chemistry, 1999. **274**(23): p. 15990-5.
62. Wang, Y.J., H.D. Zhou, and X.F. Zhou, *Clearance of amyloid-beta in Alzheimer's disease: progress, problems and perspectives.* Drug Discov Today, 2006. **11**(19-20): p. 931-8.
63. Ghiso, J., et al., *Systemic catabolism of Alzheimer's Abeta40 and Abeta42.* The Journal of Biological Chemistry, 2004. **279**(44): p. 45897-908.
64. Reitz, C., *Alzheimer's disease and the amyloid cascade hypothesis: a critical review.* International Journal of Alzheimer's Disease, 2012. **2012**: p. 369808.
65. Karran, E., M. Mercken, and B. De Strooper, *The amyloid cascade hypothesis for Alzheimer's disease: an appraisal for the development of therapeutics.* Nature Reviews Drug Discovery, 2011. **10**(9): p. 698-712.
66. Isik, A.T., *Late onset Alzheimer's disease in older people.* Clinical Interventions in Aging, 2010. **5**: p. 307-11.
67. Masters, C.L., et al., *Alzheimer's disease.* Nature Reviews Disease Primers, 2015. **1**: p. 15056.
68. Guerreiro, R., et al., *TREM2 variants in Alzheimer's disease.* The New England Journal of Medicine, 2013. **368**(2): p. 117-27.
69. Gratuze, M., C.E.G. Leyns, and D.M. Holtzman, *New insights into the role of TREM2 in Alzheimer's disease.* Molecular Neurodegeneration, 2018. **13**(1): p. 66.
70. Martinez, M., et al., *Apolipoprotein E ϵ4 Allele and Familial Aggregation of Alzheimer Disease.* Archives of Neurology, 1998. **55**(6): p. 810-816.
71. Liu, C.C., et al., *Apolipoprotein E and Alzheimer disease: risk, mechanisms and therapy.* Nature Reviews. Neurology, 2013. **9**(2): p. 106-118.
72. Mahley, R.W., *Central Nervous System Lipoproteins: ApoE and Regulation of Cholesterol Metabolism.* Arteriosclerosis, Thrombosis, and Vascular Biology, 2016. **36**(7): p. 1305-1315.
73. Kanekiyo, T., H. Xu, and G. Bu, *ApoE and Aβ in Alzheimer's disease: accidental encounters or partners?* Neuron, 2014. **81**(4): p. 740-754.
74. Wildsmith, K.R., et al., *Evidence for impaired amyloid β clearance in Alzheimer's disease.* Alzheimer's Research & Therapy, 2013. **5**(33): p. 6.
75. Ikeda, T. and M. Yamada, *Risk factors for Alzheimer's disease.* Brain and Nerve, 2010. **62**(7): p. 679-90.
76. MacKnight, C., et al., *Diabetes mellitus and the Risk of Dementia, Alzheimer's Disease and Vascular Cognitive Impairment in the Canadian Study of Health and Aging.* Dementia and Geriatric Cognitive Disorders, 2002. **14**(2): p. 77-83.
77. Pappolla, M.A., et al., *Mild hypercholesterolemia is an early risk factor for the development of Alzheimer amyloid pathology.* Neurology, 2003. **61**(2): p. 199-205.
78. Profenno, L.A., A.P. Porsteinsson, and S.V. Faraone, *Meta-Analysis of Alzheimer's Disease Risk with Obesity, Diabetes, and Related Disorders.* Biological Psychiatry, 2010. **67**(6): p. 505-512.
79. Sharp, S.I., et al., *Hypertension is a potential risk factor for vascular dementia: systematic review.* International Journal of Geriatric Psychiatry, 2011. **26**(7): p. 661-669.
80. Sivanandam, T.M. and M.K. Thakur, *Traumatic brain injury: A risk factor for Alzheimer's disease.* Neuroscience & Biobehavioral Reviews, 2012. **36**(5): p. 1376-1381.
81. Attems, J. and K.A. Jellinger, *The overlap between vascular disease and Alzheimer's disease--lessons from pathology.* BMC Medicine, 2014. **12**: p. 206.
82. De La Torre, J.C., *Alzheimer Disease as a Vascular Disorder.* Stroke, 2002. **33**(4): p. 1152-1162.

83. Stampfer, M.J., *Cardiovascular disease and Alzheimer's disease: common links.* Journal of Internal Medicine, 2006. **260**(3): p. 211-23.
84. Santos, C.Y., et al., *Pathophysiologic relationship between Alzheimer's disease, cerebrovascular disease, and cardiovascular risk: A review and synthesis.* Alzheimer's & dementia (Amsterdam, Netherlands), 2017. **7**: p. 69-87.
85. Sagare, A.P., R.D. Bell, and B.V. Zlokovic, *Neurovascular dysfunction and faulty amyloid beta-peptide clearance in Alzheimer disease.* Cold Spring Harbor Perspectives in Medicine, 2012. **2**(10).
86. Canobbio, I., et al., *Role of amyloid peptides in vascular dysfunction and platelet dysregulation in Alzheimer's disease.* Frontiers in Cellular Neuroscience, 2015. **9**.
87. Lee, C.W., Y.H. Shih, and Y.M. Kuo, *Cerebrovascular pathology and amyloid plaque formation in Alzheimer's disease.* Current Alzheimer Research, 2014. **11**(1): p. 4-10.
88. Cheung, C., et al., *Modeling cerebrovascular pathophysiology in amyloid-beta metabolism using neural-crest-derived smooth muscle cells.* Cell Reports, 2014. **9**(1): p. 391-401.
89. Salmina, A.B., et al., *Pericytes in Alzheimer's Disease: Novel Clues to Cerebral Amyloid Angiopathy Pathogenesis.* Advances in Experimental Medicine and Biology, 2019. **1147**: p. 147-166.
90. Zlokovic, B.V., *Neurovascular pathways to neurodegeneration in Alzheimer's disease and other disorders.* Nature reviews. Neuroscience, 2011. **12**(12): p. 723-738.
91. Winkler, E.A., A.P. Sagare, and B.V. Zlokovic, *The pericyte: a forgotten cell type with important implications for Alzheimer's disease?* Brain Pathology, 2014. **24**(4): p. 371-386.
92. Bell, R.D., et al., *Pericytes control key neurovascular functions and neuronal phenotype in the adult brain and during brain aging.* Neuron, 2010. **68**(3): p. 409-427.
93. Sengillo, J.D., et al., *Deficiency in mural vascular cells coincides with blood-brain barrier disruption in Alzheimer's disease.* Brain Pathology 2013. **23**(3): p. 303-310.
94. Sagare, A.P., et al., *Pericyte loss influences Alzheimer-like neurodegeneration in mice.* Nature communications, 2013. **4**: p. 2932-2932.
95. Wilhelmus, M.M., et al., *Lipoprotein receptor-related protein-1 mediates amyloid-beta-mediated cell death of cerebrovascular cells.* The American Journal of Pathology, 2007. **171**(6): p. 1989-1999.
96. Farkas, E. and P.G. Luiten, *Cerebral microvascular pathology in aging and Alzheimer's disease.* Progress in Neurobiology, 2001. **64**(6): p. 575-611.
97. Iwata, N., et al., *Metabolic Regulation of Brain Aβ by Neprilysin.* Science, 2001. **292**(5521): p. 1550-1552.
98. Yasojima, K., E.G. McGeer, and P.L. McGeer, *Relationship between beta amyloid peptide generating molecules and neprilysin in Alzheimer disease and normal brain.* Brain Research, 2001. **919**(1): p. 115-121.
99. Yasojima, K., et al., *Reduced neprilysin in high plaque areas of Alzheimer brain: a possible relationship to deficient degradation of β-amyloid peptide.* Neuroscience Letters, 2001. **297**(2): p. 97-100.
100. Eckman, E.A. and C.B. Eckman, *Abeta-degrading enzymes: modulators of Alzheimer's disease pathogenesis and targets for therapeutic intervention.* Biochemical Society Transactions, 2005. **33**(Pt 5): p. 1101-1105.
101. Maguire, J.J., et al., *Endothelin converting enzyme (ECE) activity in human vascular smooth muscle.* British Journal of Pharmacology, 1997. **122**(8): p. 1647-1654.
102. Palmer, J.C., et al., *Endothelin-converting enzyme-2 is increased in Alzheimer's disease and up-regulated by Abeta.* The American Journal of Pathology, 2009. **175**(1): p. 262-270.

103. Palmer, J.C., P.G. Kehoe, and S. Love, *Endothelin-converting enzyme-1 in Alzheimer's disease and vascular dementia.* Neuropathology and Applied Neurobiology, 2010. **36**(6): p. 487-497.
104. Funalot, B., et al., *Endothelin-converting enzyme-1 is expressed in human cerebral cortex and protects against Alzheimer's disease.* Molecular Psychiatry, 2004. **9**: p. 1122.
105. Eckman, E.A., D.K. Reed, and C.B. Eckman, *Degradation of the Alzheimer's amyloid beta peptide by endothelin-converting enzyme.* Journal of Biological Chemistry, 2001. **276**(27): p. 24540-24548.
106. Lavoie, J.L. and C.D. Sigmund, *Minireview: Overview of the Renin-Angiotensin System—An Endocrine and Paracrine System.* Endocrinology, 2003. **144**(6): p. 2179-2183.
107. Kehoe, P.G., *The Coming of Age of the Angiotensin Hypothesis in Alzheimer's Disease: Progress Toward Disease Prevention and Treatment?* Journal of Alzheimer's Disease 2018. **62**(3): p. 1443-1466.
108. Bodiga, V.L. and S. Bodiga, *Renin Angiotensin System in Cognitive Function and Dementia.* Asian Journal of Neuroscience, 2013. **2013**: p. 18.
109. Thorin, E., *Hypertension and Alzheimer Disease.* Hypertension, 2015. **65**(1): p. 36-38.
110. Amouyel, P., et al., *The Renin Angiotensin System and Alzheimer's Disease.* Annals of the New York Academy of Sciences, 2000. **903**(1): p. 437-441.
111. Skoog, I. and D. Gustafson, *Hypertension, hypertension-clustering factors and Alzheimer's disease.* Neurological Research, 2003. **25**(6): p. 675-680.
112. Chou, C.L. and H.I. Yeh, *The Role of the Renin-Angiotensin System in Amyloid Metabolism of Alzheimer's Disease.* Acta Cardiologica Sinica, 2014. **30**(2): p. 114-118.
113. Miners, J.S., et al., *Angiotensin-converting enzyme (ACE) levels and activity in Alzheimer's disease, and relationship of perivascular ACE-1 to cerebral amyloid angiopathy.* Neuropathology and Applied Neurobiology, 2008. **34**(2): p. 181-193.
114. Kehoe, P.G., et al., *Angiotensin-converting enzyme 2 is reduced in Alzheimer's disease in association with increasing amyloid-β and tau pathology.* Alzheimer's Research & Therapy, 2016. **8**(1): p. 50.
115. Xia, H. and E. Lazartigues, *Angiotensin-converting enzyme 2: central regulator for cardiovascular function.* Current Hypertension Reports, 2010. **12**(3): p. 170-175.
116. Grinberg, L.T. and D.R. Thal, *Vascular pathology in the aged human brain.* Acta Neuropathologica, 2010. **119**(3): p. 277-90.
117. Thal, D.R., W.S. Griffin, and H. Braak, *Parenchymal and vascular Abeta-deposition and its effects on the degeneration of neurons and cognition in Alzheimer's disease.* Journal of Cellular and Molecular Medicine, 2008. **12**(5b): p. 1848-62.
118. Viswanathan, A. and S.M. Greenberg, *Cerebral amyloid angiopathy in the elderly.* Annals of Neurology, 2011. **70**(6): p. 871-80.
119. Biffi, A. and S.M. Greenberg, *Cerebral amyloid angiopathy: a systematic review.* Journal of Clinical Neurology, 2011. **7**(1): p. 1-9.
120. Kawai, M., et al., *Degeneration of vascular muscle cells in cerebral amyloid angiopathy of Alzheimer disease.* Brain Research 1993. **623**(1): p. 142-6.
121. Tian, J., et al., *Relationships in Alzheimer's disease between the extent of Abeta deposition in cerebral blood vessel walls, as cerebral amyloid angiopathy, and the amount of cerebrovascular smooth muscle cells and collagen.* Neuropathology and Applied Neurobiology, 2006. **32**(3): p. 332-40.
122. Mendel, T.A., et al., *The development of cerebral amyloid angiopathy in cerebral vessels. A review with illustrations based upon own investigated post mortem cases.* Polish Journal of Pathology, 2013. **64**(4): p. 260-7.

123. Thal, D.R., et al., *Cerebral amyloid angiopathy and its relationship to Alzheimer's disease.* Acta Neuropathologica, 2008. **115**(6): p. 599-609.
124. Attems, J. and K.A. Jellinger, *Only cerebral capillary amyloid angiopathy correlates with Alzheimer pathology--a pilot study.* Acta Neuropathologica, 2004. **107**(2): p. 83-90.
125. Pezzini, A., et al., *Cerebral Amyloid Angiopathy: A Common Cause of Cerebral Hemorrhage.* Current Medicinal Chemistry, 2009. **16,**: p. 2498-2513.
126. Gurol, M.E. and S.M. Greenberg, *Cerebral Amyloid Angiopathy*, in *Uncommon Causes of Stroke*, J. Biller and L. Caplan, Editors. 2018, Cambridge University Press: Cambridge. p. 534-544.
127. Yamaguchi, H., et al., *Beta amyloid is focally deposited within the outer basement membrane in the amyloid angiopathy of Alzheimer's disease. An immunoelectron microscopic study.* The American Journal of Pathology, 1992. **141**(1): p. 249-59.
128. Vonsattel, J.P., et al., *Cerebral amyloid angiopathy without and with cerebral hemorrhages: a comparative histological study.* Annals of Neurology, 1991. **30**(5): p. 637-49.
129. Yamada, M., *Cerebral amyloid angiopathy: emerging concepts.* Journal of Stroke, 2015. **17**(1): p. 17-30.
130. Mandybur, T.I., *Cerebral amyloid angiopathy: the vascular pathology and complications.* Journal of Neuropathology and Experimental Neurology, 1986. **45**(1): p. 79-90.
131. Maeda, A., et al., *Computer-assisted three-dimensional image analysis of cerebral amyloid angiopathy.* Stroke, 1993. **24**(12): p. 1857-64.
132. Moussaddy, A., et al., *Inflammatory Cerebral Amyloid Angiopathy, Amyloid-beta-Related Angiitis, and Primary Angiitis of the Central Nervous System: Similarities and Differences.* Stroke, 2015. **46**(9): p. e210-3.
133. Vasilevko, V., et al., *Aging and cerebrovascular dysfunction: contribution of hypertension, cerebral amyloid angiopathy, and immunotherapy.* Annals of the New York Academy of Sciences, 2010. **1207**: p. 58-70.
134. Eng, J.A., et al., *Clinical manifestations of cerebral amyloid angiopathy-related inflammation.* Annals of Neurology, 2004. **55**(2): p. 250-6.
135. Viswanathan, A., et al., *Emerging concepts in sporadic cerebral amyloid angiopathy.* Brain, 2017. **140**(7): p. 1829-1850.
136. Kumar-Singh, S., *Cerebral amyloid angiopathy: pathogenetic mechanisms and link to dense amyloid plaques.* Genes, Brain, and Behavior, 2008. **7 Suppl 1**: p. 67-82.
137. Frackowiak, J., A. Zoltowska, and H.M. Wisniewski, *Non-fibrillar beta-amyloid protein is associated with smooth muscle cells of vessel walls in Alzheimer disease.* Journal of Neuropathology and Experimental Neurology, 1994. **53**(6): p. 637-45.
138. Tagliavini, F., et al., *Coexistence of Alzheimer's amyloid precursor protein and amyloid protein in cerebral vessel walls.* Laboratory Investigation 1990. **62**(6): p. 761-7.
139. Natte, R., et al., *Amyloid beta precursor protein-mRNA is expressed throughout cerebral vessel walls.* Brain Research 1999. **828**(1-2): p. 179-83.
140. Wisniewski, H.M., J. Frackowiak, and B. Mazur-Kolecka, *In vitro production of beta-amyloid in smooth muscle cells isolated from amyloid angiopathy-affected vessels.* Neuroscience Letters, 1995. **183**(1-2): p. 120-3.
141. Verbeek, M.M., et al., *Rapid degeneration of cultured human brain pericytes by amyloid beta protein.* Journal of Neurochemistry, 1997. **68**(3): p. 1135-41.
142. Weller, R.O., et al., *Cerebral amyloid angiopathy: amyloid beta accumulates in putative interstitial fluid drainage pathways in Alzheimer's disease.* American Journal of Pathology, 1998. **153**(3): p. 725-33.

143. Revesz, T., et al., *Cerebral Amyloid Angiopathies: A Pathologic, Biochemical, and Genetic View.* Journal of Neuropathology & Experimental Neurology, 2003. **62**(9): p. 885-898.
144. Fukuchi, K., et al., *High levels of circulating beta-amyloid peptide do not cause cerebral beta-amyloidosis in transgenic mice.* The American Journal of Pathology, 1996. **149**(1): p. 219-27.
145. Bakker, E.N., et al., *Lymphatic Clearance of the Brain: Perivascular, Paravascular and Significance for Neurodegenerative Diseases.* Cellular and Molecular Neurobiology, 2016. **36**(2): p. 181-94.
146. Nicoll, J.A., et al., *Cerebral amyloid angiopathy plays a direct role in the pathogenesis of Alzheimer's disease. Pro-CAA position statement.* Neurobiology of Aging, 2004. **25**(5): p. 589-97; discussion 603-4.
147. Xu, X., et al., *Age-related Impairment of Vascular Structure and Functions.* Aging and Disease, 2017. **8**(5): p. 590-610.
148. Hawkes, C.A., et al., *Disruption of arterial perivascular drainage of amyloid-beta from the brains of mice expressing the human APOE epsilon4 allele.* PLoS One, 2012. **7**(7): p. e41636.
149. Erickson, M.A. and W.A. Banks, *Blood–brain barrier dysfunction as a cause and consequence of Alzheimer's disease.* J Cereb Blood Flow Metab, 2013. **33**(10): p. 1500-1513.
150. Yamazaki, Y. and T. Kanekiyo, *Blood-Brain Barrier Dysfunction and the Pathogenesis of Alzheimer's Disease.* International Journal of Molecular Sciences, 2017. **18**(9).
151. Sevush, S., et al., *Platelet activation in Alzheimer disease.* Archives of Neurology, 1998. **55**(4): p. 530-536.
152. Ciabattoni, G., et al., *Determinants of platelet activation in Alzheimer's disease.* Neurobiology of Aging, 2007. **28**(3): p. 336-42.
153. Zhang, W., W. Huang, and F. Jing, *Contribution of blood platelets to vascular pathology in Alzheimer's disease.* Journal of Blood Medicine, 2013. **4**: p. 141-147.
154. Chen, M., et al., *Platelets Are the Primary Source of Amyloid β-Peptide in Human Blood.* Biochemical and Biophysical Research Communications, 1995. **213**(1): p. 96-103.
155. Skovronsky, D.M., V.M. Lee, and D. Pratico, *Amyloid precursor protein and amyloid beta peptide in human platelets. Role of cyclooxygenase and protein kinase C.* The Journal of Biological Chemistry, 2001. **276**(20): p. 17036-43.
156. Kucheryavykh, L.Y., et al., *Platelets are responsible for the accumulation of β-amyloid in blood clots inside and around blood vessels in mouse brain after thrombosis.* Brain Research Bulletin, 2017. **128**: p. 98-105.
157. Evin, G. and Q.X. Li, *Platelets and Alzheimer's disease: Potential of APP as a biomarker.* World Journal of Psychiatry, 2012. **2**(6): p. 102-13.
158. Ramalingam, G., N. Jones, and M. Besser, *Platelets for anaesthetists—part 1: physiology and pathology.* BJA Education, 2015. **16**(4): p. 134-139.
159. Machlus, K.R. and J.E. Italiano, *The incredible journey: From megakaryocyte development to platelet formation.* The Journal of Cell Biology, 2013. **201**(6): p. 785-796.
160. Holinstat, M., *Normal platelet function.* Cancer Metastasis Rev, 2017. **36**(2): p. 195-198.
161. Golebiewska, E.M. and A.W. Poole, *Platelet secretion: From haemostasis to wound healing and beyond.* Blood Rev, 2015. **29**(3): p. 153-62.
162. Steinhubl, S.R., *Platelets as mediators of inflammation.* Hematol Oncol Clin North Am, 2007. **21**(1): p. 115-21.
163. Koupenova, M., et al., *Circulating Platelets as Mediators of Immunity, Inflammation, and Thrombosis.* Circ Res, 2018. **122**(2): p. 337-351.

164. Eisinger, F., J. Patzelt, and H.F. Langer, *The Platelet Response to Tissue Injury.* Front Med (Lausanne), 2018. **5**: p. 317.
165. Schlesinger, M., *Role of platelets and platelet receptors in cancer metastasis.* Journal of Hematology & Oncology, 2018. **11**(1): p. 125.
166. Repsold, L., et al., *An overview of the role of platelets in angiogenesis, apoptosis and autophagy in chronic myeloid leukaemia.* Cancer Cell Int, 2017. **17**: p. 89.
167. Koupenova, M., et al., *Thrombosis and platelets: an update.* Eur Heart J, 2017. **38**(11): p. 785-791.
168. George, A.F., *Platelet Structure and Function.* Clinical Laboratory Science 2015. **28**(2): p. 125-131.
169. Lhermusier, T., H. Chap, and B. Payrastre, *Platelet membrane phospholipid asymmetry: from the characterization of a scramblase activity to the identification of an essential protein mutated in Scott syndrome.* J Thromb Haemost, 2011. **9**(10): p. 1883-91.
170. Cohen, B.M., G.S. Zubenko, and S.M. Babb, *Abnormal platelet membrane composition in Alzheimer's-type dementia.* Life Sciences, 1987. **40**(25): p. 2445-2451.
171. Zainaghi, I.A., O.V. Forlenza, and W.F. Gattaz, *Abnormal APP processing in platelets of patients with Alzheimer's disease: correlations with membrane fluidity and cognitive decline.* Psychopharmacology 2007. **192**(4): p. 547-53.
172. Selvadurai, M.V. and J.R. Hamilton, *Structure and function of the open canalicular system - the platelet's specialized internal membrane network.* Platelets, 2018. **29**(4): p. 319-325.
173. Heijnen, H. and S.J.A. Korporaal, *Platelet Morphology and Ultrastructure*, in *Platelets in Thrombotic and Non-Thrombotic Disorders*, K.N. Gresele P., Lopez J., Page C., Editor. 2017, Springer, Cham. p. 21-37.
174. Falet, H., *Anatomy of the Platelet Cytoskeleton*, in *Platelets in Thrombotic and Non-Thrombotic Disorders.*, K.N. Gresele P., Lopez J., Page C. , Editor. 2017, Springer, Cham. p. 139-156.
175. Bearer, E.L., J.M. Prakash, and Z. Li, *Actin Dynamics in Platelets.* International Review of Cytology, 2002. **217**: p. 137–182.
176. Flaumenhaft, R., *Platelet Secretion.* Platelets in Thrombotic and Non-Thrombotic Disorders, ed. K.N. Gresele P., Lopez J., Page C. 2017: Springer, Cham.
177. Rasche, H., *Haemostasis and thrombosis: an overview.* European Heart Journal Supplements, 2001. **3**(suppl_Q): p. Q3-Q7.
178. Gale, A.J., *Current understanding of hemostasis.* Toxicol Pathol, 2011. **39**(1): p. 273-80.
179. Bertina, R.M., *The role of procoagulants and anticoagulants in the development of venous thromboembolism.* Thromb Res, 2009. **123 Suppl 4**: p. S41-5.
180. Hollenhorst, M.A. and E.M. Battinelli, *Thrombosis, Hypercoagulable States, and Anticoagulants.* Prim Care, 2016. **43**(4): p. 619-635.
181. Periayah, M.H., A.S. Halim, and A.Z. Mat Saad, *Mechanism Action of Platelets and Crucial Blood Coagulation Pathways in Hemostasis.* Int J Hematol Oncol Stem Cell Res, 2017. **11**(4): p. 319-327.
182. Clark, J.F. and G. Pyne-Geithman, *Vascular smooth muscle function: The physiology and pathology of vasoconstriction.* Pathophysiology, 2005. **12**(1): p. 35-45.
183. Loscalzo, J., *Endothelial injury, vasoconstriction, and its prevention.* Tex Heart Inst J, 1995. **22**(2): p. 180-4.
184. Bergmeier, W. and R.O. Hynes, *Extracellular matrix proteins in hemostasis and thrombosis.* Cold Spring Harb Perspect Biol, 2012. **4**(2).
185. Yip, J., et al., *Primary platelet adhesion receptors.* IUBMB Life, 2005. **57**(2): p. 103-8.

186. Ruggeri, Z.M., *Platelet adhesion under flow.* Microcirculation, 2009. **16**(1): p. 58-83.
187. Sakariassen, K.S., L. Orning, and V.T. Turitto, *The impact of blood shear rate on arterial thrombus formation.* Future Sci OA, 2015. **1**(4): p. Fso30.
188. Kroll, M.H., et al., *Platelets and shear stress.* Blood, 1996. **88**(5): p. 1525-41.
189. Papaioannou, T.G. and C. Stefanadis, *Vascular wall shear stress: basic principles and methods.* Hellenic J Cardiol, 2005. **46**(1): p. 9-15.
190. Hathcock, J.J., *Flow effects on coagulation and thrombosis.* Arterioscler Thromb Vasc Biol, 2006. **26**(8): p. 1729-37.
191. Roher, A.E., et al., *Cerebral blood flow in Alzheimer's disease.* Vasc Health Risk Manag, 2012. **8**: p. 599-611.
192. Nation, D.A., *Blood Pressure and Cerebral Blood Flow in Alzheimer Disease.* Hypertension, 2018. **72**(1): p. 68-69.
193. P. A. M. M. Aarts, et al., *Blood Platelets Are Concentrated near the Wall and Red Blood Cells, in the Center in Flowing Blood.* (Arteriosclerosis, 1988. **8**: p. 819-824.
194. Goto, S., et al., *Distinct mechanisms of platelet aggregation as a consequence of different shearing flow conditions.* J Clin Invest, 1998. **101**(2): p. 479-486.
195. Shi, X., et al., *Effects of different shear rates on the attachment and detachment of platelet thrombi.* Mol Med Rep, 2016. **13**(3): p. 2447-56.
196. Uchida, Y., et al., *Characterization of coronary fibrin thrombus in patients with acute coronary syndrome using dye-staining angioscopy.* Arterioscler Thromb Vasc Biol, 2011. **31**(6): p. 1452-1460.
197. Cosemans, J.M.E.M., et al., *The effects of arterial flow on platelet activation, thrombus growth, and stabilization.* Cardiovasc Res, 2013. **99**(2): p. 342-352.
198. Ricard-Blum, S., *The collagen family.* Cold Spring Harb Perspect Biol, 2011. **3**(1): p. a004978.
199. Lodish, H., A. Berk, and S.L. Zipursky, *Collagen: the fibrous proteins of the matrix,* in *Molecular Cell Biology*. 2000, W. H. Freeman: New York.
200. Kehrel, B.E., *Platelet-collagen interactions.* Semin Thromb Hemost 1995. **21**(2): p. 123-129.
201. Manon-Jensen, T., N.G. Kjeld, and M.A. Karsdal, *Collagen-mediated hemostasis.* J Thromb Haemost, 2016. **14**(3): p. 438-448.
202. Xu, J. and G.P. Shi, *Vascular wall extracellular matrix proteins and vascular diseases.* Biochim Biophys Acta 2014. **1842**(11): p. 2106-2119.
203. Alberio, L. and G.L. Dale, *Platelet-collagen interactions: membrane receptors and intracellular signalling pathways.* European Journal of Clinical Investigation 1999. **29**: p. 1066-1076.
204. Hassan, M.I., A. Saxena, and F. Ahmad, *Structure and function of von Willebrand factor.* Blood Coagul Fibrinolysis, 2012. **23**(1): p. 11-22.
205. Peyvandi, F., I. Garagiola, and L. Baronciani, *Role of von Willebrand factor in the haemostasis.* Blood Transfus, 2011. **9 Suppl 2**: p. s3-8.
206. Joly, B.S., P. Coppo, and A. Veyradier, *Thrombotic thrombocytopenic purpura.* Blood, 2017. **129**(21): p. 2836-2846.
207. Jackson, S.P., W. Nesbitt, and E. Westein, *Dynamics of platelet thrombus formation.* J Thromb Haemost, 2009. **7 Suppl 1**: p. 17-20.
208. Canobbio, I., C. Balduini, and M. Torti, *Signalling through the platelet glycoprotein Ib-V–IX complex.* Cell Signal, 2004. **16**(12): p. 1329-1344.
209. Falati, S., C.E. Edmead, and A.W. Poole, *Glycoprotein Ib-V-IX, a receptor for von Willebrand factor, couples physically and functionally to the Fc receptor gamma-chain, Fyn, and Lyn to activate human platelets.* Blood, 1999. **94**(5): p. 1648-1656.
210. Gardiner, E.E., *A GPIb-IX-V complex signaling environment.* J Thromb Haemost, 2010. **8**(5): p. 1075-6.

211. Nieswandt, B., et al., *Glycoprotein VI but not α2β1 integrin is essential for platelet interaction with collagen.* Embo j, 2001. **20**(9): p. 2120-2130.
212. Yuan, Y., et al., *The von Willebrand factor-glycoprotein Ib/V/IX interaction induces actin polymerization and cytoskeletal reorganization in rolling platelets and glycoprotein Ib/V/IX-transfected cells.* J Biol Chem, 1999. **274**(51): p. 36241-36251.
213. Rivera, J., et al., *Platelet receptors and signaling in the dynamics of thrombus formation.* Haematologica, 2009. **94**(5): p. 700-11.
214. Dopheide, S.M., M.J. Maxwell, and S.P. Jackson, *Shear-dependent tether formation during platelet translocation on von Willebrand factor.* Blood, 2002. **99**(1): p. 159-167.
215. Gibbins, J.M., *Platelet adhesion signalling and the regulation of thrombus formation.* J Cell Sci, 2004. **117**(Pt 16): p. 3415-25.
216. Kasirer-Friede, A., M.L. Kahn, and S.J. Shattil, *Platelet integrins and immunoreceptors.* Immunol Rev, 2007. **218**: p. 247-264.
217. Ruggeri, Z.M. and S.P. Jackson, *Platelet thrombus formation in flowing blood*, in *Platelets* A.D. Michelson, Editor. 2013, Academic Press. p. 399-423.
218. Nieswandt, B., et al., *Glycoprotein VI but not α2β1 integrin is essential for platelet interaction with collagen.* Embo j, 2001. **20**(9): p. 2120-30.
219. Madamanchi, A., S.A. Santoro, and M.M. Zutter, *α2β1 integrin.* Adv Exp Med Biol, 2014. **819**: p. 41-60.
220. Moroi, A.J. and S.P. Watson, *Akt and mitogen-activated protein kinase enhance C-type lectin-like receptor 2-mediated platelet activation by inhibition of glycogen synthase kinase 3alpha/beta.* J Thromb Haemost, 2015. **13**(6): p. 1139-50.
221. Moroi, M. and S.M. Jung, *Platelet glycoprotein VI: its structure and function.* Thromb Res, 2004. **114**(4): p. 221-233.
222. Rabie, T., et al., *Diverging signaling events control the pathway of GPVI down-regulation in vivo.* Blood, 2007. **110**(2): p. 529-535.
223. Atkinson, B.T., G.E. Jarvis, and S.P. Watson, *Activation of GPVI by collagen is regulated by α2β1 and secondary mediators.* J Thromb Haemost, 2003. **1**(6): p. 1278-1287.
224. Stalker, T.J., et al., *Platelet signaling.* Handb Exp Pharmacol, 2012(210): p. 59-85.
225. Polanowska-Grabowska, R., J.M. Gibbins, and A.R. Gear, *Platelet adhesion to collagen and collagen-related peptide under flow: roles of the [alpha]2[beta]1 integrin, GPVI, and Src tyrosine kinases.* Arterioscler Thromb Vasc Biol, 2003. **23**(10): p. 1934-40.
226. Shin, E.K., et al., *Platelet Shape Changes and Cytoskeleton Dynamics as Novel Therapeutic Targets for Anti-Thrombotic Drugs.* Biomol Ther (Seoul), 2017. **25**(3): p. 223-230.
227. Gear, A.R.L. and R.K. Polanowska-Grabowska, *The platelet shape change*, in *Platelets in Thrombotic and Non-Thrombotic Disorders: Pathophysiology, Pharmacology and Therapeutics*, C.P. Page, et al., Editors. 2002, Cambridge University Press: Cambridge. p. 319-337.
228. Cerecedo, D., *Platelet cytoskeleton and its hemostatic role.* Blood Coagul Fibrinolysis, 2013. **24**(8): p. 798-808.
229. Heijnen, H. and P. van der Sluijs, *Platelet secretory behaviour: as diverse as the granules … or not?* J Thromb Haemost 2015. **13**(12): p. 2141-2151.
230. Marks, M.S., *SNARing platelet granule secretion.* Blood, 2012. **120**(12): p. 2355-2357.
231. Rendu, F. and B. Brohard-Bohn, *The platelet release reaction: granules' constituents, secretion and functions.* Platelets, 2001. **12**(5): p. 261-273.
232. Murugappa, S. and S.P. Kunapuli, *The role of ADP receptors in platelet function.* Front Biosci, 2006. **11**: p. 1977-1986.

233. Woulfe, D., J. Yang, and L. Brass, *ADP and platelets: the end of the beginning.* J Clin Invest, 2001. **107**(12): p. 1503-1505.
234. Smyth, E.M., *Thromboxane and the thromboxane receptor in cardiovascular disease.* Clin Lipidol, 2010. **5**(2): p. 209-219.
235. Nakahata, N., *Thromboxane A2: physiology/pathophysiology, cellular signal transduction and pharmacology.* Pharmacol Ther, 2008. **118**(1): p. 18-35.
236. Joo, S.J., *Mechanisms of Platelet Activation and Integrin alphaIIbeta3.* Korean Circ J, 2012. **42**(5): p. 295-301.
237. Bennett, J.S., *Structure and function of the platelet integrin alphaIIbbeta3.* J Clin Invest, 2005. **115**(12): p. 3363-3369.
238. Coller, B.S., *αIIbβ3: structure and function.* J Thromb Haemost, 2015. **13 Suppl 1**(Suppl 1): p. S17-25.
239. Durrant, T.N., M.T. van den Bosch, and I. Hers, *Integrin αIIbβ3 outside-in signaling.* Blood, 2017. **130**(14): p. 1607-1619.
240. *<FIBRINOGEN_RomBiophys.pdf>*.
241. Bennett, J.S., *Platelet-fibrinogen interactions.* Ann N Y Acad Sci, 2001. **936**: p. 340-354.
242. Ye, F., C. Kim, and M.H. Ginsberg, *Molecular mechanism of inside-out integrin regulation.* J Thromb Haemost, 2011. **9 Suppl 1**(0 1): p. 20-25.
243. Barucker, C., et al., *Abeta42-oligomer Interacting Peptide (AIP) neutralizes toxic amyloid-beta42 species and protects synaptic structure and function.* Scientific Reports, 2015. **5**: p. 15410.
244. Mehrbod, M., S. Trisno, and M.R. Mofrad, *On the activation of integrin αIIbβ3: outside-in and inside-out pathways.* Biophys J, 2013. **105**(6): p. 1304-1315.
245. Huang, J., et al., *Platelet integrin αIIbβ3: signal transduction, regulation, and its therapeutic targeting.* J Hematol Oncol, 2019. **12**(1): p. 26.
246. Shattil, S.J., H. Kashiwagi, and N. Pampori, *Integrin signaling: the platelet paradigm.* Blood, 1998. **91**(8): p. 2645-2657.
247. Smith, S.A., R.J. Travers, and J.H. Morrissey, *How it all starts: Initiation of the clotting cascade.* Crit Rev Biochem Mol Biol, 2015. **50**(4): p. 326-336.
248. Davie, E.W. and J.D. Kulman, *An overview of the structure and function of thrombin.* Semin Thromb Hemost, 2006. **32 Suppl 1**: p. 3-15.
249. Nieman, M.T., *Protease-activated receptors in hemostasis.* Blood, 2016. **128**(2): p. 169-177.
250. Estevez, B. and X. Du, *New concepts and mechanisms of platelet activation signaling.* Physiology 2017. **32**(2): p. 162-177.
251. Hawkins, C. and M. Davies, *Detection and characterisation of radicals in biological materials using EPR methodology*. Vol. 1840. 2013.
252. Soh, U.J., et al., *Signal transduction by protease-activated receptors.* Br J Pharmacol, 2010. **160**(2): p. 191-203.
253. Palta, S., R. Saroa, and A. Palta, *Overview of the coagulation system.* Indian J Anaesth, 2014. **58**(5): p. 515-523.
254. Hansson, K. and J. Stenflo, *Post-translational modifications in proteins involved in blood coagulation.* J Thromb Haemost, 2005. **3**(12): p. 2633-2648.
255. Furie, B. and B.C. Furie, *Molecular basis of vitamin K-dependent gamma-carboxylation.* Blood, 1990. **75**(9): p. 1753-1762.
256. Furie, B., B.A. Bouchard, and B.C. Furie, *Vitamin K-dependent biosynthesis of gamma-carboxyglutamic acid.* Blood, 1999. **93**(6): p. 1798-1808.
257. Hemker, H.C., et al., *Platelet membrane involvement in blood coagulation.* Blood Cells, 1983. **9**(2): p. 303-317.
258. Lentz, B.R., *Exposure of platelet membrane phosphatidylserine regulates blood coagulation.* Prog Lipid Res, 2003. **42**(5): p. 423-438.

259. Mackman, N., R.E. Tilley, and N.S. Key, *Role of the Extrinsic Pathway of Blood Coagulation in Hemostasis and Thrombosis.* Arterioscler Thromb Vasc Biol, 2007. **27**(8): p. 1687-1693.
260. Handbook of Laboratory and Diagnostic Tests. *Coagulation Process*. 2013 26-03-2019]; Available from: https://medical-dictionary.thefreedictionary.com/_/viewer.aspx?path=davis%2Flab&name=02&url=https%3A%2F%2Fmedical-dictionary.thefreedictionary.com%2Fcoagulation%2Bfactors.
261. Gailani, D. and T. Renné, *Intrinsic Pathway of Coagulation and Arterial Thrombosis.* Arterioscler Thromb Vasc Biol, 2007. **27**(12): p. 2507-2513.
262. Nikolajsen, C.L., et al., *Coagulation factor XIIIa substrates in human plasma: identification and incorporation into the clot.* J Biol Chem, 2014. **289**(10): p. 6526-34.
263. Narayanan, S., *Multifunctional roles of thrombin.* Ann Clin Lab Sci, 1999. **29**(4): p. 275-280.
264. Crawley, J.T., et al., *The central role of thrombin in hemostasis.* J Thromb Haemost, 2007. **5 Suppl 1**: p. 95-101.
265. Lenting, P.J., J.A. van-Mourik, and K. Mertens, *The life cycle of coagulation factor VIII in view of its structure and function.* Blood, 1998. **92**(11): p. 3983-3996.
266. Batty, P. and J.G. Smith, *Haemostasis.* Surgery (Oxford), 2010. **28**(11): p. 530-535.
267. Miljic, P., et al., *Thrombin activatable fibrinolysis inhibitor (TAFI): a molecular link between coagulation and fibrinolysis.* Srp Arh Celok Lek, 2010. **138 Suppl 1**: p. 74-78.
268. Yau, J.W., H. Teoh, and S. Verma, *Endothelial cell control of thrombosis.* BMC Cardiovasc Disord, 2015. **15**: p. 130.
269. Chapin, J.C. and K.A. Hajjar, *Fibrinolysis and the control of blood coagulation.* Blood Rev, 2015. **29**(1): p. 17-24.
270. James, C.T.B. and L.A. David, *The haemostatic role of tissue factor pathway Inhibitor.* Arterioscler Thromb Vasc Biol, 2008. **28**(2): p. 233-242.
271. Rajendran, P., et al., *The vascular endothelium and human diseases.* Int J Biol Sci, 2013. **9**(10): p. 1057-1069.
272. Favero, G., et al., *Endothelium and its alterations in cardiovascular diseases: life style intervention.* Biomed Res Int, 2014. **2014**: p. 801896.
273. Cortes-Canteli, M., et al., *Fibrinogen and altered hemostasis in Alzheimer's disease.* J Alzheimers Dis, 2012. **32**(3): p. 599-608.
274. Zamolodchikov, D., T. Renné, and S. Strickland, *The Alzheimer's disease peptide β-amyloid promotes thrombin generation through activation of coagulation factor XII.* J Thromb Haemost 2016. **14**(5): p. 995-1007.
275. Humpel, C., *Platelets: Their Potential Contribution to the Generation of Beta-amyloid Plaques in Alzheimer's Disease.* Current Neurovascular Research, 2017. **14**(3): p. 290-298.
276. Padovani, A., et al., *Abnormalities in the pattern of platelet amyloid precursor protein forms in patients with mild cognitive impairment and Alzheimer disease.* Arch Neurol, 2002. **59**(1): p. 71-75.
277. S., Z.G., et al., *Platelet membrane fluidity individuals at risk for Alzheimer's disease: a comparison of results from fluorescence spectroscopy and electron spin resonance spectroscopy.* Psychopharmacology, 1999. **145**: p. 175–180.
278. Zubenko, G.S., et al., *Platelet Membrane Abnormality in Alzheimer's Disease.* Annals of Neurology 1987. **22**(2).
279. Piletz, J.E., et al., *Intracellular membranes are more fluid in platelets of Alzheimer's disease patients.* Neurobiol Aging, 1991. **12**(5): p. 401-406.
280. Rosenberg, R.N., et al., *Altered amyloid protein processing in platelets of patients with Alzheimer disease.* Archives of Neurology, 1997. **54**(2): p. 139-44.

281. Catricala, S., M. Torti, and G. Ricevuti, *Alzheimer disease and platelets: how's that relevant.* Immunity & Ageing, 2012. **9**(1): p. 20.
282. Stellos, K., et al., *Predictive value of platelet activation for the rate of cognitive decline in Alzheimer's disease patients.* J Cereb Blood Flow Metab, 2010. **30**(11): p. 1817-20.
283. Stellos, K., et al., *Association of platelet activation with vascular cognitive impairment: implications in dementia development?* Current Vascular Pharmacology, 2014. **12**(1): p. 152-4.
284. Dale, G.L., *Coated-platelets: an emerging component of the procoagulant response.* J Thromb Haemost, 2005. **3**(10): p. 2185-2192.
285. Prodan, C.I., et al., *Coated-platelet levels and progression from mild cognitive impairment to Alzheimer disease.* Neurology, 2011. **76**(3): p. 247-52.
286. Arora, R.C., O.B. Emery, and H.Y. Meltzer, *Serotonin uptake in the blood platelets of Alzheimer's disease patients.* Neurology, 1991. **41**(8): p. 1307-1309.
287. Hirai, K., et al., *Mitochondrial abnormalities in Alzheimer's disease.* J Neurosci, 2001. **21**(9): p. 3017-3023.
288. Yan, M.H., X. Wang, and X. Zhu, *Mitochondrial defects and oxidative stress in Alzheimer disease and Parkinson disease.* Free Radic Biol Med, 2013. **62**: p. 90-101.
289. Parker, W.D., Jr., C.M. Filley, and J.K. Parks, *Cytochrome oxidase deficiency in Alzheimer's disease.* Neurology, 1990. **40**(8): p. 1302-3.
290. Muck-Seler, D., et al., *Platelet serotonin concentration and monoamine oxidase type B activity in female patients in early, middle and late phase of Alzheimer's disease.* Prog Neuropsychopharmacol Biol Psychiatry, 2009. **33**(7): p. 1226-1231.
291. Casoli, T., et al., *Peripheral inflammatory biomarkers of Alzheimer's disease: the role of platelets.* Biogerontology, 2010. **11**(5): p. 627-633.
292. Johnston, J.A., et al., *Platelet beta-secretase activity is increased in Alzheimer's disease.* Neurobiology of Aging, 2008. **29**(5): p. 661-8.
293. McGuinness, B., et al., *Platelet membrane β-secretase activity in mild cognitive impairment and conversion to dementia: a longitudinal study.* J Alzheimers Dis, 2016. **49**(4): p. 1095-1103.
294. Li, R., et al., *Amyloid beta peptide load is correlated with increased beta-secretase activity in sporadic Alzheimer's disease patients.* Proc Natl Acad Sci U S A, 2004. **101**(10): p. 3632-3637.
295. Gowert, N.S., et al., *Blood Platelets in the Progression of Alzheimer's Disease.* Plos One, 2014. **9**(2).
296. Shen, M.Y., et al., *Amyloid beta peptide-activated signal pathways in human platelets.* Eur J Pharmacol, 2008. **588**(2-3): p. 259-66.
297. Shen, M.Y., et al., *Expression of amyloid beta peptide in human platelets: pivotal role of the phospholipase Cgamma2-protein kinase C pathway in platelet activation.* Pharmacol Res, 2008. **57**(2): p. 151-8.
298. Jarre, A., et al., *Pre-activated blood platelets and a pro-thrombotic phenotype in APP23 mice modeling Alzheimer's disease.* Cellular Signalling, 2014. **26**(9): p. 2040-2050.
299. Canobbio, I., et al., *Platelet amyloid precursor protein is a modulator of venous thromboembolism in mice.* Blood, 2017. **130**(4): p. 527-536.
300. Canobbio, I., et al., *Immobilized amyloid A beta peptides support platelet adhesion and activation.* FEBS Letters, 2013. **587**(16): p. 2606-2611.
301. Galeazzi, L., et al., *β-Amyloid Fragment 25–35 Induces Changes in Cytosolic Free Calcium in Human Platelets.* Annals of the New York Academy of Sciences, 2000. **903**(1): p. 451-6.
302. Herczenik, E., et al., *Activation of human platelets by misfolded proteins.* Arteriosclerosis, Thrombosis, and Vascular Biology, 2007. **27**(7): p. 1657-65.

303. Canobbio, I., et al., *Amyloid beta-peptide-dependent activation of human platelets: essential role for Ca2+ and ADP in aggregation and thrombus formation.* Biochemical Journal, 2014. **462**: p. 513-523.
304. Pollard, H.B., N. Arispe, and E. Rojas, *Ion channel hypothesis for Alzheimer amyloid peptide neurotoxicity.* Cellular and Molecular Neurobiology, 1995. **15**(5): p. 513-526.
305. Arispe, N., H.B. Pollard, and E. Rojas, *Giant multilevel cation channels formed by Alzheimer disease amyloid beta-protein [A beta P-(1-40)] in bilayer membranes.* Proc Natl Acad Sci U S A, 1993. **90**(22): p. 10573-10577.
306. Sonkar, V.K., P.P. Kulkarni, and D. Dash, *Amyloid beta peptide stimulates platelet activation through RhoA-dependent modulation of actomyosin organization.* The FASEB Journal, 2014. **28**(4): p. 1819-29.
307. Donner, L., et al., *Platelets contribute to amyloid-beta aggregation in cerebral vessels through integrin alpha(IIb)beta(3)-induced outside-in signaling and clusterin release.* Science Signaling, 2016. **9**(429).
308. Fisar, Z., et al., *Mitochondrial respiration in the platelets of patients with Alzheimer's disease.* Curr Alzheimer Res, 2016. **13**(8): p. 930-941.
309. Cardoso, S.M., et al., *Cytochrome c oxidase is decreased in Alzheimer's disease platelets.* Neurobiology of Aging, 2004. **25**(1): p. 105-10.
310. Qiao, J., et al., *Regulation of platelet activation and thrombus formation by reactive oxygen species.* Redox Biology, 2018. **14**: p. 126-130.
311. Jang, J.Y., et al., *Reactive oxygen species play a critical role in collagen-induced platelet activation via SHP-2 oxidation.* Antioxid Redox Signal, 2014. **20**(16): p. 2528-2540.
312. Krotz, F., H.Y. Sohn, and U. Pohl, *Reactive oxygen species: players in the platelet game.* Arterioscler Thromb Vasc Biol, 2004. **24**(11): p. 1988-96.
313. Lopez, J.J., et al., *Thrombin induces apoptotic events through the generation of reactive oxygen species in human platelets.* J Thromb Haemost, 2007. **5**(6): p. 1283-1291.
314. Krotz, F., et al., *NAD(P)H oxidase–dependent platelet superoxide anion release increases platelet recruitment.* Hemostasis, Thrombosis, and Vascular Biology 2002. **100**(917-924).
315. Schieber, M. and N.S. Chandel, *ROS function in redox signaling and oxidative stress.* Curr Biol, 2014. **24**(10): p. R453-62.
316. Vlădăreanu, A., et al., *Role of reactive oxygen species in platelet function in normal states and chronic myeloproliferative disorders.* Romanian Journal of Biochemistry, 2008. **45**(2): p. 221–232
317. Violi, F. and P. Pignatelli, *Platelet oxidative stress and thrombosis.* Thrombosis Research, 2012. **129**(3): p. 378-81.
318. Amblard, M., et al., *Methods and protocols of modern solid phase peptide synthesis.* Mol Biotechnol, 2006. **33**(3): p. 239-254.
319. Zahn, H., *Solid phase peptide synthesis*. Angewandte Chemie, ed. V.J. M., S.J. D., and Y.W. H. Vol. 81. 1969, San Francisco-London: Freeman and Co. 796-796.
320. Palomo, J.M., *Solid-phase peptide synthesis: an overview focused on the preparation of biologically relevant peptides.* RSC Adv, 2014. **4**(62): p. 32658-32672.
321. E., K., et al., *Color test for detection of free terminal amino groups in the solid-phase synthesis of peptides.* Analytical Biochemistry, 1970. **34**(2): p. 595-598.
322. Nelson, A.R., et al., *Neurovascular dysfunction and neurodegeneration in dementia and Alzheimer's disease.* Biochim Biophys Acta, 2016. **1862**(5): p. 887-900.
323. Liu, H. and J. Zhang, *Cerebral hypoperfusion and cognitive impairment: the pathogenic role of vascular oxidative stress.* The International Journal of Neuroscience, 2012. **122**(9): p. 494-9.

324. Zhu, X., et al., *Causes of oxidative stress in Alzheimer disease.* Cell Mol Life Sci, 2007. **64**(17): p. 2202-10.
325. Verfaillie, S.C., et al., *Cerebral perfusion and glucose metabolism in Alzheimer's disease and frontotemporal dementia: two sides of the same coin?* Eur Radiol, 2015. **25**(10): p. 3050-3059.
326. De la Torre, J.C., *Cardiovascular risk factors promote brain hypoperfusion leading to cognitive decline and dementia.* Cardiovasc Psychiatry Neurol, 2012. **2012**: p. 367516.
327. Weller, R.O., et al., *Perivascular drainage of amyloid-beta peptides from the brain and its failure in cerebral amyloid angiopathy and Alzheimer's disease.* Brain Pathol, 2008. **18**(2): p. 253-66.
328. Di Luca, M., et al., *Abnormal pattern of platelet APP isoforms in Alzheimer disease and Down syndrome.* Archives of Neurology, 1996. **53**(11): p. 1162-6.
329. Parker, W.D., Jr. and J.K. Parks, *Cytochrome c oxidase in Alzheimer's disease brain: purification and characterization.* Neurology, 1995. **45**(3 Pt 1): p. 482-6.
330. Cardoso, S.M., et al., *Mitochondria dysfunction of Alzheimer's disease cybrids enhances Abeta toxicity.* Journal of Neurochemistry, 2004. **89**(6): p. 1417-26.
331. Valla, J., et al., *Impaired platelet mitochondrial activity in Alzheimer's disease and mild cognitive impairment.* Mitochondrion, 2006. **6**(6): p. 323-30.
332. Kniewallner, K.M., et al., *Platelets in the Alzheimer's Disease Brain: do they Play a Role in Cerebral Amyloid Angiopathy?* Current Neurovascular Research, 2015. **12**(1): p. 4-14.
333. Canobbio, I., et al., *Increased platelet adhesion and thrombus formation in a mouse model of Alzheimer's disease.* Cellular Signalling, 2016. **28**(12): p. 1863-1871.
334. Bu, X.L., et al., *Blood-derived amyloid-beta protein induces Alzheimer's disease pathologies.* Molecular Psychiatry 2017.
335. Nostrand, W., et al., *Protease nexin-2/amyloid β-protein precursor in blood is a platelet-specific protein.* Biochemical and Biophysical Research Communications, 1991. **175**(1): p. 15-21.
336. Kowalska, M.A. and K. Badellino, *beta-Amyloid protein induces platelet aggregation and supports platelet adhesion.* Biochemical and Biophysical Research Communications, 1994. **205**(3): p. 1829-35.
337. Ozaki, Y., et al., *Platelet GPIb-IX-V-dependent signaling.* J Thromb Haemost, 2005. **3**(8): p. 1745-51.
338. Ozaki, Y., *GPIb-Related Signaling Pathways in Platelets*, in *Recent Advances in Thrombosis and Hemostasis 2008*, D.E.W. Tanaka K., Ikeda Y., Iwanaga S., Saito H., Sueishi K., Editor. 2008, Springer: Tokyo. p. 253-264.
339. Senis, Y.A., A. Mazharian, and J. Mori, *Src family kinases: at the forefront of platelet activation.* Blood, 2014. **124**(13): p. 2013-24.
340. Sonkar, V.K., et al., *Plasma Fibrinogen Is a Natural Deterrent to Amyloid beta-Induced Platelet Activation and Neuronal Toxicity.* Molecular Medicine, 2016. **22**: p. 224-232.
341. Donner, L., et al., *Relevance of N-terminal residues for amyloid-beta binding to platelet integrin alpha(IIb)beta(3), integrin outside-in signaling and amyloid-beta fibril formation.* Cellular Signalling, 2018. **50**: p. 121-130.
342. Behrendt, R., P. White, and J. Offer, *Advances in Fmoc solid-phase peptide synthesis.* J Pept Sci, 2016. **22**(1): p. 4-27.
343. Schupf, N., et al., *Elevated plasma amyloid β-peptide 1–42 and onset of dementia in adults with Down syndrome.* Neuroscience Letters, 2001. **301**(3): p. 199-203.
344. Muller, J., et al., *Profiling of active thrombin in human blood by supramolecular complexes.* Angewandte Chemie (International Ed English), 2011. **50**(27): p. 6075-6078.

345. Elaskalani, O., et al., *Oligomeric and fibrillar amyloid beta 42 induce platelet aggregation partially through GPVI.* Platelets, 2018. **29**(4): p. 415-420.
346. Ahn, H.J., et al., *Alzheimer's disease peptide beta-amyloid interacts with fibrinogen and induces its oligomerization.* Proc Natl Acad Sci U S A, 2010. **107**(50): p. 21812-7.
347. Mangin, P.H., et al., *Immobilized fibrinogen activates human platelets through glycoprotein VI.* Haematologica, 2018. **103**(5): p. 898-907.
348. Induruwa, I., et al., *Platelet collagen receptor Glycoprotein VI-dimer recognizes fibrinogen and fibrin through their D-domains, contributing to platelet adhesion and activation during thrombus formation.* J Thromb Haemost, 2018. **16**(2): p. 389-404.
349. Siljander, P.R., et al., *Integrin activation state determines selectivity for novel recognition sites in fibrillar collagens.* J Biol Chem, 2004. **279**(46): p. 47763-72.
350. Farndale, R.W., et al., *Collagen-platelet interactions: recognition and signalling.* Biochem Soc Symp, 2003(70): p. 81-94.
351. Alsheikh-Abubaker, A., et al., *Amyloid Peptide β1-42 Induces Integrin αIIbβ3 Activation, Platelet Adhesion, and Thrombus Formation in a NADPH Oxidase-Dependent Manner.* Oxidative Medicine and Cellular Longevity, 2019. **2019**: p. 1-12.
352. Handtke, S., et al., *Toward the Relevance of Platelet Subpopulations for Transfusion Medicine.* Frontiers in Medicine, 2018. **5**: p. 17.
353. Lorenzo, A., et al., *Amyloid β interacts with the amyloid precursor protein: a potential toxic mechanism in Alzheimer's disease.* Nature Neuroscience, 2000. **3**(5): p. 460-464.
354. Visconte, C., et al., *Amyloid precursor protein is required for in vitro platelet adhesion to amyloid peptides and potentiation of thrombus formation.* Cellular Signalling, 2018. **52**: p. 95-102.
355. Vara, D., et al., *A novel combinatorial technique for simultaneous quantification of oxygen radicals and aggregation reveals unexpected redox patterns in the activation of platelets by different physiopathological stimuli.* Haematologica, 2019: p. haematol.2018.208819.
356. Jang, J.Y., et al., *Resveratrol inhibits collagen-induced platelet stimulation through suppressing NADPH oxidase and oxidative inactivation of SH2 domain-containing protein tyrosine phosphatase-2.* Free Radic Biol Med, 2015. **89**: p. 842-51.
357. Carrim, N., et al., *Thrombin-induced reactive oxygen species generation in platelets: A novel role for protease-activated receptor 4 and GPIbalpha.* Redox Biology, 2015. **6**: p. 640-7.
358. Wachowicz, B., et al., *Generation of reactive oxygen species in blood platelets.* Platelets, 2002. **13**(3): p. 175-82.
359. Olas, B., et al., *Free radicals are involved in cancer procoagulant-induced platelet activation.* Thromb Res, 2000. **97**(3): p. 169-75.
360. Lander, H.M., *An essential role for free radicals and derived species in signal transduction.* Faseb Journal, 1997. **11**(2): p. 118-24.
361. Klann, E. and E. Thiels, *Modulation of protein kinases and protein phosphatases by reactive oxygen species: implications for hippocampal synaptic plasticity.* Prog Neuropsychopharmacol Biol Psychiatry, 1999. **23**(3): p. 359-76.
362. Chiarugi, P. and P. Cirri, *Redox regulation of protein tyrosine phosphatases during receptor tyrosine kinase signal transduction.* Trends Biochem Sci, 2003. **28**(9): p. 509-14.
363. Ostman, A. and F.D. Bohmer, *Regulation of receptor tyrosine kinase signaling by protein tyrosine phosphatases.* Trends Cell Biol, 2001. **11**(6): p. 258-66.
364. Freedman, J.E., *Oxidative stress and platelets.* Arterioscler Thromb Vasc Biol, 2008. **28**(3): p. s11-6.

365. Mironczuk-Chodakowska, I., A.M. Witkowska, and M.E. Zujko, *Endogenous non-enzymatic antioxidants in the human body.* Advances in Medical Sciences, 2018. **63**(1): p. 68-78.
366. Valko, M., et al., *Free radicals and antioxidants in normal physiological functions and human disease.* The International Journal of Biochemisty & Cell Biology, 2007. **39**(1): p. 44-84.
367. Seno, T., et al., *Involvement of NADH/NADPH oxidase in human platelet ROS production.* Thrombosis Research, 2001. **103**(5): p. 399-409.
368. Dzhatdoeva, A.A., et al., *Mitochondria As a Source of Superoxide in Human Platelets.* Biologicheskie Membrany, 2017. **34**(6): p. 116-123.
369. Moro, M.A., et al., *Paradoxical fate and biological action of peroxynitrite on human platelets.* Proc Natl Acad Sci U S A, 1994. **91**(14): p. 6702-6.
370. Eitan, F. and D. Mutaz, *Oxidative Stress and Platelet Dysfunction.* Thrombosis & Haemostasis: Research, 2018. **2**(2).
371. Kohen, R. and A. Nyska, *Oxidation of biological systems: oxidative stress phenomena, antioxidants, redox reactions, and methods for their quantification.* Toxicol Pathol, 2002. **30**(6): p. 620-50.
372. Berlett, B.S. and E.R. Stadtman, *Protein oxidation in aging, disease, and oxidative stress.* J Biol Chem, 1997. **272**(33): p. 20313-6.
373. Cordeiro, R.M., *Reactive oxygen species at phospholipid bilayers: distribution, mobility and permeation.* Biochim Biophys Acta, 2014. **1838**(1 Pt B): p. 438-44.
374. Taverne, Y.J.H.J., et al., *Reactive Oxygen Species and the Cardiovascular System.* Oxidative Medicine and Cellular Longevity, 2013. **2013**: p. 15.
375. Chen, X., C. Guo, and J. Kong, *Oxidative stress in neurodegenerative diseases.* Neural Regen Res, 2012. **7**(5): p. 376-85.
376. Chauhan, V. and A. Chauhan, *Oxidative stress in Alzheimer's disease.* Pathophysiology, 2006. **13**(3): p. 195-208.
377. Thakur, P., A. Kumar, and A. Kumar, *Targeting oxidative stress through antioxidants in diabetes mellitus.* J Drug Target, 2018. **26**(9): p. 766-776.
378. Liochev, S.I., *Reactive oxygen species and the free radical theory of aging.* Free Radic Biol Med, 2013. **60**: p. 1-4.
379. Violi, F. and P. Pignatelli, *Platelet NOX, a novel target for anti-thrombotic treatment.* Thrombosis Haemostasis, 2014. **111**(5): p. 817-23.
380. Pastori, D., et al., *Nox-2 up-regulation and platelet activation: Novel insights.* Prostaglandins Other Lipid Mediat, 2015. **120**: p. 50-5.
381. Altenhofer, S., et al., *The NOX toolbox: validating the role of NADPH oxidases in physiology and disease.* Cellular and Molecular Life Sciences, 2012. **69**(14): p. 2327-43.
382. Bedard, K. and K.H. Krause, *The NOX family of ROS-generating NADPH oxidases: physiology and pathophysiology.* Physiol Rev, 2007. **87**(1): p. 245-313.
383. Vara, D., M. Campanella, and G. Pula, *The novel NOX inhibitor 2-acetylphenothiazine impairs collagen-dependent thrombus formation in a GPVI-dependent manner.* Br J Pharmacol, 2013. **168**(1): p. 212-24.
384. Schröder, K., N. Weissmann, and R.P. Brandes, *Organizers and activators: Cytosolic Nox proteins impacting on vascular function.* Free Radical Biology and Medicine, 2017. **109**: p. 22-32.
385. Banfi, B., et al., *Two novel proteins activate superoxide generation by the NADPH oxidase NOX1.* THE JOURNAL OF BIOLOGICAL CHEMISTRY, 2003. **278**(6): p. 3510-3.
386. Serino, A. and G. Salazar, *Protective Role of Polyphenols against Vascular Inflammation, Aging and Cardiovascular Disease.* Nutrients, 2018. **11**(1).

387. Begonja, A.J., et al., *Platelet NAD(P)H-oxidase-generated ROS production regulates alphaIIbbeta3-integrin activation independent of the NO/cGMP pathway.* Blood, 2005. **106**(8): p. 2757-60.
388. Begonja, A.J., et al., *Platelet regulation by NO/cGMP signaling and NAD(P)H oxidase-generated ROS.* Blood Cells, Molecules, and Diseases 2006. **36**(2): p. 166-70.
389. Walsh, T.G., et al., *The role of Nox1 and Nox2 in GPVI-dependent platelet activation and thrombus formation.* Redox Biology, 2014. **2**: p. 178-86.
390. Magwenzi, S., et al., *Oxidized LDL activates blood platelets through CD36/NOX2-mediated inhibition of the cGMP/protein kinase G signaling cascade.* Blood, 2015. **125**(17): p. 2693-703.
391. Delaney, M.K., et al., *Differential Roles of the NADPH-Oxidase 1 and 2 in Platelet Activation and Thrombosis.* Arterioscler Thromb Vasc Biol, 2016. **36**(5): p. 846-54.
392. Bakdash, N. and M.S. Williams, *Spatially distinct production of reactive oxygen species regulates platelet activation.* Free Radic Biol Med, 2008. **45**(2): p. 158-66.
393. Vara, D. and G. Pula, *Reactive oxygen species: physiological roles in the regulation of vascular cells.* Curr Mol Med, 2014. **14**(9): p. 1103-25.
394. Griendling, K.K., et al., *Measurement of Reactive Oxygen Species, Reactive Nitrogen Species, and Redox-Dependent Signaling in the Cardiovascular System: A Scientific Statement From the American Heart Association.* Circ Res, 2016. **119**(5): p. e39-75.
395. Dikalov, S.I. and D.G. Harrison, *Methods for detection of mitochondrial and cellular reactive oxygen species.* Antioxid Redox Signal, 2014. **20**(2): p. 372-82.
396. Eruslanov, E. and S. Kusmartsev, *Identification of ROS using oxidized DCFDA and flow-cytometry.* Methods Mol Biol, 2010. **594**: p. 57-72.
397. Wojtala, A., et al., *Methods to monitor ROS production by fluorescence microscopy and fluorometry.* Methods Enzymol, 2014. **542**: p. 243-62.
398. Sun, S.Y., *N-acetylcysteine, reactive oxygen species and beyond.* Cancer Biol Ther, 2010. **9**(2): p. 109-10.
399. Hosseini, E., et al., *ROS scavenger, N-acetyl-l-cysteine and NOX specific inhibitor, VAS2870 reduce platelets apoptosis while enhancing their viability during storage.* Transfusion, 2019.
400. Owusu-Ansah, E., A. Yavari, and U. Banerjee, *A protocol for in vivo detection of Reactive Oxygen Species*. 2008.
401. Alsheikh-Abubaker, A., et al., *A novel flow cytometry assay using dihydroethidium as redox-sensitive probe reveals NADPH oxidase-dependent generation of superoxide anion in human platelets exposed to amyloid peptide beta.* Platelets, 2017: p. 1-9.
402. Sahu, I.D., R.M. McCarrick, and G.A. Lorigan, *Use of electron paramagnetic resonance to solve biochemical problems.* Biochemistry, 2013. **52**(35): p. 5967-84.
403. Mrakic-Sposta, S., et al., *A quantitative method to monitor reactive oxygen species production by electron paramagnetic resonance in physiological and pathological conditions.* Oxid Med Cell Longev, 2014. **2014**: p. 306179.
404. Berg, K., et al., *A high precision method for quantitative measurements of reactive oxygen species in frozen biopsies.* PLoS One, 2014. **9**(3): p. e90964.
405. Dikalov, S., K.K. Griendling, and D.G. Harrison, *Measurement of reactive oxygen species in cardiovascular studies.* Hypertension, 2007. **49**(4): p. 717-27.
406. Dikalov, S.I., Y.F. Polienko, and I. Kirilyuk, *Electron Paramagnetic Resonance Measurements of Reactive Oxygen Species by Cyclic Hydroxylamine Spin Probes.* Antioxid Redox Signal, 2018. **28**(15): p. 1433-1443.
407. Cifuentes-Pagano, E., D.N. Meijles, and P.J. Pagano, *The quest for selective nox inhibitors and therapeutics: challenges, triumphs and pitfalls.* Antioxid Redox Signal, 2014. **20**(17): p. 2741-54.

408. Cifuentes-Pagano, M.E., D.N. Meijles, and P.J. Pagano, *Nox Inhibitors & Therapies: Rational Design of Peptidic and Small Molecule Inhibitors.* Curr Pharm Des, 2015. **21**(41): p. 6023-35.
409. Ranayhossaini, D.J., et al., *Selective recapitulation of conserved and nonconserved regions of putative NOXA1 protein activation domain confers isoform-specific inhibition of Nox1 oxidase and attenuation of endothelial cell migration.* J Biol Chem, 2013. **288**(51): p. 36437-50.
410. Cifuentes-Pagano, E., G. Csanyi, and P.J. Pagano, *NADPH oxidase inhibitors: a decade of discovery from Nox2ds to HTS.* Cell Mol Life Sci, 2012. **69**(14): p. 2315-25.
411. Deyts, C., G. Thinakaran, and A.T. Parent, *APP Receptor? To Be or Not To Be.* Trends Pharmacol Sci, 2016. **37**(5): p. 390-411.
412. Cotman, C.W., et al., *Cell adhesion molecules in neural plasticity and pathology: similar mechanisms, distinct organizations?* Progress in Neurobiology 1998. **55**: p. 659-669.
413. Sunde, M., et al., *Common core structure of amyloid fibrils by synchrotron X-ray diffraction.* J Mol Biol, 1997. **273**(3): p. 729-39.
414. Jiménez, J.L., et al., *Cryo-electron microscopy structure of an SH3 amyloid fibril and model of the molecular packing.* Embo j, 1999. **18**(4): p. 815-21.
415. Williams, A.D., et al., *Mapping abeta amyloid fibril secondary structure using scanning proline mutagenesis.* J Mol Biol, 2004. **335**(3): p. 833-42.
416. Kumar, S. and J. Udgaonkar, *Mechanisms of amyloid fibril formation by proteins*. Vol. 98. 2010. 639-656.
417. Biancalana, M. and S. Koide, *Molecular mechanism of Thioflavin-T binding to amyloid fibrils.* Biochim Biophys Acta, 2010. **1804**(7): p. 1405-12.
418. Hoshino, M., *Fibril formation from the amyloid-beta peptide is governed by a dynamic equilibrium involving association and dissociation of the monomer.* Biophys Rev, 2017. **9**(1): p. 9-16.
419. Chatani, E. and N. Yamamoto, *Recent progress on understanding the mechanisms of amyloid nucleation.* Biophys Rev, 2018. **10**(2): p. 527-534.
420. Stokes, K.Y., et al., *Platelet-associated NAD(P)H oxidase contributes to the thrombogenic phenotype induced by hypercholesterolemia.* Free Radic Biol Med, 2007. **43**(1): p. 22-30.
421. Kalyanaraman, B., et al., *Measuring reactive oxygen and nitrogen species with fluorescent probes: challenges and limitations.* Free Radic Biol Med, 2012. **52**(1): p. 1-6.
422. Rota, C., C. F Chignell, and R. Mason, *Evidence for free radical formation during the oxidation of 2',7-dichlorofluorescin to the fluorescent dye 2',7-dichlorofluorescin by horseradish peroxidase: Possible implications for oxidative stress measurements*. Vol. 27. 1999. 873-881.
423. Wang, Z., et al., *The role of mitochondria-derived reactive oxygen species in hyperthermia-induced platelet apoptosis.* PLoS One, 2013. **8**(9): p. e75044.
424. Gibson, K.R., et al., *Therapeutic potential of N-acetylcysteine as an antiplatelet agent in patients with type-2 diabetes.* Cardiovasc Diabetol, 2011. **10**: p. 43.
425. Paul, M., et al., *Methotrexate Promotes Platelet Apoptosis via JNK-Mediated Mitochondrial Damage: Alleviation by N-Acetylcysteine and N-Acetylcysteine Amide.* PLoS One, 2015. **10**(6): p. e0127558.
426. Dietrich-Muszalska, A. and A. Kwiatkowska, *Generation of superoxide anion radicals and platelet glutathione peroxidase activity in patients with schizophrenia.* Neuropsychiatr Dis Treat, 2014. **10**: p. 703-9.
427. Vara, D., et al., *A novel combinatorial technique for simultaneous quantification of oxygen radicals and aggregation reveals unexpected redox patterns in the activation of platelets by different physiopathological stimuli.* Haematologica, 2019.

428. Greenwald, J. and R. Riek, *Biology of amyloid: structure, function, and regulation.* Structure, 2010. **18**(10): p. 1244-60.
429. Serpell, L.C., *Alzheimer's amyloid fibrils: structure and assembly.* Biochimica et Biophysica Acta, 2000. **1502**: p. 16-30.
430. Roche, J., et al., *Monomeric Aβ(1-40) and Aβ(1-42) Peptides in Solution Adopt Very Similar Ramachandran Map Distributions That Closely Resemble Random Coil.* Biochemistry, 2016. **55**(5): p. 762-75.
431. Itoh, N., et al., *Not Oligomers but Amyloids are Cytotoxic in the Membrane-Mediated Amyloidogenesis of Amyloid-beta Peptides.* Chembiochem, 2018. **19**(5): p. 430-433.
432. Bhatia, R., H. Lin, and R. Lal, *Fresh and globular amyloid beta protein (1-42) induces rapid cellular degeneration: evidence for AbetaP channel-mediated cellular toxicity.* Faseb j, 2000. **14**(9): p. 1233-43.
433. Pietraforte, D., et al., *Redox control of platelet functions in physiology and pathophysiology.* Antioxid Redox Signal, 2014. **21**(1): p. 177-93.
434. Stuart, M.J. and H. Holmsen, *Hydrogen peroxide, an inhibitor of platelet function: Effect on adenine nucleotide metabolism, and the release reaction.* American Journal of Hematology, 1977. **2**(1): p. 53-63.
435. Canoso, R.T., et al., *Hydrogen peroxide and platelet function.* Blood, 1974. **43**(5): p. 645-656.
436. Levine, P.H., et al., *Leukocyte-platelet interaction. Release of hydrogen peroxide by granulocytes as a modulator of platelet reactions.* The Journal of Clinical Investigation, 1976. **57**(4): p. 955-963.
437. Del Principe, D., et al., *Hydrogen peroxide has a role in the aggregation of human platelets.* FEBS Lett, 1985. **185**(1): p. 142-6.
438. del principe, D., et al., *Hydrogen peroxide is an intermediate in the platelet activation cascade triggered by collagen, but not by thrombin*. Vol. 62. 1991. 365-75.
439. Forde, R.C. and D.J. Fitzgerald, *Reactive oxygen species and platelet activation in reperfusion injury.* Circulation, 1997. **95**(4): p. 787-9.
440. Clutton, P., A. Miermont, and J.E. Freedman, *Regulation of endogenous reactive oxygen species in platelets can reverse aggregation.* Arterioscler Thromb Vasc Biol, 2004. **24**(1): p. 187-92.
441. Trovati, M. and G. Anfossi, *Mechanisms involved in platelet hyperactivation and platelet-endothelium interrelationships in diabetes mellitus.* Curr Diab Rep, 2002. **2**(4): p. 316-22.
442. Israels, S.J., et al., *Markers of platelet activation are increased in adolescents with type 2 diabetes.* Diabetes Care, 2014. **37**(8): p. 2400-3.
443. Pula, G., et al., *Functional interaction of protein kinase Calpha with the tyrosine kinases Syk and Src in human platelets.* J Biol Chem, 2005. **280**(8): p. 7194-205.
444. Wentworth, J.K., G. Pula, and A.W. Poole, *Vasodilator-stimulated phosphoprotein (VASP) is phosphorylated on Ser157 by protein kinase C-dependent and -independent mechanisms in thrombin-stimulated human platelets.* Biochem J, 2006. **393**(Pt 2): p. 555-64.
445. Taylor, L., et al., *Discovery of novel GPVI receptor antagonists by structure-based repurposing.* PLoS One, 2014. **9**(6): p. e101209.
446. Harper, M.T. and A.W. Poole, *Diverse functions of protein kinase C isoforms in platelet activation and thrombus formation.* J Thromb Haemost, 2010. **8**(3): p. 454-62.
447. Cosentino-Gomes, D., N. Rocco-Machado, and J.R. Meyer-Fernandes, *Cell signaling through protein kinase C oxidation and activation*. Int J Mol Sci, 2012. **13**(9): p. 10697-721.
448. Bamberger, M.E., et al., *A cell surface receptor complex for fibrillar beta-amyloid mediates microglial activation.* J Neurosci, 2003. **23**(7): p. 2665-2674.

449. Moore, K.J., et al., *A CD36-initiated signaling cascade mediates inflammatory effects of beta-amyloid.* J Biol Chem, 2002. **277**(49): p. 47373-47379.
450. Wilkinson, B., et al., *Fibrillar beta-amyloid-stimulated intracellular signaling cascades require Vav for induction of respiratory burst and phagocytosis in monocytes and microglia.* J Biol Chem, 2006. **281**(30): p. 20842-20850.
451. Garcia-Bonilla, L., L. Park, and C. Iadecola, *Commentary on Myers et al.: growing role of the innate immunity receptor CD36 in central nervous system diseases.* Exp Neurol, 2014. **261**: p. 633-7.
452. Yang, M., et al., *Platelet CD36 promotes thrombosis by activating redox sensor ERK5 in hyperlipidemic conditions.* Blood, 2017. **129**(21): p. 2917-2927.
453. Gandhi, D.M., et al., *Characterization of Protease-Activated Receptor (PAR) ligands: Parmodulins are reversible allosteric inhibitors of PAR1-driven calcium mobilization in endothelial cells*. Vol. 26. 2018.
454. Jagroop, I.A. and D.P. Mikhailidis, *Angiotensin II can induce and potentiate shape change in human platelets: effect of losartan*. Journal of Human Hypertension, 2000. **14**(9): p. 581-585.
455. Alexandru, N., et al., *Platelet activation in hypertension associated with hypercholesterolemia: effects of irbesartan.* Journal of Thrombosis and Haemostasis, 2011. **9**(1): p. 173-184.
456. Kehoe, P.G., et al., *The Rationale and Design of the Reducing Pathology in Alzheimer's Disease through Angiotensin TaRgeting (RADAR) Trial.* Journal of Alzheimers Disease, 2018. **61**(2): p. 803-814.
457. Voko, Z., et al., *Aspirin use and risk of stroke in the elderly: the Rotterdam Study.* Neuroepidemiology, 2001. **20**(1): p. 40-44.
458. Hong, Y.M., *Atherosclerotic cardiovascular disease beginning in childhood.* Korean Circulation Journal, 2010. **40**(1): p. 1-9.
459. Bagyinszky, E., et al., *Role of inflammatory molecules in the Alzheimer's disease progression and diagnosis.* Journal of the Neurological Sciences, 2017. **376**: p. 242-254.
460. Honjo, K., S.E. Black, and N.P.L.G. Verhoeff, *Alzheimer's Disease, cerebrovascular Disease, and the β−amyloid cascade.* Canadian Journal of Neurological Sciences, 2012. **39**: p. 712-728.

APPENDIX

HPLC and MS for Aβ peptide from Life-Protein

Order ID	:LT1148-2
Name	:1(**Aβ1-42**)
Sequence	:DAEFRHDSGYEVHHQKLVFFAEDVGSNKGAIIGLMVGGVVIA
Lot. No	:LT1148-2-0125
Pump A	:0.1%Trifluoroacetic in 100% water
Pump B	:0.1%Trifluoroacetic in 100% acetonrtrile
Total Flow	:1ml/min
Wavelength	:214nm
Analytial column type	:SHIMADZU Inertsil ODS-SP(4.6*250mm*5um)
Dissolution method	:15%ACN+85%H2O
Inj. Volume	: 95ul

Time	Module	Action	Value
0.01	Pumps	B.Conc	20
20.00	Pumps	B.Conc	65
30.00	Pumps	B.Conc	100
38.00	Pumps	B.Conc	100
40.00	Pumps	B.Conc	20
50.00	Controller	Stop	

Chromatogram

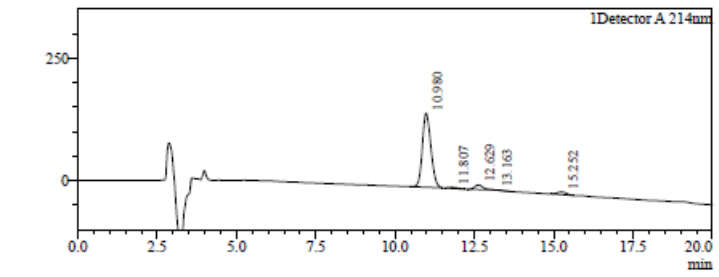

Peak Table

Detector A 214nm

Peak#	Ret. Time	Area	Height	Area%
1	10.980	2820092	151189	90.037
2	11.807	33289	1828	1.063
3	12.629	163115	9245	5.208
4	13.163	8243	54	0.263
5	15.252	107397	5567	3.429
Total		3132136	167884	100.000

MS Spectrum

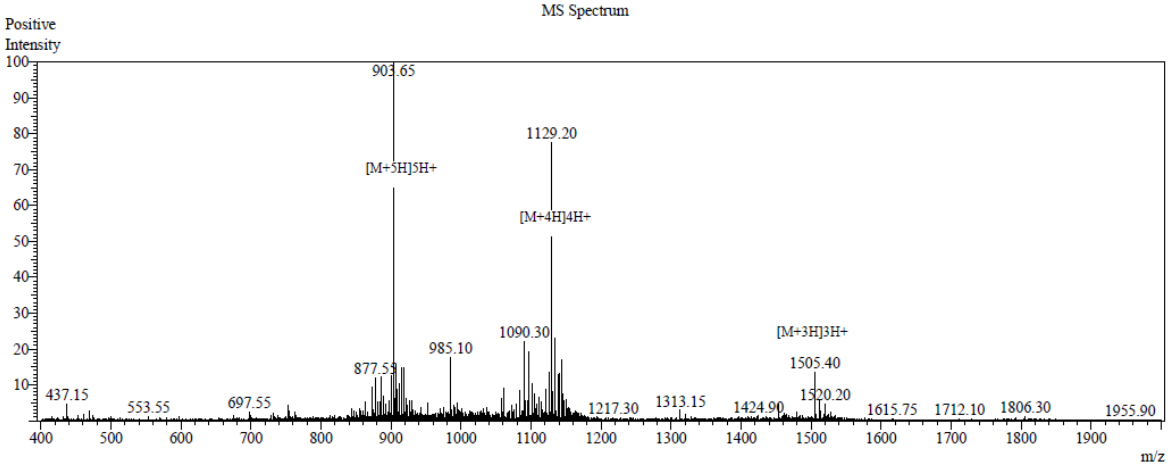

Sample Information

Dissolution method	:5%HAC+8%ACN+87%H2O	Interface	:ESI	Prerod Bias	:+4.5kv
Date Acquired	:2016/03/28 15:43:01	Nebulizing Gas Flow	:1.50L/min	Detector	:-0.2kv
Injection Volume	:1ul	CDL Temp	:250C	T.Flow	:0.2ml/min
Block Temp	:200	CDL Volt	:0v	B.conc	:50%H2O/50%MEOH

Order ID	:LT1148-2
Name	:1
Sequence	:DAEFRHDSGYEVHHQKLVFFAEDVGSNKGAIIGLMVGGVVIA
Lot.No	:LT1148-2-0125
Theoretical	:4514.07
Observed	:4513.25

Order ID	:LT1148-6
Name	:5 **(Aβ25-35)**
Sequence	:GSNKGAIIGLM
Lot. No	:LT1148-6-0125
Pump A	:0.1%Trifluoroacetic in 100% water
Pump B	:0.1%Trifluoroacetic in 100% acetonrtrile
Total Flow	:1ml/min
Wavelength	:214nm
Analytial column type	:Waters ODS-SP(4.6*250mm*5um)
Dissolution method	:100%H2O
Inj. Volume	: 85ul

Time	Module	Action	Value
0.01	Pumps	B.Conc	2
30.00	Pumps	B.Conc	65
33.00	Pumps	B.Conc	100
38.00	Pumps	B.Conc	100
40.00	Pumps	B.Conc	2
50.00	Controller	Stop	

Chromatogram

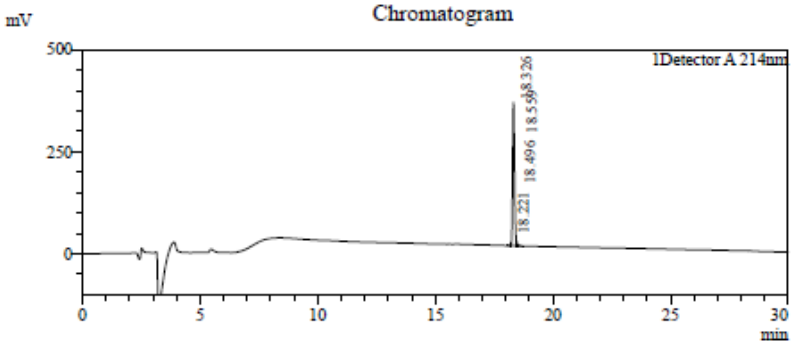

Peak Table

Detector A 214nm

Peak#	Ret. Time	Area	Height	Area%
1	18.221	17329	4410	0.870
2	18.326	1946381	350786	97.673
3	18.496	17665	3353	0.886
4	18.559	11376	2047	0.571
Total		1992751	360597	100.000

MS Spectrum

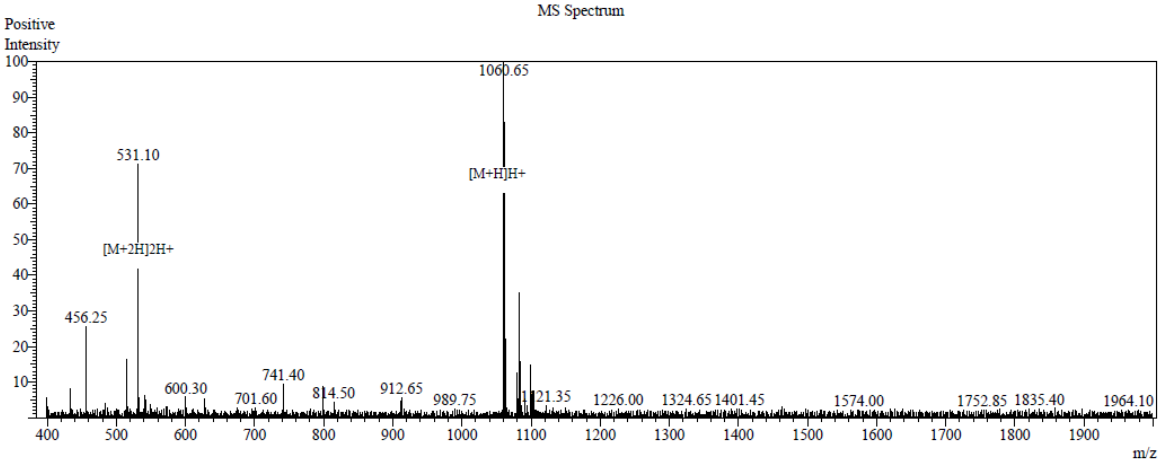

Sample Information

Dissolution method	:5%HAC+8%ACN+87%H2O	Interface	:ESI	Prerod Bias	:+4.5kv
Date Acquired	:2016/02/01 14:12:56	Nebulizing Gas Flow	:1.50L/min	Detector	:-0.2kv
Injection Volume	:1ul	CDL Temp	:250C	T.Flow	:0.2ml/min
Block Temp	:200	CDL Volt	:0v	B.conc	:50%H2O/50%MEOH

Order ID	:LT1148-6
Name	:5
Sequence	:GSNKGAIIGLM
Lot.No	:LT1148-6-0125
Theoretical	:1060.28
Observed	:1059.65

Order ID	:LT1148-3
Name	:2 **(Aβ1-40)**
Sequence	:DAEFRHDSGYEVHHQKLVFFAEDVGSNKGAIIGLMVGGVV
Lot. No	:LT1148-3-0125
Pump A	:0.1%Trifluoroacetic in 100% water
Pump B	:0.1%Trifluoroacetic in 100% acetonrtrile
Total Flow	:1ml/min
Wavelength	:214nm
Analytial column type	:SHIMADZU Inertsil ODS-SP(4.6*250mm*5um)
Dissolution method	:15%ACN+85%H2O
Inj. Volume	: 55ul

Time	Module	Action	Value
0.01	Pumps	B.Conc	20
25.00	Pumps	B.Conc	85
30.00	Pumps	B.Conc	100
38.00	Pumps	B.Conc	100
40.00	Pumps	B.Conc	20
50.00	Controller	Stop	

Chromatogram

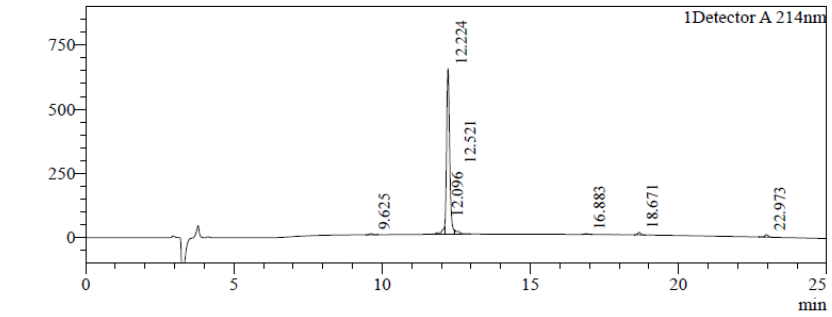

Peak Table

Detector A 214nm

Peak#	Ret. Time	Area	Height	Area%
1	9.625	32266	4406	0.616
2	12.096	188382	21927	3.594
3	12.224	4718014	644219	90.023
4	12.521	143600	10518	2.740
5	16.883	22139	2742	0.422
6	18.671	66295	9779	1.265
7	22.973	70179	9928	1.339
Total		5240875	703519	100.000

MS Spectrum

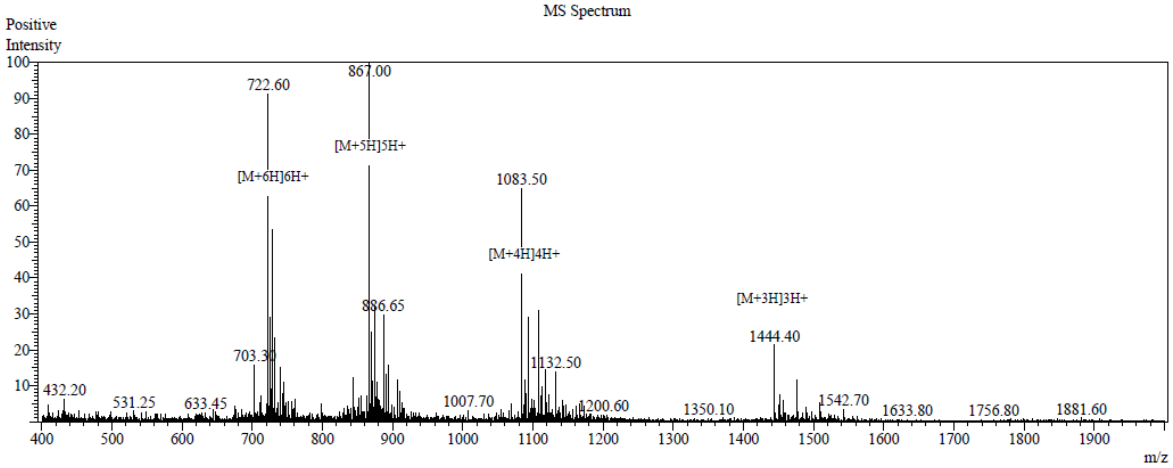

Sample Information

Dissolution method	:5%HAC+8%ACN+87%H2O	Interface	:ESI	Prerod Bias	:+4.5kv
Date Acquired	:2016/02/25 14:57:37	Nebulizing Gas Flow	:1.50L/min	Detector	:-0.2kv
Injection Volume	:1ul	CDL Temp	:250C	T.Flow	:0.2ml/min
Block Temp	:200	CDL Volt	:0v	B.conc	:50%H2O/50%MEOH

Order ID	:LT1148-3
Name	:2
Sequence	:DAEFRHDSGYEVHHQKLVFFAEDVGSNKGAIIGLMVGGVV
Lot.No	:LT1148-3-0125
Theoretical	:4329.84
Observed	:4330.00

Order ID	:LT1148-5
Name	:4 **(Scrambled Aβ1-42)**
Sequence	:DEFAKNIGHHDGVAVHMYKGRQVEFIGSIALVFEDVGSAGLV
Lot. No	:LT1148-5-0125
Pump A	:0.1%Trifluoroacetic in 100% water
Pump B	:0.1%Trifluoroacetic in 100% acetonrtrile
Total Flow	:1ml/min
Wavelength	:214nm
Analytial column type	:SHIMADZU Inertsil ODS-SP(4.6*250mm*5um)
Dissolution method	:15%ACN+85%H2O
Inj. Volume	: 80ul

Time	Module	Action	Value
0.01	Pumps	B.Conc	20
25.00	Pumps	B.Conc	85
30.00	Pumps	B.Conc	100
38.00	Pumps	B.Conc	100
40.00	Pumps	B.Conc	20
50.00	Controller	Stop	

Chromatogram

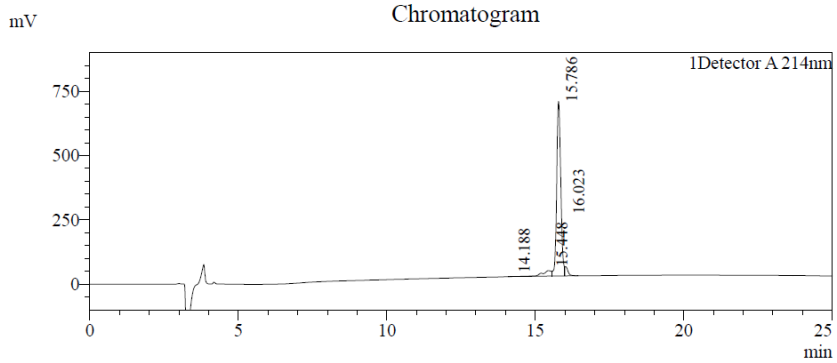

Peak Table

Detector A 214nm

Peak#	Ret. Time	Area	Height	Area%
1	14.188	4276	694	0.060
2	15.448	449579	21428	6.280
3	15.786	6447021	678735	90.054
4	16.023	258183	35738	3.606
Total		7159059	736596	100.000

MS Spectrum

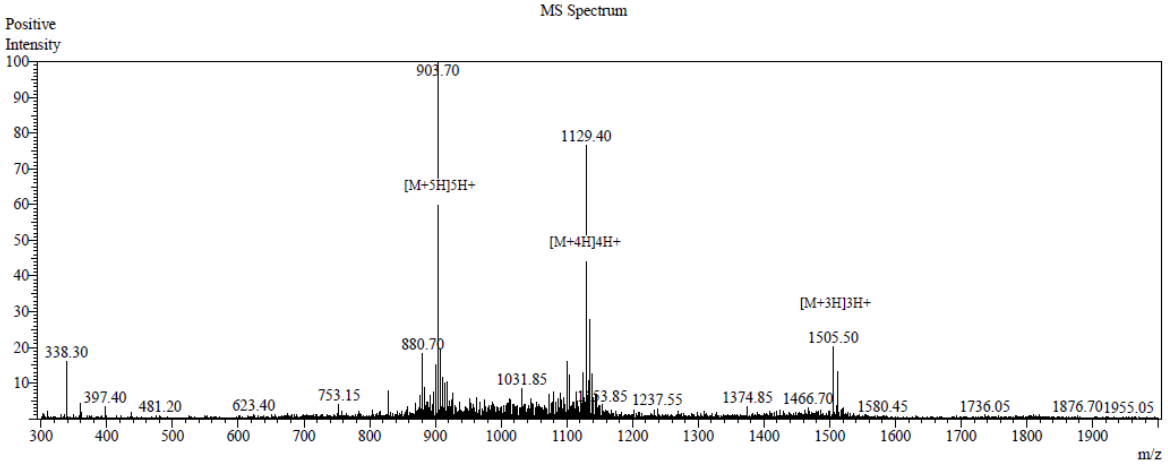

Sample Information

Dissolution method	:5%HAC+8%ACN+87%H2O	Interface	:ESI	Prerod Bias	:+4.5kv
Date Acquired	:2016/03/18 13:17:31	Nebulizing Gas Flow	:1.50L/min	Detector	:-0.2kv
Injection Volume	:1ul	CDL Temp	:250C	T.Flow	:0.2ml/min
Block Temp	:200	CDL Volt	:0v	B.conc	:50%H2O/50%MEOH

Order ID	:LT1148-5
Name	:4
Sequence	:DEFAKNIGHHDGVAVHMYKGRQVEFIGSIALVFEDVGSAGLV
Lot.No	:LT1148-5-0125
Theoretical	:4514.07
Observed	:4513.50

Publications